



Universiteit
Leiden
The Netherlands

Control of early plant development by light quality

Spaninks, K.

Citation

Spaninks, K. (2023, May 10). *Control of early plant development by light quality*. Retrieved from <https://hdl.handle.net/1887/3618264>

Version: Publisher's Version

License: [Licence agreement concerning inclusion of doctoral thesis in the Institutional Repository of the University of Leiden](#)

Downloaded from: <https://hdl.handle.net/1887/3618264>

Note: To cite this publication please use the final published version (if applicable).

Control of early plant development by light quality



Kiki Spaninks

Control of early plant development by light quality

Kiki Spaninks

Funding: This work was part of the research program “LED it be 50%” with project number 14212, which is partly financed by the Dutch Research Council (NWO).

Front cover: Tomato leaf mosaic art by Vanita Ruardy (tattoo artist, Marco Bratt tattoo, Noordwijk)

Printed and bound by: Ridderprint, www.ridderprint.nl

ISBN/EAN: 978-94-6483-051-4

Control of early plant development by light quality

Proefschrift

ter verkrijging van
de graad van doctor aan de Universiteit Leiden,
op gezag van rector magnificus prof.dr.ir. H. Bijl,
volgens besluit van het college voor promoties
te verdedigen op woensdag 10 mei 2023
klokke 16.15 uur

door

Kiki Spaninks

geboren te Voorburg, Nederland

25 November 1990

Promotores:

Prof. dr. R. Offringa

Prof. dr. P.J.J. Hooykaas

Co-promotor:

Dr. ir. W. van Ieperen (Wageningen University & Research)

Promotiecommissie:

Prof. dr. A.H. Meijer

Prof. dr. J. Memelink

Prof. dr. ir. L. Marcelis (Wageningen University & Research)

Prof. dr. R. Pierik (Universiteit Utrecht)

Dr. B.S. de Pater

Contents

Chapter 1

Light signalling pathways during early plant development. 7

Chapter 2

Local phytochrome signalling limits root growth in light by repressing auxin biosynthesis. 91

Chapter 3

Regulation of early plant development by red and blue light: A comparative analysis between *Arabidopsis thaliana* and *Solanum lycopersicum*. 137

Chapter 4

Light quality regulates apical and primary radial growth of *Arabidopsis thaliana* and *Solanum lycopersicum*. 193

Chapter 5

Light quality regulates flowering through the photoperiodic and age pathways. 231

Summary 291

Samenvatting 299

List of abbreviations 307

Curriculum vitae 317



Chapter 1

Light signalling pathways during early plant
development.

(General introduction)

Kiki Spaninks¹ and Remko Offringa¹

¹Plant Developmental Genetics, Institute of Biology Leiden,
Leiden University, Sylviusweg 72, 2333 BE, Leiden, Netherlands.



Abstract

For a horticultural crop such as tomato, the initial growth phase is crucial for the success of the whole production cycle. During this phase, the light requirements are relatively low, opening up possibilities to grow young plants in multi-layers that require less space and energy. Since light-emitting diodes (LEDs) make it possible to decouple light intensity from heating, building highly efficient multi-layer growth chambers is becoming more and more feasible. In order to optimise the use of LED lighting systems for vertical farming, more research has to be done on the effects of light quality on different developmental phases in multiple plant species. Moreover, by understanding the molecular mechanisms behind light-mediated plant development, we might be able to predict the effects of different wavelengths, and even circumvent possible negative effects of these wavelengths. Here we discuss the discovery, structure, and downstream signalling of plant light receptors, and new insights on early light-mediated plant development. Since these developmental processes are highly influenced by phytohormones, we also discuss the interplay between light and hormonal pathways. Finally, because this thesis is focused on the growth and development of young tomato plants, while using *Arabidopsis thaliana* (Arabidopsis) as a genetic model plant, we discuss similarities and differences in light-mediated plant development between these two species.

Keywords: LEDs, light quality, photoreceptors, photomorphogenesis, tomato, Arabidopsis



Light quality and LED technology

In the 17th century, Isaac Newton discovered that light can be broken down into different colours (Newton, 1704). The portion of the electromagnetic spectrum that is visible to the human eye, spanning a wavelength range between 400 and 700 nanometres (nm), is commonly referred to as “light”. However, in the 19th century, colours outside the visible spectrum, such as infrared and ultraviolet (UV) light, were discovered and correlated to specific wavelengths and frequencies of electromagnetic radiation (Young, 1804). Spectral colours only span a narrow range of wavelengths and include red, orange, yellow, green, cyan, blue, and violet (Bruno and Svoronos, 2005) (**Table 1**), whereas unsaturated colours such as magenta are mixes of multiple wavelengths. The spectral distribution of the different wavelengths or colours within a light source is referred to as “light quality”. Many artificial lights that are used in horticulture try to mimic the spectrum of sunlight by including fractions of all light colours and are commonly referred to as “white” lights. Not only does this term suggest that its spectrum consists of a single colour, but it also leads to the general misconception that all “white” lights have the same spectral quality. Therefore a more suitable term would be “multi-coloured” lights. Since different types or brands of white lights vary in light quality, it is incorrect to assume that plants will behave the same under each type or brand. Plants and algae respond to changes in light quality, mainly from colours at the end of the visible spectrum (i.e. red (R) and blue (B)), whereas the intermediate wavelengths (green and yellow) play minor roles. Moreover, land plants also respond to colours outside of the visible spectrum, being far-



Table 1: The electromagnetic radiation spectrum and its perception by land plants.

Spectral colours correspond to specific wavelengths and frequencies. This table indicates the characteristics of each colour within the plant visible spectrum and the photoreceptor families that perceive these colours. Photoreceptor families include phytochromes (PHYs), cryptochromes (CRYs), phototropins (PHOTs), Zeirlupes (ZTLs) and UV-RESISTANCE LOCUS 8 (UVR8). *Although CRYs have been reported to perceive green light, they are mainly sensitive to cyan, blue, and violet spectral ranges.

Colour	Wavelength (nm)	Frequency (THz)	Perception
Far-red	720-800	389-405	PHYs
Red	625-720	405-479	PHYs
Orange	590-625	479-508	-
Yellow	565-590	508-530	-
Green	520-565	530-576	*CRYs
Cyan	500-520	576-600	CRYs, PHOTs, ZTLs
Blue	435-500	600-689	CRYs, PHOTs, ZTLs
UV-A	315-435	689-952	CRYs, PHOTs, ZTLs
UV-B	280-315	952-1070	UVR8
UV-C	100-280	1070-3000	-

red (FR, 720-800 nm) and UV-B (280-350 nm) (Morrow, 2008). For this reason, the ratio of FR, R, B and UV-B fractions within “multi-colour” lighting systems influences the overall growth and development of plants. The development of LED technology has opened up new possibilities for more energy-efficient and economic lighting in horticulture. LEDs turn approximately 50% of the energy input directly into light. Moreover, less energy is lost in heat production, making LEDs not only more efficient, but also suitable for multi-layered growth chambers (SharathKumar et al., 2020). Because of their longer life span, additional costs for replacement and its



associated labour costs are limited. Furthermore, since LEDs lack dangerous materials such as mercury and glass casing, they are less harmful to the environment when discarded (Morrow, 2008). However, the most interesting trait of LEDs, that makes them fundamentally different from traditional lighting systems, is the possibility for spectral quality control. By matching the LED spectral output to specific light-detecting proteins and their downstream signalling pathways, optimal plant performance may be achieved without wasting energy on non-productive wavelengths (Heo et al., 2002). However, effects of these specific LED spectra have been shown to vary between species (Dougher and Bugbee, 2001). To optimise the use of LED lighting systems in horticulture, it is necessary to understand how differences in light quality influence plant development, not solely on the level of the whole organism, but also on a cellular and molecular level. In order to achieve this, we must start at the beginning of the process: the perception of light.

Light perception in land plants

As photo-autotrophic organisms, plants are capable of transforming light into chemical energy via photosynthesis by two large light-harvesting complexes consisting of proteins and pigments in chloroplasts. At the same time, plants “sense” light and translate this information into physiological and developmental responses, collectively referred to as photomorphogenesis (Arsovski et al., 2012), to optimise their stature to the light environment. Similar to the visible spectrum for human eyes, photosynthesis occurs within the spectral range of 400-700 nm. Therefore this spectral range is also referred to as photosynthetically active radiation (PAR). Photons at shorter wavelengths can be too energetic resulting in damage of cells, whereas photons



Chapter 1: General introduction

at longer wavelengths do not carry enough energy for photosynthesis (Pattison et al., 2018). Initially, the irradiance of PAR was measured in energy flux (W/m^2) which is based on the energy contained in the photons. However, for agricultural purposes it appeared to be more relevant to measure the number of photons received per area per time unit. Thus, photosynthetic photon flux (PPF), in $\mu\text{mol}/\text{m}^2/\text{s}$, was introduced as a more accurate method for measuring PAR, assuming that photons of B and R wavelengths drive the same amount of photosynthesis (McCree, 1972). Although in some cases the spectral response of photosynthesis did not follow the McCree curve (Barnes et al., 1993; Hogewoning et al., 2012; Kume, 2017), these are beyond the scope of this thesis, but are summarised in some excellent reviews (Krizek, 2004; Amthor, 2010; Wu et al., 2019). In contrast to photosynthesis, photomorphogenesis is regulated by specialised chromoproteins, or photoreceptors, that induce a downstream signal transduction cascade in response to light (Galvão and Fankhauser, 2015). Each class of photoreceptors is activated by a specific range of wavelengths (**Table 1**), and this specificity is determined by the characteristic absorption spectrum of the photosensory domain or photopigment, consisting of an amino acid sequence that binds to a chromophore (Briggs and Christie, 2002; Nagy and Schäfer, 2002; Lin and Shalitin, 2003; Li et al., 2013). Three distinct families of photoreceptors are sensitive to B light: the cryptochromes (CRYs) (Wang et al., 2018), the phototropins (PHOTs) and the Zeitelupes (ZTLs) (Suetsugu and Wada, 2013). The phytochrome (PHY) family responds mainly to R and FR light, although some sensitivity to B light has also been reported (Legris et al., 2019). Finally, the *UV RESISTANCE LOCUS8* (UVR8) photoreceptor responds to UV-B light (Yin and Ulm, 2017).



Phytochromes (PHYs)

In the early 1950s, the observation by Borthwick and colleagues that the germination of lettuce seeds was promoted by R light and inhibited or reversed by FR light (Borthwick et al., 1952) suggested the presence of a photo-reversible pigment in plants which was later isolated and identified as “phytochrome” (Sage, 1992). In the 1980s, the first *PHY* gene sequence was published (Hershey et al., 1985). Since then, members of the *PHY* family have been identified in many plant species, and even in prokaryotes and fungi (Li et al., 2015; Rockwell and Lagarias, 2020). PHYs consist of an N-terminal photosensory region that covalently binds the chromophore phytychromobilin tetrapyrrole (PΦB), and a C-terminal histidine kinase-related domain (HKRD) that is required for dimerisation (Burgie and Vierstra, 2014) (**Figure 1**). In the cytoplasm, PHYs occur in two photo-interconvertible conformations, an R-absorbing form (Pr) which is considered biologically inactive, and an FR-absorbing, biologically active form (Pfr) (Legris et al., 2019). The crystal structure of Pr shows that these conformational changes in the protein structure are a result of chromophore isomerisation (Burgie et al., 2014). This mode of action is referred to as low fluence response (LFR) and suggests that PHYs act as modular switches that are mostly activated by R light and deactivated by FR light (Franklin and Quail, 2010). PHYs can be classified into either Type I PHYs, which are activated by FR light, or Type II PHYs, which are activated by R light. Type II PHYs follow the LFR described above, whereas Type I PHYs respond to low amounts of any wavelength (very low fluence response (VLFR)) or by continuous irradiation with high intensity FR light (high irradiance response (HIR)) (Shinomura et al., 2000). In *Arabidopsis*, PHYA



(Type I) and PHYB-E (Type II) have roles in many developmental processes, including seed germination, de-etiolation, shade avoidance and floral transition (Galvão and Fankhauser, 2015). Many of these developmental responses are initiated by translocation of PHYs into the nucleus after their photoactivation (Kevei et al., 2007). Nuclear translocation of photoactivated PHYA requires two homologous chaperone proteins: FAR-RED ELONGATED HYPOCOTYL 1 (FHY1) and FHY1-LIKE (FHL). PHYA directly interacts with these chaperones and utilises their nuclear localisation signals (NLS) to reach the nucleus (Hiltbrunner et al., 2006). In Type II PHYs, putative NLS might be exposed after conversion of Pr to Pfr (Chen et al., 2005), but so far no canonical NLS sequences have been identified, suggesting that nuclear translocation of Type II PHYs relies on chaperone proteins as well (Pfeiffer et al., 2012). After nuclear import, PHYs accumulate into subnuclear foci called nuclear bodies (NBs) or speckles (Kircher et al., 2002). For PHYA and PHYB, interactions with the PHYTOCHROME-INTERACTING FACTOR (PIF) transcription factors are required for the formation of NBs. For PHYC-E, this process is not yet elucidated, although it is clearly independent of PIFs (Klose et al., 2015). Inside NBs, PHYA interacts with PIF1 and PIF3 (Huq et al., 2004; Al-Sady et al., 2006) whereas PHYB has been shown to interact with all members of the PIF family. These interactions lead to PIF phosphorylation and their subsequent degradation, altering gene expression, and ultimately leading to physiological responses (Pham et al., 2018) (**Figure 2**). Aside from PHY-PIF interactions, photoactivated PHYs can suppress the activities of CONSTITUTIVE PHOTOMORPHOGENIC 1 (COP1) and the COP9 signalosome (CSN), and thereby induce accumulation of several photomorphogenesis-promoting transcription factors, including



ELONGATED HYPOCOTYL 5 (HY5), HY5 HOMOLOGUE (HYH), LONG HYPOCOTYL IN FAR-RED (HFR1), and LONG AFTER FAR-RED LIGHT (LAF1) (Osterlund et al., 2000; Soo Seo et al., 2003; Duek et al., 2004) (**Figure 2**). Moreover, several studies also identified interactions between PIFs and COP1 or SUPPRESSOR OF PHYA1 (SPA1) repressors suggesting that regulation of gene transcription by PHYs is highly controlled and complex (Dong et al., 2014, 2015; Xu et al., 2014).

Cryptochromes (CRYs)

Shortly after the identification of PHYs, the first B light-responsive photoreceptors were described. One of these pigments was first identified in *Arabidopsis* as *ELONGATED HYPOTOCOTYL 4* (HY4), named after its phenotype that was specific for B light only (Ahmad and Cashmore, 1993). Based on its protein structure, HY4 was first thought to be a DNA photolyase, which catalyses B light-dependent repair of DNA lesions that result from UV damage in many other organisms. However, it was later found that HY4 lacks any photolyase activity (Malhotra et al., 1995), and instead binds to a flavin adenine dinucleotide (FAD) (Lin et al., 1995a), which strongly suggested that HY4 was in fact a CRY and thus renamed CRY1 (Lin et al., 1995b). A second CRY (*CRY2*) was identified by screening an *Arabidopsis* mutant population (Lin et al., 1996), and finally a third family member (*CRY3*) was identified through gene sequencing and phylogenetic analysis (Brudler et al., 2003; Kleine et al., 2003). In contrast to other photoreceptors, CRYs are found to be highly conserved and present across all kingdoms of life (Lin and Todo, 2005; Mei and Dvornyk, 2015).



Chapter 1: General introduction

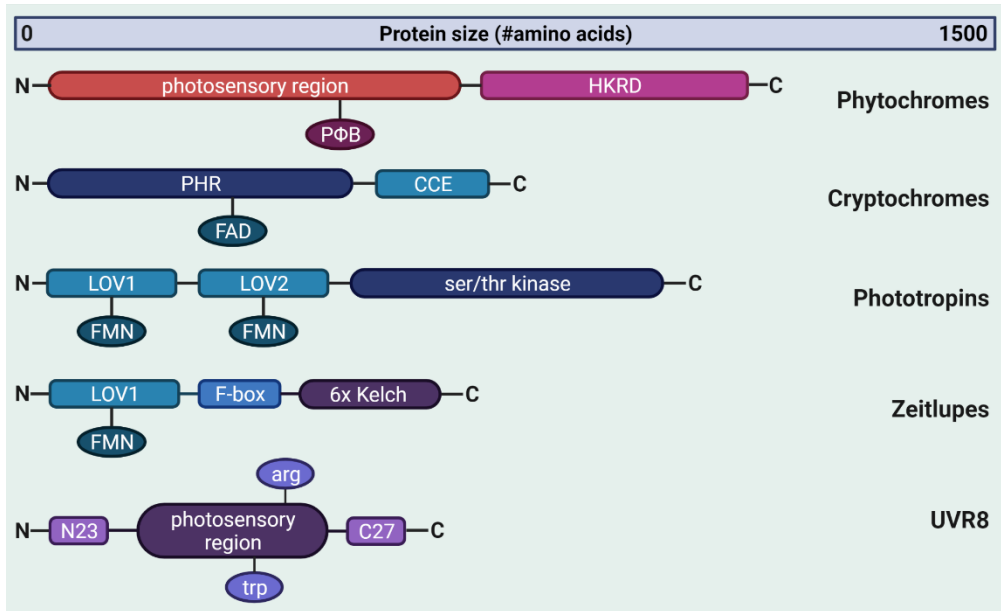


Figure 1: Protein domains in photoreceptors.

Schematic representation of the protein structures of different photoreceptor families. PHYs consist of an N-terminal photosensory region that covalently binds the PΦB chromophore, and a C-terminal histidine kinase-related signalling domain (HKRD) that is required for dimerisation and protein interactions. After photoactivation, PHYs are transported to the nucleus with the help of chaperone proteins, or via a yet to be identified nuclear localisation signal (NLS) in the active Pfr conformation. CRYs consist of an N-terminal Photolyase Homologous Region (PHR) domain bound to the fully oxidised cofactor flavin adenine dinucleotide (FAD) and a CRY C-terminal Extension (CCE) domain. The PHR domain is required for homo-dimerisation and CIB interaction, while the CCE effector domain is required for protein interactions and nuclear transport. The chromophore of PHOTs consists of two N-terminal LOV domains bound to the FMN cofactor and is linked to the C-terminal ser/thr kinase domain that phosphorylates downstream targets. Zeitzlupe (ZTL) chromophores contain only one LOV-FMN domain linked to an F-box domain and to six Kelch repeats. UVR8 consists of an N-terminal NLS N23 and a C-terminal interaction domain C27. Its photosensory region comprises a chromophore consisting of three tryptophan (trp triad) residues and arginine (arg) residues for homodimerisation.



Therefore, CRYs and photolyases can be subdivided into five groups: cyclobutane pyrimidine dimer (CPD) photolyases, (6–4) pyrimidine–pyrimidone adduct [(6–4) photoproduct] photolyases, cry-DASH proteins, animal CRYs and plant CRYs (Mei and Dvornyk, 2015). Many excellent reviews about animal and prokaryotic CRYs (Losi and Gärtner, 2017; Michael et al., 2017) have been published but these are beyond the scope of this thesis. In land plants, CRY1 and CRY2 function as photoreceptors, whereas CRY3 resembles a DASH-type CRY that is thought to act as a B light-activated single-stranded DNA-repair enzyme inside mitochondria and chloroplasts (Pokorny et al., 2008). The photoreceptors CRY1 and CRY2 function as dimers (Sang et al., 2005; Yu et al., 2007) with monomers that consist of two major domains: an N-terminal Photolyase Homologous Region (PHR) domain and a diverged CRY C-terminal Extension (CCE) domain. The PHR domain binds to the fully oxidised FAD (Brautigam et al., 2004) (**Figure 1**). Upon absorption of B light, an electron transfer from tryptophan (trp) to tyrosine residues reduces the chromophore of CRY1 *in vitro*, resulting in conformational modifications in the FAD domain (Giovani et al., 2003). However, mutations of trp-triad residues in CRY2 did not decrease its photoactivation *in vivo* (Li et al., 2011), suggesting another mechanism for photoactivation of CRYs. Similar to PHYs, photoactivated CRYs can alter gene expression directly and indirectly. CRY1 interacts with SPA1, thereby mediating suppression of the COP1-dependent degradation of the photomorphogenesis-promoting transcription factors HY5, HYH, and HFR1 (Lian et al., 2011). Similarly, photoactivated CRY2 suppresses COP1-dependent protein degradation of the flowering-promoting CONSTANS (CO) (Liu et al., 2008). Moreover, the PHR domain of CRY2 binds to the N-terminal



domain of the transcription factor CRY2-INTERACTING bHLH 1 (CIB1) resulting in heterodimerisation of CIB1 with CIB3, CIB4 and CIB5 to activate *FLOWERING LOCUS T* (*FT*) transcription (Liu et al., 2013) (**Figure 2**). Aside from COP1/SPA1 complexes and CIBs, PHYs and PIFs have also been identified as CRY-binding proteins (Mas et al., 2000; Pedmale et al., 2016), suggesting synergy between R/FR and B light responses, and thus adding another layer of complexity to light signalling pathways.

Phototropins (PHOTs)

Although plant bending responses to unidirectional light were already documented by Charles Darwin in the 19th century (Darwin et al., 1880), it took more than a hundred years to identify the photoreceptors responsible for this phenomenon. While auxin, the key phytohormone in phototropism, was identified already early in the 20th century (Went, 1926), the PHOTs were only identified at the end of the 20th century. In 1989, a genetic screen in *Arabidopsis* for mutants defective in phototropic growth identified the *JK224* mutation (Khurana and Poff, 1989), which was later renamed to *non-phototropic hypocotyl 1* (*nph1*) (Liscum and Briggs, 1995). Cloning and sequencing of the *NPH1* gene showed that it encodes a plasma membrane-associated protein with two light, oxygen, or voltage (LOV) domains in the N-terminal half and a ser/thr protein kinase in the C-terminal half (Hanks and Hunter, 1995; Briggs et al., 2001a), suggesting that autophosphorylation was the initial step in the signalling pathway (Huala et al., 1997). When expression of the NPH1 protein in insect cells confirmed its light-dependent autophosphorylation, the protein was renamed to PHOT1 after its role in the regulation of phototropism (Christie et al., 1998, 1999). Among other loci



involved in phototropism, *NPH1-like 1* (*NPL1*) was identified in *Arabidopsis* with 67% similarity to *PHOT1* (Jarillo, 1998), and based on its function and the similar structure of the encoded protein the gene was renamed to *PHOT2* (Briggs et al., 2001a). The LOV domains bind the cofactor flavin mononucleotide (FMN) and together form the chromophore (Christie et al., 1999) (**Figure 1**). Photoactivation of this chromophore triggers conformational changes that liberate the C-terminal kinase domain resulting in fluence-dependent autophosphorylation of residues in both their sensory and kinase domains (Christie et al., 1998; Sakai et al., 2001). PHOTs regulate chloroplast movement and phototropism in a fluence-dependent manner, where PHOT1 is activated at both low and high light intensities, while PHOT2 only responds to high fluence rates (Inada et al., 2004). Since autophosphorylation requires more photons than are needed to induce PHOT-mediated responses, it is likely that autophosphorylation is not the main mechanism of PHOT signalling (Briggs et al., 2001b). Possibly low/intermediate fluence phosphorylation sites are important for signalling, whereas high fluence autophosphorylation sites are involved in receptor desensitisation (Salomon et al., 2003). In their inactive state, PHOTs are tightly associated with the plasma membrane. Upon photoactivation, autophosphorylation is believed to be required for plasma membrane dissociation and targeting of PHOT1 to the cytoplasm (Wan et al., 2008) and of PHOT2 to the Golgi apparatus (Kong et al., 2006). In the last decades, more and more downstream targets of PHOTs have been identified. Both *Arabidopsis* PHOTs have been shown to enhance cytosolic calcium increase that might act as an intermediate signalling component (Harada et al., 2003; Zhao et al., 2013). Furthermore, phototropism studies led to the discovery of PHOT1-interacting proteins: NON-PHOTOTROPIC



HYPOCOTYL 3 (NPH3), ROOT PHOTOTROPISM 2 (RTP2), and ATP-BINDING CASSETTE B19 (ABCB19) (Motchoulski and Liscum, 1999; Sakai et al., 2000; Lariguet et al., 2006; Christie et al., 2011). Moreover, RTP2 phosphorylation by PHOT1 is also required for stomatal opening (Inada et al., 2004). So far, PHOT2 has been shown to interact with PROTEIN PHOSPHATASE 2A (PP2A) and 14-3-3 λ (Tseng and Briggs, 2010; Tseng et al., 2012) (**Figure 2**). Additionally, PHOTs have been shown to interact with components of R/FR light signalling. For example, PHYA binds to PHOT1 at the plasma membrane where it likely enhances phototropic growth (Jaedicke et al., 2012), and PHYTOCHROME KINASE SUBSTRATE 1 (PKS1) and PKS2 bind PHOTs during phototropism to control leaf positioning and flattening (Lariguet et al., 2006; Boccalandro et al., 2008; de Carbonnel et al., 2010).

Other photoreceptors in land plants

Alongside the PHOTs, land plants have another family of LOV domain-containing B-light receptors: the ZEITLUPE (ZTL) family, named after its founding member. The three members of this family, *ZTL*; *FLAVIN-BINDING KELCH REPEAT 1 (FKF1)* and *LOV KELCH PROTEIN 2 (LKP2)*, were first identified in genetic screens for period length *Arabidopsis* mutants (Nelson et al., 2000; Somers et al., 2000; Schultz et al., 2001) and contain one FMN-binding LOV domain for photoreception together with an F-box domain and six Kelch repeats (Ito et al., 2012) (**Figure 1**). F-box proteins are typically components of Skp, Cullin, and F-box (SCF)-type ubiquitin E3 ligases, and ZTLs were found to participate in light-regulated proteolysis of circadian clock-associated proteins including TIMING OF CAB EXPRESSION 1

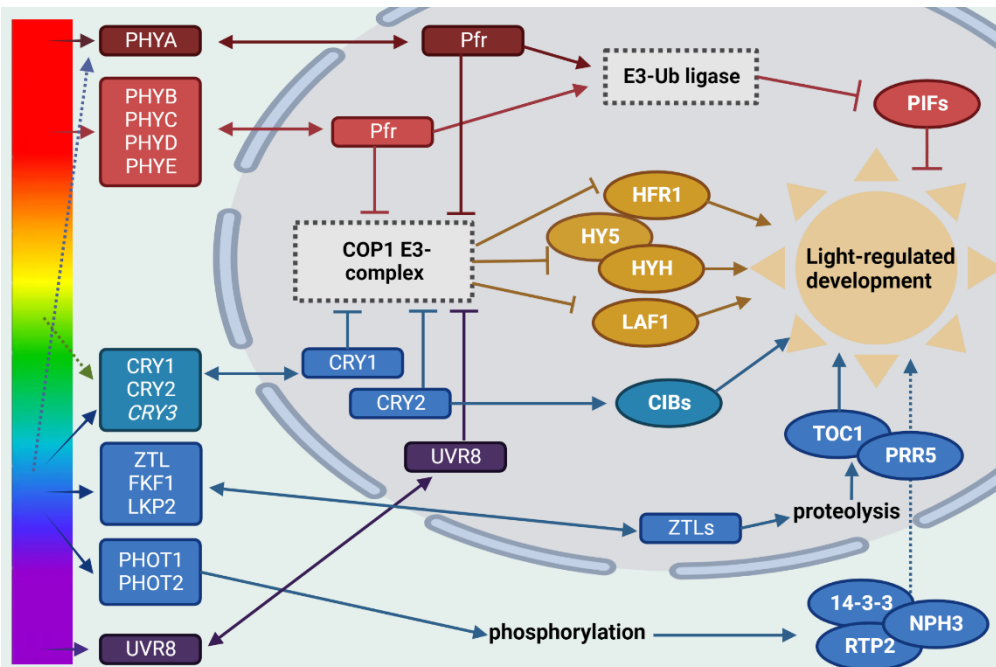


Figure 2: Signal transduction pathways of Arabidopsis photoreceptor families.

FR/R light: PHYA is activated by FR light and to some extent by B light, whereas PHYB to PHYE are activated by R light. In their active conformation, PHYs (Pfr) move to the nucleus where they inhibit the COP1 E3-complex, resulting in the accumulation of transcription factors such as HFR1, HY5 and LAF1. In addition, photoactivated PHYA and PHYB promote the ubiquitination and degradation of PIFs that repress light-regulated development. **B light:** CRYs, PHOTs, and ZTLs are all activated by B light, and CRYs to some extent by green light. Upon photoactivation, CRYs move to the nucleus where they inhibit the COP1 E3-complex to regulate photomorphogenesis. In addition, CRY2 binds to CIB transcription factors to promote flowering. PHOT signalling relies on (auto)phosphorylation. PHOTs are known to phosphorylate 14-3-3 proteins, NPH3 and RTP2 that ultimately influence phototropism and stomatal opening. Photoactivated ZTLs move to the nucleus where their F-box domains target various circadian clock proteins such as TOC1 and PRR5 for degradation by the 26S proteasome. **UV-B light:** UVR8 is activated by UV-B light. Upon its activation, UVR8 moves to the nucleus and binds COP1 to inhibit its activity, resulting in stabilisation of transcription factors such as HY5/HYH.



Chapter 1: General introduction

(TOC1) and its homolog PSEUDO-RESPONSE REGULATOR 5 (PRR5) by the 26S proteasome (Más et al., 2003; Kiba et al., 2007; Harmon et al., 2008; Gil et al., 2017) (**Figure 2**). Moreover, it has been shown that ZTL indirectly controls PRR9 protein levels, and the interaction between TOC1 and PRR3 (Fujiwara et al., 2008). By controlling protein levels, ZTLs not only regulate the timing of circadian events throughout the day, but also photoperiodic timing of flowering (Song et al., 2013; Serrano-Bueno et al., 2017). A last class of plant photoreceptors responds to UV-B radiation. UV-B (280-315 nm) is a small fraction of the solar spectrum that is potentially harmful to any organism that is exposed to sunlight. Even though solar light only contains 0.5% UV-B radiation (Blumthaler, 1993), these photons are highly energetic and can be absorbed by a number of biologically active components, including nucleic acids, ultimately leading to DNA damage. A well-known defect in animals resulting from UV-B-induced DNA damage is the induction of cancerous melanoma cells. However, plants can be exposed to UV-B radiation at substantial levels with hardly any DNA damage occurring in the cells. This UV-B tolerance is a result of a signalling pathway that is initiated when UV-B is perceived by its receptor UVR8 (Kliebenstein et al., 2002). Rather than depending on a cofactor chromophore, UVR8 uses a triad of closely packed trp residues (W233, W285 and W337) to perceive light (Di Wu et al., 2012) (**Figure 1**). At low levels of UV-B radiation, UVR8 exists as a homodimer bound by hydrogen bonds facilitated by arginine (arg286 and arg338) (Tilbrook et al., 2013). Upon UV-B exposure, these homodimers undergo rapid monomerisation, a process that depends on conformational changes in the light-perceiving trp residues (Rizzini et al., 2011). UVR8 monomers bind to the WD40 domain of COP1 to stabilise the HY5 and HYH transcription



factors, which ultimately alter gene expression (Brown and Jenkins, 2008; Favory et al., 2009; Yin et al., 2015) (**Figure 2**). These UV-B responsive genes include proteins involved in UV protection such as antioxidants and photolyases (Tilbrook et al., 2013). Furthermore, WD40-repeat proteins REPRESSOR OF UV-B PHOTOMORPHOGENESIS (RUP)1 and RUP2 are among the target genes that facilitate negative feedback of the UV-B signalling pathway by directly inactivating UVR8 (Gruber et al., 2010; Heijde and Ulm, 2013). In addition to R, FR, B, and UV-B light, it has been suggested that green sensory mechanisms monitor and adjust plant growth and development (Folta and Maruhnich, 2007; Wang and Folta, 2013). Although 10-50% of the green light is reflected by chloroplasts, the remaining photons are absorbed for photosynthesis, or for activation of CRYs or putative green light photoreceptors, suggesting that green light may be important for optimal plant performance (Terashima et al., 2009; Smith et al., 2017). Altogether, the different photoreceptor families influence many, if not all, developmental processes in land plants. Next, we discuss the interplay between light signalling and hormonal pathways during early plant development.

Seedling emergence: Transition from darkness to light

During seed germination, plant embryos mature from being heterotrophic (dependent on seed reserves) to fully photoautotrophic seedlings. When germination occurs in the absence of light (e.g. in the soil), seedlings undergo a developmental process that is characterised by rapid hypocotyl elongation, little root development, and the formation and maintenance of an apical hook that protects the shoot apical meristem (SAM) while the seedling shoot grows through the dark soil. These traits are collectively referred to as



Chapter 1: General introduction

skotomorphogenesis, or etiolation, and aid seedling shoots to rapidly emerge into the light (Arsovski et al., 2012; Armarego-Marriott et al., 2020). During skotomorphogenesis, the limited energy resources of the seed reserves are mainly allocated to the hypocotyl to achieve rapid seedling emergence. As a result, root development is delayed until the cotyledons have expanded and are photosynthetically active. Addition of sucrose to etiolated seedlings promotes root development in darkness, suggesting that lack of energy resources (or sugar signalling), and not direct photoreceptor signalling, is the main cause for short roots in etiolated seedlings (Kircher and Schopfer, 2012). In contrast, hypocotyl elongation and apical hook formation have been shown to be directly regulated by downstream signalling of photoreceptors (Arsovski et al., 2012; Mazzella et al., 2014). Skotomorphogenesis results from PHY- and CRY-dependent degradation of transcription factors such as HY5 and HYH via the COP1-SPA E3 ubiquitin ligase complex (Osterlund et al., 2000). As a result, HY5 and HYH no longer suppress auxin signalling, thus creating auxin maxima that enhance hypocotyl growth (Sibout et al., 2006) (**Figure 3A**). In addition, maintenance of skotomorphogenic growth is regulated by various PIFs that are stable in the dark and degraded after seedling emergence into the light (Leivar et al., 2008). During skotomorphogenesis, ethylene (ET) balances hypocotyl elongation through ETHYLENE-INSENSITIVE 3 (EIN3), which enhances expression of *ETHYLENE RESPONSE FACTOR 1* (*ERF1*) that inhibits hypocotyl growth in darkness. (Zhong et al., 2012). (**Figure 3A**). Finally, seedling emergence is enhanced by gravitropism and PHOT-mediated phototropism which aids the seedlings to efficiently direct their growth upwards and towards the light source (Masson et al., 2002; Christie and Murphy, 2013). After emergence, light exposure initiates a new developmental

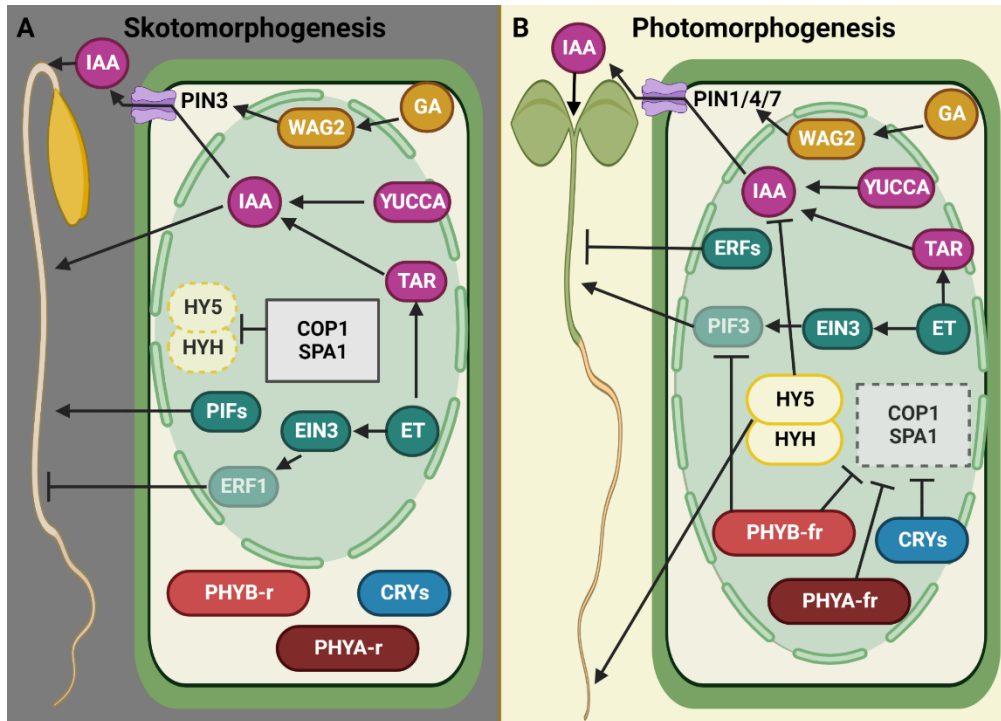


program referred to as photomorphogenesis, or de-etiolation, that causes hypocotyl growth arrest, unfolding of the apical hook and induction of root development (Arsovski et al., 2012; Armarego-Marriott et al., 2020). During photomorphogenesis, COP1-dependent degradation of HY5 and other transcription factors is relieved, resulting in their accumulation (Osterlund et al., 2000). Downstream targets of HY5 include signalling components of the phytohormones auxin, cytokinin (CK), ET, brassinosteroids (BR), gibberellic acid (GA) and jasmonic acid (JA), making this transcription factor a key integrator of light signalling and hormonal pathways (Zhang et al., 2011). HY5 inhibition of auxin signalling, along with accumulation of light-stable ERFs, cause the hypocotyl growth arrest that characterises photomorphogenesis (Zhong et al., 2012). Similar to skotomorphogenic growth, ET balances the hypocotyl growth arrest via EIN3. By EIN3-mediated stabilisation of *PIF3* expression, hypocotyl growth is promoted in the light (Sibout et al., 2006; Zhong et al., 2012; de Wit et al., 2016) (**Figure 3B**). Apical hook formation, maintenance and opening rely on asymmetrical cell growth at opposite sides of the hypocotyl regulated by the phytohormone auxin (Mazzella et al., 2014). The mechanism that underlies this asymmetrical cell growth is the establishment of local auxin maxima in the cortex and epidermal cells through a combination of auxin biosynthesis and polar auxin transport (PAT) (Žádníková et al., 2010). Mutations in auxin biosynthesis genes of the *YUCCA* (*YUC*) and *TRYPTOPHAN AMINOTRANSFERASE OF ARABIDOPSIS1* / *TRYPTOPHAN AMINOTRANSFERASE RELATED* (*TAA1/TAR*) families impair hook development (Zhao et al., 2001; Stepanova et al., 2005). Moreover, chemical inhibition of the PIN-FORMED (PIN) auxin transporters that drive PAT by 1-naphthylphthalamic acid (NPA) resulted in a reduced



Chapter 1: General introduction

hook, confirming that PAT is required for hook formation (Žádníková et al., 2010). Auxin synthesised in the apical part of the seedling is transported through the stele towards the root by the PIN1 auxin efflux carriers and assisted by the AUXIN RESISTANT 1 (AUX1) auxin influx carrier. Expression studies revealed an important role for PIN3 in apical hook formation by redistributing auxin to create an auxin maximum on the inner (concave) side of the hypocotyl (**Figure 3A**). In contrast, during the transition from apical hook maintenance to opening, PIN1, PIN4 and PIN7 that are expressed at the inner cell layers of the hook redistribute auxin towards the stele (Vandenbussche et al., 2010; Žádníková et al., 2010) (**Figure 3B**). Auxin





signalling is initiated by binding of auxin to co-receptor complexes that consist of a TRANSPORT INHIBITOR RESPONSE 1 / AUXIN BINDING F-BOX PROTEIN (TIR1/AFB) and an AUXIN / INDOLE-3-ACETIC ACID PROTEIN (AUX/IAA). This results in the subsequent ubiquitination and degradation of the AUX/IAA repressors, thereby releasing AUXIN RESPONSE FACTORS (ARFs) that activate the expression of auxin-responsive genes, ultimately leading to asymmetrical growth (Leyser, 2018). Finally, this process is enhanced by interaction with other hormonal pathways. The AGC-3 kinase WAG2 connects GA (and light) signalling to the auxin gradient. GA (and darkness) lead to PIF5 accumulation which induces WAG2

Figure 3: Hormonal regulation of skoto- and photomorphogenesis.

A. Skotomorphogenesis is characterised by a short root, an elongated hypocotyl, and an apical hook. Auxin signalling (pink) that results from degradation of HY5 and HYH by the COP1-SPA1 E3 complex, and dark-stable PIFs, promote hypocotyl elongation. In contrast, ET (green) inhibits hypocotyl growth in darkness through its transcriptional activation of the light-stable ERF1 via EIN3. Apical hook formation and maintenance is directly regulated by auxin biosynthesis and transport and indirectly by GA (orange) and ET signalling. Auxin efflux via PIN3, assisted by PIN4 and PIN7, results in an auxin maximum on the inner (concave) side of the hypocotyl, leading to hypocotyl bending. **B.** After exposure to light, the developmental program of photomorphogenesis is initiated, leading to inhibition of hypocotyl elongation, promotion of root growth and unfolding of the apical hook. Photoactivated PHYs and CRYs move to the nucleus where they inhibit the COP1-SPA1 E3 complex, resulting in stabilisation of the photomorphogenesis-promoting HY5 and HYH. Hypocotyl growth arrest results from HY5/HYH inhibition of auxin signalling and from light-stable ERFs that inhibit hypocotyl growth. In contrast, ET promotes hypocotyl growth in light through its transcriptional activation of the dark-stable PIF3 via EIN3. During opening of the apical hook, PIN1, PIN4 and PIN7 alleviate the asymmetric auxin distribution in the hypocotyl.



expression. By phosphorylating the central intracellular loop of PIN1, PIN3, PIN4, and PIN7 proteins, WAG2 in turn regulates PAT to maintain the apical hook (Willige et al., 2012). In addition, ET influences auxin biosynthesis and transport at the inner side of the hook by upregulation of *TAR2*, *AUX1*, *LAX1*, *PIN1*, *PIN3*, *PIN4* and *PIN7* (Vandenbussche et al., 2010; Žádníková et al., 2010) (**Figure 3**).

Light-directed seedling development

After seedlings emerge from the soil, the apical hook unfolds, and cotyledons expand. As a result, the SAM is now exposed to light and the seedling has become fully photoautotrophic. However, when seedlings are growing under a canopy of other plants, they have to compete with these other plants for light in order to avoid overall delays in growth (Weiner, 1985). To keep up with their competition, plants channel their energy resources to apical elongation, at the expense of other tissues. In seedlings, this leads to elongated hypocotyls, hyponastic leaves, and reduced leaf lamina size, whereas older plants show elongated stems, petioles, or internodes, reduced leaf surface area and early flowering. Collectively these traits are referred to as the shade avoidance syndrome (Courbier and Pierik, 2019). The most widely studied trait of the shade avoidance syndrome is the elongated hypocotyl. Whereas hypocotyl growth during skotomorphogenesis is dependent on ET signalling, shade-induced hypocotyl elongation relies mainly on auxin. Initially, shade is detected by PHYs that monitor R:FR ratios. Sunlight reaches the top of the canopy with a high R:FR ratio where the green leaves absorb R light and reflect FR light. As a result, the R:FR ratio in the shade below the canopy is lower (Ballaré et al., 1990). The main sensor for changes in the R:FR ratio is PHYB,



while PHYC-E play minor roles in shade avoidance. In high R:FR ratios, PHYB is abundant in its active Pfr state that translocates to the nucleus where it inactivates PIF4, PIF5 and PIF7 (Buti et al., 2020) (**Figure 4A**). In contrast, in low R:FR ratios, PHYB is mainly abundant in its inactive Pr state, resulting in PIF stabilisation and subsequently into PIF-mediated changes in gene transcription. Accumulation of PIF4, PIF5 and PIF7 promotes transcription of *YUC*, *AUX/IAA* and *PIN* genes, ultimately leading to auxin-mediated hypocotyl elongation in shade (Lorrain et al., 2008; Leivar et al., 2012; Li et al., 2012a; Buti et al., 2020) (**Figure 4B**). Once the seedling has reached the top of the canopy, the SAM is fully exposed to all wavelengths within the solar spectrum. Subsequently, the SAM grows to its mature size to start the formation of new leaf primordia. During seedling development only a few first leaves are initiated in the SAM that will enhance the availability of sugars through photosynthesis. After formation of these first leaves, the higher level of available sugars activates the root apical meristem (RAM). In fact, studies with decapitated seedlings showed that cotyledon-derived sugars are essential for the initiation of root growth (Kircher and Schopfer, 2012). Furthermore, these sugars can act as shoot-to-root signals resulting in the upregulation of nutrient transporters within the root to optimise seedling growth (Lejay et al., 2008) (**Figure 4C**). However, shoot-to-root sugar signalling is a slow process since it requires both photosynthesis and sugar biosynthesis. Therefore the role of shoot-to-root signalling via sugars is likely to be subordinate to other more rapid light-induced shoot-to-root signals. Likely candidates for this are transcription factors that are downstream photoreceptor targets. Recently, HY5 was identified as a mobile signal that travels to the root upon photoreceptor activation in the shoot. Moreover, it was shown that upon arrival in the root,



Chapter 1: General introduction

HY5 promotes root growth and nitrate uptake (Chen et al., 2016) (**Figure 4C**). Aside from mobile transcription factors such as HY5, phytohormones have been shown to move from shoot-to-root to modulate root growth. Auxin that is produced in the shoot is transported to the root via the vascular cylinder in two ways: bulk transport of auxin via the phloem that is unloaded in the root apex by AUX1 (1), and auxin carrier-mediated transport that relies mainly on PIN proteins (2) (Casson and Lindsey, 2003). While *PIN1*, *PIN3* and *PIN7* are all expressed in hypocotyls, PIN1 has been shown to be the main efflux carrier for light-driven shoot-to-root auxin transport (Keuskamp et al., 2010; Sassi et al., 2012). Within the root, auxin accumulates in the quiescent centre (QC) of the RAM where primary root growth is tightly controlled by auxin and CK interplay. In the QC, auxin acts antagonistically with CK, to maintain a balanced stem cell pool. In addition, CK influences the auxin gradient to create auxin maxima that induce primary root growth. However, when the auxin levels in the RAM become too high, primary root growth is inhibited (Thimann, 1937). Next, basipetal transport of auxin (from the tip towards the base of the root) controls gravitropism and the outgrowth of lateral root primordia in the elongation zone (Rashotte et al., 2000; Casimiro et al., 2001). Within the elongation zone of the root, auxin and CK regulate the initiation and outgrowth of lateral root primordia (Jing and Strader, 2019) (**Figure 4D**). Aside from auxin, it has been reported that a biologically inactive form of GA, GA₁₂, travels from shoot to root where it is converted into the active forms GA₂₀- and GA₃-oxidases that ultimately stimulate root growth (Regnault et al., 2015). However, it remains unclear whether or not GA₁₂ transport is light-dependent. In summary, mobile signals (sugars, HY5, auxin and other yet to



be identified molecules) travel from shoot-to-root to influence root development in a light-dependent manner.

Light-regulated initiation and outgrowth of lateral organs.

After the seedling stage, early plant development shifts from only apical growth to the formation of lateral organs to enhance nutrient uptake and photosynthetic capacity. In many plant species, new shoot organs are initiated in the SAM following a Fibonacci spiral pattern, which allows for optimal light capture (Strauss et al., 2020). To ensure proper phyllotaxis, a tight balance between proliferation and differentiation of meristem cells is required. Within the central zone (CZ) at the tip of the SAM, proliferation of pluripotent stem cells is tightly controlled by a feedback loop between WUSCHEL (WUS) and CLAVATA (CLV) proteins (Schoof et al., 2000). The homeobox transcription factor WUS, which is required for specification of stem cell identity, is expressed in the organizing centre (OC) within the rib zone (RZ) of the SAM (Mayer et al., 1998) (**Figure 5A, B**). WUS moves upwards to the CZ via plasmodesmata, where together with another homeobox protein SHOOT MERISTEMLESS (STM), it induces expression of the *CLV3* gene in stem cells (Brand et al., 2002; Daum et al., 2014). Subsequently, CLV3 peptides are secreted from the stem cells and are perceived by a CLV1/CLV2 receptor kinase complex in the OC to repress WUS activity, thus creating a negative feedback loop that is required for stem cell homeostasis (Brand et al., 2000) (**Figure 5B**). In addition, WUS levels are controlled by either CLV-dependent or CLV-independent CK signalling (Gordon et al., 2009). CKs and their precursors are mainly synthesised within the root and loaded by ATP-BINDING CASSETTE G14 (ABCG14) into the xylem through which they

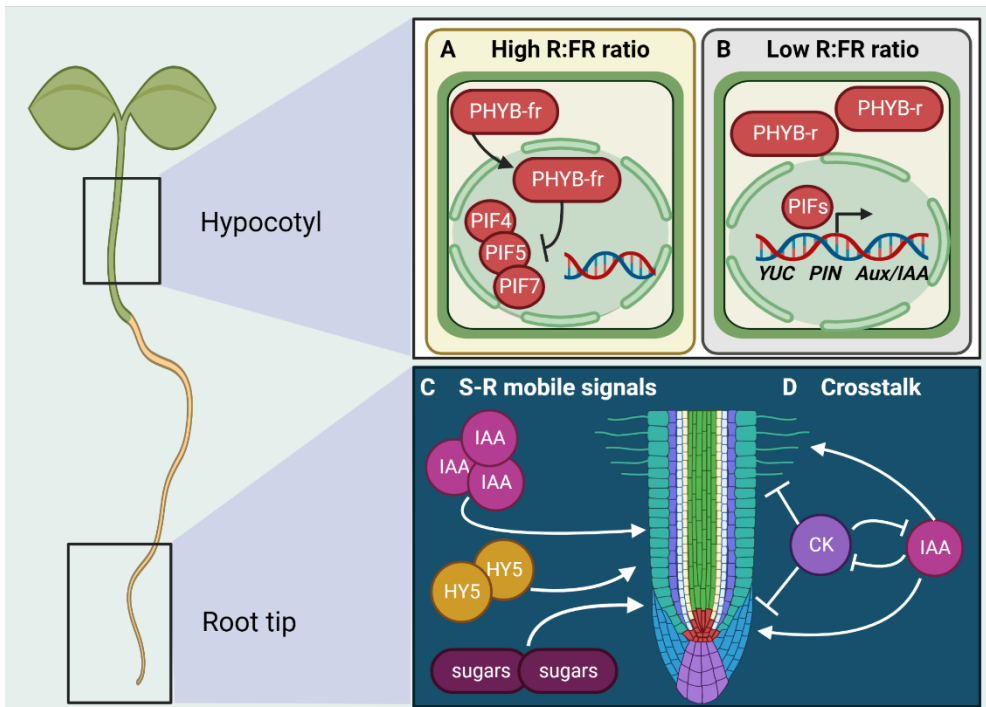


Figure 4: Light-directed hypocotyl and root development in seedlings.

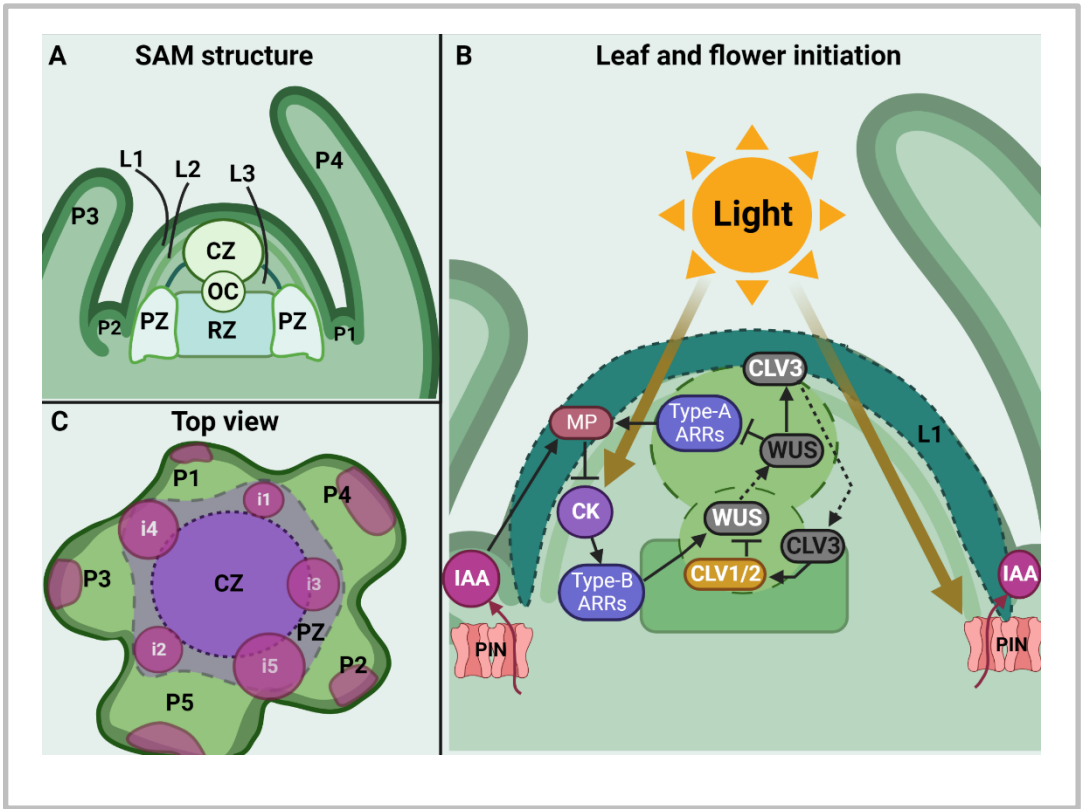
In order for seedlings to optimise their photosynthetic capacity, the shoot needs to be exposed to light. **A.** In light conditions with high R:FR ratios, PHYB is activated (PHYB-fr) and moves to the nucleus where it induces the degradation of the bHLH transcription factors PIF4, PIF5 and PIF7. **B.** Shade reduces the R:FR ratio and induces the shade avoidance response. Due to the low R:FR ratio, PHYB proteins are kept in the inactive state (PHYB-r) and remain in the cytosol. This results in nuclear accumulation of PIF4, PIF5 and PIF7 that promote expression of auxin biosynthesis genes (*YUC*), transporters (*PIN*) and downstream signalling targets (*Aux/IAAs*), ultimately resulting in hypocotyl growth. **C.** Sugars available from photosynthesis in the shoot travel to the root to activate the RAM and promote root growth and nutrient uptake. Further root development depends on the shoot-to-root (S-R) transport of other mobile signals such as HY5 and auxin (IAA). Upon light detection in the shoot, both molecules travel to the root where they enhance root growth and nutrient uptake. **D.** Furthermore, auxin acts antagonistically with CK to control the size of the stem cell pool in the QC, and the formation and outgrowth of lateral root primordia.



travel to the shoot and accumulate in the OC (Ko et al., 2014; Zhang et al., 2014). Within the OC, CK signalling results in elevated *WUS* expression via type-B ARABIDOPSIS RESPONSE REGULATOR (ARR) 1, ARR10 and ARR12 (Meng et al., 2017; Xie et al., 2018). Moreover, *WUS* represses expression of type-A *ARR5*, *ARR6*, *ARR7* and *ARR15*, which are important for negative feedback of CK signalling, to further enhance CK-mediated stem cell proliferation (Leibfried et al., 2005) (**Figure 5B**). Finally, the interplay between *WUS*-*CLV* and CK is regulated by tissue-specific HECATE (*HEC*) transcription factors (Schuster et al., 2014). When stem cells divide in the CZ, their daughter cells move outwards to the peripheral zone (PZ) where new organ primordia are initiated (**Figure 5A**). Organ initiation mainly relies on *PAT* in the epidermis via *PIN1* (Benková et al., 2003). In fact, *PIN*s were even discovered because of their “pin-shaped” inflorescence, a result of lacking organ initiation at the inflorescence meristem (IM) (Okada et al., 1991; Gälweiler et al., 1998). Although rosette leaf formation is generally not abolished in plants that exhibit “pin-shaped” inflorescences, organ initiation by auxin is expected to rely on the same mechanisms in the SAM as well as in the IM. Studies in tomato, where the SAM is larger and more accessible than in *Arabidopsis*, have confirmed that leaf formation in the SAM relies on *PAT* via *PIN1* (Reinhardt et al., 2000; Bayer et al., 2009). In the SAM, polar localisation of *PIN1* in the L1 layer creates an auxin flux towards incipient primordia sites and depletion around these sites, thus generating a chemical inhibitory field (together with CK signalling) that defines the primordium boundaries (Reinhardt et al., 2003; Heisler et al., 2005; Vernoux et al., 2011; Kierzkowski et al., 2013; Besnard et al., 2014a). (**Figure 5C**). As cellular auxin levels increase at the primordium site, *AUX/IAAs* are targeted for



Chapter 1: General introduction



ubiquitination via TIR1/AFBs, resulting in their proteolytic degradation, and ultimately leading to the release of ARFs. MONOPTEROS (MP / ARF5), together with ETTIN (ARF3) and ARF4, regulates initiation of new primordia through activation of genes that specify cell fate (Przemeck et al., 1996; Galvan-Ampudia et al., 2020). In the SAM, MP is present at low levels in the CZ where it aids stem cell homeostasis (Luo et al., 2018), and at high levels in the PZ where it induces primordium fate by upregulation of *PIN1*, *LEAFY* (*LFY*), *AINTEGUMENTA* (*ANT*), *AINTEGUMENTA-LIKE6* / *PLETHORA3* (*AIL6* / *PLT3*), and *FILAMENTOUS FLOWER* (*FIL*) (Weigel et al., 1992; Elliott et al., 1996; Sawa et al., 1999; Krizek, 2009; Krogan et al., 2016).



Figure 5: Light-regulated initiation and outgrowth of lateral shoot organs.

New shoot organs are initiated in the SAM, where stem cell proliferation and differentiation are tightly balanced to ensure proper phyllotaxis. **A.** The SAM consists of three layers: L1 (epidermal cell layer), L2 (subepidermal cell layer) and L3 (corpus cell layer) and can be divided into five regions: the central zone (CZ), organizing centre (OC), rib zone (RZ), peripheral zone (PZ), and outgrowing primordia (P1 to P4). **B.** To induce stem cell proliferation, *WUS* is expressed in the OC and moves to the CZ to induce *CLV3* expression in pluripotent stem cells. Subsequently, *CLV3* moves to the OC to repress *WUS* via a *CLV1/2* receptor kinase complex, creating a negative feedback loop that is required for stem cell homeostasis. *WUS* expression is enhanced by CK through type-B ARR in response to light, and through a positive feedback loop via type-A ARRs that maintains CK signalling, and thus stem cell proliferation. Moreover, through MP, auxin slightly enhances *WUS* via the type-A ARR-CK feedback loop. To induce stem cell differentiation, light stabilises polar PIN protein localisation to create the auxin gradient that is required for initiation of new primordia. **C.** Incipient organs (i1 to i5) are initiated at the sites of enhanced auxin flow (pink) and are confined by chemical inhibitory fields that result from auxin depletion and cytokinin signalling (purple).

Moreover, MP has been shown to target the CK signalling inhibitor ARABIDOPSIS HISTIDINE PHOSPHOTRANSFER PROTEIN 6 (AHP6) that increases the robustness of phyllotaxis by creating a secondary inhibitory field around the site of primordium initiation (Besnard et al., 2014b) (**Figure 5B, C**). Following initiation, leaf primordia undergo primary morphogenesis which is mainly regulated by *ANT* and *YABBY* genes resulting in lamina initiation and specification, and the formation of marginal structures such as serrations (Mizukami and Fischer, 2000; Sarojam et al., 2010). Finally, during secondary morphogenesis, the mature leaf is shaped by expansion, tissue differentiation and differential growth through a tight balance between CK and



Chapter 1: General introduction

GA (Achard et al., 2009; Holst et al., 2011). The newly formed leaf is part of a morphogenic unit called phytomere which also includes an internode and an axillary meristem (AM) (Galinat 1959). In *Arabidopsis*, the shoot meristem produces three different types of phytomers depending on the age of the plant. Type 1 phytomers form the rosette and consist of a rosette leaf, an extremely short internode, and an AM that may produce a branch. Type 2 phytomers form the inflorescence base and consist of a cauline leaf, a long internode, and an axillary branch, whereas type 3 phytomers carry the floral meristem that produces flowers instead of leaves (Schultz and Haughn, 1991). Finally, branches that arise from AMs of phytomeres can divide into second-order and third-order paraclades which can be divided between rosette paraclades that arise from type 1 phytomers, and cauline paraclades that are produced from type 2 phytomers (Talbert et al., 1995). For a long time, it was believed that stem cells in the SAM were shielded from possibly dangerous abiotic influences, and that organ formation was therefore self-regulatory (Airy, 1873). However, a first clue that light might regulate leaf initiation was found in pea plants that arrested leaf development when transferred to darkness (Low, 1971). Furthermore, microarray analysis has shown that light-regulated CK-associated genes are differentially expressed between seedlings and adult leaves, suggesting a light-dependent hormone response throughout shoot development (Ma et al., 2001). Moreover, auxin, ET, CK and GA genes are modulated in the SAM of etiolated seedlings after exposure to light. In addition, it was shown that phytochromes and cryptochromes contribute redundantly to SAM activity, possibly by modulation of these hormonal pathways (López-Juez et al., 2008). Finally, a breakthrough study by Yoshida and colleagues combined *Arabidopsis* and tomato research to show how light



regulates SAM activity through auxin and CK. Light was shown to activate CK signalling in the SAM, which likely activates the stem cell pool via WUS-CLV. In addition, light stabilises PIN1 proteins at the plasma membrane, to establish the auxin gradient required for primordia initiation (Yoshida et al., 2011) (**Figure 5B**). A more recent study showed that light-induced SAM activation by CK coincides with elevated sugars that promote the *TARGET OF RAPAMYCIN (TOR)* kinase pathway, indicating the importance of metabolic in addition to hormonal signals (Pfeiffer et al., 2016). Aside from its effect on leaf initiation, light also influences leaf morphology. For example, low light intensity promotes petiole elongation and inhibits leaf blade expansion, a leaf phenotype that is well characterised as part of shade avoidance syndrome (Kozuka et al., 2005). As a response to low R:FR ratios, this altered leaf shape provides a better position for light exposure to drive photosynthesis (Tsukaya, 2004). Furthermore, darkness causes a local starvation state in the SAM that arrests cell proliferation in young primordia (Mohammed et al., 2018), and in the long term, results in leaf senescence (Weaver and Amasino, 2001). In summary, light has been shown to modulate both leaf initiation and morphology, thereby opening up many new research possibilities in identifying wavelength-specific responses and applications for horticulture.

Light-regulated primary and secondary stem growth

Similar to other shoot organs, the stem is initiated in the SAM. However, while lateral organs are initiated in the PZ, stem growth originates from the RZ of the SAM. The central region of the RZ gives rise to the pith, the peripheral regions of the RZ produces stem epidermis and cortex, and the boundary between these two regions develops the vasculature (Sachs, 1965). Elongation

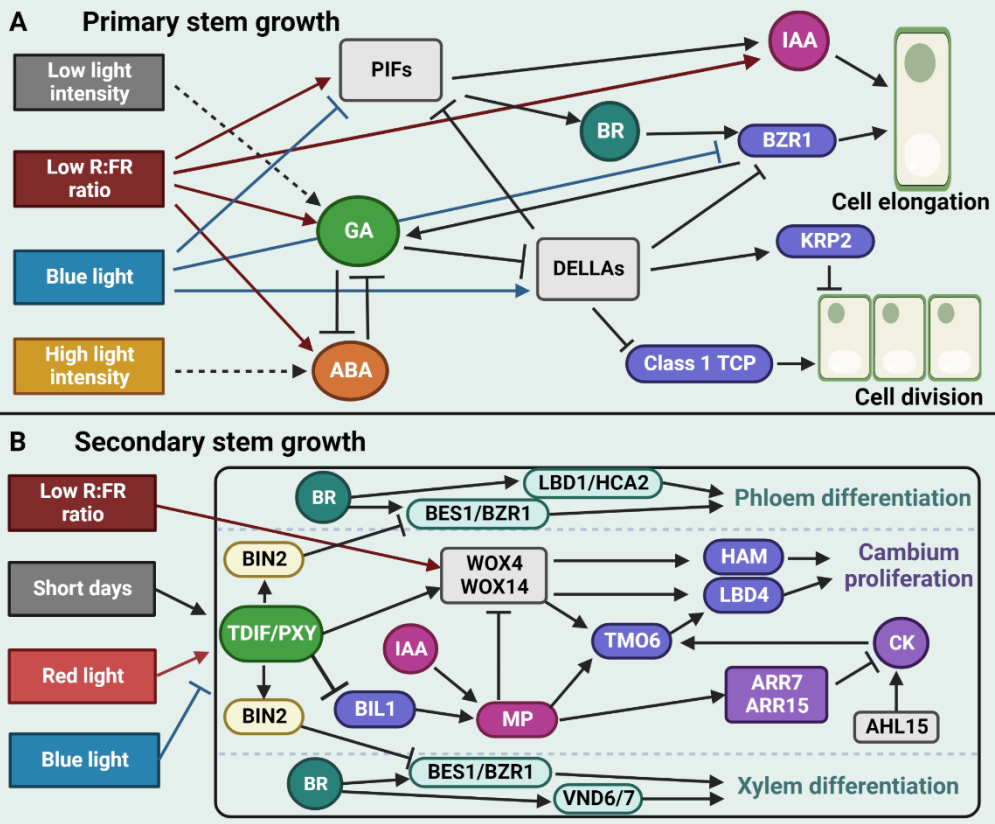


Chapter 1: General introduction

of the stem relies on the interplay between GA, BR, auxin, and abscisic acid (ABA) signalling, with a key role for GA and the growth-inhibiting DELLA proteins that act downstream of the GA receptor (Ross et al., 2003; Unterholzner et al., 2015; Davière and Achard, 2016; Shu et al., 2016). The role of GA in primary growth is well characterised by the dwarfed GA biosynthesis mutants that are defective in leaf expansion and stem elongation (Thomas and Sun, 2004). GA promotes cell division in the RZ by inducing degradation of DELLAs that repress class I TCP (TEOSINTE BRANCHED 1, CYCLOIDEA, PROLIFERATING CELL FACTOR) cell cycle progression transcription factors (Davière et al., 2014). DELLAs have also been shown to directly inhibit cell division in the RZ through activation of the cell cycle inhibitor KRP2 (KIP-RELATED PROTEIN 2), thus further enhancing the role of GA in primary stem growth (Serrano-Mislata et al., 2017). In addition, DELLAs physically interact with and inhibit BRASSINAZOLE-RESISTANT 1 (BZR1) proteins, which are positive regulators of the growth-promoting BR response, suggesting that GA (partially) regulates BR-induced stem growth (Gallego-Bartolomé et al., 2012; Li et al., 2012b). However, some studies indicate that BR may also enhance stem growth by modulation of GA levels, thus highlighting the importance of both phytohormones (Tong et al., 2014; Unterholzner et al., 2015). Similarly, auxin has been shown to enhance biosynthesis of GA, and to inhibit its deactivation, to promote stem internode elongation in pea (Ross et al., 2003). Finally, to control stem growth, high levels of ABA act antagonistically on GA biosynthesis, whereas low levels of ABA promote GA biosynthesis (Seo et al., 2006; Oh et al., 2007) (**Figure 6A**). The effects of light quality and intensity on plant height are well established and have been reported in several species (Zheng et al., 2019; Paradiso and



Proietti, 2021). Low light intensity has been shown to result in increased stem elongation that is correlated to higher levels of GA in pea and *Brassica napus* (Gawronska et al., 1995; Potter et al., 1999). Stem elongation in response to low R:FR ratios is proposed to depend on a similar auxin-mediated shade avoidance mechanism that was identified in the hypocotyl and is described earlier in this chapter (**Figure 4B**). In addition, analysis of the *phyB gal* double mutant in *Arabidopsis* revealed that the PHYB-mediated shade avoidance response requires functional GA signalling (Peng and Harberd, 1997), which was further supported by enhanced GA synthesis and sensitivity under low R:FR ratios (Reed et al., 1996; Hisamatsu et al., 2005). PIF stabilisation under low R:FR ratios is enhanced by GA signalling through relieving the inhibiting interaction between DELLAs and PIF1, PIF3, PIF4 and PIF6 (Feng et al., 2008; Gallego-Bartolomé et al., 2010; Lucas et al., 2008). Moreover, stabilised PIF4 promotes BR production, thus further enhancing stem elongation (Martínez et al., 2018). In contrast to shade avoidance, stem growth is inhibited by blue light via CRY1-mediated stabilisation of DELLA proteins (Yan et al., 2021), and through inhibition of PIFs and BZR1 (He et al., 2019; Ma et al., 2016). Finally, low R:FR ratios, as well as high light intensity, induce the biosynthesis and signalling of ABA to further prevent indeterminate primary growth (Huang et al., 2019; Ortiz-Alcaide et al., 2019) (**Figure 6A**). While primary (apical) stem growth depends on apical meristems, secondary (radial) stem growth depends on lateral meristems being the vascular cambium that produces xylem and phloem, and the cork cambium which gives rise to cork and phelloderm (Barra-Jiménez and Ragni, 2017). These vascular tissues provide the stem with strength and resilience, while facilitating long-range



transport of water and nutrients. In young stems, vascular tissues are organised in bundles that contain procambium, primary xylem, and primary phloem. As the plant ages, and secondary growth increases, the procambium, along with interfascicular parenchyma cells, mature into a circular vascular cambium that produces phloem towards the outside of the stem, and xylem towards the centre (Spicer and Groover, 2010; Ragni and Greb, 2018). Proliferation of cambium stem cells relies on a mechanism similar to CLV-WUS in the SAM. The



Figure 6: Regulation of primary and secondary stem growth.

Both primary (apical) and secondary (radial) stem growth respond to light. **A.** Primary stem growth relies mainly on GA inhibition of DELLA proteins that regulate cell division via KRP2 and class I TCPs, and cell elongation via BZR1. Interplay between GA and other phytohormones rely largely on PIFs, that promote cell elongation via auxin (IAA), and via BR. Additionally, ABA acts antagonistically on GA-dependent primary growth. Low R:FR ratios and low light intensities stimulate primary growth in a GA- and auxin-dependent manner. In contrast, blue light and high light intensities inhibit primary growth via ABA, or through modulation of PIFs, DELLAs and BZR1. **B.** Secondary stem growth relies on cambium proliferation, and differentiation into xylem and phloem cells. Stem cell homeostasis is regulated by proliferation-promoting WOX4/14, and by proliferation-inhibiting ARR7/15 signalling modules. The TDIF/PXY ligand-receptor complex stimulates cell division via WOX4/14 that activates HAM and LBD4 transcription factors, and through inhibition of BIL1, and its subsequent reduction in ARR7/15 via MP. TMO6 integrates CK and auxin signalling pathways to promote cambium proliferation. CK promotes cambium proliferation in an AHL15-dependent manner, while IAA stabilises ARR7/15 via MP, to inhibit cambium proliferation and promote xylem differentiation. BR stimulates xylem differentiation via VND6 and 7, and phloem differentiation via LBD1 and HCA2. In addition, BES1 and BZR1 are key factors for both xylem and phloem differentiation. R light, short days, and low R:FR ratios stimulate secondary growth, while B light represses secondary growth.

ligand-receptor complex TRACHEARY ELEMENT DIFFERENTIATION (TDIF) / PHLOEM INTERCALATED WITH XYLEM (PXY) promotes stem cell division and inhibits xylem cell differentiation via activation of the *WUSCHEL-RELATED HOMEODOMAIN 4* (WOX4) and *WOX14* transcription factors (Etchells et al., 2013, 2016). Subsequently, WOX4 and WOX14 promote stem cell proliferation through interaction with the LATERAL ORGAN BOUNDARIES DOMAIN 4 (LBD4) and HAIRY MERISTEM



(HAM) transcription factors (Suer et al., 2011; Etchells et al., 2013; Smit et al., 2020). In addition, PXY represses *BRASSINOSTEROID-INSENSITIVE 2-LIKE 1* (*BIL1*), that phosphorylates the cambium-inhibiting MP, to promote cambium proliferation via TARGET OF MONOPTEROS 6 (TMO6) (Han et al., 2018; Smit et al., 2020) (**Figure 6B**). Stem cell homeostasis relies greatly on the phytohormones auxin and CK. Auxin-dependent regulation of stem cell proliferation relies on WOX4, and its direct attenuation by MP. (Suer et al., 2011; Brackmann et al., 2018). Cambium activity and maintenance relies on CK levels that are modulated by LONELY GUY (LOG), CYTOKININ DEHYDROGENASE 2 (CKX2), and ARR7/15 (Kurakawa et al., 2007; Nieminen et al., 2008). Moreover, CK biosynthesis is promoted by the longevity-enhancing AT-HOOK MOTIF CONTAINING NUCLEAR LOCALIZED 15 (AHL15) transcriptional regulator (Rahimi et al., 2022b). Finally, TMO6 integrates auxin and CK signalling pathways to regulate cambium proliferation via LBD4 (Smit et al., 2020) (**Figure 6B**). Further towards the inside and outside of the stem, differentiation is initiated by stem cell fate identification into xylem and phloem precursors, and later on into secondary xylem and phloem cells. HIGH CAMBIAL ACTIVITY 2 (HCA2) and LATERAL ORGAN BOUNDARIES DOMAIN 1 (LBD1) have been identified as phloem-forming transcription factors (Guo et al., 2008; Yordanov et al., 2010), whereas VASCULAR-RELATED NAC-DOMAIN 6 (VND6) and VND7 are important for xylem production (Kubo et al., 2005). In addition, BRI1-EMS-SUPPRESSOR 1 (BES1) and BZR1 have been identified as key regulators of both xylem and phloem differentiation (Saito et al., 2018) (**Figure 6B**). Although the exact mechanism remains relatively unknown, BR appears to be involved in both xylem and phloem differentiation, likely via the above-



mentioned transcription factors (Miyashima et al., 2013). Light has been shown to affect secondary stem growth, mostly through intensity and day length, where shorter days (and thus less photons) result in thicker stems (MacMillan et al., 2013). In addition, low R:FR ratios have been shown to induce xylem formation in hypocotyls through activation of WOX4 (Botterweg-Paredes et al., 2020). Other light quality studies in three different plant species show that, higher fractions of (F)R light enhance stem thickness, while higher fractions of B light reduce secondary growth (Rehman et al., 2020; Cao et al., 2016; Li-Li et al., 2020) (**Figure 6B**). However, the underlying mechanisms remain to be elucidated.

Light-mediated timing of developmental phase transitions

Throughout their life cycle, plants undergo distinct developmental phases from embryonic growth all the way up to reproduction. After the formation and outgrowth of the first lateral organs, plants progress from juvenile phase to adult phase during vegetative phase change (VPC). In *Arabidopsis*, this transition can be easily identified by leaf heteroblasty, phyllotaxis and plastochron (Huijser and Schmid, 2011; Poethig, 2013). Conserved throughout angiosperms, the age pathway regulates developmental phase shifts including VPC (Weigel and Meyerowitz, 1993). In juvenile plants, *microRNA156* (*miR156*) levels are high, resulting in inhibition of its target genes encoding SQUAMOSA PROMOTER BINDING PROTEIN-LIKE (SPL) transcription factors. As plants age, *miR156* levels gradually decrease, subsequently resulting in stabilisation of SPL expression. In addition, SPL levels are also promoted through GA signalling, indirectly of *miR156* (Wang et al., 2009; Jung et al., 2012; Yu et al., 2012). Six of these factors (SPL2, 9, 10, 11, 13,



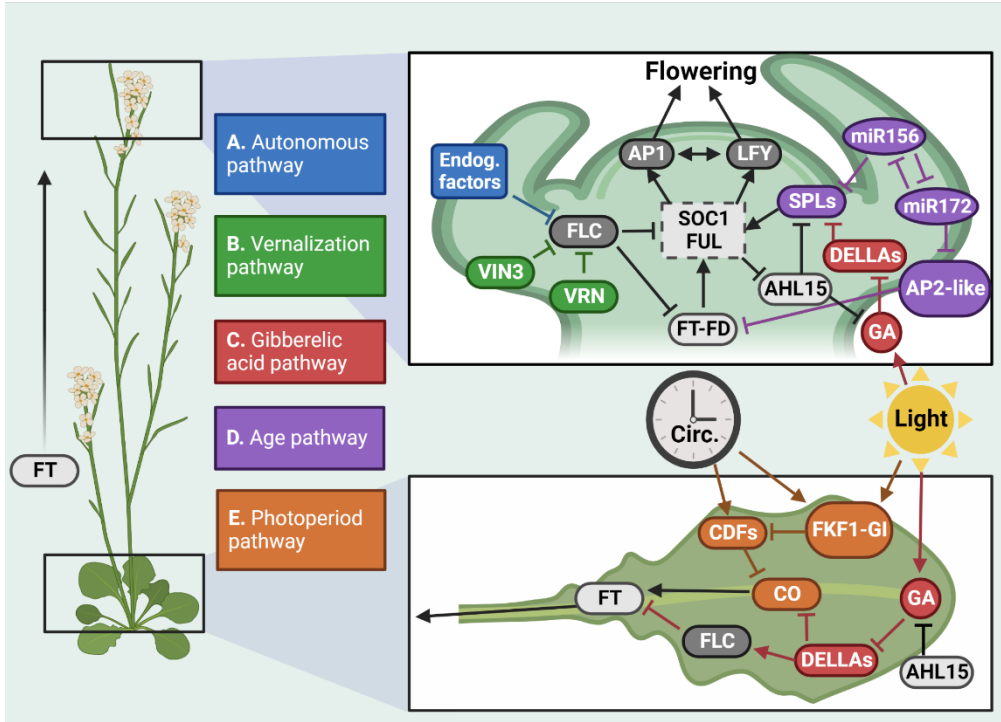
and 15) regulate VPC directly via induction of leaf elongation and serration, or indirectly through activation of *miR172* (Xu et al., 2016a). As *miR172* levels gradually increase, this promotes the formation of abaxial trichomes by inhibiting *APETALA2* (*AP2*) and *AP2*-like genes *TARGET OF EARLY ACTIVATION TAGGED 1* (*TOE1*) and *TOE2* (Aukerman and Sakai, 2004; Chen, 2004). So far, only few publications indicate that VPC may be regulated by light. For example, VPC can be accelerated by high light intensity (Guo et al., 2017). In addition, *FHY3* and *FAR-RED IMPAIRED RESPONSE 1* (*FAR1*), that are required for *PHYA* signalling, have been identified recently as integrators of light and the *miRNA156*-*SPL* module of VPC (Xie et al., 2020). After acquisition of flowering competence following VPC, the SAM switches to an IM during the floral transition. A flowering hormone, or “florigen” was proposed to be synthesised in the leaves and transmitted to the SAM to acquire floral identity (Chailakhyan, 1937; Zeevaart, 1976). Later, *Arabidopsis* *FLOWERING LOCUS T* (*FT*) has been identified as such a leaf-to-SAM florigen that induces flowering (Corbesier et al., 2007). Moreover, *FT* homologues have been identified as florigens in several economically important, yet fundamentally different species, such as tomato, rice and apple (Lifschitz et al., 2006; Tamaki et al., 2007; Kotoda et al., 2010). Once inside the SAM, *FT* forms a complex with the bZIP transcription factor *FD* to induce floral meristem identity genes *API* and *LFY* via *AGAMOUS-LIKE 24* (*AGL24*), and *SUPPRESSOR OF OVEREXPRESSION OF CONSTANS 1* (*SOC1*), *SEPALLATA3* (*SEP3*), and *FRUITFULL* (*FUL*) (Weigel et al., 1992; Abe et al., 2005; Teper-Bamnolker and Samach, 2005; Lee et al., 2008) (**Figure 7**). In contrast to *FT*, *TERMINAL FLOWER 1* (*TFL1*) acts as an “anti-florigen” that binds to *FD* to suppress flowering by antagonizing *FT*-*FD*



complex activity (Abe et al., 2005; Conti and Bradley, 2007). The balance between florigens and anti-florigens determines the timing of the floral transition in long-day (LD), short-day (SD) and day-neutral (DN) plant species (Higuchi, 2018). In *Arabidopsis*, this balance is determined via five distinct flowering pathways: (1) the autonomous pathway, (2) the vernalization pathway, (3) the GA pathway, (4) the age pathway and (5) the photoperiodic pathway. **(1)** In the autonomous pathway, endogenous factors repress the activity of the MADS-box protein FLOWERING LOCUS C (FLC), thereby relieving its inhibition of *FT* and *SOC1*, ultimately leading to flower induction (Simpson, 2004) (**Figure 7A**). **(2)** Vernalization is the requirement for exposure to long-term cold to induce flowering. Upon cold exposure, VERNALIZATION INSENSITIVE 3 (VIN3), VERNALIZATION 1 (VRN1) and VRN2 induce flowering by inhibiting *FLC* and *FLC-like* floral repressors (Kim and Sung, 2014) (**Figure 7B**). Since the autonomous and vernalization pathways are not likely to be influenced by light, we will not discuss their mechanisms in detail, and instead focus on the other three pathways that are (partially) regulated by light. **(3)** The importance of GA during floral transition was shown clearly by major flowering defects in loss of function mutants of GA biosynthesis and signalling components (Wilson et al., 1992; Jacobsen and Olszewski, 1993). Regulation of flowering by GA occurs both in the SAM and in the leaves by interacting with components of other hormonal and flowering pathways, or by direct modulation of (anti-)florigens (Bao et al., 2020). In leaves, GAs inhibit DELLA proteins that modulate the activity of a variety of transcription factors, including FT activators such as CONSTANS (CO) and WRKY75, and *FT* suppressors such as FLC and MYC3 (Li et al., 2016; Xu et



Chapter 1: General introduction



al., 2016b; Zhang et al., 2018; Bao et al., 2019). In the SAM, GA-mediated proteolysis of DELLAs leads to accumulation of *miR159*, WRKY12, NUCLEAR FACTOR Ys (NFYs) and SPLs, that activate *FUL* and *SOC1*, and subsequently *LFY* and *AP1* to promote flowering (Achard et al., 2004; Yu et al., 2012; Hou et al., 2014; Li et al., 2016b). Although most evidence for light-regulated flowering via the GA pathway depends on day length through stabilisation of the CO transcription factor, some studies also suggest



Figure 7: Light regulates flowering through GA signalling and day length.

In the facultative long-day plant *Arabidopsis*, the floral transition is controlled via five distinct flowering pathways that rely on a group of key floral integrators and floral meristem identity genes. The florigen *FT* is expressed in leaves and moves to the SAM, where it forms a complex with *FD* to induce *SOC1* and *FUL*, among others, that subsequently enhance *AP1* and *LFY* to promote flowering. **A.** In the autonomous pathway, *FLC* activity is repressed by endogenous factors, resulting in relieved inhibition of *FT* and *SOC1*. **B.** The vernalization pathway is activated by exposure to long-term cold, resulting in *FLC* inhibition by *VIN3*, *VRN1* and *VRN2*, and thus in elevation of *FT* and *SOC1*. **C.** In leaves, GA signalling induces flowering by inhibition of *DELLA* proteins that repress *FT* expression via *CO* or *FLC* proteins. In the SAM, GA signalling inhibits *DELLA*s, thereby relieving their repression of *SPL*s and other flower-inducing transcription factors that enhance *SOC1* and *FUL*. In both tissues, GA signalling is enhanced by light through *PHY* signalling, or day length. **D.** Plant ageing influences flowering depending on the balance between *miR156* and *miR172*. As plants age, *miR156* levels gradually decrease, resulting in *SPL* accumulation that promote flowering, while *miR172* levels increase and promote flowering through inhibition of *AP2*-like floral repressors. The longevity-enhancing *AHL15* protein delays flowering by direct inhibition of the *SPL*s and through repressing GA signalling. **E.** In long-day photoperiods, *FKF1*, together with *ZTL* and *LKP2*, associates with the clock-associated component *GI* to inhibit *CDF*s that repress *CO* expression. Subsequently, the *CO* expression peak in the late afternoon of long days, results in enhanced *FT* expression at dusk.

regulation of the GA pathway by light quality through *PHY*s and light intensity via *MYB-RELATED PROTEIN*s (Hisamatsu and King, 2008; Zhao et al., 2011) (**Figure 7C**). (4) The age pathway mostly influences flowering through the timing of VPC as described above. As plants age and *miR172* levels increase, *AP2-like* genes that act as floral repressors are inhibited. Alleviated of its inhibition by *AP2-like* transcription factors, *FT* levels are elevated, ultimately leading to flowering (Teotia and Tang, 2015; Zheng et al., 2019). In addition,



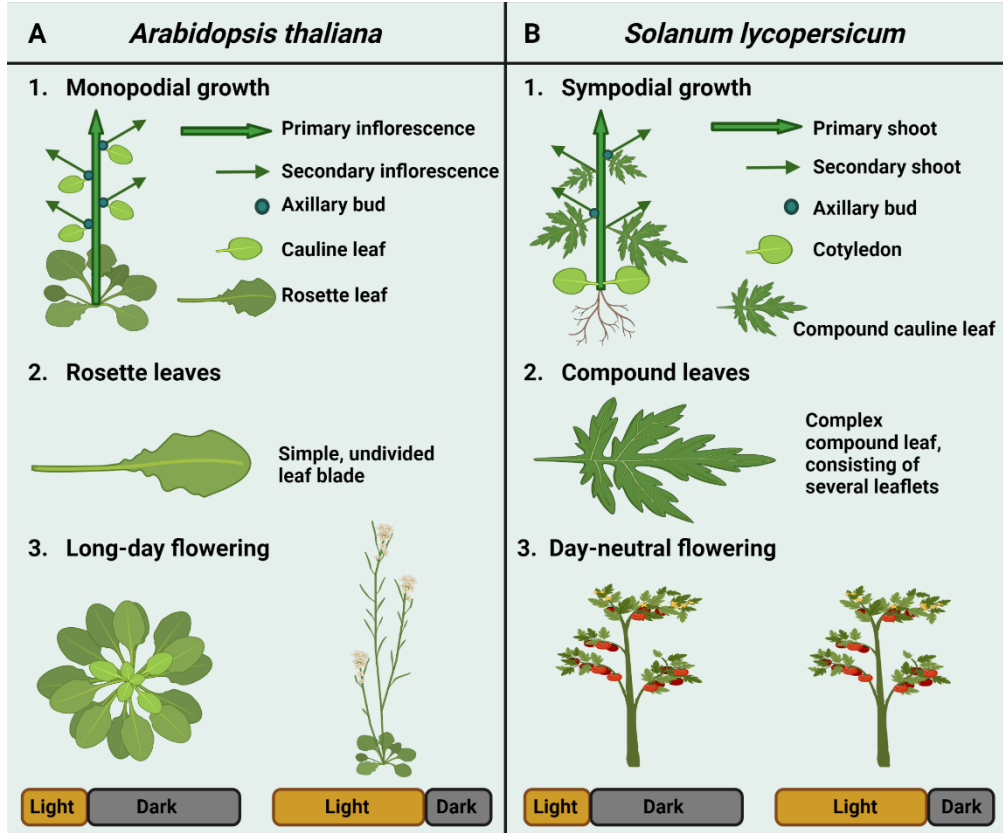
higher SPL levels in adult plants activate *SOC1* transcription in the SAM, resulting in expression of *API* and *LFY* (Lee et al., 2008; Immink et al., 2012). To delay flowering, the longevity-promoting AHL15 protein decreases SPL levels in a *miR156*-independent manner. In addition, AHL15 has been shown to suppress GA biosynthesis, resulting in delayed flowering (Karami et al., 2020; Rahimi et al., 2022a). So far, an effect of light quality on age-dependent floral transition has not yet been identified, but some studies on VPC suggest a putative role for light in ageing (Guo et al., 2017; Xie et al., 2020) (**Figure 7D**). (5) Although light may influence flowering through the GA pathway and the age pathway, its main effect is through the photoperiodic pathway. This specific pathway depends on day length (photoperiod) and circadian clock components that are integrated via the light-dependent zinc-finger transcription factor CO (Samach et al., 2000; Suárez-López et al., 2001). In LD plants such as *Arabidopsis*, the floral transition occurs once the day length increases in late spring (Garner and Allard, 1920). During LD photoperiods, the blue-light FKF1 photoreceptor associates with the nuclear protein GIGANTEA (GI) to inhibit CYCLING DOF FACTORS (CDFs) that act as repressors of *CO* expression (Sawa et al., 2007). Its other two family members, ZTL and LKP2, both interact with FKF1 and GI to aid in the targeted degradation of CDFs (Fornara et al., 2009). The inhibition of these CDFs facilitates *CO* expression during the late afternoon resulting in a peak in *FT* expression at dusk. This FT peak promotes expression of *API*, *FUL*, and *CAULIFLOWER* (*CAL*) that induce the switch of the SAM to an IM (Hayama and Coupland, 2004; Abe et al., 2005; Wigge et al., 2005) (**Figure 7E**). In SD plants, such as rice, flowering occurs once daylength decreases in early autumn (Garner & Allard, 1920), and this also relies on CO-FT regulation. In rice, SD



conditions promote transcription of the florigen *Heading date 3A* (*Hd3a*, an orthologue of FT) which promotes floral transition (Tamaki et al., 2007). Similar to the GI-CO pathway in Arabidopsis, the rice orthologue of GI activates both Heading date 1 (*Hd1*, an orthologue of CO) and Early heading date 1 (*Ehd1*, a type B ARR) in response to the circadian clock (Yano et al., 2000; Hayama et al., 2003). Interestingly, *Hd1* functions as an activator of *Hda3* in SD conditions and as a repressor of *Hda3* in LD conditions, indicating it is one of the main regulators of flowering in SD plants (Hayama and Coupland, 2004). Finally, in DN plants, such as tomato, flowering occurs regardless of photoperiod (Garner & Allard, 1920).

Horticultural crop versus genetic model plant: Differences between tomato and Arabidopsis.

Since this thesis focuses on Arabidopsis as a genetic model plant, and tomato as an important commercial crop, we should consider the differences and similarities between these two species. For example, germination of Arabidopsis seeds requires light, whereas tomato seeds germinate better in darkness (Mancinelli et al., 1966; Casal and Sánchez, 1998). As both species are dicots, seedling development is quite similar in Arabidopsis and tomato. However, after the seeding stage, Arabidopsis and tomato differ greatly in plant architecture, day length sensitivity, and life cycle. Differences in plant architecture between Arabidopsis and tomato are clearly visible in the shoot. Arabidopsis is an annual, monopodial plant in which the vegetative SAM produces leaves to form a spiral rosette that continues to grow until the vegetative SAM switches to a reproductive IM (Benlloch et al., 2007; Bartlett



and Thompson, 2014) (**Figure 8A**). In contrast, tomato is a semi-perennial, sympodial plant that produces 8-12 compound leaves before the vegetative SAM splits into an IM that will produce flowers, and an axillary bud that will produce new compound leaves (**Figure 8B**). After the first IM, tomato SAMs continue to split after production of three new compound leaves (Benlloch et al., 2007; Bartlett and Thompson, 2014). Not only do *Arabidopsis* and tomato differ in shoot meristems, they also greatly differ in leaf morphology. Rosette leaves of *Arabidopsis* are simple with an undivided leaf blade, whereas the

**Figure 8: *Arabidopsis thaliana* versus *Solanum lycopersicum*.**

Because molecular mechanisms identified in the genetic model plant *Arabidopsis thaliana* are not always conserved in important crops, the most important differences in architecture and life cycle between *Arabidopsis* and tomato are highlighted above. In addition, there are many differences on a genetic level resulting from mutations, duplications, and deletions. **A.** *Arabidopsis* is a monopodial plant that produces a spiral rosette from the vegetative SAM, until its switch to IM (1). The rosette leaves are simple, consisting of an undivided leaf blade (2). The floral transition depends greatly on day-length, with induction in long-day photoperiods (3). **B.** Tomato is a sympodial plant that produces a predetermined number of leaves before the SAM splits into an IM producing an inflorescence with flowers and an axillary bud producing a fixed set of phytomers with new leaves before it splits again in an IM and axillary bud (1). The tomato compound leaves are complex, consisting of leaflets that are separated by a bladeless region (2). As a day-neutral plant, tomato plants acquire flowering competence based on plant architecture, regardless of photoperiod (3).

compound leaves of tomato are more complex, consisting of separate subunits (leaflets) divided by a bladeless region (Bar and Ori, 2014; Du et al., 2018) (**Figure 8**). These differences in plant architecture and life cycle between *Arabidopsis* and tomato might be correlated to flowering competence. As a LD plant, *Arabidopsis* responds to changes in circadian rhythm and temperature to start flowering under increasing day length (Johansson and Staiger, 2015) (**Figure 8A**). In contrast, the DN tomato acquires flowering competence based on plant architecture (after a certain number of leaves), regardless of changes



in day length (Lifschitz and Eshed, 2006) (**Figure 8B**). Because *Arabidopsis* and tomato differ greatly in many aspects of plant development, photoreceptor responses most likely differ as well. All the different photoreceptor families that have been identified in *Arabidopsis* are also present in tomato, however evolutionary differences in photoreceptor lineage can make translation of light signalling pathways from model plant to crop quite challenging. For example, although the R/FR-sensitive PHY family in *Arabidopsis* consist of five members (PHYA to PHYE), this is not the case for all land plants. *PHYA* and *PHYB* lineages are greatly conserved among species. *PHYC* most likely arose from a gene duplication in the *PHYA* lineage, whereas *PHYD* and *PHYE* are a result of *PHYB* lineage duplication within *Brassicaceae* and dicots, respectively (Mathews and Sharrock, 1997). The tomato PHY family also consists of five members: *PHYA*, *PHYB1*, *PHYB2*, *PHYE* and *PHYF* (Van Tuinen et al., 1997; Alba et al., 2000). Tomato *PHYA*, *PHYE*, and *PHYF* have been identified as true orthologues of *Arabidopsis* *PHYA*, *PHYE*, and *PHYC*, respectively (Hauser et al., 1995; Alba et al., 2000). Tomato *PHYB1* and *PHYB2* however, arose from an independent duplication in *Solanaceae*, and are not exact functional orthologues of *Arabidopsis* *PHYB* and *PHYD* (Pratt et al., 1995). For perception of B light, the tomato CRY family consists of 4 members: *CRY1a*, *CRY1b*, *CRY2* and *CRY3*. Similar to *Arabidopsis*, tomato *CRY3* is a DASH-type that is active in DNA repair (Facella et al., 2006). *CRY1a* and *CRY2* have been identified as homologues of *Arabidopsis* *CRY1* and *CRY2* (Perrotta et al., 2000). Although there are many functional similarities with their *Arabidopsis* counterparts, tomato *CRY1a* and *CRY2* functions differ from *Arabidopsis* in shoot and root elongation, circadian leaf movements and flowering (Fantini et al., 2019). Finally, tomato *CRY1b* turned



out to be a truncated copy of *CRY1a* resulting from a whole genome triplication in the common *Solanaceae* progenitor, and is likely not functional (Sato et al., 2012). Homologues of another B light-sensing receptor family, the PHOTs, have been identified as tomato *PHOT1* (Sharma & Sharma, 2007) and *PHOT2* (Sharma *et al.*, 2007). Unfortunately, functional gene studies remain limited in the tomato PHOT family. Recently, an orthologue of Arabidopsis *UVR8* has been identified to mediate acclimation to UV-B stress in tomato (Li et al., 2018). Finally, studies on the *ZTL* family in tomato are unfortunately almost non-existent. Altogether, the many differences between these two species show that translation from a genetic model plant to a horticultural crop remains challenging, and in some cases close to impossible. This indicates just how important it is to include crops in experimental studies on plant development.

Thesis outline

In this thesis, we set out to elucidate how different developmental processes during early plant development are influenced by light. In **chapter 2**, we used white TL lights to compare light and dark treatments, whereas in **chapters 3-5**, we investigated the effect of light quality on early plant development with the use of white, red, and blue LED modules. In **chapter 2**, we show that exposure of roots to light represses their primary elongation in Arabidopsis and tomato seedlings. Genetic analysis of mutants, combined with reporter lines, identified that the mechanism that regulates this phenotype depends on PHYA and PHYB that, upon their activation by FR and R light respectively, inhibit PIF transcription factors that modulate local auxin biosynthesis in the RAM. In **chapter 3**, we provide a clear and detailed overview of the early Arabidopsis and tomato phenotypes that arise when grown in red, blue, and white LED



Chapter 1: General introduction

conditions. A comparative analysis showed that primary growth responses to light quality were highly conserved between *Arabidopsis* and tomato. In contrast, *Arabidopsis* developmental phase transitions were extremely sensitive to light quality, whereas tomato phase transitions were remarkably indifferent to R or B light. In **chapter 4**, we further investigated *Arabidopsis* and tomato apical and radial growth responses to light quality. Microscopic and histological analyses of hypocotyls and stems throughout plant development showed that light quality can modulate both apical and primary radial growth in *Arabidopsis*, whereas tomato responses to R or B light are limited to apical growth. Finally, in **chapter 5**, we further analysed the major difference between *Arabidopsis* and tomato in light quality responses: flowering time. By combining genetic analysis of *Arabidopsis* plants with flowering studies in long-day and day-neutral plant species we show that B light promotes flowering through modulation of major components of the photoperiodic pathway. Moreover, we show that R light delays flowering through inhibition of important components of the age pathway. Altogether, this thesis gives a clear overview of light quality-regulated early plant development of *Arabidopsis* and tomato.

Author contributions

KS and RO structured the manuscript. KS wrote the manuscript and created the figures using BioRender software. All authors contributed to manuscript revision.



Funding

This work was part of the research program “LED it be 50%” with project number 14212, which is partly financed by the Dutch Research Council (NWO).



References

- Abe, M., Kobayashi, Y., Yamamoto, S., Daimon, Y., Yamaguchi, A., Ikeda, Y., Ichinoki, H., Notaguchi, M., Goto, K., and Araki, T.** (2005). FD, a bZIP protein mediating signals from the floral pathway integrator FT at the shoot apex. *Science* 309, 1052–1056.
- Achard, P., Gusti, A., Cheminant, S., Alioua, M., Dhondt, S., Coppens, F., Beemster, G. T. S., and Genschik, P.** (2009). Gibberellin signaling controls cell proliferation rate in Arabidopsis. *Curr. Biol.* 19, 1188–1193.
- Achard, P., Herr, A., Baulcombe, D. C., and Harberd, N. P.** (2004). Modulation of floral development by a gibberellin-regulated microRNA. *Development* 131, 3357–3365.
- Ahmad, M., and Cashmore, A. R.** (1993). HY4 gene of *A. thaliana* encodes a protein with characteristics of a blue-light photoreceptor. *Nature* 366, 162–166.
- Al-Sady, B., Ni, W., Kircher, S., Schäfer, E., and Quail, P. H.** (2006). Photoactivated phytochrome induces rapid PIF3 phosphorylation prior to proteasome-mediated degradation. *Mol. Cell* 23, 439–446.
- Alba, R., Kelmenson, P. M., Cordonnier-Pratt, M. M., and Pratt, L. H.** (2000). The phytochrome gene family in tomato and the rapid differential evolution of this family in angiosperms. *Mol. Biol. Evol.* 17, 362–373.
- Amthor, J. S.** (2010). From sunlight to phytomass: On the potential efficiency of converting solar radiation to phyto-energy. *New Phytol.* 188, 939–959.
- Armarego-Marriott, T., Sandoval-Ibañez, O., and Kowalewska, Ł.** (2020). Beyond the darkness: Recent lessons from etiolation and de-etiolation studies. *J. Exp. Bot.* 71, 1215–1225.
- Arsovski, A. A., Galstyan, A., Guseman, J. M., and Nemhauser, J. L.** (2012). Photomorphogenesis. *Arab. B.* 10, e0147.
- Aukerman, M. J., and Sakai, H.** (2004). Regulation of flowering time and floral organ identity by a microRNA and its apetala2-like target genes. *Plant Cell* 15, 2730–2741.



- Ballaré, C. L., Scopel, A. L., and Sánchez, R. A.** (1990). Far-red radiation reflected from adjacent leaves: An early signal of competition in plant canopies. *Science* 247, 329–332.
- Bao, S., Hua, C., Huang, G., Cheng, P., Gong, X., Shen, L., and Yu, H.** (2019). Molecular basis of natural variation in photoperiodic flowering responses. *Dev. Cell* 50, 90–101.
- Bao, S., Hua, C., Shen, L., and Yu, H.** (2020). New insights into gibberellin signaling in regulating flowering in Arabidopsis. *J. Integr. Plant Biol.* 62, 118–131.
- Bar, M., and Ori, N.** (2014). Leaf development and morphogenesis. *Dev.* 141, 4219–4230.
- Barnes, C., Tibbitts, T., Sager, J., Deitzer, G., Bubenheim, D., Koerner, G., and Bugbee, B.** (1993). Accuracy of quantum sensors measuring yield photon flux and photosynthetic photon flux. *HortScience* 28, 1197–1200.
- Barra-Jiménez, A., and Ragni, L.** (2017). Secondary development in the stem: when Arabidopsis and trees are closer than it seems. *Curr. Opin. Plant Biol.* 35, 145–151.
- Bartlett, M. E., and Thompson, B.** (2014). Meristem identity and phyllotaxis in inflorescence development. *Front. Plant Sci.* 5, 1–11.
- Bayer, E. M., Smith, R. S., Mandel, T., Nakayama, N., Sauer, M., Prusinkiewicz, P., and Kuhlemeier, C.** (2009). Integration of transport-based models for phyllotaxis and midvein formation. *Genes Dev.* 23, 373–384.
- Benková, E., Michniewicz, M., Sauer, M., Teichmann, T., Seifertová, D., Jürgens, G., and Friml, J.** (2003). Local, efflux-dependent auxin gradients as a common module for plant organ formation. *Cell* 115, 591–602.
- Benlloch, R., Berbel, A., Serrano-Mislata, A., and Madueño, F.** (2007). Floral initiation and inflorescence architecture: A comparative view. *Ann. Bot.* 100, 659–676.
- Besnard, F., Refahi, Y., Morin, V., Marteaux, B., Brunoud, G., Chambrier, P., Rozier, F., Mirabet, V., Legrand, J., Lainé, S., Thévenon, E., Farcot, E.,**



Chapter 1: General introduction

- Cellier, C., Das, P., Bishopp, A., Dumas, R., Parcy, F., Helariutta, Y., Boudaoud, A., Godin, C., Traas, J., Guédon, Y., and Vernoux, T. (2014a).** Cytokinin signalling inhibitory fields provide robustness to phyllotaxis. *Nature* 505, 417–421.
- Besnard, F., Rozier, F., and Vernoux, T. (2014b).** The AHP6 cytokinin signaling inhibitor mediates an auxin-cytokinin crosstalk that regulates the timing of organ initiation at the shoot apical meristem. *Plant Signal. Behav.* 9, 4–7.
- Boccalandro, H. E., De Simone, S. N., Bergmann-Honsberger, A., Schepens, I., Fankhauser, C., and Casal, J. J. (2008).** Phytochrome kinase substrate1 regulates root phototropism and gravitropism. *Plant Physiol.* 146, 108–115.
- Borthwick, H. A., Hendricks, S. B., Parker, M. W., Toole, E. H., and Toole, V. K. (1952).** A reversible photoreaction controlling seed germination. *Proc. Natl. Acad. Sci. U. S. A.* 38, 662–666.
- Botterweg-Paredes, E., Blaakmeer, A., Hong, S. Y., Sun, B., Mineri, L., Kruusvee, V., Xie, Y., Straub, D., Ménard, D., Pesquet, E., and Wenkel, S. (2020).** Light affects tissue patterning of the hypocotyl in the shade-avoidance response. *PLOS Genet.* 16, e1008678.
- Brackmann, K., Qi, J., Gebert, M., Jouannet, V., Schlamp, T., Grünwald, K., Walner, E. S., Novikova, D. D., Levitsky, V. G., Augustí, J., Sanchez, P., Lohmann, J. U., and Greb, T. (2018).** Spatial specificity of auxin responses coordinates wood formation. *Nat. Commun.* 9.
- Brand, U., Fletcher, J. C., Hobe, M., Meyerowitz, E. M., and Simon, R. (2000).** Dependence of stem cell fate in Arabidopsis on a feedback loop regulated by CLV3 activity. *Science* 289, 617–619.
- Brand, U., Grünwald, M., Hobe, M., and Simon, R. (2002).** Regulation of CLV3 expression by two homeobox genes in Arabidopsis. *Plant Physiol.* 129, 565–575.
- Brautigam, C. A., Smith, B. S., Ma, Z., Palnitkar, M., Tomchick, D. R., Machius, M., and Deisenhofer, J. (2004).** Structure of the photolyase-like domain of cryptochrome 1 from *Arabidopsis thaliana*. *Proc. Natl. Acad. Sci. U. S. A.* 101, 12142–12147.



- Briggs, W. R., Beck, C. F., Cashmore, A. R., Christie, J. M., Hughes, J., Jarillo, J. A., Kagawa, T., Kanegae, H., Liscum, E., Nagatani, A., Okada, K., Salomon, M., Rüdiger, W., Sakai, T., Takano, M., Wada, M., and Watson, J. C.** (2001a). The phototropin family of photoreceptors. *Plant Cell* 13, 993–997.
- Briggs, W. R., Christie, J. M., and Salomon, M.** (2001b). Phototropins: A new family of flavin-binding blue light receptors in plants. *Antioxidants Redox Signal.* 3, 775–788.
- Briggs, W. R., and Christie, J. M.** (2002). Phototropins 1 and 2: Versatile plant blue-light receptors. *Trends Plant Sci.* 7, 204–210.
- Brown, B. A., and Jenkins, G. I.** (2008). UV-B signaling pathways with different fluence-rate response profiles are distinguished in mature arabidopsis leaf tissue by requirement for UVR8, HY5, and HYH. *Plant Physiol.* 146, 576–588.
- Brudler, R., Hitomi, K., Daiyasu, H., Toh, H., Kucho, K. I., Ishiura, M., Kanehisa, M., Roberts, V. A., Todo, T., Tainer, J. A., and Getzoff, E. D.** (2003). Identification of a new cryptochrome class: Structure, function, and evolution. *Mol. Cell* 11, 59–67.
- Bruno, T. J., and Svoronos, P. D.** (2005). CRC Handbook of fundamental spectroscopic correlation charts.
- Burgie, E. S., Bussell, A. N., Walker, J. M., Dubiel, K., and Vierstra, R. D.** (2014). Crystal structure of the photosensing module from a red/far-red light-absorbing plant phytochrome. *Proc. Natl. Acad. Sci. U. S. A.* 111, 10179–10184.
- Burgie, E. S., and Vierstra, R. D.** (2014). Phytochromes: An atomic perspective on photoactivation and signaling. *Plant Cell* 26, 568–4583.
- Buti, S., Hayes, S., and Pierik, R.** (2020). The bHLH network underlying plant shade-avoidance. *Physiol. Plant.* 169, 312–324.
- Cao, K., Cui, L., Ye, L., Zhou, X., Bao, E., Zhao, H., and Zou, Z.** (2016). Effects of red light night break treatment on growth and flowering of tomato plants. *Front. Plant Sci.* 7, 527.
- Casal, J. J., and Sánchez, R. A.** (1998). Phytochromes and seed germination. *Seed*



Chapter 1: General introduction

Sci. Res. 8, 317–329.

Casimiro, I., Marchant, A., Bhalerao, R. P., Beeckman, T., Dhooge, S., Swarup, R., Graham, N., Inzé, D., Sandberg, G., Casero, P. J., and Bennet, M. (2001). Auxin transport promotes *Arabidopsis* lateral root initiation. *Plant Cell* 13, 843–852.

Casson, S. A., and Lindsey, K. (2003). Genes and signalling in root development. *New Phytol.* 158, 11–38.

Chailakhyan, M. K. (1937). Hormonal theory of plant development. *Bull. Acad. Sci. U. R. S. S.* 198.

Chen, M., Tao, Y., Lim, J., Shaw, A., and Chory, J. (2005). Regulation of phytochrome B nuclear localization through light-dependent unmasking of nuclear-localization signals. *Curr. Biol.* 15, 637–642.

Chen, X. (2004). A microRNA as a transcriptional repressor of *APETALA2* in *Arabidopsis* flower development. *Science* 303, 2022–2025.

Chen, X., Yao, Q., Gao, X., Jiang, C., Harberd, N. P., and Fu, X. (2016). Shoot-to-root mobile transcription factor HY5 coordinates plant carbon and nitrogen acquisition. *Curr. Biol.* 26, 640–646.

Christie, J. M., and Murphy, A. S. (2013). Shoot phototropism in higher plants: New light through old concepts. *Am. J. Bot.* 100, 35–46.

Christie, J. M., Reymond, P., Powell, G. K., Bernasconi, P., Raibekas, A. A., Liscum, E., and Briggs, W. R. (1998). *Arabidopsis* NPH1: A flavoprotein with the properties of a photoreceptor for phototropism. *Science* 282, 1698–1701.

Christie, J. M., Salomon, M., Nozue, K., Wada, M., and Briggs, W. R. (1999). LOV (light, oxygen, or voltage) domains of the blue-light photoreceptor phototropin (nph1): Binding sites for the chromophore flavin mononucleotide. *Proc. Natl. Acad. Sci. U. S. A.* 96, 8779–8783.

Christie, J. M., Yang, H., Richter, G. L., Sullivan, S., Thomson, C. E., Lin, J., Titapiwatanakun, B., Ennis, M., Kaiserli, E., Lee, O. R., Adamec, J., Peer, W. A., and Murphy, A. S. (2011). Phot1 inhibition of ABCB19 primes lateral auxin fluxes in the shoot apex required for phototropism. *PLoS Biol.* 9:



e1001076.

- Conti, L., and Bradley, D.** (2007). TERMINAL FLOWER1 is a mobile signal controlling Arabidopsis architecture. *Plant Cell* 19, 767–778.
- Corbesier, L., Vincent, C., Jang, S., Fornara, F., Fan, Q., Searle, I., Giakountis, A., Farrona, S., Gissot, L., Turnbull, C., and Coupland, G.** (2007). FT protein movement contributes to long-distance signaling in floral induction of Arabidopsis. *Science* 316, 1030–1033.
- Courbier, S., and Pierik, R.** (2019). Canopy light quality modulates stress responses in plants. *iScience* 22, 441–452.
- Darwin, C., Darwin, C., Darwin, F., and Leeds., U.** (1880). *The power of movement in plants*. London : John Murray, doi:10.5962/bhl.title.102319.
- Daum, G., Medzihradszky, A., Suzaki, T., and Lohmann, J. U.** (2014). A mechanistic framework for noncell autonomous stem cell induction in Arabidopsis. *Proc. Natl. Acad. Sci. U. S. A.* 111, 14619–14624.
- Davière, J. M., and Achard, P.** (2016). A pivotal role of DELLAs in regulating multiple hormone signals. *Mol. Plant* 9, 10–20.
- Davière, J. M., Wild, M., Regnault, T., Baumberger, N., Eisler, H., Genschik, P., and Achard, P.** (2014). Class I TCP-DELLA interactions in inflorescence shoot apex determine plant height. *Curr. Biol.* 24, 1923–1928.
- de Carbonnel, M., Davis, P., Roelfsema, M. R. G., Inoue, S. I., Schepens, I., Lariguet, P., Geisler, M., Shimazaki, K. I., Hangarter, R., and Fankhauser, C.** (2010). The Arabidopsis PHYTOCHROME KINASE SUBSTRATE2 protein is a phototropin signaling element that regulates leaf flattening and leaf positioning. *Plant Physiol.* 152, 1391–1405.
- de Wit, M., Galvão, V. C., and Fankhauser, C.** (2016). Light-mediated hormonal regulation of plant growth and development. *Annu. Rev. Plant Biol.* 67, 513–537.
- Di Wu, Hu, Q., Yan, Z., Chen, W., Yan, C., Huang, X., Zhang, J., Yang, P., Deng, H., Wang, J., Deng, X., Shi, Y.** (2012). Structural basis of ultraviolet-B perception by UVR8. *Nature* 484, 214–219.



Chapter 1: General introduction

- Dong, J., Tang, D., Gao, Z., Yu, R., Li, K., He, H., Terzaghi, W., Deng, X. W., and Chen, H.** (2014). Arabidopsis DE-ETIOLATED1 represses photomorphogenesis by positively regulating phytochrome-interacting factors in the dark. *Plant Cell* 26, 3630–3645.
- Dong, J., Terzaghi, W., Deng, X. W., and Chen, H.** (2015). Multiple photomorphogenic repressors work in concert to regulate Arabidopsis seedling development. *Plant Signal. Behav.* 10, 33–36.
- Dougher, T. A. O., and Bugbee, B.** (2001). Differences in the response of wheat, soybean and lettuce to reduced blue radiation. *Photochem. Photobiol.* 73, 199.
- Du, F., Guan, C., and Jiao, Y.** (2018). Molecular mechanisms of leaf morphogenesis. *Mol. Plant* 11, 1117–1134.
- Duek, P. D., Elmer, M. V., Van Oosten, V. R., and Fankhauser, C.** (2004). The degradation of HFR1, a putative bHLH class transcription factor involved in light signaling, is regulated by phosphorylation and requires COP1. *Curr. Biol.* 14, 2296–2301.
- Elliott, R. C., Betzner, A. S., Huttner, E., Oakes, M. P., Tucker, W. Q. J., Gerentes, D., Perez, P., and Smyth, D. R.** (1996). AINTEGUMENTA, an APETALA2-like gene of Arabidopsis with pleiotropic roles in ovule development and floral organ growth. *Plant Cell* 8, 155–168.
- Etchells, J. P., Provost, C. M., Mishr, L., and Turner, S. R.** (2013). WOX4 and WOX14 act downstream of the PXY receptor kinase to regulate plant vascular proliferation independently of any role in vascular organisation. *Development* 140, 2224–2234.
- Etchells, J. P., Smit, M. E., Gaudinier, A., Williams, C. J., and Brady, S. M.** (2016). A brief history of the TDIF-PXY signalling module: balancing meristem identity and differentiation during vascular development. *New Phytol.* 209, 474–484.
- Facella, P., Lopez, L., Chiappetta, A., Bitonti, M. B., Giuliano, G., and Perrotta, G.** (2006). CRY-DASH gene expression is under the control of the circadian clock machinery in tomato. *FEBS Lett.* 580, 4618–4624.



- Fantini, E., Sulli, M., Zhang, L., Aprea, G., Jiménez-Gómez, J. M., Bendahmane, A., Perrotta, G., Giuliano, G., and Facella, P. (2019).** Pivotal roles of cryptochromes 1a and 2 in tomato development and physiology 1. *Plant Physiol.* 179, 732–748.
- Favory, J. J., Stec, A., Gruber, H., Rizzini, L., Oravecz, A., Funk, M., Albert, A., Cloix, C., Jenkins, G. I., Oakely, E. J., Seidlitz, H. K., Nagy, F., and Ulm, R. (2009).** Interaction of COP1 and UVR8 regulates UV-B-induced photomorphogenesis and stress acclimation in Arabidopsis. *EMBO J.* 28, 591–601.
- Feng, S., Martinez, C., Gusmaroli, G., Wang, Y., Zhou, J., Wang, F., Chen, L., Yu, L., Iglesias-Pedraz, J. M., Kircher, S., Schäfer, E., Fu, X., Fan, L. M., and Deng, X. W. (2008).** Coordinated regulation of Arabidopsis thaliana development by light and gibberellins. *Nature*, 451, 475–479.
- Folta, K. M., and Maruhnich, S. A. (2007).** Green light: A signal to slow down or stop. *J. Exp. Bot.* 58, 3099–3111.
- Fornara, F., Panigrahi, K. C. S., Gissot, L., Sauerbrunn, N., Rühl, M., Jarillo, J. A., and Coupland, G. (2009).** Arabidopsis DOF transcription factors act redundantly to reduce CONSTANS expression and are essential for a photoperiodic flowering response. *Dev. Cell* 17, 75–86.
- Franklin, K. A., and Quail, P. H. (2010).** Phytochrome functions in Arabidopsis development. *J. Exp. Bot.* 61, 11–24.
- Fujiwara, S., Wang, L., Han, L., Suh, S. S., Salomé, P. A., McClung, C. R., and Somers, D. E. (2008).** Post-translational regulation of the Arabidopsis circadian clock through selective proteolysis and phosphorylation of pseudo-response regulator proteins. *J. Biol. Chem.* 283, 23073–23083.
- Gallego-Bartolomé, J., Minguet, E. G., Marín, J. A., Prat, S., Blázquez, M. A., and Alabadí, D. (2010).** Transcriptional diversification and functional conservation between DELLA proteins in Arabidopsis. *Mol. Biol. Evol.* 27, 1247–1256.
- Gallego-Bartolomé, J., Minguet, E. G., Grau-Enguix, F., Abbas, M., Locascio, A., Thomas, S. G., Alabadí, D., and Blázquez, M. A. (2012).** Molecular



Chapter 1: General introduction

mechanism for the interaction between gibberellin and brassinosteroid signaling pathways in *Arabidopsis*. *Proc. Natl. Acad. Sci. U. S. A.* 109, 13446–13451.

Galinat, W. C. (1959). The phytomer in relation to floral homologies in the American Maydeae. *JSTOR*. 19, 1-32.

Galvan-Ampudia, C. S., Cerutti, G., Legrand, J., Brunoud, G., Martin-Arevalillo, R., Azais, R., Bayle, V., Moussu, S., Wenzl, C., Jaillais, Y., Lohmann, J. U., Godin, C., and Vernoux, T. (2020). Temporal integration of auxin information for the regulation of patterning. *Elife* 9, 1–65.

Galvão, V. C., and Fankhauser, C. (2015). Sensing the light environment in plants: Photoreceptors and early signaling steps. *Curr. Opin. Neurobiol.* 34, 46–53.

Gälweiler, L., Guan, C., Müller, A., Wisman, E., Mendgen, K., Yephremov, A., and Palme, K. (1998). Regulation of polar auxin transport by AtPIN1 in *Arabidopsis* vascular tissue. *Science* 282, 2226–2230.

Gawronska, H., Yang, Y. Y., Furukawa, K., Kendrick, R. E., Takahashi, N., and Kamiya, Y. (1995). Effects of low irradiance stress on gibberellin levels in pea seedlings. *Plant Cell Physiol.* 36, 1361–1367.

Gil, K. E., Kim, W. Y., Lee, H. J., Faisal, M., Saquib, Q., Alatar, A. A., and Park, C. M. (2017). ZEITLUPE contributes to a thermoresponsive protein quality control system in *Arabidopsis*. *Plant Cell* 29, 2882–2894.

Giovani, B., Byrdin, M., Ahmad, M., and Brettel, K. (2003). Light-induced electron transfer in a cryptochrome blue-light photoreceptor. *Nat. Struct. Biol.* 10, 489–490.

Gordon, S. P., Chickarmane, V. S., Ohno, C., and Meyerowitz, E. M. (2009). Multiple feedback loops through cytokinin signaling control stem cell number within the *Arabidopsis* shoot meristem. *Proc. Natl. Acad. Sci. U. S. A.* 106, 16529–16534.

Gruber, H., Heijde, M., Heller, W., Albert, A., Seidlitz, H. K., and Ulm, R. (2010). Negative feedback regulation of UV-B-induced photomorphogenesis and stress acclimation in *Arabidopsis*. *Proc. Natl. Acad. Sci. U. S. A.* 107, 20132–20137.

Guo, C., Xu, Y., Shi, M., Lai, Y., Wu, X., Wang, H., Zhu, Z., Poethig, R. S., and



- Wu, G.** (2017). Repression of miR156 by miR159 regulates the timing of the juvenile-to-adult transition in arabidopsis. *Plant Cell* 29, 1293–1304.
- Guo, M., Thomas, J., Collins, G., and Timmermans, M. C. P.** (2008). Direct repression of KNOX loci by the ASYMMETRIC LEAVES1 complex of Arabidopsis. *Plant Cell* 20, 48–58.
- Han, S., Cho, H., Noh, J., Qi, J., Jung, H. J., Nam, H., Lee, S., Hwang, D., Greb, T., and Hwang, I.** (2018). BIL1-mediated MP phosphorylation integrates PXY and cytokinin signalling in secondary growth. *Nat. Plants* 48(4), 605–614.
- Hanks, S. K., and Hunter, T.** (1995). The eukaryotic protein kinase superfamily: kinase (catalytic) domain structure and classification 1. *FASEB J.* 9, 576–596.
- Harada, A., Sakai, T., and Okada, K.** (2003). Phot1 and phot2 mediate blue light-induced transient increases in cytosolic Ca²⁺ differently in Arabidopsis leaves. *Proc. Natl. Acad. Sci. U. S. A.* 100, 8583–8588.
- Harmon, F., Imaizumi, T., and Gray, W. M.** (2008). CUL1 regulates TOC1 protein stability in the Arabidopsis circadian clock. *Plant J.* 55, 568–579.
- Hauser, B. A., Cordonnier-Pratt, M. M., Daniel-Vedele, F., and Pratt, L. H.** (1995). The phytochrome gene family in tomato includes a novel subfamily. *Plant Mol. Biol.* 29, 1143–1155.
- Hayama, R., and Coupland, G.** (2004). The molecular basis of diversity in the photoperiodic flowering responses of arabidopsis and rice. *Plant Physiol.* 135, 677–684.
- Hayama, R., Yokoi, S., Tamaki, S., Yano, M., and Shimamoto, K.** (2003). Adaptation of photoperiodic control pathways produces short-day flowering in rice. *Nature* 422, 719–722.
- He, G., Liu, J., Dong, H., and Sun, J.** (2019). The blue-light receptor CRY1 interacts with BZR1 and BIN2 to modulate the phosphorylation and nuclear function of BZR1 in repressing BR signaling in Arabidopsis. *Mol. Plant* 12, 689–703.
- Heijde, M., and Ulm, R.** (2013). Reversion of the Arabidopsis UV-B photoreceptor UVR8 to the homodimeric ground state. *Proc. Natl. Acad. Sci. U. S. A.* 110, 1113–1118.



Chapter 1: General introduction

- Heisler, M. G., Ohno, C., Das, P., Sieber, P., Reddy, G. V., Long, J. A., and Meyerowitz, E. M.** (2005). Patterns of auxin transport and gene expression during primordium development revealed by live imaging of the Arabidopsis inflorescence meristem. *Curr. Biol.* 15, 1899–1911.
- Heo, J., Lee, C., Chakrabarty, D., and Paek, K.** (2002). Growth responses of marigold and salvia bedding plants as affected by monochromatic or mixture radiation provided by a Light-Emitting Diode (LED). *Plant Growth Regul.* 38, 225–230.
- Hershey, H. P., Barker, R. F., Idler, K. B., Lissemore, J. L., and Quail, P. H.** (1985). Analysis of cloned cDNA and genomic sequences for phytochrome: Complete amino acid sequences for two gene products expressed in etiolated Avena. *Nucleic Acids Res.* 13, 8543–8559.
- Higuchi, Y.** (2018). Florigen and anti-florigen: Flowering regulation in horticultural crops. *Breed. Sci.* 68, 109–118.
- Hiltbrunner, A., Tscheuschler, A., Viczián, A., Kunkel, T., Kircher, S., and Schäfer, E.** (2006). FHY1 and FHL act together to mediate nuclear accumulation of the phytochrome A photoreceptor. *Plant Cell Physiol.* 47, 1023–1034.
- Hisamatsu, T., and King, R. W.** (2008). The nature of floral signals in Arabidopsis. II. Roles for FLOWERING LOCUS T (FT) and gibberellin. *J. Exp. Bot.* 59, 3821–3829.
- Hisamatsu, T., King, R. W., Helliwell, C. A., and Koshioka, M.** (2005). The involvement of gibberellin 20-oxidase genes in phytochrome-regulated petiole elongation of Arabidopsis. *Plant Physiol.* 138, 1106–1116.
- Hogewoning, S. W., Wientjes, E., Douwstra, P., Trouwborst, G., van Ieperen, W., Croce, R., and Harbinson, J.** (2012). Photosynthetic quantum yield dynamics: From photosystems to leaves. *Plant Cell* 24, 1921–1935.
- Holst, K., Schmölling, T., and Werner, T.** (2011). Enhanced cytokinin degradation in leaf primordia of transgenic Arabidopsis plants reduces leaf size and shoot organ primordia formation. *J. Plant Physiol.* 168, 1328–1334.



- Hou, X., Zhou, J., Liu, C., Liu, L., Shen, L., and Yu, H.** (2014). Nuclear factor Y-mediated H3K27me3 demethylation of the SOC1 locus orchestrates flowering responses of Arabidopsis. *Nat. Commun.* 5, 4601.
- Huala, E., Oeller, P. W., Liscum, E., Han, I. S., Larsen, E., and Briggs, W. R.** (1997). Arabidopsis NPH1: A protein kinase with a putative redox-sensing domain. *Science* 278, 2120–2123.
- Huang, J., Zhao, X., and Chory, J.** (2019). The Arabidopsis transcriptome responds specifically and dynamically to high light stress. *Cell Rep.* 29, 4186–4199.
- Huijser, P., and Schmid, M.** (2011). The control of developmental phase transitions in plants. *Development* 138, 4117–4129.
- Huq, E., Al-Sady, B., Hudson, M., Kim, C., Apel, K., and Quail, P. H.** (2004). Phytochrome-interacting factor 1 is a critical bHLH: Regulator of chlorophyll biosynthesis. *Science* 305, 1937–1941.
- Immink, R. G. H., Posé, D., Ferrario, S., Ott, F., Kaufmann, K., Valentim, F. L., de Folter, S., van der Wal, F., van Dijk, A. D. J., Schmid, M., and Angenent, G. C.** (2012). Characterization of SOC1's central role in flowering by the identification of its upstream and downstream regulators. *Plant Physiol.* 160, 433–449.
- Inada, S., Ohgishi, M., Mayama, T., Okada, K., and Sakai, T.** (2004). RPT2 is a signal transducer involved in phototropic response and stomatal opening by association with phototropin 1 in *Arabidopsis thaliana*. *Plant Cell* 16, 887–896.
- Ito, S., Song, Y. H., and Imaizumi, T.** (2012). LOV domain-containing F-box proteins: Light-dependent protein degradation modules in Arabidopsis. *Mol. Plant* 5, 573–582.
- Jacobsen, S. E., and Olszewski, N. E.** (1993). Mutations at the SPINDLY locus of Arabidopsis alter gibberellin signal transduction. *Plant Cell* 5, 887–896.
- Jaedicke, K., Lichtenthäler, A. L., Meyberg, R., Zeidler, M., and Hughes, J.** (2012). A phytochrome-phototropin light signaling complex at the plasma membrane. *Proc. Natl. Acad. Sci. U. S. A.* 109, 12231–12236.
- Jing, H., and Strader, L. C.** (2019). Interplay of auxin and cytokinin in lateral root



Chapter 1: General introduction

- development. *Int. J. Mol. Sci.* 20, 486.
- Johansson, M., and Staiger, D.** (2015). Time to flower: Interplay between photoperiod and the circadian clock. *J. Exp. Bot.* 66, 719–730.
- Jung, J. H., Ju, Y., Seo, P. J., Lee, J. H., and Park, C. M.** (2012). The SOC1-SPL module integrates photoperiod and gibberellic acid signals to control flowering time in *Arabidopsis*. *Plant J.* 69, 577–588.
- Karami, O., Rahimi, A., Khan, M., Bemer, M., Hazarika, R. R., Mak, P., Compier, M., van Noort, V., and Offringa, R.** (2020). A suppressor of axillary meristem maturation promotes longevity in flowering plants. *Nat. Plants* 6, 368–376.
- Keuskamp, D. H., Pollmann, S., Voeselek, L. A. C. J., Peeters, A. J. M., and Pierik, R.** (2010). Auxin transport through PIN-FORMED 3 (PIN3) controls shade avoidance and fitness during competition. *Proc. Natl. Acad. Sci. U. S. A.* 107, 22740–22744.
- Kevei, E., Schafer, E., and Nagy, F.** (2007). Light-regulated nucleo-cytoplasmic partitioning of phytochromes. *J. Exp. Bot.* 58, 3113–3124.
- Khurana, J. P., and Poff, K. L.** (1989). Mutants of *Arabidopsis thaliana* with altered phototropism. *Planta* 178, 400–406.
- Kiba, T., Henriques, R., Sakakibara, H., and Chua, N. H.** (2007). Targeted degradation of PSEUDO-RESPONSE REGULATOR5 by an SCFZTL complex regulates clock function and photomorphogenesis in *Arabidopsis thaliana*. *Plant Cell* 19, 2516–2530.
- Kierzkowski, D., Lenhard, M., Smith, R., and Kuhlemeier, C.** (2013). Interaction between meristem tissue layers controls phyllotaxis. *Dev. Cell* 26, 616–628.
- Kim, D.-H., and Sung, S.** (2014). Genetic and epigenetic mechanisms underlying vernalization. *Arab. B.* 12, e0171.
- Kircher, S., Gil, P., Kozma-Bognár, L., Fejes, E., Speth, V., Husselstein-Muller, T., Bauer, D., Adám, E., Schäfer, E., and Nagy, F.** (2002). Nucleocytoplasmic partitioning of the plant photoreceptors phytochrome A, B, C, D, and E is regulated differentially by light and exhibits a diurnal rhythm.



Plant Cell 14, 1541–1555.

- Kircher, S., and Schopfer, P.** (2012). Photosynthetic sucrose acts as cotyledon-derived long-distance signal to control root growth during early seedling development in *Arabidopsis*. *Proc. Natl. Acad. Sci. U. S. A.* 109, 11217–11221.
- Kleine, T., Lockhart, P., and Batschauer, A.** (2003). An *Arabidopsis* protein closely related to *Synechocystis* cryptochrome is targeted to organelles. *Plant J.* 35, 93–103.
- Kliebenstein, D. J., Lim, J. E., Landry, L. G., and Last, R. L.** (2002). *Arabidopsis* UVR8 regulates ultraviolet-B signal transduction and tolerance and contains sequence similarity to human Regulator of Chromatin Condensation 1. *Plant Physiol.* 130, 234–243.
- Klose, C., Viczián, A., Kircher, S., Schäfer, E., and Nagy, F.** (2015). Molecular mechanisms for mediating light-dependent nucleo/cytoplasmic partitioning of phytochrome photoreceptors. *New Phytol.* 206, 965–971.
- Ko, D., Kang, J., Kiba, T., Park, J., Kojima, M., Do, J., Kim, K. Y., Kwon, M., Endler, A., Song, W. Y., Martinoia, E., Sakakibara, H., and Lee, Y.** (2014). *Arabidopsis* ABCG14 is essential for the root-to-shoot translocation of cytokinin. *Proc. Natl. Acad. Sci. U. S. A.* 111, 7150–7155.
- Kong, S. G., Suzuki, T., Tamura, K., Mochizuki, N., Hara-Nishimura, I., and Nagatani, A.** (2006). Blue light-induced association of phototropin 2 with the Golgi apparatus. *Plant J.* 45, 994–1005.
- Kotoda, N., Hayashi, H., Suzuki, M., Igarashi, M., Hatsuyama, Y., Kidou, S. I., Igasaki, T., Nishiguchi, M., Yano, K., Shimizu, T., Takahashi, S., Iwanami, H., Moriya, S., and Abe, K.** (2010). Molecular characterization of flowering LOCUS t-like genes of apple (*malus* × *domestica* borkh.). *Plant Cell Physiol.* 51, 561–575.
- Kozuka, T., Horiguchi, G., Kim, G. T., Ohgishi, M., Sakai, T., and Tsukaya, H.** (2005). The different growth responses of the *Arabidopsis thaliana* leaf blade and the petiole during shade avoidance are regulated by photoreceptors and sugar. *Plant Cell Physiol.* 46, 213–223.



Chapter 1: General introduction

- Krizek, B. A.** (2009). AINTEGUMENTA and AINTEGUMENTA-LIKE6 act redundantly to regulate Arabidopsis floral growth and patterning. *Plant Physiol.* 150, 1916–1929.
- Krizek, D. T.** (2004). Influence of PAR and UV-A in determining plant sensitivity and photomorphogenic responses to UV-B Radiation. *Photochem. Photobiol.* 79, 307.
- Krogan, N. T., Marcos, D., Weiner, A. I., and Berleth, T.** (2016). The auxin response factor MONOPTEROS controls meristem function and organogenesis in both the shoot and root through the direct regulation of PIN genes. *New Phytol.* 212, 42–50.
- Kubo, M., Udagawa, M., Nishikubo, N., Horiguchi, G., Yamaguchi, M., Ito, J., Mimura, T., Fukuda, H., and Demura, T.** (2005). Transcription switches for protoxylem and metaxylem vessel formation. *Genes Dev.* 19, 1855–1860.
- Kume, A.** (2017). Importance of the green color, absorption gradient, and spectral absorption of chloroplasts for the radiative energy balance of leaves. *J. Plant Res.* 130, 501–514.
- Kurakawa, T., Ueda, N., Maekawa, M., Kobayashi, K., Kojima, M., Nagato, Y., Sakakibara, H., and Kyojuka, J.** (2007). Direct control of shoot meristem activity by a cytokinin-activating enzyme. *Nature* 445, 652–655.
- Lariguet, P., Schepens, I., Hodgson, D., Pedmale, U. V., Trevisan, M., Kami, C., de Carbonnel, M., Alonso, J. M., Ecker, J. R., Liscum, E., and Fankhauser, C.** (2006). Phytochrome kinase substrate 1 is a phototropin 1 binding protein required for phototropism. *Proc. Natl. Acad. Sci. U. S. A.* 103, 10134–10139.
- Lee, J., Oh, M., Park, H., and Lee, I.** (2008). SOC1 translocated to the nucleus by interaction with AGL24 directly regulates LEAFY. *Plant J.* 55, 832–843.
- Legris, M., Ince, Y. Ç., and Fankhauser, C.** (2019). Molecular mechanisms underlying phytochrome-controlled morphogenesis in plants. *Nat. Commun.* 10, 5219.
- Leibfried, A., To, J. P. C., Busch, W., Stehling, S., Kehle, A., Demar, M., Kieber, J. J., and Lohmann, J. U.** (2005). WUSCHEL controls meristem function by



direct regulation of cytokinin-inducible response regulators. *Nature* 438, 1172–1175.

Leivar, P., Monte, E., Al-Sady, B., Carle, C., Storer, A., Alonso, J. M., Ecker, J. R., and Quail, P. H. (2008). The Arabidopsis phytochrome-interacting factor PIF7, together with PIF3 and PIF4, regulates responses to prolonged red light by modulating phyB levels. *Plant Cell* 20, 337–352.

Leivar, P., Tepperman, J. M., Cohn, M. M., Monte, E., Al-Sady, B., Erickson, E., and Quail, P. H. (2012). Dynamic antagonism between phytochromes and PIF family basic helix-loop-helix factors induces selective reciprocal responses to light and shade in a rapidly responsive transcriptional network in Arabidopsis. *Plant Cell* 24, 1398–1419.

Lejay, L., Wirth, J., Pervent, M., Cross, J. M. F., Tillard, P., and Gojon, A. (2008). Oxidative pentose phosphate pathway-dependent sugar sensing as a mechanism for regulation of root ion transporters by photosynthesis. *Plant Physiol.* 146, 2036–2053.

Leyser, O. (2018). Auxin signaling. *Plant Physiol.* 176, 465–479.

Li-Li, C., Zhang, K., Gong, X.-C., Wang, H.-Y., You-Hui, G., Wang, X.-Q., Zeng, Z. H., and Hu, Y. G. (2020). Effects of different LEDs light spectrum on the growth, leaf anatomy, and chloroplast ultrastructure of potato plantlets in vitro and minituber production after transplanting in the greenhouse. *J. Integr. Agric.* 2020, 108–119.

Li, F. W., Melkonian, M., Rothfels, C. J., Villarreal, J. C., Stevenson, D. W., Graham, S. W., Wong, G. K. S., Pryer, K. M., and Mathews, S. (2015). Phytochrome diversity in green plants and the origin of canonical plant phytochromes. *Nat. Commun.* 6, 7852.

Li, H., Li, Y., Deng, H., Sun, X., Wang, A., Tang, X., Gao, Y., Zhang, N., Wang, L., Yang, S., Liu, Y., and Wang, S. (2018). Tomato UV-B receptor *SIUVR8* mediates plant acclimation to UV-B radiation and enhances fruit chloroplast development via regulating *SlGLK2*. *Sci. Rep.* 8, 1–12.

Li, J., Yang, L., Jin, D., Nezames, C. D., Terzaghi, W., and Deng, X. W. (2013). UV-B-induced photomorphogenesis in Arabidopsis. *Protein Cell* 4, 485–492.



Chapter 1: General introduction

- Li, L., Ljung, K., Breton, G., Schmitz, R. J., Pruneda-Paz, J., Cowing-Zitron, C., Cole, B. J., Ivans, L. J., Pedmale, U. V., Jung, H. S., Ecker, J. R., Kay, S. A., and Chory, J.** (2012a). Linking photoreceptor excitation to changes in plant architecture. *Genes Dev.* 26, 785–790.
- Li, M., An, F., Li, W., Ma, M., Feng, Y., Zhang, X., and Guo, H.** (2016a). DELLA proteins interact with FLC to repress flowering transition. *J. Integr. Plant Biol.* 58, 642–655.
- Li, Q. F., Wang, C., Jiang, L., Li, S., Sun, S. S. M., and He, J. X.** (2012b). An interaction between BZR1 and DELLAs mediates direct signaling crosstalk between brassinosteroids and gibberellins in Arabidopsis. *Sci. Signal.* 5, 244.
- Li, W., Wang, H., and Yu, D.** (2016b). Arabidopsis WRKY transcription factors WRKY12 and WRKY13 oppositely regulate flowering under short-day conditions. *Mol. Plant* 9, 1492–1503.
- Li, X., Wang, Q., Yu, X., Liu, H., Yang, H., Zhao, C., Liu, X., Tan, C., Klejnot, J., Zhong, D., and Lin, C.** (2011). Arabidopsis cryptochrome 2 (CRY2) functions by the photoactivation mechanism distinct from the tryptophan (trp) triad-dependent photoreduction. *Proc. Natl. Acad. Sci. U. S. A.* 108, 20844–20849.
- Lian, H. L., He, S. B., Zhang, Y. C., Zhu, D. M., Zhang, J. Y., Jia, K. P., Sun, S. X., Li, L., and Yang, H. Q.** (2011). Blue-light-dependent interaction of cryptochrome 1 with SPA1 defines a dynamic signaling mechanism. *Genes Dev.* 25, 1023–1028.
- Lifschitz, E., and Eshed, Y.** (2006). Universal florigenic signals triggered by FT homologues regulate growth and flowering cycles in perennial day-neutral tomato. *J. Exp. Bot.* 57, 3405–3414.
- Lifschitz, E., Eviatar, T., Rozman, A., Shalit, A., Goldshmidt, A., Amsellem, Z., Alvarez, J. P., and Eshed, Y.** (2006). The tomato FT ortholog triggers systemic signals that regulate growth and flowering and substitute for diverse environmental stimuli. *Proc. Natl. Acad. Sci. U. S. A.* 103, 6398–6403.
- Lin, C., Ahmad, M., Gordon, D., and Cashmore, A. R.** (1995a). Expression of an Arabidopsis cryptochrome gene in transgenic tobacco results in hypersensitivity



- to blue, UV-A, and green light. *Proc. Natl. Acad. Sci. U. S. A.* 92, 8423–8427.
- Lin, C., Robertson, D. E., Ahmad, M., Raibekas, A. A., Jorns, M. S., Dutton, P. L., and Cashmore, A. R.** (1995b). Association of flavin adenine dinucleotide with the Arabidopsis blue light receptor CRY1. *Science* 269, 968–970.
- Lin, C., and Shalitin, D.** (2003). Cryptochrome structure and signal transduction. *Annu. Rev. Plant Biol.* 54, 469–496.
- Lin, C., and Todo, T.** (2005). The cryptochromes. *Genome Biol.* 6(5) 220.
- Liscum, E., and Briggs, W. R.** (1995). Mutations in the NPH1 locus of Arabidopsis disrupt the perception of phototropic stimuli. *Plant Cell* 7, 473.
- Liu, L. J., Zhang, Y. C., Li, Q. H., Sang, Y., Mao, J., Lian, H. L., Wang, L., and Yang, H. Q.** (2008). COP1-mediated ubiquitination of CONSTANS is implicated in cryptochrome regulation of flowering in Arabidopsis. *Plant Cell* 20, 292–306.
- Liu, Y., Li, X., Li, K., Liu, H., and Lin, C.** (2013). Multiple bHLH proteins form heterodimers to mediate CRY2-dependent regulation of flowering-time in Arabidopsis. *PLoS Genet.* 9(10): e1003861.
- López-Juez, E., Dillon, E., Magyar, Z., Khan, S., Hazeldine, S., De Jager, S. M., Murray, J. A. H., Beemster, G. T. S., Bögre, L., and Shanahan, H.** (2008). Distinct light-initiated gene expression and cell cycle programs in the shoot apex and cotyledons of Arabidopsis. *Plant Cell* 20, 947–968.
- Lorrain, S., Allen, T., Duek, P. D., Whitelam, G. C., and Fankhauser, C.** (2008). Phytochrome-mediated inhibition of shade avoidance involves degradation of growth-promoting bHLH transcription factors. *Plant J.* 53, 312–323.
- Losi, A., and Gärtner, W.** (2017). Solving blue light riddles: New lessons from flavin-binding LOV photoreceptors. *Photochem. Photobiol.* 93, 141–158.
- Low, V. H. K.** (1971). Effects of light and darkness on the growth of peas. *Aust. J. Biol. Sci.* 24, 187–196.
- Lucas, M. Daviere, J. M., Rodríguez-Falcon, M., Pontin, M., Iglesias-Pedras, J. M., Lorrain, S., Fankhauser, C., Blázquez, M. A., Titarenko, E., and Prat,**



Chapter 1: General introduction

- S. (2008). A molecular framework for light and gibberellin control of cell elongation. *Nature* 451, 480–484.
- Luo, L., Zeng, J., Wu, H., Tian, Z., and Zhao, Z.** (2018). A molecular framework for auxin-controlled homeostasis of shoot stem cells in *Arabidopsis*. *Mol. Plant* 11, 899–913.
- Ma, D., Li, X., Guo, Y., Chu, J., Fang, S., Yan, C., Noel, J. P., and Liu, H.** (2016). Cryptochrome 1 interacts with PIF4 to regulate high temperature-mediated hypocotyl elongation in response to blue light. *Proc. Natl. Acad. Sci. U. S. A.* 113, 224–229.
- Ma, L., Li, J., Qu, L., Hager, J., Chen, Z., Zhao, H., and Deng, X. W.** (2001). Light control of *Arabidopsis* development entails coordinated regulation of genome expression and cellular pathways. *Plant Cell* 13, 2589–2607.
- MacMillan, C. P., O'Donnell, P. J., Smit, A. M., Evans, R., Stachurski, Z. H., Torr, K., West, M., Baltunis, J., and Strabala, T. J.** (2013). A survey of the natural variation in biomechanical and cell wall properties in inflorescence stems reveals new insights into the utility of *Arabidopsis* as a wood model. *Funct. Plant Biol.* 40, 662–676.
- Malhotra, K., Kim, S. T., Batschauer, A., Dawut, L., and Sancar, A.** (1995). Putative blue-light photoreceptors from *Arabidopsis thaliana* and *Sinapis alba* with a high degree of sequence homology to DNA photolyase contain the two photolyase cofactors but lack DNA repair activity. *Biochemistry* 34, 6892–6899.
- Mancinelli, A. L., Borthwick, H. A., and Hendricks, S. B.** (1966). Phytochrome action in tomato seed germination. *Bot. Gaz.* 127, 1–5.
- Martínez, C., Espinosa-Ruíz, A., Lucas, M. de, Bernardo-García, S., Franco-Zorrilla, J. M., and Prat, S.** (2018). PIF4-induced BR synthesis is critical to diurnal and thermomorphogenic growth. *EMBO J.* 37, e99552.
- Mas, P., Devlin, P. F., Panda, S., and Kay, S. A.** (2000). Functional interaction of phytochrome B and cryptochrome 2. *Nature* 408, 207–211.
- Más, P., Kim, W. Y., Somers, D. E., and Kay, S. A.** (2003). Targeted degradation of TOC1 by ZTL modulates circadian function in *Arabidopsis thaliana*. *Nature*



426, 567–570.

- Masson, P. H., Tasaka, M., Morita, M. T., Guan, C., Chen, R., and Boonsirichai, K.** (2002). *Arabidopsis thaliana*: A model for the study of root and shoot gravitropism. *Arab. B.* 1, e0043.
- Mathews, S., and Sharrock, R. A.** (1997). Phytochrome gene diversity. *Plant, Cell Environ.* 20, 666–671.
- Mayer, K. F. X., Schoof, H., Haecker, A., Lenhard, M., Jürgens, G., and Laux, T.** (1998). Role of WUSCHEL in regulating stem cell fate in the *Arabidopsis* shoot meristem. *Cell* 95, 805–815.
- Mazzella, M. A., Casal, J. J., Muschietti, J. P., and Fox, A. R.** (2014). Hormonal networks involved in apical hook development in darkness and their response to light. *Front. Plant Sci.* 5, 1–13.
- McCree, K. J.** (1972). Test of current definitions of photosynthetically active radiation against leaf photosynthesis data. *Agric. Meteorol.* 10, 443–453.
- Mei, Q., and Dvornyk, V.** (2015). Evolutionary history of the photolyase/cryptochrome superfamily in eukaryotes. *PLoS One* 10, 1–20.
- Meng, W. J., Cheng, Z. J., Sang, Y. L., Zhang, M. M., Rong, X. F., Wang, Z. W., Tang, Y. Y., and Zhang, X. S.** (2017). Type-B ARABIDOPSIS RESPONSE REGULATORS specify the shoot stem cell niche by dual regulation of WUSCHEL. *Plant Cell* 29, 1357–1372.
- Michael, A. K., Fribourgh, J. L., Van Gelder, R. N., and Partch, C. L.** (2017). Animal cryptochromes: divergent roles in light perception, circadian timekeeping and beyond. *Photochem. Photobiol.* 93, 128–140.
- Miyashima, S., Sebastian, J., Lee, J. Y., and Helariutta, Y.** (2013). Stem cell function during plant vascular development. *EMBO J.* 32, 178–193.
- Mizukami, Y., and Fischer, R. L.** (2000). Plant organ size control: AINTEGUMENTA regulates growth and cell numbers during organogenesis. *Proc. Natl. Acad. Sci. U. S. A.* 97, 942–947.
- Mohammed, B., Bilooei, S. F., Dóczy, R., Grove, E., Railo, S., Palme, K., Ditengou,**



Chapter 1: General introduction

- F. A., Bögre, L., and López-Juez, E.** (2018). Converging light, energy and hormonal signaling control meristem activity, leaf initiation, and growth. *Plant Physiol.* 176, 1365–1381.
- Morrow, R. C.** (2008). LED lighting in horticulture. *HortScience* 43, 1947–1950.
- Motchoulski, A., and Liscum, E.** (1999). Arabidopsis NPH3: A NPH1 photoreceptor-interacting protein essential for phototropism. *Science* 286, 961–964.
- Nagy, F., and Schäfer, E.** (2002). Phytochromes control photomorphogenesis by differentially regulated, interacting signaling pathways in higher plants. *Annu. Rev. Plant Biol.* 53, 329–355.
- Nelson, D. C., Lasswell, J., Rogg, L. E., Cohen, M. A., and Bartel, B.** (2000). FKF1, a clock-controlled gene that regulates the transition to flowering in Arabidopsis. *Cell* 101, 331–340.
- Newton, I., and Hemming, G.** (2020). Opticks: or, A treatise of the reflections, refractions, inflexions and colours of light : also two treatises of the species and magnitude of curvilinear figures. doi:10.5479/SIL.302475.39088000644674.
- Nieminen, K., Immanen, J., Laxell, M., Kauppinen, L., Tarkowski, P., Dolezal, K., Tähtiharju, S., Elo, A., Decourteix, M., Ljung, K., Bhalerao, R., Keinonen, K., Albert, V. A., and Helariutta, Y.** (2008). Cytokinin signaling regulates cambial development in poplar. *Proc. Natl. Acad. Sci. U. S. A.* 105, 20032–20037.
- Oh, E., Yamaguchi, S., Hu, J., Yusuke, J., Jung, B., Paik, I., Lee, H. S., Sun, T. P., Kamija, Y., and Choi, G.** (2007). PIL5, a phytochrome-interacting bHLH protein, regulates gibberellin responsiveness by binding directly to the GAI and RGA promoters in Arabidopsis seeds. *Plant Cell* 19, 1192–1208.
- Okada, K., Ueda, J., Komaki, M. K., Bell, C. J., and Shimura, Y.** (1991). Requirement of the auxin polar transport system in early stages of Arabidopsis floral bud formation. *Plant Cell* 3, 677–684.
- Ortiz-Alcaide, M., Llamas, E., Gomez-Cadenas, A., Nagatani, A., Martínez-García, J. F., and Rodríguez-Concepción, M.** (2019). Chloroplasts modulate



elongation responses to canopy shade by retrograde pathways involving HY5 and Abscissic Acid. *Plant Cell* 31, 384–398.

Osterlund, M. T., Hardtke, C. S., Ning, W., and Deng, X. W. (2000). Targeted destabilization of HY5 during light-regulated development of Arabidopsis. *Nature* 405, 462–466.

Paradiso, R., and Proietti, S. (2021). Light-Quality Manipulation to Control Plant Growth and Photomorphogenesis in Greenhouse Horticulture: The State of the Art and the Opportunities of Modern LED Systems. *J. Plant Growth Regul.* 41, 742–780.

Pattison, P. M., Tsao, J. Y., Brainard, G. C., and Bugbee, B. (2018). LEDs for photons, physiology and food. *Nature* 563, 493–500.

Pedmale, U. V., Huang, S. S. C., Zander, M., Cole, B. J., Hetzel, J., Ljung, K., Reis, P. A. B., Sridevi, P., Nito, K., Nery, J. R., Ecker, J. R., and Chory, J. (2016). Cryptochromes interact directly with PIFs to control plant growth in limiting blue light. *Cell* 164, 233–245.

Peng, J., and Harberd, N. P. (1997). Gibberellin deficiency and response mutations suppress the stem elongation phenotype of phytochrome-deficient mutants of Arabidopsis. *Plant Physiol.* 113, 1051–1058.

Perrotta, G., Ninu, L., Flamma, F., Weller, J. L., Kendrick, R. E., Nebuloso, E., and Giuliano, G. (2000). Tomato contains homologues of Arabidopsis cryptochromes 1 and 2. *Plant Mol. Biol.* 42, 765–773.

Pfeiffer, A., Janocha, D., Dong, Y., Medzihradszky, A., Schöne, S., Daum, G., Suzaki, T., Forner, J., Langenecker, T., Rempel, E., Schmid, M., Wirtz, M., Hell, R., and Lohmann, J. U. (2016). Integration of light and metabolic signals for stem cell activation at the shoot apical meristem. *Elife* 5, e17023.

Pfeiffer, A., Nagel, M. K., Popp, C., Wüst, F., Bindics, J., Viczián, A., Hiltbrunner, A., Nagy, F., Kunkel, T., and Schäfer, E. (2012). Interaction with plant transcription factors can mediate nuclear import of phytochrome B. *Proc. Natl. Acad. Sci. U. S. A.* 109, 5892–5897.

Pham, V. N., Kathare, P. K., and Huq, E. (2018). Phytochromes and phytochrome



Chapter 1: General introduction

- interacting factors. *Plant Physiol.* 176, 1025–1038.
- Poethig, R. S.** (2013). Vegetative phase change and shoot maturation in plants. *Curr. Top. Dev. Biol.* 105, 125–152.
- Pokorný, R., Klar, T., Hennecke, U., Carell, T., Batschauer, A., and Essen, L. O.** (2008). Recognition and repair of UV lesions in loop structures of duplex DNA by DASH-type cryptochrome. *Proc. Natl. Acad. Sci. U. S. A.* 105, 21023–21027.
- Potter, T. I., Rood, S. B., and Zanewich, K. P.** (1999). Light intensity, gibberellin content and the resolution of shoot growth in Brassica. *Planta* 207, 505–511.
- Pratt, L. H., Cordonnier-Pratt, M. M., Hauser, B., and Caboche, M.** (1995). Tomato contains two differentially expressed genes encoding B-type phytochromes, neither of which can be considered an ortholog of Arabidopsis phytochrome B. *Planta* 197, 203–206.
- Przemeck, G. K. H., Mattsson, J., Hardtke, C. S., Sung, Z. R., and Berleth, T.** (1996). Studies on the role of the Arabidopsis gene MONOPTEROS in vascular development and plant cell axialization. *Planta* 200, 229–237.
- Ragni, L., and Greb, T.** (2018). Secondary growth as a determinant of plant shape and form. *Semin. Cell Dev. Biol.* 79, 58–67.
- Rahimi, A., Karami, O., Balazadeh, S., and Offringa, R.** (2022a). miR156-independent repression of the ageing pathway by longevity-promoting AHL proteins in Arabidopsis. *New Phytol.* 235, 2424–2438.
- Rahimi, A., Karami, O., Lestari, A. D., de Werk, T., Amakorová, P., Shi, D., Novák, O., Greb, T., and Offringa, R.** (2022b). Control of cambium initiation and activity in Arabidopsis by the transcriptional regulator AHL15. *Curr. Biol.* 32, 1764–1775.
- Rashotte, A. M., Brady, S. R., Reed, R. C., Ante, S. J., and Muday, G. K.** (2000). Basipetal auxin transport is required for gravitropism in roots of Arabidopsis. *Plant Physiol.* 122, 481–490.
- Reed, J. W., Foster, K. R., Morgan, P. W., and Chory, J.** (1996). Phytochrome B affects responsiveness to gibberellins in Arabidopsis. *Plant Physiol.* 112, 337–342.



- Regnault, T., Davière, J.-M., Wild, M., Sakvarelidze-Achard, L., Heintz, D., Carrera Bergua, E., Diaz, I. L., Gong, F., Hedden, P., and Achard, P.** (2015). The gibberellin precursor GA12 acts as a long-distance growth signal in *Arabidopsis*. *Nat. Plants* 1, 1–6.
- Rehman, M., Fahad, S., Saleem, M., Hafeez, M., Rahman, M. U., Liu, F., and Deng, G.** (2020). Red light optimized physiological traits and enhanced the growth of ramie (*Boehmeria nivea* L.). *Photosynthetica* 58, 922–931.
- Reinhardt, D., Mandel, T., and Kuhlemeier, C.** (2000). Auxin regulates the initiation and radial position of plant lateral organs. *Plant Cell* 12, 507–518.
- Reinhardt, D., Pesce, E. R., Stieger, P., Mandel, T., Baltensperger, K., Bennett, M., Traas, J., Friml, J., and Kuhlemeier, C.** (2003). Regulation of phyllotaxis by polar auxin transport. *Nature* 426, 255–260.
- Rizzini, L., Favory, J. J., Cloix, C., Faggionato, D., O'Hara, A., Kaiserli, E., Baumeister, R., Schäfer, E., Nagy, F., Jenkins, G. I., and Ulm, R.** (2011). Perception of UV-B by the *Arabidopsis* UVR8 protein. *Science* 332, 103–106.
- Rockwell, N. C., and Lagarias, J. C.** (2020). Phytochrome evolution in 3D: deletion, duplication, and diversification. *New Phytol.* 225, 2283–2300.
- Ross, J. J., O'Neill, D. P., and Rathbone, D. A.** (2003). Auxin-gibberellin interactions in pea: integrating the old with the new. *J. Plant Growth Regul.* 22, 99–108.
- Sachs, R. M.** (1965). Stem Elongation. *Annu. Rev. Plant Physiol.* 16, 73–96.
- Sage, L. C.** (1992). Pigment of the imagination : a history of phytochrome research. 562.
- Saito, M., Kondo, Y., and Fukuda, H.** (2018). BES1 and BZR1 redundantly promote phloem and xylem differentiation. *Plant Cell Physiol.* 59, 590–600.
- Sakai, T., Kagawa, T., Kasahara, M., Swartz, T. E., Christie, J. M., Briggs, W. R., Wada, M., and Okada, K.** (2001). *Arabidopsis* nph1 and npl1: Blue light receptors that mediate both phototropism and chloroplast relocation. *Proc. Natl. Acad. Sci. U. S. A.* 98, 6969–6974.



Chapter 1: General introduction

- Sakai, T., Wada, T., Ishiguro, S., and Okada, K.** (2000). RPT2: A signal transducer of the phototropic response in Arabidopsis. *Plant Cell* 12, 225–236.
- Salomon, M., Knieb, E., Von Zeppelin, T., and Rüdiger, W.** (2003). Mapping of low- and high-fluence autophosphorylation sites in phototropin 1. *Biochemistry* 42, 4217–4225.
- Samach, A., Onouchi, H., Gold, S. E., Ditta, G. S., Schwarz-Sommer, Z., Yanofsky, M. F., and Coupland, G.** (2000). Distinct roles of constans target genes in reproductive development of Arabidopsis. *Science* 288, 1613–1616.
- Sang, Y., Li, Q. H., Rubio, V., Zhang, Y. C., Mao, J., Deng, X. W., and Yang, H. Q.** (2005). N-terminal domain-mediated homodimerization is required for photoreceptor activity of Arabidopsis Cryptochrome 1. *Plant Cell* 17, 1569–1584.
- Sarojam, R., Suppl, P. G., Goldshmidt, A., Efroni, I., Floyd, S. K., Eshed, Y., and Bowman, J. L.** (2010). Differentiating Arabidopsis shoots from leaves by combined YABBY activities. *Plant Cell* 22, 2113–2130.
- Sassi, M., Lu, Y., Zhang, Y., Wang, J., Dhonukshe, P., Blilou, I., Dai, M., Li, J., Gong, X., Jaillais Y., Yu, X., Traas, J., Ruberti, I., Wang, H., Scheres, B., Vernoux, T., and Xu, J.** (2012). COP1 mediates the coordination of root and shoot growth by light through modulation of PIN1- and PIN2-dependent auxin transport in Arabidopsis. *Dev.* 139, 3402–3412.
- Sato, S., Tabata, S., Hirakawa, H., Asamizu, E., Shirasawa, K., and Isobe, S.** (2012). The tomato genome sequence provides insights into fleshy fruit evolution. *Nature* 485, 635–641.
- Sawa, M., Nusinow, D. A., Kay, S. A., and Imaizumi, T.** (2007). FKF1 and GIGANTEA complex formation is required for day-length measurement in Arabidopsis. *Science* 318, 261–265.
- Sawa, S., Watanabe, K., Goto, K., Kanaya, E., Morita, E. H., and Okada, K.** (1999). FILAMENTOUS FLOWER: A meristem and organ identity gene of Arabidopsis, encodes a protein with a zinc finger and HMG-related domains. *Genes Dev.* 13, 1079–1088.



- Schoof, H., Lenhard, M., Haecker, A., Mayer, K. F. X., Jürgens, G., and Laux, T.** (2000). The stem cell population of Arabidopsis shoot meristems is maintained by a regulatory loop between the CLAVATA and WUSCHEL genes. *Cell* 100, 635–644.
- Schultz, E. A., and Haughn, G. W.** (1991). LEAFY, a homeotic gene that regulates inflorescence development in arabidopsis. *Plant Cell* 3, 771–781.
- Schultz, T. F., Kiyosue, T., Yanovsky, M., Wada, M., and Kay, S. A.** (2001). A role for LKP2 in the circadian clock of Arabidopsis. *Plant Cell* 13, 2659–2670.
- Schuster, C., Gaillochet, C., Medzihradsky, A., Busch, W., Daum, G., Krebs, M., Kehle, A., and Lohmann, J. U.** (2014). A regulatory framework for shoot stem cell control integrating metabolic, transcriptional, and phytohormone signals. *Dev. Cell* 28, 438–449.
- Seo, M., Hanada, A., Kuwahara, A., Endo, A., Okamoto, M., Yamauchi, Y., North, H., Marion-Poll, A., Sun, T. P., Koshiba, T., Kamiya, Y., Yamguchi, S., and Nambara, E.** (2006). Regulation of hormone metabolism in Arabidopsis seeds: phytochrome regulation of abscisic acid metabolism and abscisic acid regulation of gibberellin metabolism. *Plant J.* 48, 354–366.
- Serrano-Bueno, G., Romero-Campero, F. J., Lucas-Reina, E., Romero, J. M., and Valverde, F.** (2017). Evolution of photoperiod sensing in plants and algae. *Curr. Opin. Plant Biol.* 37, 10–17.
- Serrano-Mislata, A., Bencivenga, S., Bush, M., Schiessl, K., Boden, S., and Sablowski, R.** (2017). DELLA genes restrict inflorescence meristem function independently of plant height. *Nat. plants* 3, 749–754.
- SharathKumar, M., Heuvelink, E., and Marcelis, L. F. M.** (2020). Vertical farming: moving from genetic to environmental modification. *Trends Plant Sci.* 25, 724–727.
- Shinomura, T., Uchida, K., and Furuya, M.** (2000). Elementary processes of photoperception by phytochrome A for high-irradiance response of hypocotyl elongation in Arabidopsis. *Plant Physiol.* 122, 147–156.
- Shu, K., Chen, Q., Wu, Y., Liu, R., Zhang, H., Wang, P., Li, Y., Wang, S., Tang,**



Chapter 1: General introduction

- S., Liu, C., Yang, W., Cao, X., Serino, G., and Xie, Q.** (2016). ABI4 mediates antagonistic effects of abscisic acid and gibberellins at transcript and protein levels. *Plant J.* 85, 348–361.
- Sibout, R., Sukumar, P., Hettiarachchi, C., Holm, M., Muday, G. K., and Hardtke, C. S.** (2006). Opposite root growth phenotypes of *hy5* versus *hy5* *hyh* mutants correlate with increased constitutive auxin signaling. *PLoS Genet.* 2, 1898–1911.
- Simpson, G. G.** (2004). The autonomous pathway: Epigenetic and post-transcriptional gene regulation in the control of Arabidopsis flowering time. *Curr. Opin. Plant Biol.* 7, 570–574.
- Smit, M. E., McGregor, S. R., Sun, H., Gough, C., Bågman, A. M., Soyars, C. L., Kroon, J. T., Gaudinier, A., Williams, C. J., Yang, X., Nimchuk, Z. L., Weijers, D., Turner, S. R., Brady, S. M., and Etchells, J. P.** (2020). A PXY-Mediated Transcriptional Network Integrates Signaling Mechanisms to Control Vascular Development in Arabidopsis. *Plant Cell* 32, 319–335.
- Smith, H. L., Mcausland, L., and Murchie, E. H.** (2017). Don't ignore the green light: Exploring diverse roles in plant processes. *J. Exp. Bot.* 68, 2099–2110.
- Somers, D. E., Schultz, T. F., Milnamow, M., and Kay, S. A.** (2000). ZEITLUPE encodes a novel clock-associated PAS protein from Arabidopsis. *Cell* 101, 319–329.
- Song, Y. H., Ito, S., and Imaizumi, T.** (2013). Flowering time regulation: Photoperiod- and temperature-sensing in leaves. *Trends Plant Sci.* 18, 575–583.
- Soo Seo, H., Yang, J. Y., Ishikawa, M., Bolle, C., Ballesteros, M. L., and Chua, N. H.** (2003). LAF1 ubiquitination by COP1 controls photomorphogenesis and is stimulated by SPA1. *Nature* 423, 995–999.
- Spicer, R., and Groover, A.** (2010). Evolution of development of vascular cambia and secondary growth. *New Phytol.* 186, 577–592.
- Stepanova, A. N., Hoyt, J. M., Hamilton, A. A., and Alonso, J. M.** (2005). A link between ethylene and auxin uncovered by the characterization of two root-specific ethylene-insensitive mutants in arabidopsis. *Plant Cell* 17, 2230–2242.



- Strauss, S., Lempe, J., Prusinkiewicz, P., Tsiantis, M., and Smith, R. S.** (2020). Phyllotaxis: is the golden angle optimal for light capture? *New Phytol.* 225, 499–510.
- Suárez-López, P., K. Wheatley, F. Robson, H. Onouchi, F. Valverde, and G. Coupland** (2001). CONSTANS mediates between the circadian clock and the control of flowering in *Arabidopsis*. *Nature* 410, 1116–1120.
- Suer, S., Agusti, J., Sanchez, P., Schwarz, M., and Greb, T.** (2011). WOXA imparts auxin responsiveness to cambium cells in *Arabidopsis*. *Plant Cell* 23, 3247–3259.
- Suetsugu, N., and Wada, M.** (2013). Evolution of three LOV blue light receptor families in green plants and photosynthetic stramenopiles: Phototropin, ZTL/FKF1/LKP2 and aureochrome. *Plant Cell Physiol.* 54, 8–23.
- Talbert, P. B., Adler, H. T., Parks, D. W., and Comai, L.** (1995). The REVOLUTA gene is necessary for apical meristem development and for limiting cell divisions in the leaves and stems of *Arabidopsis thaliana*. *Development* 121, 2723–2735.
- Tamaki, S., Matsuo, S., Hann, L. W., Yokoi, S., and Shimamoto, K.** (2007). Hd3a protein is a mobile flowering signal in rice. *Science* 316, 1033–1036.
- Teotia, S., and Tang, G.** (2015). To bloom or not to bloom: Role of microRNAs in plant flowering. *Mol. Plant* 8, 359–377.
- Teper-Bamnolker, P., and Samach, A.** (2005). The flowering integrator FT regulates SEPALLATA3 and FRUITFULL accumulation in *Arabidopsis* leaves. *Plant Cell* 17, 2661–2675.
- Terashima, I., Fujita, T., Inoue, T., Chow, W. S., and Oguchi, R.** (2009). Green light drives leaf photosynthesis more efficiently than red light in strong white light: Revisiting the enigmatic question of why leaves are green. *Plant Cell Physiol.* 50, 684–697.
- Thimann, K. V.** (1937). On the nature of inhibitions caused by auxin. *Am. J. Bot.* 24, 407.
- Thomas, S. G., and Sun, T. P.** (2004). Update on gibberellin signaling. A tale of the tall and the short. *Plant Physiol.* 135, 668–676.



Chapter 1: General introduction

- Tilbrook, K., Arongaus, A. B., Binkert, M., Heijde, M., Yin, R., and Ulm, R.** (2013). The UVR8 UV-B Photoreceptor: Perception, Signaling and Response. *Arab. B.* 11, e0164.
- Tong, H., Xiao, Y., Liu, D., Gao, S., Liu, L., Yin, Y., Jin, Y., Qian, Q., and Chu, C.** (2014). Brassinosteroid regulates cell elongation by modulating gibberellin metabolism in rice. *Plant Cell* 26, 4376-4393.
- Tseng, T. S., and Briggs, W. R.** (2010). The Arabidopsis rcn1-1 mutation impairs dephosphorylation of phot2, resulting in enhanced blue light responses. *Plant Cell* 22, 392–402.
- Tseng, T. S., Whippo, C., Hangarter, R. P., and Briggs, W. R.** (2012). The role of a 14-3-3 protein in stomatal opening mediated by PHOT2 in Arabidopsis. *Plant Cell* 24, 1114–1126.
- Tsukaya, H.** (2004). Leaf shape: genetic controls and environmental factors. *Int. J. Dev. Biol.* 49, 547–555.
- Unterholzner, S. J., Rozhon, W., Papacek, M., Ciomas, J., Lange, T., Kugler, K. G., Mayer, K. F., Sieberer, T., and Poppenberger, B.** (2015). Brassinosteroids are master regulators of gibberellin biosynthesis in Arabidopsis. *Plant Cell* 27, 2261–2272.
- Van Tuinen, A., Cordonnier-Pratt, M. M., Pratt, L. H., Verkerk, R., Zabel, P., and Koornneef, M.** (1997). The mapping of phytochrome genes and photomorphogenic mutants of tomato. *Theor. Appl. Genet.* 94, 115–122.
- Vandenbussche, F., Petrášek, J., Žádníková, P., Hoyerová, K., Pešek, B., Raz, V., Swarup, R., Bennet, M., Zazímalová, E., Benková, E., and van der Straeten, D.** (2010). The auxin influx carriers AUX1 and LAX3 are involved in auxin-ethylene interactions during apical hook development in Arabidopsis thaliana seedlings. *Development* 137, 597–606.
- Vernoux, T., Brunoud, G., Farcot, E., Morin, V., Van Den Daele, H., Legrand, J., Oliva, M., Das, P., Larrieu, A., Wells, D., Guédon, Y., Armitage, L., Picard, F., Guyomarch, S., Cellier, C., Parry, G., Koumprouglu, R., Doonan, J. H., Estelle, M., Godin, C., Kepinski, S., Bennet, M., de Veylder, L., and Traas, J.** (2011). The auxin signalling network translates dynamic input



- into robust patterning at the shoot apex. *Mol. Syst. Biol.* 7, 508.
- Wan, Y. L., Eisinger, W., Ehrhardt, D., Kubitscheck, U., Baluska, F., and Briggs, W.** (2008). The subcellular localization and blue-light-induced movement of phototropin 1-GFP in etiolated seedlings of *Arabidopsis thaliana*. *Mol. Plant* 1, 103–117.
- Wang, J. W., Czech, B., and Weigel, D.** (2009). miR156-regulated SPL transcription factors define an endogenous flowering pathway in *Arabidopsis thaliana*. *Cell* 138, 738–749.
- Wang, Q., Zuo, Z., Wang, X., Liu, Q., Gu, L., Oka, Y., and Lin, C.** (2018). Beyond the photocycle — how cryptochromes regulate photoresponses in plants? *Curr. Opin. Plant Biol.* 45, 120–126.
- Wang, Y., and Folta, K. M.** (2013). Contributions of green light to plant growth and development. *Am. J. Bot.* 100, 70–78.
- Weaver, L. M., and Amasino, R. M.** (2001). Senescence is induced in individually darkened *Arabidopsis* leaves, but inhibited in whole darkened plants. *Plant Physiol.* 127, 876–886.
- Weigel, D., Alvarez, J., Smyth, D. R., Yanofsky, M. F., and Meyerowitz, E. M.** (1992). LEAFY controls floral meristem identity in *Arabidopsis*. *Cell* 69, 843–859.
- Weigel, D., and Meyerowitz, E. M.** (1993). Activation of floral homeotic genes in *Arabidopsis*. *Science* 261, 1723–1726.
- Weiner, J.** (1985). Size hierarchies in experimental populations of annual plants. *Ecology* 66, 743–752.
- Went, F.** (1926). On growth-accelerating substances in the coleoptile of *Avena sativa*. *Proc. K. Ned. Akad. van Wet.* 30, 10–19.
- Wigge, P. A., Kim, M. C., Jaeger, K. E., Busch, W., Schmid, M., Lohmann, J. U., and Weigel, D.** (2005). Integration of spatial and temporal information during floral induction in *Arabidopsis*. *Science* 309, 1056–1059.
- Willige, B. C., Ogiso-Tanaka, E., Zourelidou, M., and Schwechheimer, C.** (2012).



Chapter 1: General introduction

WAG2 represses apical hook opening downstream from gibberellin and PHYTOCHROME INTERACTING FACTOR 5. *Dev.* 139, 4020–4028.

- Wilson, R. N., Heckman, J. W., and Somerville, C. R.** (1992). Gibberellin is required for flowering in *Arabidopsis thaliana* under short days. *Plant Physiol.* 100, 403–408.
- Wu, B. Sen, Rufyikiri, A. S., Orsat, V., and Lefsrud, M. G.** (2019). Re-interpreting the photosynthetically action radiation (PAR) curve in plants. *Plant Sci.* 289, 110272.
- Xie, M., Chen, H., Huang, L., O’Neil, R. C., Shokhirev, M. N., and Ecker, J. R.** (2018). A B-ARR-mediated cytokinin transcriptional network directs hormone cross-regulation and shoot development. *Nat. Commun.* 9, 1–13.
- Xie, Y., Zhou, Q., Zhao, Y., Li, Q., Liu, Y., Ma, M., Wang, B., Shen, R., Zheng, Z., and Wang, H.** (2020). FHY3 and FAR1 integrate light signals with the miR156-SPL module-mediated aging pathway to regulate *Arabidopsis* flowering. *Mol. Plant* 13, 483–498.
- Xu, F., Li, T., Xu, P. B., Li, L., Du, S. S., Lian, H. L., and Yang, H. Q.** (2016a). DELLA proteins physically interact with CONSTANS to regulate flowering under long days in *Arabidopsis*. *FEBS Lett.* 590, 541–549.
- Xu, M., Hu, T., Zhao, J., Park, M. Y., Earley, K. W., Wu, G., Yang, L., and Poethig, R. S.** (2016b). Developmental functions of miR156-regulated SQUAMOSA PROMOTER BINDING PROTEIN-LIKE (SPL) genes in *Arabidopsis thaliana*. *PLoS Genet.* 12, 1–29.
- Xu, X., Paik, I., Zhu, L., Bu, Q., Huang, X., Deng, X. W., and Huq, E.** (2014). PHYTOCHROME INTERACTING FACTOR1 enhances the E3 ligase activity of CONSTITUTIVE PHOTOMORPHOGENIC1 to synergistically repress photomorphogenesis in *Arabidopsis*. *Plant Cell* 26, 1992–2006.
- Yan, B., Yang, Z., He, G., Jing, Y., Dong, H., Ju, L., Zhang, Y., Zhu, Y., Zhou, Y., and Sun, J.** (2021). The blue light receptor CRY1 interacts with GID1 and DELLA proteins to repress gibberellin signaling and plant growth. *Plant Commun.* 2, 100245.
- Yano, M., Katayose, Y., Ashikari, M., Yamanouchi, U., Monna, L., Fuse, T.,**



- Baba, T., Yamamoto, K., Umehara, Y., Nagamura, Y., and Sasaki, T.** (2000). Hd1, a major photoperiod sensitivity quantitative trait locus in rice, is closely related to the Arabidopsis flowering time gene CONSTANS. *Plant Cell* 12, 2473–2483.
- Yin, R., Arongaus, A. B., Binkert, M., and Ulm, R.** (2015). Two distinct domains of the UVR8 photoreceptor interact with COP1 to initiate UV-B signaling in Arabidopsis. *Plant Cell* 27, 202–213.
- Yin, R., and Ulm, R.** (2017). How plants cope with UV-B: from perception to response. *Curr. Opin. Plant Biol.* 37, 42–48.
- Yordanov, Y. S., Regan, S., and Busov, V.** (2010). Members of the LATERAL ORGAN BOUNDARIES DOMAIN transcription factor family are involved in the regulation of secondary growth in Populus. *Plant Cell* 22, 3662–3677.
- Yoshida, S., Mandel, T., and Kuhlemeier, C.** (2011). Stem cell activation by light guides plant organogenesis. *Genes Dev.* 25, 1439–1450.
- Young, T.** (1804). I. The Bakerian Lecture. Experiments and calculations relative to physical optics. *Philos. Trans. R. Soc.* 94, 1–16.
- Yu, S., Galvão, V. C., Zhang, Y. C., Horrer, D., Zhang, T. Q., Hao, Y. H., Feng, Y. Q., Wang, S., Schmid, M., and Wang, J. W.** (2012). Gibberellin regulates the Arabidopsis floral transition through miR156-targeted SQUAMOSA PROMOTER BINDING-LIKE transcription factors. *Plant Cell* 24, 3320–3332.
- Yu, X., Shalitin, D., Liu, X., Maymon, M., Klejnot, J., Yang, H., Lopez, J., Zhao, X., Bendehakalu, K. T., and Lin, C.** (2007). Derepression of the NC80 motif is critical for the photoactivation of Arabidopsis CRY2. *Proc. Natl. Acad. Sci. U. S. A.* 104, 7289–7294.
- Žádníková, P., Petrášek, J., Marhavý, P., Raz, V., Vandenbussche, F., Ding, Z., Schwarzerová, K., Morita, M. T., Tasaka, M., Hejátko, J., van der Straeten, D., Friml, J., and Benková E.** (2010). Role of PIN-mediated auxin efflux in apical hook development of *Arabidopsis thaliana*. *Development* 137, 607–617.
- Zeevaart, J. A. D.** (1976). Physiology of flower formation. *Annu. Rev. Plant Physiol.* 27, 321–348.



Chapter 1: General introduction

- Zhang, H., He, H., Wang, X., Wang, X., Yang, X., Li, L., and Deng, X. W.** (2011). Genome-wide mapping of the HY5-mediated gene networks in Arabidopsis that involve both transcriptional and post-transcriptional regulation. *Plant J.* 65, 346–358.
- Zhang, K., Novak, O., Wei, Z., Gou, M., Zhang, X., Yu, Y., Yang, H., Cai, Y., Strnad, M., and Liu, C. J.** (2014). Arabidopsis ABCG14 protein controls the acropetal translocation of root-synthesized cytokinins. *Nat. Commun.* 5, 3274.
- Zhang, L., Chen, L., and Yu, D.** (2018). Transcription factor WRKY75 interacts with DELLA proteins to affect flowering. *Plant Physiol.* 176, 790–803.
- Zhao, C., Hanada, A., Yamaguchi, S., Kamiya, Y., and Beers, E. P.** (2011). The Arabidopsis Myb genes MYR1 and MYR2 are redundant negative regulators of flowering time under decreased light intensity. *Plant J.* 66, 502–515.
- Zhao, X., Wang, Y. L., Qiao, X. R., Wang, J., Wang, L. D., Xu, C. S., and Zhang, X.** (2013). Phototropins function in high-intensity blue light-induced hypocotyl phototropism in Arabidopsis by altering cytosolic calcium. *Plant Physiol.* 162, 1539–1551.
- Zhao, Y., Christensen, S. K., Fankhauser, C., Cashman, J. R., Cohen, J. D., Weigel, D., and Chory, J.** (2001). A role for flavin monooxygenase-like enzymes in auxin biosynthesis. *Science* 291, 306–309.
- Zheng, C., Ye, M., Sang, M., and Wu, R.** (2019). A regulatory network for mir156-spl module in *Arabidopsis thaliana*. *Int. J. Mol. Sci.* 20, 6166.
- Zheng, L., He, H., and Song, W.** (2019). Application of light-emitting diodes and the effect of light quality on horticultural crops: A review. *HortScience.* 54, 1656–1661.
- Zhong, S., Shi, H., Xue, C., Wang, L., Xi, Y., Li, J., Quail, P. H., Deng, X. W., and Guo, H.** (2012). A molecular framework of light-controlled phytohormone action in Arabidopsis. *Curr. Biol.* 22, 1530–1535.



Chapter 2

Local phytochrome signalling limits root growth in light by repressing auxin biosynthesis.

Kiki Spaninks¹ and Remko Offringa¹

¹Plant Developmental Genetics, Institute of Biology Leiden,
Leiden University, Sylviusweg 72, 2333 BE, Leiden, Netherlands.

Abstract

In nature, plant shoots are exposed to light whereas the roots grow in darkness. Surprisingly, many root studies rely on *in vitro* systems that leave the roots exposed to light whilst ignoring the possible effects of this light on root development. Here, we investigated how direct root illumination affects root growth and development in Arabidopsis and tomato. Our results show that in light-grown Arabidopsis roots activation of local phytochrome A and B by far-red or red light inhibits respectively PHYTOCHROME INTERACTING FACTORs 1 or 4, resulting in decreased *YUCCA4* and *YUCCA6* expression. As a result, the auxin levels in the root apex become suboptimal, ultimately resulting in reduced growth of light-grown roots. These findings highlight once more the importance of using *in vitro* systems where roots are grown in darkness, for studies that focus on root system architecture. Moreover, we show that the response and components of this mechanism are conserved in tomato roots, thus signifying its importance for horticulture as well. Our findings open up new research possibilities to investigate the importance of light-induced root growth inhibition for plant development, possibly by exploring putative correlations with responses to other abiotic signals, such as temperature, gravity, touch, or salt stress.

Keywords: Root growth, PHY signalling, Auxin biosynthesis, Arabidopsis, tomato

Introduction

Light is an essential energy source for life on earth. Aside from driving photosynthesis in cyanobacteria and plants, light also acts as an environmental cue that regulates almost all aspects of plant growth and development. Perception of light by photoreceptors initiates a variety of physiological responses that are collectively referred to as photomorphogenesis (Arsoovski et al., 2012). The blue light photoreceptor families of cryptochromes, phototropins and Zeitlupes act together with the red (R) / far-red (FR)-sensitive family of phytochromes (PHYs) to regulate developmental processes ranging from germination to flowering, often by influencing hormonal pathways (de Wit et al., 2016). Generally, only the plant shoot is considered when light perception is discussed, as in nature, plant roots grow in darkness. However, root morphology and development are greatly influenced by light (Lee et al., 2017). Photoreceptors regulate root development either by detecting light in the shoot and inducing transmission of mobile signalling molecules, or by perceiving direct or stem-piped light in the roots (Lejay et al., 2008; Sassi et al., 2012; Chen et al., 2016; Lee et al., 2016). A healthy root system is vital for plants for the absorption of water and nutrients, for mechanical support, and as a sink organ (Petricka et al., 2012). Root-localised light perception is physiologically relevant when growing plants *in vitro* or in aeroponic systems. Therefore, elucidation of the local light perception and signalling pathways in the roots is particularly important for studies that focus on root system architecture (RSA), and that have been conducted in *in vitro* systems where the plant roots are exposed to light. Excluding the effect of light, while using light-grown root (LGR) systems in these studies, might result in inadequate

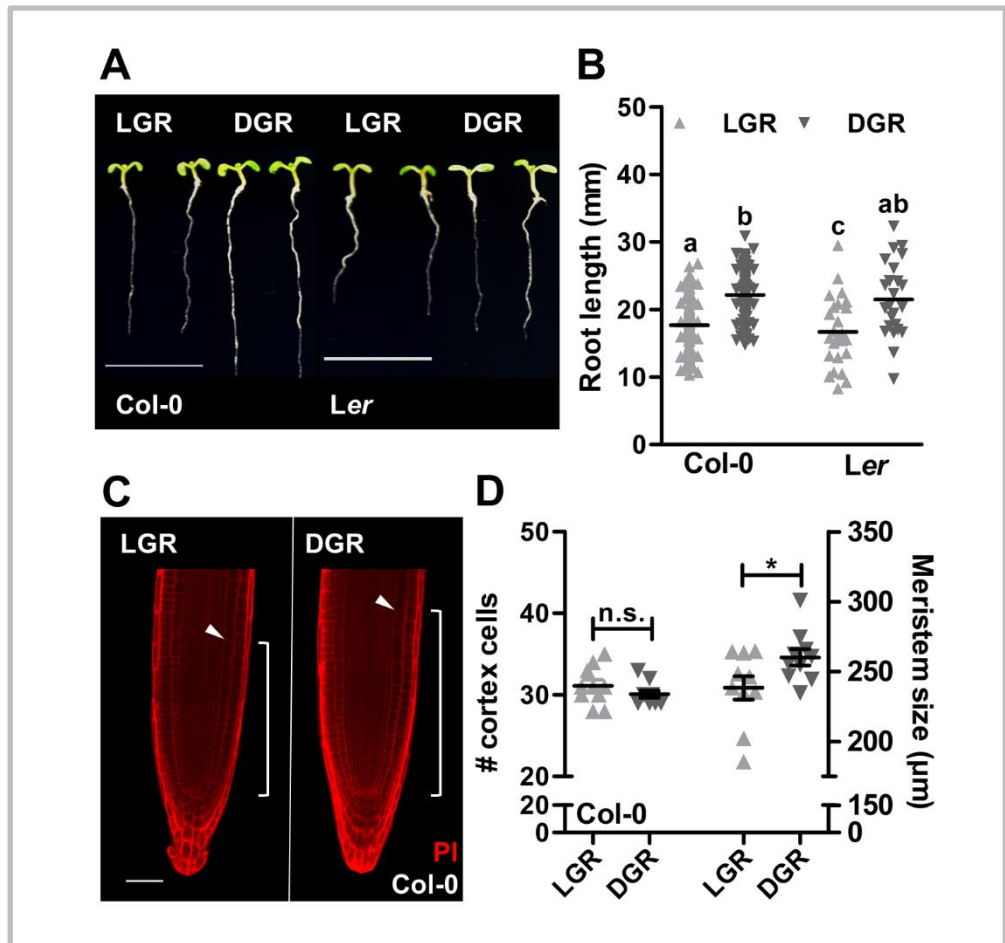
predictive models for RSA phenotypes. For example, an immediate and strong outburst of reactive oxygen species (ROS) has been observed in roots grown in LGR conditions, which might influence the overall RSA (Yokawa et al., 2011). To avoid such stresses, and their adverse effects on the RSA, a dark-grown root (DGR) system, such as the D-root system, should be used for future RSA studies (Silva-Navas et al., 2015). Also in horticulture, where plants are often grown in aeroponic systems or on light-transmittable substrates, such as glass wool, the unintended LGR conditions may influence the growth and development of crop plants. Although crop breeding programs mainly focus on shoot-related phenotypes, changes in RSA might improve crop tolerance to a range of abiotic stresses including drought, salinity, and nutrient limitations (Koevoets et al., 2016).

Here we show that when *Arabidopsis thaliana* (*Arabidopsis*) seedlings are grown in the DGR condition, the bHLH transcription factors PHYTOCHROME INTERACTING FACTOR 1 (PIF1) and PIF4 promote local auxin biosynthesis through upregulation of *YUCCA4* (*YUC4*) and *YUC6* genes, which results in close-to-optimal auxin levels in the RAM, and thus in normal root development. However, in the LGR condition, FR or R light activation of respectively PHYA and PHYB triggers the targeted degradation of these PIFs, resulting in reduced expression of *YUC4* and *YUC6*, and ultimately in shorter roots due to suboptimal auxin levels in the RAM. In addition to the identification of this molecular mechanism, we show that the LGR response and components of this pathway are conserved between *Arabidopsis* and the horticultural crop tomato (*Solanum lycopersicum*).

Results

Cell growth in the proximal root meristem is decreased in light-grown roots.

Arabidopsis seedlings of ecotypes Columbia (Col-0) and Landsberg *erecta* (*Ler*) were grown in the LGR or DGR condition for seven days. Seedlings of both ecotypes showed significantly shorter roots in the LGR condition compared to the DGR condition (**Figures 1A, B**). These results were in line with previously published data using the D-root system (Silva-Navas et al., 2015). Interestingly, hypocotyls of LGR seedlings were also significantly shorter than those of DGR seedlings (**Figures 1A, S2A**). However, since the shoot/root ratio of LGR seedlings was significantly higher than that of DGR seedlings (**Figure S2B**), we conclude that root growth inhibition in the LGR condition is independent of reduced hypocotyl growth. Root growth depends on the balance between cell proliferation and cell expansion in the RAM and on vast asymmetric cell expansion in the elongation zone. In general, a higher number of cortex cells in the proximal meristem of the root apex correlates with longer roots (Baskin, 2013). However, root length can also be determined by the size of these cortex cells (Aceves-García et al., 2016). Propidium iodide (PI) staining and imaging by confocal microscopy detected no significant differences in the number of cortex cells between root tips of LGR and DGR seedlings, whereas the proximal meristem size (in μm) was significantly smaller in LGR seedlings (**Figure 1C, D**). These data showed that direct illumination of roots results in a reduced cell growth in the proximal meristem of the root apex, ultimately leading to a shorter primary root.



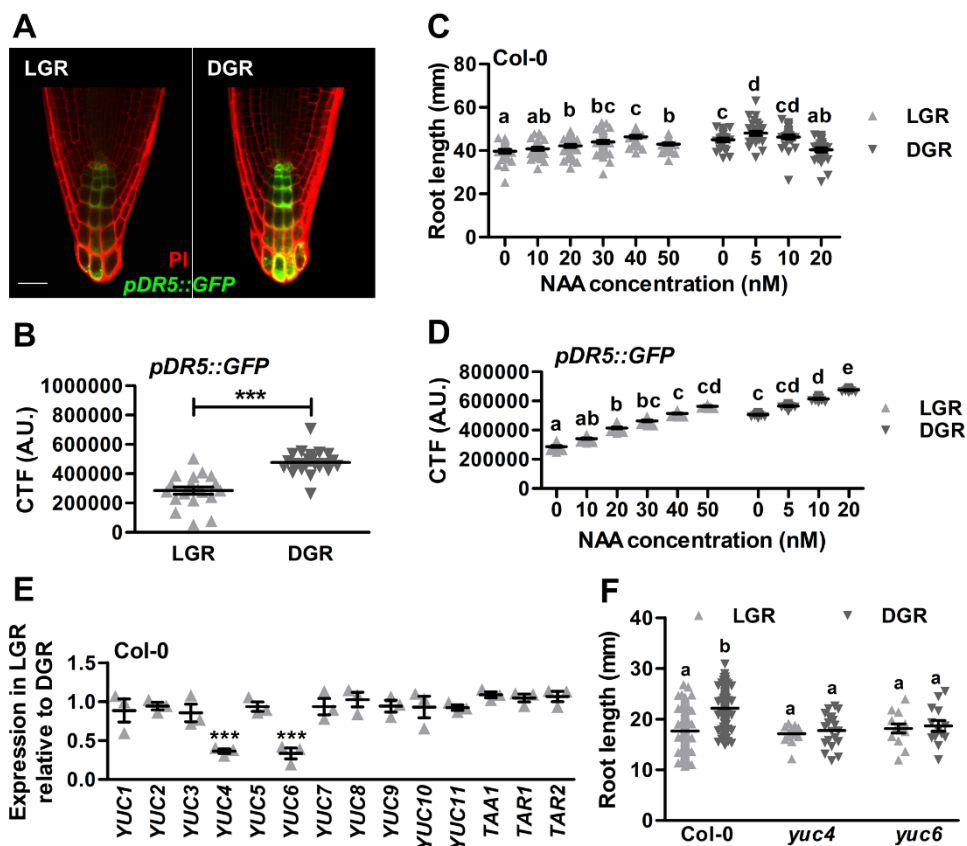
Reduced growth of light-grown roots correlates with a decrease in local auxin biosynthesis in the RAM.

As a key regulator of root growth and development, auxin might be the driving force behind cortex cell growth in the DGR condition. Confocal analysis of the *pDR5::GFP* auxin response reporter in Arabidopsis Col-0 seedlings showed a significant reduction of the GFP signal in the RAM of LGR seedlings,

Figure 1: Cell growth in the proximal meristem is decreased in light-grown roots.

A. Representative 7-day-old *Arabidopsis* seedlings of ecotypes Columbia (Col-0) and Landsberg *erecta* (*Ler*) grown in the light-grown roots (LGR) or the dark-grown roots (DGR) condition. For presentation purposes, seedlings were transferred to black agarose plates before photographing. **B.** Quantification of the primary root length of 7-day-old Col-0 and *Ler* seedlings grown in the LGR or DGR condition. **C.** Confocal images of Col-0 root tips that were stained with propidium iodide (PI). Arrowheads indicate the end of the proximal meristem and white brackets indicate the meristem size. **D.** Quantification of the proximal meristem size in number of cortex cells (left) or in μm (right) of Col-0 seedlings grown in the LGR or DGR condition. Primary root lengths in **B** were compared using a one-way ANOVA followed by a Tukey's test. Letters **a**, **b**, and **c** indicate statistically different values, $p < 0.05$. The LGR condition in **D** was compared to the DGR condition using a two-sided Student's *t*-test (* $p < 0.05$, n.s. = not significant). Scale bars indicate 1 cm in **A**, and 50 μm in **C**. In **B** ($n=30$) and **D** ($n=20$) the horizontal line indicates the mean, error bars represent standard error of the mean (for some not visible due to limited variation) and triangles indicate values of biologically independent observations. Similar results were obtained from three (**A-B**), or from two independent experiments (**C-D**).

compared to DGR seedlings (**Figures 2A, B**), suggesting that light inhibits the auxin response in the RAM. To investigate if reduced root growth in the LGR condition was caused by a decrease in auxin levels, wild-type Col-0 seedlings were grown on medium supplemented with 1-naphthaleneacetic acid (NAA) concentrations varying between 0 and 50 nanomolar. In LGR seedlings, NAA concentrations up to 40 nM maximised root growth, whereas addition of 50 nM NAA reduced root growth (**Figure 2C**). In contrast, for DGR seedlings the

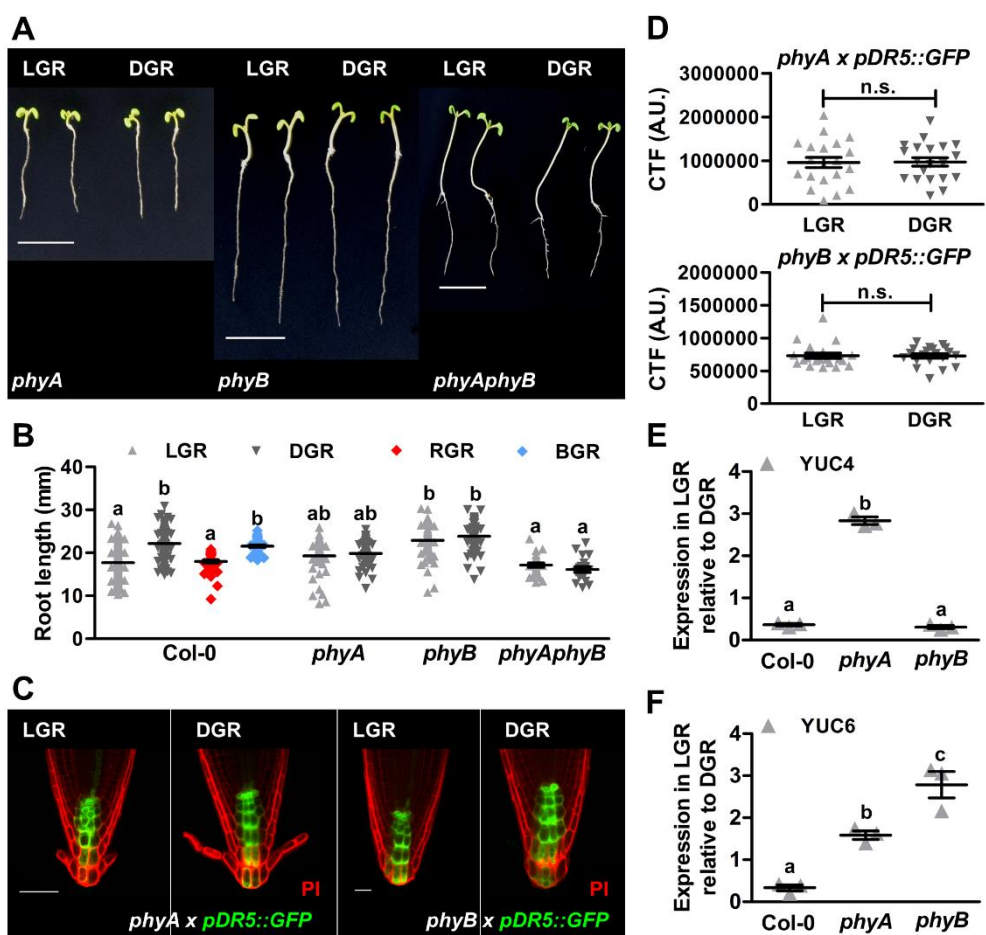


addition of 5 nM NAA maximised root growth, whereas 20 nM NAA resulted in clear root growth inhibition. The 8-fold increase in NAA concentration for optimal root growth of LGR seedlings was in line with the reduced *DR5::GFP* expression. NAA treatment of LGR- and DGR-grown *pDR5::GFP* seedlings confirmed that reporter gene expression increased with increasing NAA concentrations, and that expression in DGR RAMs was always significantly higher compared to LGR RAMs (**Figure 2D**), and thus that reduced primary root growth in the LGR condition was caused by the reduced auxin response

Figure 2: Growth inhibition of roots by light is caused by a decrease in local auxin biosynthesis in the RAM.

A. Confocal images of the root apical meristem (RAM) of 7-day-old *pDR5::GFP* (green signal) seedlings grown in the LGR or the DGR condition. The roots were stained with propidium iodide (PI, red signal). **B.** Quantification of the corrected total fluorescence (CTF) of the RAM. **C-D.** Quantification of the primary root length of Col-0 seedlings (**C**) and the CTF of *pDR5::GFP* seedlings (**D**) grown in the LGR or DGR condition on medium containing different concentrations of 1-naphthaleneacetic acid (NAA). **E.** Quantitative RT-PCR analysis of *YUC1-11*, *TAA1*, *TAR1* and *TAR2* expression in the RAM of 7-day-old Col-0 seedlings that were grown in the LGR condition, relative to gene expression levels of seedlings grown in the DGR condition. **F.** Quantification of the primary root length of 7-day-old Col-0, *yuc4* and *yuc6* seedlings grown in the LGR or DGR condition. In **B** and **E**, the LGR condition was compared to the DGR condition using a two-sided Student's *t*-test (***p*<0.001). In **C**, **D** and **F**, NAA concentrations and primary root lengths were compared using a one-way ANOVA followed by a Tukey's test. Letters **a**, **b**, **c**, **d**, and **e** indicate statistically different values, *p*<0.05. The scale bar indicates 50 μ m in **A**. In **B** (n=20), **C**, **D**, **F** (n=30) and **E** (n=3), the horizontal line indicates the mean, error bars represent standard error of the mean (for some not visible due to limited variation) and triangles indicate values of biologically independent observations. Similar results were obtained from two (**A-B**), or from three independent experiments (**C-F**).

in the RAM. For both conditions, there was a strong positive correlation between increase in GFP signal and increasing NAA concentrations. This correlation was linear with a statistically indistinguishable regression coefficient *b* (**Table S1**), indicating that the reduced auxin response in LGR RAMs was caused by lower endogenous auxin levels, rather than a reduced auxin responsiveness. It is therefore most likely that either auxin biosynthesis or transport is affected in LGR seedlings, resulting in a reduced auxin response



in the RAM. Expression analysis of the auxin biosynthesis genes *YUC1-11*, *TAA1*, *TAR1* and *TAR2* in LGR or DGR RAMs by qRT-PCR showed that *YUC4* and *YUC6* expression was significantly lower in LGR compared to DGR seedlings (**Figure 2E**). Moreover, the dark-induced enhancement of root growth was lost in *yuc4* and *yuc6* mutant seedlings grown in the DGR condition (**Figure 2F**). In contrast, mutants of important auxin influx and

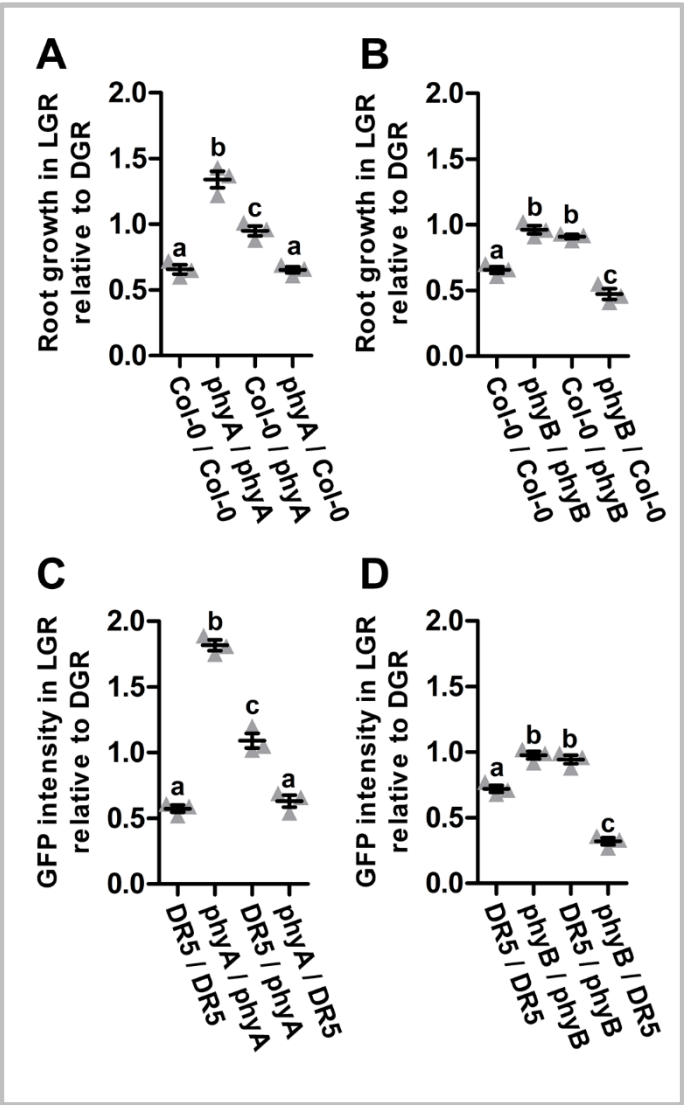
Figure 3: PHYA and PHYB trigger root growth inhibition in response to light.

A. Representative 7-day-old *phy* mutant seedlings grown in the LGR or the DGR condition. For presentation purposes, seedlings were transferred to black agarose plates before photographing. **B.** Quantification of the primary root length of 7-day-old Col-0 seedlings grown in the LGR, DGR, red light-grown roots (RGR) or blue light-grown roots (BGR) condition, and *phy* seedlings grown in the LGR or DGR condition. **C.** Confocal images of the root apical meristem (RAM) of *phyA* \times *pDR5::GFP* and *phyB* \times *pDR5::GFP* (green signal) seedlings grown in the LGR or DGR condition. Root tips were stained with propidium iodide (PI, red signal). **D.** Quantification of the corrected total fluorescence (CTF) of the RAM of *phyA* \times *pDR5::GFP* and *phyB* \times *pDR5::GFP* seedlings. **E-F.** Quantitative RT-PCR analysis of *YUC4* (**E**) and *YUC6* (**F**) expression in the RAM of 7-day-old Col-0, *phyA* and *phyB* seedlings that were grown in the LGR condition, relative to gene expression levels in the RAM of seedlings grown in the DGR condition. In **B**, **E** and **F**, primary root lengths and relative gene expression were compared using a one-way ANOVA followed by a Tukey's test. Letters **a**, **b** and **c** indicate statistically different values, $p < 0.05$. The LGR condition in **D** was compared to the DGR condition using a two-sided Student's *t*-test (n.s. = not significant). Scale bars indicate 1 cm in **A**, and 50 μ m in **C**. In **B** ($n=30$), **D** ($n=20$) and **E-F** ($n=3$), the horizontal line indicates the mean, error bars represent standard error of the mean (for some not visible due to limited variation) and triangles indicate values of biologically independent observations. Similar results were obtained from three (**A-B**, **E-F**), or from two independent experiments (**C-D**).

efflux carriers remained sensitive to the different light conditions, suggesting that auxin transport is not affected in LGR seedlings (**Figure S3A**). Altogether, these experiments indicated that lower *YUC4* and *YUC6* expression in the RAM of LGR seedlings causes a reduction in local auxin biosynthesis that ultimately leads to shorter roots.

Root-localised PHYA and PHYB mediate light-induced inhibition of root growth.

Since the differential auxin levels in LGR and DGR seedlings must be initiated by detection of light, we next investigated the LGR response in mutants of the three main photoreceptor families in land plants: the R/FR-inducible PHYs, and the blue light-induced cryptochromes (CRYs) and phototropins (PHOTs). Although their main functions might be above-ground, many photoreceptors of these families are also expressed in roots (Van Gelderen et al., 2018), and thus might be involved in root growth inhibition of LGR seedlings. For most of the single *phy*, *cry* and *phot* mutants, light-grown roots were significantly shorter



than dark-grown roots, indicating that the response of root growth to light was not affected (**Figure S3B**). For the *phyA* and *phyB* mutants, however, LGR and DGR roots were of the same length, suggesting that the sensitivity of the roots to light was lost in these mutants (**Figures 3A, B**). Moreover, analysis of the *phyAphyB* double mutant showed a similar loss of light sensitivity. Since PHYs

Figure 4: Grafting: local PHYA and PHYB trigger root growth inhibition in response to light.

A-B. Quantification of the root growth of *phyA* and wild-type (Col-0) grafts (**A**), or *phyB* and Col-0 grafts (**B**) in the LGR condition, relative to the DGR condition, at 5 days post-grafting. **C-D.** Quantification of the corrected total fluorescence (CTF) of *pDR5::GFP* in the root apical meristem (RAM) of indicated grafts at 5 days post-grafting in the LGR relative to the DGR condition. Scion / rootstock combinations were grafted using 4-day-old *phyA* and Col-0 (**A**), *phyB* and Col-0 (**B**), *pDR5::GFP* and *phyA* \times *pDR5::GFP* (**C**) or *pDR5::GFP* and *phyB* \times *pDR5::GFP* (**D**) seedlings. Graft combinations were compared using a one-way ANOVA followed by a Tukey's test. Letters **a**, **b**, and **c** indicate statistically different values, $p < 0.05$. In the graphs, the horizontal line indicates the mean, error bars represent standard error of the mean and triangles indicate values of biologically independent observations ($n=5$). Similar results were obtained from two independent experiments.

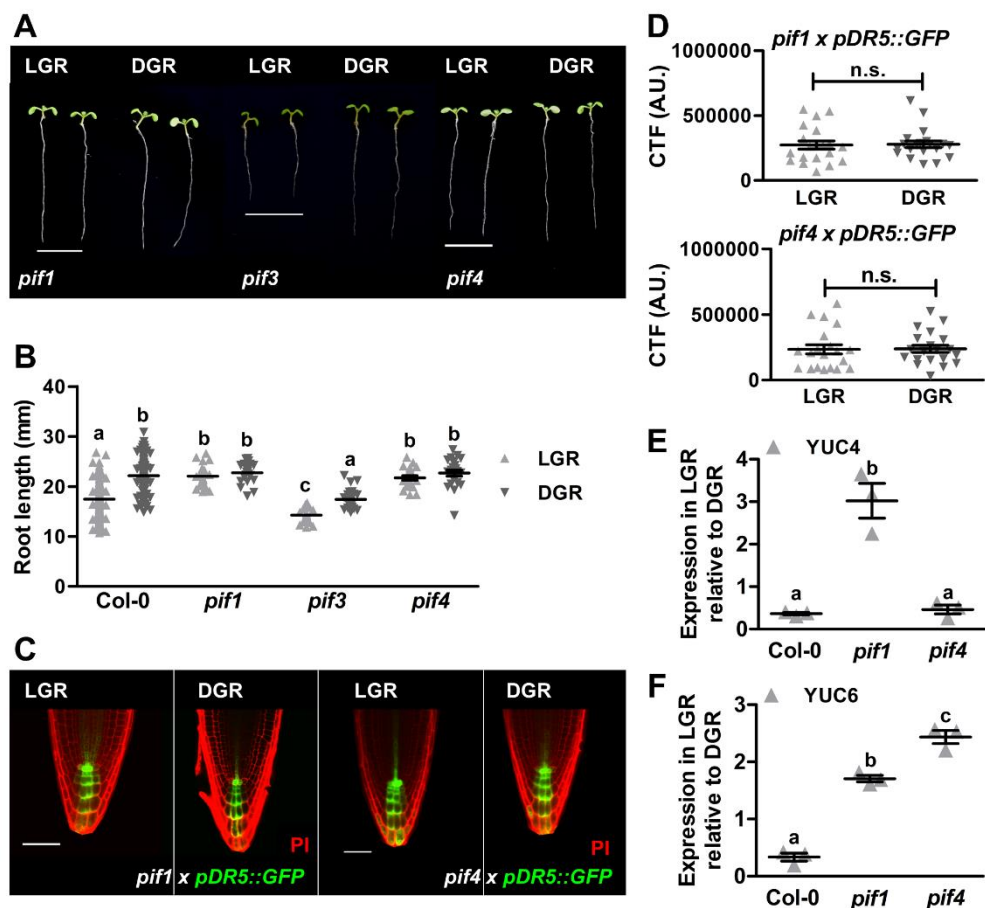
are R/FR-responsive photoreceptors, we expected that only exposure of roots to spectra that contain R or FR wavelengths would result in root growth inhibition. To monitor root growth in response to different wavelengths, Arabidopsis seedlings were grown with their roots covered by clear (LGR), red (RGR) or blue (BGR) translucent plastic, or black paper covers (DGR). Primary root growth was significantly inhibited

in LGR and RGR seedlings, but not in BGR or DGR seedlings (**Figure 3B**), confirming that inhibition of root growth is specific for R and FR light. The *pDR5::GFP* reporter showed a similar auxin response in the LGR and DGR condition in both the *phyA* and *phyB* mutant background (**Figures 3C, D**). In addition, quantitative RT-PCR analysis showed that expression of *YUC4* was significantly increased in the RAM of *phyA* seedlings grown in the LGR condition, compared to the DGR condition, whereas it was decreased in LGR Col-0 and *phyB* RAMs (**Figure 3E**). Moreover, *YUC6* was significantly increased in LGR *phyA* and *phyB* seedlings (**Figure 3F**). Together, this data suggests that inhibition of *YUC4* and *YUC6* expression by light is regulated by PHYA and partially by PHYB. Finally, to confirm that signalling through PHYA and PHYB is truly initiated in the root and not in the shoot, a series of grafting experiments were performed. The following scion / rootstock combinations were included: wild type / wild type (positive control), mutant / mutant (negative control), wild type / mutant (to study photoactivation in the shoot), and mutant / wild type (to study photoactivation in the root). As expected, the positive control grafts showed sensitivity to light, and the negative control grafts were insensitive. For both mutants, the grafts with wild-type roots retained light sensitivity, whereas the grafts with mutant roots had lost light sensitivity (**Figures 4A, B**), confirming that root-localised photoactivation of PHYA or PHYB initiates root growth inhibition by light. Finally, grafting of *phy x pDR5::GFP* seedlings with wild-type *pDR5::GFP* seedlings confirmed the correlation between primary root growth and auxin response in the RAM of grafted seedlings (**Figures 4C, D**). Altogether, the experiments described above showed that FR and R light directly activate root-localised PHYA and PHYB, respectively, to inhibit *YUC4* (PHYA) and *YUC6*

(PHYA and PHYB) expression, thus lowering local auxin levels to reduce primary root growth.

Light-activated root-localised phytochromes repress local auxin biosynthesis via PIF1 and PIF4.

Photoactivated PHYs can affect gene expression either through inhibition of ubiquitin E3 ligases, such as COP1/SPA, or by inhibition of the basic helix-loop-helix (bHLH) family of PIF transcription factors (Pham et al., 2018; Podolec and Ulm, 2018). Since PIF inhibition is exclusive for PHYA and PHYB signalling, we investigated PIFs as putative signalling components for root growth inhibition in LGR conditions. We selected PIF1 and PIF3, as they are targeted by both PHYA and PHYB, and the PHYB-exclusive target PIF4 for its known role in regulation of auxin biosynthesis (Franklin et al., 2011; Pham et al., 2018). Primary root growth measurements of *pif1*, *pif3* and *pif4* mutants grown in the LGR and DGR condition revealed that *pif1* and *pif4* seedlings were insensitive to root illumination, whereas *pif3* responded similar to wild-type seedlings (**Figures 5A, B**). In line with our results in *phyA* and *phyB* mutants, the *pDR5::GFP* response was the same in LGR and DGR conditions in *pif1* and *pif4* mutants (**Figures 5C, D**). Moreover, quantitative RT-PCR analysis showed a significant increase in *YUC4* in the RAM of light-grown *pif1* seedlings, compared to dark-grown seedlings, whereas LGR Col-0 and *pif4* RAMs showed a significant decrease (**Figure 5E**). Moreover, *YUC6* expression was significantly increased in the RAMs of LGR *pif1* and *pif4* but decreased in LGR Col-0 RAMs (**Figure 5F**). Since the *YUC4* and *YUC6* levels in *pif1* mutants were similar to those in *phyA* mutants (**Figure 3E, F**), PIF1 is most likely targeted by PHYA in response to FR light exposure of roots.



Likewise, the RAMs of LGR *pif4* mutants showed a significant decrease in *YUC4* expression and increase in *YUC6* expression, which was similar to *phyB* mutants (**Figure 3E, F**), suggesting that PHYB inhibits PIF4 in response to illumination of roots with R light.

Light-induced inhibition of root growth is partially conserved between Arabidopsis and tomato.

Figure 5: Light represses local auxin biosynthesis through PIF1 and PIF4.

A. Representative 7-day-old *pif* mutant seedlings grown in the LGR or the DGR condition. For presentation purposes, seedlings were transferred to black agarose plates before photographing. **B.** Quantification of the primary root length of 7-day-old Col-0 and *pif* seedlings grown in the LGR or DGR condition. **C.** Confocal images of the root apical meristem (RAM) of *pif1* \times *pDR5::GFP* and *pif4* \times *pDR5::GFP* (green signal) seedlings grown in the LGR or DGR condition. Root tips were stained with propidium iodide (PI, red signal). **D.** Quantification of the corrected total fluorescence (CTF) of *pDR5::GFP* in the RAM. **E-F.** Quantitative RT-PCR analysis of *YUC4* (**E**) and *YUC6* (**F**) expression in the RAM of 7-day-old Col-0, *pif1* and *pif4* seedlings grown in the LGR condition relative to the DGR condition. In **B**, **E** and **F**, primary root lengths were compared using a one-way ANOVA followed by a Tukey's test. Letters **a**, **b**, and **c** indicate statistically different values, $p < 0.05$. In **D**, the LGR condition was compared to the DGR condition using a two-sided Student's *t*-test (n.s. = not significant). Scale bars indicate 1 cm in **A**, and 50 μ m in **C**. In **B** ($n=30$), **D** ($n=20$) and **E-F** ($n=3$), the horizontal line indicates the mean, error bars represent standard error of the mean (for some not visible due to limited variation) and triangles indicate values of biologically independent observations. Similar results were obtained from three (**A-B**, **E-F**), or from two independent experiments (**C-D**).

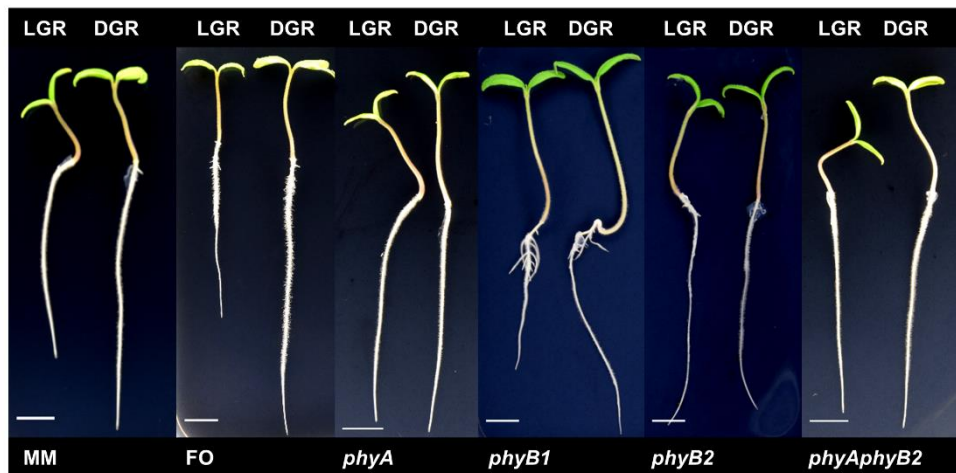
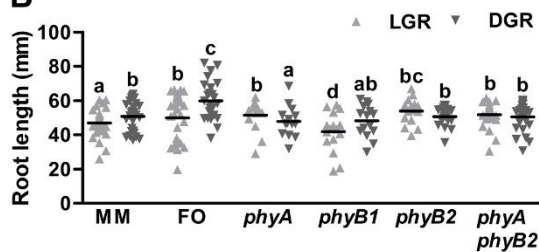
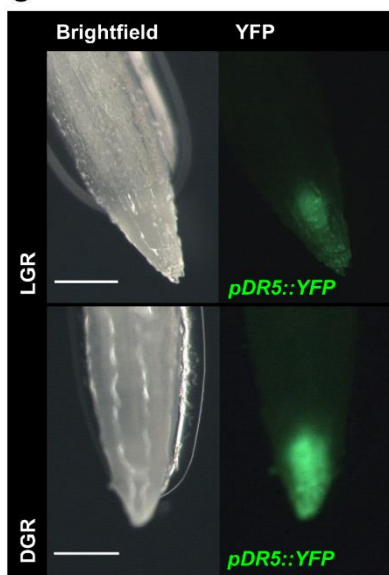
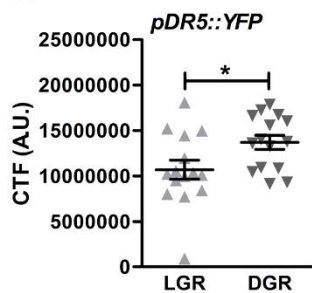
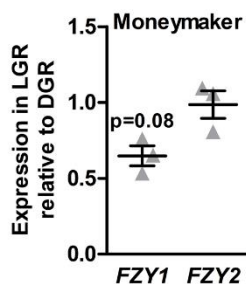
The results described above clearly showed how the widely used LGR *in vitro* system results in suboptimal root growth in Arabidopsis. To investigate if the LGR condition can also lead to suboptimal root growth in horticulture, we included the economically important crop tomato in our experiments. Similar to Arabidopsis, wild-type tomato seedlings of both Moneymaker (MM) and the commercial hybrid Foundation (FO) showed a significant reduction in primary root growth in the LGR condition, compared to the DGR condition

(**Figures 6A, B**). Analysis of MM *phy* mutants in the LGR and DGR condition, showed that both *phyB2* single and *phyAphyB2* double mutant seedling roots were insensitive to light, whereas *phyB1* roots responded the same as wild-type roots. Interestingly, tomato *phyA* roots were significantly longer in the LGR condition, compared to the DGR condition, which is not the case for Arabidopsis *phyA* roots (**Figures 6A, B**). As in Arabidopsis, the tomato *pDR5::YFP* reporter line showed that the auxin response in the RAM was significantly reduced in the LGR condition compared to the DGR condition (**Figures 6C, D**). However, gene expression of the tomato orthologue of *AtYUC6*, *ToFZY2* (Expósito-Rodríguez et al., 2011), was similar in both conditions, indicating that this gene does not play a role in light-induced root growth inhibition (**Figure 6E**). For the *AtYUC4* orthologue, *ToFZY1* (Expósito-Rodríguez et al., 2011), a close to significant ($p=0.08$) decrease in expression was observed in LGR seedlings. To summarise, our data suggests that the PHY-triggered and auxin-modulated growth inhibition by light is conserved between Arabidopsis and tomato, but that not all components of the signalling pathway act in the same way or are shared between these two species.

Discussion

Culturing Arabidopsis seedlings on growth medium in petri dishes allows for an easy way to study root growth and development. However, the majority of these *in vitro* systems leave the roots exposed to light, making this system quite different from natural growth conditions in the soil. Although a number of studies have warned about negative effects of direct light on root growth and development (Yokawa et al., 2014; Moni et al., 2015), most studies still rely

on LGR systems for *in vitro* Arabidopsis research. To demonstrate the consequences of using LGR systems, we aimed to elucidate exactly how direct root illumination affects root growth. Whereas light perception in the shoot stimulates root growth and development, direct illumination of roots has been shown to reduce root growth. Furthermore, direct illumination of roots also influences lateral root emergence and distribution, anthocyanin accumulation and even flowering time (Sassi et al., 2012; Silva-Navas et al., 2015). Since the effects of root illumination are so diverse, they are more likely to be caused by photoreceptor signalling than by light-induced stresses such as ROS or DNA damage. So far, studies on root-localised photoreceptor signalling have been somewhat contradictory. Analysis of root growth in double cryptochrome and phototropin mutants, alongside blue LED treatments indicated that inhibition of root growth is likely to be mediated by blue light photoreceptors (Silva-Navas et al., 2015). In contrast, experiments with tissue-specific deficiency in PHY chromophores suggested that root PHYs, and not shoot PHYs, are required for inhibition of primary root elongation (Costigan et al., 2011). In this study, we identified PHYA and PHYB as regulators of root growth based on a screen of single photoreceptor mutants. For this reason, we cannot fully exclude some functional redundancy with blue light photoreceptors, as was indicated by Silva-Navas and colleagues (Silva-Navas et al., 2015). However, our experiments with coloured plastic indicated that R and FR, but not blue light, are reducing root growth. Additional grafting experiments confirmed that both root-localised PHYA and PHYB are required for light sensitivity, indicating that these photoreceptors are the main regulators of root growth inhibition in the LGR condition. When we considered downstream signalling components, PIFs seemed the most likely targets, since

A**B****C****D****E**

PIF signalling is exclusive for PHYA and PHYB. Although PIF3 has been shown to induce primary root growth inhibition in Arabidopsis (Bai et al., 2014), *pif3* mutants remained sensitive to the LGR condition, indicating that

Figure 6: Light-induced inhibition of root growth is (partially) conserved between Arabidopsis and tomato.

A. Representative 5-day-old tomato seedlings of wild-type cultivars Moneymaker (MM) and Foundation (FO), and of *phy* mutants (in MM background) grown in the LGR or the DGR condition. For presentation purposes, seedlings were transferred to black agarose plates before photographing. **B.** Quantification of the primary root length of 5-day-old MM, FO, and *phy* seedlings grown in the LGR or DGR condition. **C.** Stereo-fluorescence images of the root apical meristem (RAM) of *pDR5::YFP* tomato (M82) seedlings grown in the LGR or DGR condition. **D.** Quantification of the corrected total fluorescence (CTF) of *pDR5::YFP* in the RAM. **E.** Quantitative RT-PCR analysis of expression of *AtYUC4* orthologue *ToFZY1* and *AtYUC6* orthologue *ToFZY2* in the RAM of 5-day-old MM tomato seedlings grown in the LGR condition, relative to the DGR condition. Primary root lengths in **B** were compared using a one-way ANOVA followed by a Tukey's test. Letters **a**, **b**, **c**, and **d** indicate statistically different values, $p < 0.05$. In **D-E**, the LGR condition was compared to the DGR condition using a two-sided Student's *t*-test ($*p < 0.05$). Scale bars indicate 1 cm in **A**, and 0.5 mm in **C**. In **B** ($n=30$), **D** ($n=20$) and **E** ($n=3$), the horizontal line indicates the mean, error bars represent standard error of the mean (for some not visible due to limited variation) and triangles indicate values of biologically independent observations. Similar results were obtained from three (**A-B**, **E**), or from two independent experiments (**C-D**).

its function in primary root growth inhibition is initiated in the shoot and not in the root. Until now, no clear role has been described for PIF1 and PIF4 in regulation of root growth. Here we show for the first time that PIF1 and PIF4

have specific functions in regulation of root growth. Our analysis of the *pDR5::GFP* reporter and quantitative RT-PCR in *pif* mutants showed that, in the DGR condition, PIF1 and PIF4 stimulate local auxin biosynthesis in the RAM by elevating *YUC4* and *YUC6* expression. Since root cells are extremely sensitive to auxin, slight changes in local auxin concentrations can have great consequences (Thimann, 1937). Our analysis of the *pDR5::GFP* reporter in combination with NAA treatments revealed that endogenous auxin levels in dark-grown roots are close to optimal, whereas, in light-grown roots, they are greatly reduced, resulting in shorter roots. The close-to-optimal auxin levels in the DGR condition might explain previously reported increased sensitivity to indole-3-acetic acid (IAA) in DGR seedlings as well (Silva-Navas et al., 2015). With this experiment, we showed not only that inhibition of root growth by light is mediated by auxin, but we also demonstrated once more that the LGR *in vitro* system leads to suboptimal root growth. Based on our observations in *Arabidopsis* we propose a model where under natural circumstances, when roots are grown in darkness, PIF1 and PIF4 promote expression of *YUC6*, whereas PIF1 also promotes *YUC4* expression (**Figure 7**). This results in local auxin biosynthesis in the RAM, and thus in auxin levels that are close-to-optimal for root growth. When roots are exposed to light, however, such as in the widely used LGR *in vitro* system or in aeroponics, local PHYA and PHYB photoreceptors are activated. In light conditions with a low R/FR ratio, PHYA converts from the inactive PHYA_{fr} conformation to the active PHYA_r conformation that inhibits PIF1. Conversely, a high R/FR ratio converts the inactive PHYB_r to the active PHYB_{fr} that inhibits PIF4. Therefore, all light conditions that include either R or FR light, or both, will result in PIF inhibition, leading to a decrease in local auxin biosynthesis. As a result,

suboptimal auxin levels in the RAM lead to reduced primary root growth in LGR seedlings. However, light responses observed in the genetic model *Arabidopsis* do not always translate to an economically important crop such as

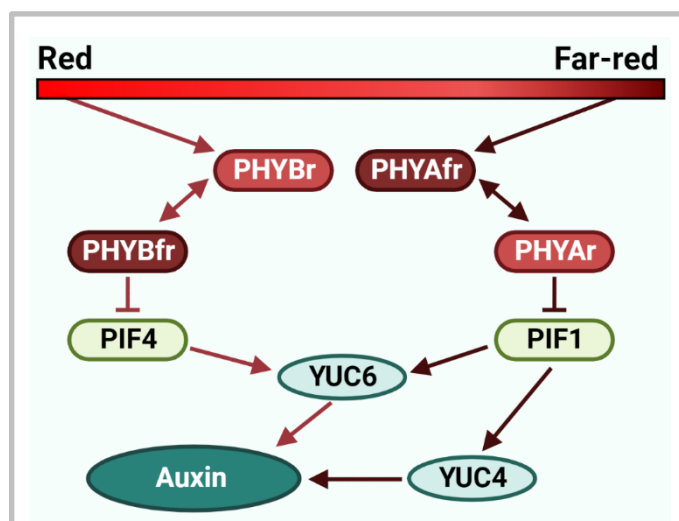


Figure 7: Model for root growth inhibition by local light perception in *Arabidopsis* roots.

Direct illumination of seedling roots with either red (R) or far-red (FR) light inhibits auxin biosynthesis which ultimately results in decreased primary root growth. In response to FR light, phytochrome A (PHYA) converts from the inactive PHYAfr state to the active PHYAr state and translocates to the nucleus where it inhibits PHYTOCHROME INTERACTING FACTOR 1 (PIF1). As a result, expression levels of *YUCCA 4* (*YUC4*) and *YUCCA 6* (*YUC6*) are decreased. Similarly, in response to R light, PHYB converts from the inactive PHYBr state to the active PHYBfr state and inhibits PIF4 in the nucleus, thereby reducing *YUC6* expression. In both cases this leads to lower auxin levels in the RAM that are suboptimal for root growth.

tomato (**chapter 3**). By including tomato seedlings in this study, we could show that this mechanism is also present in a horticultural crop, albeit that the components of the signalling pathway are not completely conserved. This implies that the use of aeroponics or light-transmittable substrates could lead to suboptimal root growth in crops, which could result in decreased tolerance to a range of abiotic stresses (Koevoets et al., 2016). On the other

hand, additional research into the root response to different spectral qualities might provide us with new ways to steer root architecture towards better crop performance. For example, light quality responses in the roots might be genetically linked to yield-associated traits in tomato (Alaguero-Cordovilla et al., 2018). Moreover, root illumination can influence flowering time in *Arabidopsis* (Silva-Navas et al., 2015), suggesting that light responses in the root might even influence shoot development and the timing of developmental phase transitions, thereby opening up new research possibilities towards crop improvement. Finally, the big question that remains to be answered is why plants have developed this molecular mechanism in response to root illumination. Since roots are actively stimulated to grow into the soil via gravitropism and negative phototropism (Harmer and Brooks, 2018), it is not entirely surprising that roots develop better in the darkness. But why would plants actively inhibit root growth when exposed to light? A possible reason might be that root inhibition by light somehow relates to negative phototropism. Previous studies have shown that light affects root halotropism and the gravitropic response, indicating its importance in tropic responses (Yokawa et al., 2011; Silva-Navas et al., 2015). Although negative phototropism is primarily regulated by the blue light receptor PHOT1, it has been suggested that PHYA interacts with PHOT1 during root phototropism, possibly by modulating its intracellular distribution, or through induction of PHYTOCHROME KINASE SUBSTRATE 1 (Boccalandro et al., 2008; Han et al., 2008). Moreover, a PHYA-mediated decrease of auxin in the RAM of light-grown roots might aid to establish the auxin gradient that is required for root bending during tropic responses. This, however, does not explain the PHYB response in the LGR condition. Aside from its role in light signalling,

PHYB is a known thermosensor that, together with PIF4, embodies the main signalling hub in regulation of temperature responses (Casal and Balasubramanian, 2019). Since exposure of roots to light likely rises the root temperature as well, the PHYB light response in roots could be correlated to temperature responses. Substantial increases in root temperature result in decreased nutrient uptake, enhanced respiration, and overall growth inhibition (Du and Tachibana, 1994). A light-induced decrease in RAM size could contribute to, or be a result of, root cell respiration induced by high temperature. In addition, PHYB-PIF4 signalling regulates auxin biosynthesis in hypocotyls in response to heat stress (Sun et al., 2012), suggesting the possibility that, in roots, light and temperature coregulate auxin levels via PHYB-PIF4 to avoid water and nutrient loss.

Materials and Methods

Growth conditions and light treatments.

In all experiments, seedlings were grown at a 16h photoperiod, under white TL lights with a measured photon flux density of $150 \pm 10 \mu\text{mol m}^{-2} \text{s}^{-1}$, a temperature of 21°C and 50% relative humidity. Two different light treatments were included: (1) seedlings were grown completely exposed to light (light-grown roots or LGR); or (2) seedlings were grown in a more “natural” light environment with shoots exposed to light and roots shielded from light using black paper covers: (dark-grown roots or DGR) (**Figure S1**) (based on Silva-Navas et al., 2015).

Plant lines and seed germination.

Wild-type seedlings of *Arabidopsis thaliana* (Arabidopsis) and *Solanum lycopersicum* (tomato) were used as controls in this study. For Arabidopsis two ecotypes were included: Columbia (Col-0) and Landsberg *erecta* (Ler). For tomato, the Moneymaker (MM) cultivar and the commercial hybrid line Foundation (FO) were used. All Arabidopsis and tomato mutants and reporter lines that were used are listed in **Table S2**. Arabidopsis single mutants *phyA*, *phyB*, *pif1*, and *pif4* (all in Col-0 background) have been described before (Mayfield et al., 2007; Ruckle et al., 2007; Leivar et al., 2008a; Stephenson et al., 2009), and were crossed with *pDR5::GFP* to monitor auxin responses in these lines. Prior to the experiments all mutant lines and crosses were genotyped using the primers listed in **Table S3** and if required CAPS / PCR-RFLP markers described in **Table S4** (Nam et al., 1989; Konieczny and Ausubel, 1993). Arabidopsis and tomato seeds were surface sterilised by incubating for 1 minute in 70% ethanol and 10 minutes in a 2-fold diluted commercial bleach solution (1% chlorine). Subsequently the seeds were washed five times with sterile water. Arabidopsis seeds were stratified for 5 days at 4°C in darkness and germinated on square plates (#688102, Greiner Bio-One™) containing MA medium (Masson and Paszkowski, 1992) supplemented with 1% (w/v) sucrose and 0.8% (w/v) Daishin agar. Arabidopsis seeds were germinated by placing the plates vertically in the two light conditions described above. Sterile tomato seeds were placed on sterilised, wet filter paper (#1001325, Whatman®) using forceps and were germinated in darkness at 21°C for 5 days. Germinated seeds were moved from

the filters to square plates containing solid MA medium and placed vertically in the two light conditions described above.

***In vitro* analysis of seedling growth.**

At 7 days after germination (DAG), *Arabidopsis* seedlings were photographed, and primary root length and hypocotyl length were measured. The shoot-root ratio was calculated based on these measurements. Tomato seedlings were photographed at 5 DAG for primary root length measurements. To monitor the response of *Arabidopsis* seedlings to exogenous auxin, 4-day-old seedlings were transferred to square plates containing MA medium supplemented with 0, 5, 10, 20, 30, 40 or 50 nM 1-naphthaleneacetic acid (NAA). The increase in primary root length between 0 and 6 days after NAA treatment was measured. At 6 days after NAA treatment, *pDR5::GFP* seedlings were analysed under the confocal microscope. To analyse root-localised versus shoot-localised phytochrome functions, 4-day-old *Arabidopsis* seedlings grown in the LGR condition were grafted as described previously (Marsch-Martínez et al., 2013) in the following combinations: wild type/wild type (positive control); mutant/mutant (negative control); wild type/mutant (mutation only present in roots) and mutant/wild type (mutation only present in shoots). At 5 days after grafting, successful grafts were photographed to measure the post-grafting increase in primary root growth and analysed under the confocal microscope. To analyse the response of roots to light quality, the roots were covered with red translucent plastic (RGR) or blue translucent plastic (BGR). To avoid any additional effects of decreased light intensity, LGR seedlings were wrapped with white translucent plastic in this experiment. The primary root length was

measured after 7 days of growth under coloured plastic. All measurements were performed with ImageJ (Fiji) (Schindelin et al., 2012).

Microscopy analysis.

For confocal images of Arabidopsis roots, 7-day-old seedlings were stained with 10 µg/ml propidium iodide (PI) for 5 minutes and then mounted onto a glass slide in water with a cover slip. To visualise *pDR5::GFP* and PI staining in root tips, a Zeiss LSM5 Exciter/AxioImager equipped with a 40x oil objective and respectively a 488 nm argon laser and a 505-530 nm band pass filter or 600 nm long pass filter was used. For images of tomato roots, 5-day-old seedlings were mounted on a glass slide and imaged with a Leica MZ16FA equipped with a Leica DFC420C camera. YFP fluorescence was detected using a 510/20 nm excitation filter and a 560/40 nm emission filter. To quantify the fluorescent signals, the corrected total cell fluorescence method (McCloy et al., 2014) was slightly adjusted to quantify the corrected total fluorescence (CTF) of the root apex. $CTF = \text{integrated density (sum of all pixel intensities)} - (\text{area of root apex} * \text{mean fluorescence of background readings})$. All CTF measurements were performed in ImageJ (Fiji) and are expressed in Arbitrary Units (A.U.).

RNA extraction and qRT-PCR.

Root tips of 7-day-old Arabidopsis seedlings or 5-day-old tomato seedlings were pooled (± 80 per RNA sample), frozen in liquid nitrogen, and ground with a TissueLyser II (#85300, Qiagen). Total RNA was extracted from the ground tissue using a RNeasy® Plant Mini kit (#74904, Qiagen), and used for first strand cDNA synthesis with the RevertAid First Strand cDNA Synthesis kit

(#K1621, Thermo Scientific™). For qRT-PCR, the cDNA was diluted 10x and used with TB Green Premix Ex Taq II (Tli RNase H Plus) (#RR820B, Takara) and the CFX96 Touch™ Real-Time PCR Detection System (#1855196, Bio-Rad). CT values were obtained using Bio-Rad CFX manager 3.1. Normalisation was done according to the $\Delta\Delta C_t$ method with *PP2A* (At2g42500) and *TIP41* (Solyc10g049850) as reference genes for Arabidopsis and tomato, respectively (Pfaffl, 2001). All primers that were used for qRT-PCR are listed in **Table S3**.

Linear regression analysis.

The correlation coefficient (r) was calculated using the equation below, where x represents the NAA concentration, and y represents the *pDR5::GFP* signal.

$$r = \frac{\sum(x_i - \bar{x})(y_i - \bar{y})}{\sqrt{\sum(x_i - \bar{x})^2 \sum(y_i - \bar{y})^2}}$$

To calculate the linear regression coefficients a (y-intercept) and b (slope), the following equations were used, where $\sigma(x,y)$ represents the covariance of x and y , and $\sigma(x)$ represents the variance of x .

$$a = \bar{y} - b\bar{x} \qquad b = \frac{\sigma(x,y)}{\sigma(x)}$$

Statistical analysis and figures.

All phenotyping and microscopy experiments were performed with 20 or 30 biologically independent seedlings for tomato or Arabidopsis, respectively. In experiments that included only wild-type seedlings, the LGR condition was compared to the DGR condition using a two-sided Student's *t*-test. Experiments that included NAA treatments, or wild type versus mutant comparisons were statistically analysed using a one-way ANOVA followed by a Tukey's honestly significant different (HSD) post hoc test. In qRT-PCR experiments, three biological replicates (RNA isolated from \pm 80 root tips) were included, with three technical replicates each. For each plant line, normalised levels of gene expression in the LGR condition were compared to the DGR condition using a two-sided Student's *t*-test. For the linear regression analysis, regression coefficient *b* of the LGR condition was compared to regression coefficient *b* of the DGR condition as previously described (Andrade and Estévez-Pérez, 2014). All measurements were plotted into graphs using GraphPad Prism 5 software. All photographs were taken with a Nikon D5300 camera and edited in ImageJ (Fiji). Schematic models were generated with BioRender software. Final figures were assembled using Microsoft PowerPoint.

Author Contributions

KS and RO conceived and designed the experiments. KS performed the experiments and the statistical analysis. KS and RO analysed the results and wrote the manuscript. Both authors contributed to manuscript revision.

Funding

This work was part of the research programme “LED it be 50%” with project number 14212, which is partly financed by the Dutch Research Council (NWO).

Acknowledgements

We would like to thank Nunhems Netherlands BV for providing seeds of their commercial tomato hybrid line Foundation, and Cris Kuhlemeier for providing seeds of the tomato M82 *pDR5::YFP* reporter line. We thank Dália Alves Carvalho for help with propagation and genotyping of tomato mutants. Furthermore we acknowledge Thomas van der Toorn and Daan Kloosterman for help in optimizing the DGR system, Gerda Lamers for assistance with microscopy, Yohanna Miotto for help in optimizing grafting protocols, and Nick Surtel for assistance with the “coloured plastic” experiments.

References

- Aceves-García, P., Álvarez-Buylla, E. R., Garay-Arroyo, A., García-Ponce, B., Muñoz, R., and Sánchez, M. de la P. (2016). Root architecture diversity and meristem dynamics in different populations of *Arabidopsis thaliana*. *Front. Plant Sci.* 7, 1–14.
- Alaguero-Cordovilla, A., Gran-Gómez, F. J., Tormos-Moltó, S., and Pérez-Pérez, J. M. (2018). Morphological characterization of root system architecture in diverse tomato genotypes during early growth. *Int. J. Mol. Sci.* 19, 3888.
- Andrade, J. M., and Estévez-Pérez, M. G. (2014). Statistical comparison of the slopes of two regression lines: A tutorial. *Anal. Chim. Acta* 838, 1–12.
- Arsovski, A. A., Galstyan, A., Guseman, J. M., and Nemhauser, J. L. (2012). Photomorphogenesis. *Arab. B.* 10, e0147.
- Bai, S., Yao, T., Li, M., Guo, X., Zhang, Y., Zhu, S., and He, Y. (2014). PIF3 is involved in the primary root growth inhibition of *Arabidopsis* induced by nitric oxide in the light. *Mol. Plant* 7, 616–625.
- Bainbridge, K., Guyomarc'h S., Bayer, E., Swarup, R., Bennet, M., Mandel, T., and Kuhlemeier, C. (2008). Auxin influx carriers stabilize phyllotactic patterning. *Genes Dev.* 22, 810–823.
- Baskin, T. I. (2013). Patterns of root growth acclimation: Constant processes, changing boundaries. *Wiley Interdiscip. Rev. Dev. Biol.* 2, 65–73.
- Ben-Gera, H., Shwartz, I., Shao, M. R., Shani, E., Estelle, M., and Ori, N. (2012). ENTIRE and GOBLET promote leaflet development in tomato by modulating auxin response. *Plant J.* 70, 903–915.
- Boccalandro, H. E., De Simone, S. N., Bergmann-Honsberger, A., Schepens, I., Fankhauser, C., and Casal, J. J. (2008). Phytochrome kinase substrate1 regulates root phototropism and gravitropism. *Plant Physiol.* 146, 108–115.
- Casal, J. J., and Balasubramanian, S. (2019). Thermomorphogenesis. *Annu. Rev. Plant Biol.* 70, 321–346.

- Chen, X., Yao, Q., Gao, X., Jiang, C., Harberd, N. P., and Fu, X.** (2016). Shoot-to-root mobile transcription factor HY5 coordinates plant carbon and nitrogen acquisition. *Curr. Biol.* 26, 640–646.
- Cheng, Y., Dai, X., and Zhao, Y.** (2006). Auxin biosynthesis by the YUCCA flavin monooxygenases controls the formation of floral organs and vascular tissues in Arabidopsis. *Genes Dev.* 20, 1790–1799.
- Christians, M. J., Gingerich, D. J., Hua, Z., Lauer, T. D., and Vierstra, R. D.** (2012). The light-response BTB1 and BTB2 proteins assemble nuclear ubiquitin ligases that modify phytochrome B and D signaling in Arabidopsis. *Plant Physiol.* 160, 118–134.
- Costigan, S. E., Warnasooriya, S. N., Humphries, B. A., and Montgomery, B. L.** (2011). Root-localized phytochrome chromophore synthesis is required for photoregulation of root elongation and impacts root sensitivity to jasmonic acid in Arabidopsis. *Plant Physiol.* 157, 1138–1150.
- de Wit, M., Galvão, V. C., and Fankhauser, C.** (2016). Light-mediated hormonal regulation of plant growth and development. *Annu. Rev. Plant Biol.* 67, 513–537.
- Du, Y. C., and Tachibana, S.** (1994). Effect of supraoptimal root temperature on the growth, root respiration and sugar content of cucumber plants. *Sci. Hortic.* 58, 289–301.
- Expósito-Rodríguez, M., Borges, A. A., Borges-Pérez, A., and Pérez, J. A.** (2011). Gene structure and spatiotemporal expression profile of tomato genes encoding YUCCA-like flavin monooxygenases: The ToFZY gene family. *Plant Physiol. Biochem.* 49, 782–791.
- Franklin, K. A., Lee, S. H., Patel, D., Kumar, S. V., Spartz, A. K., Gu, C., Ye, S., Yu, P., Breen, G., Cohen, J. D., Wigge, P. A., and Gray, W.M.** (2011). Phytochrome-Interacting Factor 4 (PIF4) regulates auxin biosynthesis at high temperature. *Proc. Natl. Acad. Sci. U. S. A.* 108, 20231–20235.
- Guenot, B., Bayer, E., Kierzkowski, D., Smith, R. S., Mandel, T., Zádňíková, P., Benková, E.,**

- and Kuhlmeier, C.** (2012). PIN1-independent leaf initiation in *Arabidopsis*. *Plant Physiol.* 159, 1501-1510.
- Guo, H., Yang, H., Mockler, T. C., and Lin, C.** (1998). Regulation of flowering time by *Arabidopsis* photoreceptors. *Science* 279, 1360-1363.
- Han, I. S., Tseng, T. S., Eisinger, W., and Briggs, W. R.** (2008). Phytochrome A regulates the intracellular distribution of phototropin 1-green fluorescent protein in *Arabidopsis thaliana*. *Plant Cell* 20, 2835–2847.
- Harmer, S. L., and Brooks, C. J.** (2018). Growth-mediated plant movements: hidden in plain sight. *Curr. Opin. Plant Biol.* 41, 89–94.
- Kim, J., Yi, H., Choi, G., Shin, B., Song, P. S., and Choi, G.** (2003). Functional characterization of phytochrome interacting factor 3 in phytochrome-mediated light signal transduction. *Plant Cell* 15, 2399-2407.
- Koevoets, I. T., Venema, J. H., Elzenga, J. T. M., and Testerink, C.** (2016). Roots withstanding their environment: Exploiting root system architecture responses to abiotic stress to improve crop tolerance. *Front. Plant Sci.* 7, 1–19.
- Konieczny, A., and Ausubel, F. M.** (1993). A procedure for mapping *Arabidopsis* mutations using co-dominant ecotype-specific PCR-based markers. *Plant J.* 4, 403–410.
- Lee, H. J., Ha, J. H., Kim, S. G., Choi, H. K., Kim, Z. H., Han, Y. J., Kim, J. Il, Oh, Y., Frago, V., Shin, K., Hyeon, T., Choi, H. G., Oh, K. H., Baldwin, I. T., and Park, C. M.** (2016). Stem-piped light activates phytochrome B to trigger light responses in *Arabidopsis thaliana* roots. *Sci. Signal.* 9, 1–10.
- Lee, H. J., Park, Y. J., Ha, J. H., Baldwin, I. T., and Park, C. M.** (2017). Multiple routes of light signaling during root photomorphogenesis. *Trends Plant Sci.* 22, 803–812.
- Leivar, P., Monte, E., Al-Sady, B., Carle, C., Storer, A., Alonso, J. M., Ecker, J. R., and Quail, P. H.** (2008a). The *Arabidopsis* phytochrome-interacting factor

PIF7, together with PIF3 and PIF4, regulates responses to prolonged red light by modulating phyB levels. *Plant Cell* 20, 337–352.

Leivar, P., Monte, E., Oka, Y., Liu, T., Carle, C., Castillon, A., Huq, E., and Quail, P. H. (2008b). Multiple phytochrome-interacting bHLH transcription factors repress premature seedling photomorphogenesis in darkness. *Curr. Biol.* 18, 1815–1823.

Lejay, L., Wirth, J., Pervent, M., Cross, J. M. F., Tillard, P., and Gojon, A. (2008). Oxidative pentose phosphate pathway-dependent sugar sensing as a mechanism for regulation of root ion transporters by photosynthesis. *Plant Physiol.* 146, 2036–2053.

Marsch-Martínez, N., Franken, J., Gonzalez-Aguilera, K. L., de Folter, S., Angenent, G., and Alvarez-Buylla, E. R. (2013). An efficient flat-surface collar-free grafting method for *Arabidopsis thaliana* seedlings. *Plant Methods* 9, 1–9.

Masson, J., and Paszkowski, J. (1992). The culture response of *Arabidopsis thaliana* protoplasts is determined by the growth conditions of donor plants. *Plant J.* 2, 829–833.

Mayfield, J. D., Folta, K. M., Paul, A. L., and Ferl, R. J. (2007). The 14-3-3 proteins μ and ν influence transition to flowering and early phytochrome response. *Plant Physiol.* 145, 1692–1702.

McCloy, R. A., Rogers, S., Caldon, C. E., Lorca, T., Castro, A., and Burgess, A. (2014). Partial inhibition of Cdk1 in G2 phase overrides the SAC and decouples mitotic events. *Cell Cycle* 13, 1400–1412.

McElver, J., Tzafrir, I., Aux, G., Rogers, R., Ashby, C., Smith, K., Thomas, C., Schetter, A., Zhou, Q., Cushman, M. A., Tossberg, J., Nickle, T., Levin, J. Z., Law, M., Meinke, D., and Patton, D. (2001). Insertional mutagenesis of genes required for seed development in *Arabidopsis thaliana*. *Genetics* 159, 1751–1763.

Moni, A., Lee, A. Y., Briggs, W. R., and Han, I. S. (2015). The blue light receptor Phototropin 1 suppresses lateral root growth by controlling cell elongation. *Plant Biol.* 17, 34–40.

- Monte, E., Alonso, J. M., Ecker, J. R., Zhang, Y., Li, X., Young, J., Austin-Phillips, S., and Quail, P. H.** (2003). Isolation and characterization of phyC mutants in *Arabidopsis* reveals complex crosstalk between phytochrome signaling pathways. *Plant Cell* 15, 1962–1980.
- Nam, H. G., Giraudat, J., Den Boer, B., Moonan, F., Loos, W., Hauge, B. M., and Goodman, H. M.** (1989). Restriction fragment length polymorphism linkage map of *Arabidopsis thaliana*. *Plant Cell* 1, 699–705.
- Ottenschlager, I., Wolff, P., Wolverton, C., Bhalerao, R. P., Sandberg, G., Ishikawa, H., Evans, M., and Palme, K.** (2003). Gravity-regulated differential auxin transport from columella to lateral root cap cells. *Proc. Natl. Acad. Sci. U. S. A.* 100, 2987–2991.
- Petricka, J. J., Winter, C. M., and Benfey, P. N.** (2012). Control of *Arabidopsis* root development. *Annu. Rev. Plant Biol.* 63, 563–590.
- Pfaffl, M. W.** (2001). A new mathematical model for relative quantification in real-time RT-PCR. *Nucleic Acids Res.* 29, e45.
- Pham, V. N., Kathare, P. K., and Huq, E.** (2018). Phytochromes and phytochrome interacting factors. *Plant Physiol.* 176, 1025–1038.
- Podolec, R., and Ulm, R.** (2018). Photoreceptor-mediated regulation of the COP1/SPA E3 ubiquitin ligase. *Curr. Opin. Plant Biol.* 45, 18–25.
- Redei, G. P.** (1992). A heuristic glance at the past of *Arabidopsis* genetics. *Methods in Arabidopsis Research*, 1–15.
- Reed, J. W., Nagatani, A., Elich, T. D., Fagan, M., and Chory, J.** (1994). Phytochrome A and phytochrome B have overlapping but distinct functions in *Arabidopsis* development. *Plant Physiol.* 104, 1139–1149.
- Ruckle, M. E., DeMarco, S. M., and Larkin, R. M.** (2007). Plastid signals remodel light signaling networks and are essential for efficient chloroplast biogenesis in *Arabidopsis*. *Plant Cell* 19, 3944–3960.
- Sassi, M., Lu, Y., Zhang, Y., Wang, J., Dhonukshe, P., Blilou, I., Dai, M., Li, J., Gong, X., Jaillais, Y., Yu, X., Traas, J., Ruberti, I., Wang, H., Scheres, B., Vernoux, T., and Xu, J.** (2012). COP1 mediates the coordination of root and

shoot growth by light through modulation of PIN1- and PIN2-dependent auxin transport in *Arabidopsis*. *Dev.* 139, 3402–3412.

Schindelin, J., Arganda-Carreras, I., Frise, E., Kaynig, V., Longair, M., Pietzsch, T., Preibisch, S., Rueden, C., Saalfeld, S., Schmid, B., Tinevez, J. Y., White, D. J., Hartenstein, V., Eliceiri, K., Tomancak, P., and Cardona, A. (2012). Fiji: An open-source platform for biological-image analysis. *Nat. Methods* 9, 676–682.

Silva-Navas, J., Moreno-Risueno, M. A., Manzano, C., Pallero-Baena, M., Navarro-Neila, S., Téllez-Robledo, B., Garcia-Mina, J. M., Baigorri, R., Gallego, F. J., and Del Pozo, J. C. (2015). D-Root: A system for cultivating plants with the roots in darkness or under different light conditions. *Plant J.* 84, 244–255.

Smith, R. S., Guyomarc'h, S., Mandel, T., Reinhardt, D., Kuhlemeier, C., and Prusinkiewicz, P. (2006). A plausible model of phyllotaxis. *Proc. Natl. Acad. Sci. U. S. A.* 103, 1301–1306.

Stephenson, P. G., Fankhauser, C., and Terry, M. J. (2009). PIF3 is a repressor of chloroplast development. *Proc. Natl. Acad. Sci. U. S. A.* 106, 7654–7659.

Sun, J., Qi, L., Li, Y., Chu, J., and Li, C. (2012). Pif4-mediated activation of *yucca8* expression integrates temperature into the auxin pathway in regulating *Arabidopsis* hypocotyl growth. *PLoS Genet.* 8, e1002594.

Thimann, K. V. (1937). On the nature of inhibitions caused by auxin. *Am. J. Bot.* 24, 407.

Van Gelderen, K., Kang, C., and Pierik, R. (2018). Light signaling, root development, and plasticity. *Plant Physiol.* 176, 1049–1060.

Van Tuinen, A., Kerckhoffs, L. H. J., Nagatani, A., Kendrick, R. E., and Koornneef, M. (1995a). Far-red light-insensitive, phytochrome A-deficient mutants of tomato. *Mol. Gen. Genet.* 246, 133–141.

Van Tuinen, A., Kerckhoffs, L. H. J., Nagatani, A., Kendrick, R. E., and Koornneef, M. (1995b). A temporarily red light-insensitive mutant of tomato lacks a light-stable, B-like phytochrome. *Plant Physiol.* 108, 939–947.

- Warnasooriya, S. N., Porter, K. J., and Montgomery, B. L.** (2011). Tissue- and isoform-specific phytochrome regulation of light-dependent anthocyanin accumulation in *Arabidopsis thaliana*. *Plant Signal. Behav.* 6, 624-631.
- Weller, J. L., Schreuder, M. E. L., Smith, H., Koornneef, M., and Kendrick, R. E.** (2000). Physiological interactions of phytochromes A, B1 and B2 in the control of development in tomato. *Plant J.* 24, 345-356.
- Yokawa, K., Kagenishi, T., Kawano, T., Mancuso, S., and Baluška, F.** (2011). Illumination of Arabidopsis roots induces immediate burst of ROS production. *Plant Signal. Behav.* 6, 1460–1464.
- Yokawa, K., Fasano, R., Kagenishi, T., and Baluška, F.** (2014). Light as stress factor to plant roots – Case of root halotropism. *Front. Plant Sci.* 5, 1–9.

Supplementary Material (Tables S1-S4 and Figures S1-S3)

Table S1: Linear regression analysis.

Linear regression analysis of the correlation between NAA concentration and *pDR5::GFP* expression in the RAM. \bar{y} -values are the mean values of the dot plot shown in Figure 2D. $\sigma(x,y)$ = covariance of x - and y -values, $\sigma(x)$ = variance of x -values, and $\sigma(y)$ = variance of y -values. Regression coefficient a indicates the y -intercept, and regression coefficient b indicates the slope.

Light condition	NAA concentration (x)	GFP signal (y)	$x_i - x_{mean}$	$y_i - y_{mean}$	$\sigma(x,y)$	$\sigma(x)$	$\sigma(y)$
LGR	0	277979	-25	-151755	3793879	625	23029630610
	10	333101	-15	-96633	1449497	225	9337968900
	20	414728	-5	-15006	75031	25	225185038
	30	454278	5	24544	122719	25	602399755
	40	534336	15	104601	1569027	225	10941543537
	50	563983	25	134249	3356221	625	18022749251
Mean	25	429734	0	0	1727729	292	10359912848
DGR	0	525449	-8.75	-64573	565011	76.6	4169640043
	5	565031	-3.75	-24991	93715	14.1	624537586
	10	614962	1.25	24940	31175	1.6	622016070
	20	654645	11.25	64623	727012	126.6	4176164441
Mean	8.75	590022	0	0	354228	54.7	2398089535
	Correlation coefficient (r)		Regression coefficient (a)		Regression coefficient (b)		
LGR	0.993		281643		5924		
DGR	0.978		533345		6477		
	p-value slope comparison (b)						
LGR vs DGR	0.609						

Table S2: Plant lines used in this study.

Arabidopsis mutant lines were obtained from Nottingham Arabidopsis Stock Centre (NASC). Tomato mutant lines were obtained from Tomato Genetics Resource Centre (TGRC).

Plant line	Description	Source	Reference
Arabidopsis			
Columbia (Col-0)	Natural Arabidopsis accession	-	Redei, 1992
Landsberg <i>erecta</i> (Ler)	Natural Arabidopsis accession	-	Redei, 1992
Moneymaker (MM)	Standard non-hybrid cultivar	Nunhems	-
Foundation (FO)	Commercial hybrid	Nunhems	-
<i>yuc4</i> (SM_3_16128)	Transposon insertion in exon of At5g11320	-	Cheng et al., 2006
<i>yuc6</i> (SALK_093708)	T-DNA insertion in intron of At5g25620	-	Cheng et al., 2006
<i>phyA</i> (SALK_014575)	T-DNA insertion in exon of At1g09570	NASC	Ruckle et al., 2007
<i>phyB</i> (SALK_022035)	T-DNA insertion in exon of At2g18790	NASC	Mayfield et al., 2007
<i>phyC</i> (phyC-3)	3 kbp deletion in At5g35840	NASC	Monte et al., 2003
<i>phyD</i> (SALK_027956)	T-DNA insertion in exon of At4g16250	NASC	Christians et al., 2012
<i>phyE</i> (SALK_092529)	T-DNA insertion in exon of At4g18130	NASC	Warnasooriya et al., 2011
<i>cry1</i> (SALK_069292)	T-DNA insertion in exon of At4g08920	NASC	Ruckle et al., 2007
<i>cry2</i> (<i>cry2-1</i>)	Large deletion (2/3) in At1g04400	NASC	Guo et al., 1998
<i>phot1</i> (SAIL_1232_C01)	T-DNA insertion in exon of At3g45780	NASC	McElver et al., 2001
<i>phot2</i> (SALK_142275)	T-DNA insertion in exon of At5g58140	NASC	Ruckle et al., 2007
<i>phyAphyB</i> (phyA-201 phyB-5)	Substitution Q980STOP in At1g09570 x substitution W552STOP in At2g18790	NASC	Reed et al., 1994
<i>pif1</i> (SAIL_256_G07)	T-DNA insertion in exon of At2g20180	NASC	Stephenson et al., 2009
<i>pif3</i> (SALK_030753)	T-DNA insertion in intron of At1g09530	NASC	Kim et al., 2003
<i>pif4</i> (SAIL_1288_E07)	T-DNA insertion in intron of At2g43010	NASC	Leivar et al., 2008a
<i>pif1pif3pif4</i> (SAIL_256_G01, pif3-3, SAIL_1288_E07)	2.5 kbp deletion in At1g09530 x T-DNA insertion in At2g20180 and At2g43010	NASC	Leivar et al., 2008b
<i>pin1</i> (SALK_047613)	T-DNA insertion in exon of At1g73590	NASC	Smith et al., 2006
<i>pin2</i> (<i>eir1-1</i>)	Diepoxbutane mutation in exon of At5g57090	NASC	Guenot et al., 2012
<i>pin4-3</i>	Transposon insertion in exon of At2g01420	NASC	Guenot et al., 2012
<i>pin7-2</i>	T-DNA insertion in exon of At1g23080	NASC	Guenot et al., 2012
<i>auxlaxq</i> (<i>aux1-21</i> , <i>lax1</i> , <i>lax2</i> , <i>lax3</i>)	EMS mutation in exon of At2g38120 x T-DNA insertion in exon of At5g01240 x T-DNA insertion in exon of At2g21050 x T-DNA insertion in exon of At1g77690	NASC	Bainbridge et al., 2008
<i>pDR5::GFP</i>	Synthetic auxin-responsive reporter (Col-0)	-	Ottenschlager et al., 2003
<i>phyA</i> x <i>pDR5::GFP</i>	SALK_014575 crossed with DR5 reporter	-	This study
<i>phyB</i> x <i>pDR5::GFP</i>	SALK_022035 crossed with DR5 reporter	-	This study
<i>pif1</i> x <i>pDR5::GFP</i>	SAIL_256_G07 crossed with DR5 reporter	-	This study
<i>pif4</i> x <i>pDR5::GFP</i>	SAIL_1288_E07 crossed with DR5 reporter	-	This study
Tomato			
<i>phyA</i> (phyA-1)	Null-mutant (<i>fri</i> ¹)	TGRC	Van Tuinen et al., 1995a
<i>phyB1</i> (phyB1-1)	Null-mutant (<i>tri</i> ¹)	TGRC	Van Tuinen et al., 1995b
<i>phyB2</i> (phyB2-1)	Null-mutant (70F)	TGRC	Weller et al., 2000
<i>phyAphyB2</i>	Null-mutant (<i>fri</i> ¹) x Null mutant (70F)	TGRC	Weller et al., 2000
<i>pDR5::YFP</i>	Synthetic auxin-responsive reporter (M82)	Kuhlemeier	Ben-Gera et al., 2012

Table S3: Primers used in this study.

Primer name	Target gene	Sequence 5'→3'	Experiment
LB1 (SAIL T-DNA)	N/A	GCCTTTTCAGAAATGGATAAATA	Genotyping
LBb1.3 (SALK T-DNA)	N/A	ATTTTGCCGATTTCGGAAC	Genotyping
Border seq (SM transposon)	N/A	TACGAATAAGAGCGTCCATTTTAGAGTGA	Genotyping
SALK_014575 (<i>phyA</i>) FW	At1g09570	CCAGTCAGCTCAGCAATTTTC	Genotyping
SALK_014575 (<i>phyA</i>) RV	At1g09570	AATGCAAAACATGCTAGGGTG	Genotyping
SALK_022035 (<i>phyB</i>) FW	At2g18790	CATCATCAGCATCATGTCCACC	Genotyping
SALK_022035 (<i>phyB</i>) RV	At2g18790	TTCACGAAGGCAAAAGAGTTG	Genotyping
SM_3_16128 (<i>yuc4</i>) FW	At5g11320	CCCTTCTTAGACCTACTCTAC	Genotyping
SM_3_16128 (<i>yuc4</i>) RV	At5g11320	GCCCAACGTAGAATTAGCAAG	Genotyping
SALK_093708 (<i>yuc6</i>) FW	At5g25620	CCAGCCTTTGTATTTTCCCGT	Genotyping
SALK_093708 (<i>yuc6</i>) RV	At5g25620	CCGAAAAAGGGTCTTGTGCG	Genotyping
<i>phyA-201</i> (double mutant) FW	At1g09570	GAAGTGTGACTGCTTCCACGAGT	Genotyping
<i>phyA-201</i> (double mutant) RV	At1g09570	TAGCAAGATGCACAGAACGCC	Genotyping
<i>phyB-5</i> (double mutant) FW	At2g18790	CGTGACGCGCCTGCTGGAATTGTT	Genotyping
<i>phyB-5</i> (double mutant) RV	At2g18790	TCCATTGATGCAGCCTCCGGCA	Genotyping
<i>phyC-3</i> FW	At5g35840	ATGTCATCGAACACTTCACG	Genotyping
<i>phyC-3</i> RV	At5g35840	TCAAATCAAGGGAAATTTCTG	Genotyping
SALK_027956 (<i>phyD</i>) FW	At4g16250	AACCCGGTGAATCAGAATGG	Genotyping
SALK_027956 (<i>phyD</i>) RV	At4g16250	ATCGGTTACAGTGAAAATGCG	Genotyping
SALK_092529 (<i>phyE</i>) FW	At4g18130	AAAGAGGCGGTCTAGTTCAGC	Genotyping
SALK_092529 (<i>phyE</i>) RV	At4g18130	TATCAGTGGTTAAACCCGTCG	Genotyping
SALK_069292 (<i>cry1</i>) FW	At4g08920	TTCATGCCACTTGGTTAGACC	Genotyping
SALK_069292 (<i>cry1</i>) RV	At4g08920	TCCCACAGACTGGATACATC	Genotyping
<i>cry2-1</i> FW	At1g04400	ATGAAGATGGACAAAAAGAC	Genotyping
<i>cry2-1</i> RV	At1g04400	TCATTTGCAACCATTTTTTC	Genotyping
SAIL_1232_C01 (<i>phot1</i>) FW	At3g45780	ACATAGGATGCAGCAGAAACG	Genotyping
SAIL_1232_C01 (<i>phot1</i>) RV	At3g45780	CAGTAGACTGGTGGGCTCTTG	Genotyping
SALK_142275 (<i>phor2</i>) FW	At5g58140	TCCATCTCCTTTGAATGATGC	Genotyping
SALK_142275 (<i>phor2</i>) RV	At5g58140	AGTGTCATTGCTCACGGATTTC	Genotyping
<i>phyA-1</i> FW	Solyc10g044670	TAAC TGAATACACCATTCCTTAACC	Genotyping
<i>phyA-1</i> RV	Solyc10g044670	ATAATCGCTCTATAGTCACC	Genotyping
<i>phyB1-1</i> FW	Solyc01g059870	CTAAAATTCAAAGAGGAGGTGAGATT	Genotyping
<i>phyB1-1</i> RV	Solyc01g059870	GAAGGGGTAAAAAGGGTCTCTAA	Genotyping
<i>phyB2-1</i> FW	Solyc05g053410	GACGAGTAACATTACATGA	Genotyping
<i>phyB2-1</i> RV	Solyc05g053410	GCTTAGGCAACACTAGGTTA	Genotyping
SAIL_256_G07 (<i>pif1</i>) FW	At2g20180	AAGGAAGGAGGAGGAATAGGC	Genotyping
SAIL_256_G07 (<i>pif1</i>) RV	At2g20180	CATGAATTTCTCGAGGCTGAG	Genotyping
SALK_030753 (<i>pif3</i>) FW	At1g09530	AGTCTGTGCTTCTGCTACGC	Genotyping
SALK_030753 (<i>pif3</i>) RV	At1g09530	TTGCATAAGGCATTCCCATAC	Genotyping
SAIL_1288_E07 (<i>pif4</i>) FW	At2g43010	AATACATTTTGCAGGCAATCG	Genotyping
SAIL_1288_E07 (<i>pif4</i>) RV	At2g43010	CGTAATGAAGTTGCACGTTTACTC	Genotyping
<i>pif3-3</i> WT (triple mutant) FW	At1g09530	AGAAGCAATTTGGTCACCATGCTC	Genotyping
<i>pif3-3</i> WT (triple mutant) RV	At1g09530	TGCATACAAATAGTCGATCGTATG	Genotyping
<i>pif3-3</i> DEL (triple mutant) FW	At1g09530	GGTGTGTATGTGAGAAGGTACATCCATCG	Genotyping
<i>pif3-3</i> DEL (triple mutant) RV	At1g09530	AAGCTTAGCTTTGGTGAGCCTGAAAAGCT	Genotyping
SALK_047613 (<i>pin1</i>) FW	At1g73590	TTCCATAAAGTCATGATTAAGCACA	Genotyping
SALK_047613 (<i>pin1</i>) RV	At1g73590	CGGTGGGAACAACATAAGCAA	Genotyping
<i>eir1-1</i> (<i>pin2</i>) FW	At5g57090	GGTACCAATGATCACCGGCAAAGACAT	Genotyping
<i>eir1-1</i> (<i>pin2</i>) RV	At5g57090	GAAGAGATCATTGATGAGGC	Genotyping
<i>pin4-3</i> FW	At2g01420	CAACGCCGTTAAATATGG	Genotyping
<i>pin4-3</i> RV	At2g01420	TGCAGCAAAACCCACATTTTACTTC	Genotyping
<i>pin7-2</i> FW	At1g23080	TTTACTTGAACAATGGCCACAC	Genotyping
<i>pin7-2</i> RV	At1g23080	GGTAAAGGAAGTGCTTAACGG	Genotyping
<i>aux1-21</i> FW	At2g38120	TGCTACCAAAGCACTACTACTAC	Genotyping
<i>aux1-21</i> RV	At2g38120	GAAATGGGCTGAAACCAACTCAA	Genotyping

<i>lax1</i> FW	At5g01240	ATATGGTTGCAGGTGGCACA	Genotyping
<i>lax1</i> RV	At5g01240	GTAACCGGCAAAAGCTGCA	Genotyping
<i>lax2</i> FW	At2g21050	ATGGAGAACGGTGAGAAAGCAGC	Genotyping
<i>lax2</i> RV	At2g21050	CGCAGAAGGCAGCGTTAGCG	Genotyping
<i>lax3</i> FW	At1g77690	TACTTCACCGGAGCCACCA	Genotyping
PP2A-3 FW	At2g42500	ACGTGGCCAAAATGATGCAA	qRT-PCR
PP2A-3 RV	At2g42500	TCATGTTCTCCACAACCGCT	qRT-PCR
YUCCA1 FW	At4g32540	TTAGCTTAGACCTCGTCGGACAT	qRT-PCR
YUCCA1 RV	At4g32540	TGGCAACACATGAACGGTGT	qRT-PCR
YUCCA2 FW	At4g13260	TGTTTTGGACGTTGGCACTCT	qRT-PCR
YUCCA2 RV	At4g13260	TACCCGTTTCAACTCCGGATA	qRT-PCR
YUCCA3 FW	At1g04610	CCTACGCAGCCAACTTTGACA	qRT-PCR
YUCCA3 RV	At1g04610	GCCCGAACGTCTCATCATATTT	qRT-PCR
YUCCA4 FW	At5g11320	TCTAGCCGTAGCGGCTTGTTT	qRT-PCR
YUCCA4 RV	At5g11320	AAACAATCGGTTCTCTCGAGGA	qRT-PCR
YUCCA5 FW	At5g43890	TGTCCAGTCTGCTCGATACGA	qRT-PCR
YUCCA5 RV	At5g43890	CACCGGCAGATATATTCATCTC	qRT-PCR
YUCCA6 FW	At5g25620	CGGTATGGAGGTTGTTTGGAT	qRT-PCR
YUCCA6 RV	At5g25620	ATGGACAGCCCAAAAGTTGAAG	qRT-PCR
YUCCA7 FW	At2g33230	CCCGGAGTATCCAACGAAGTAC	qRT-PCR
YUCCA7 RV	At2g33230	TGATTGGACCGTCTCATTGAAC	qRT-PCR
YUCCA8 FW	At4g28720	TGACCTAGCAAACCATTCGCT	qRT-PCR
YUCCA8 RV	At4g28720	CATCTTCATTGCAAGCTCAAACG	qRT-PCR
YUCCA9 FW	At1g04180	TTCTCAGAGCGGCGATGTGT	qRT-PCR
YUCCA9 RV	At1g04180	CACAACGAATGGGACTCCTTGA	qRT-PCR
YUCCA10 FW	At1g48910	AAGTATGCTCCAGTGGCGATG	qRT-PCR
YUCCA10 RV	At1g48910	GGAAGAGTCCGTACTTGGAGAGATC	qRT-PCR
YUCCA11 FW	At1g21430	GACGAATACGCCACACGTTTC	qRT-PCR
YUCCA11 RV	At1g21430	ACCATCTTTGAAGTACGCGGA	qRT-PCR
TAA1 FW	At1g70560	GCAGAGCTGGAGAGCGTTGTG	qRT-PCR
TAA1 RV	At1g70560	CTTCATGTTGGCGAGTCTCTCGAG	qRT-PCR
TAR1 FW	At1g23320	CAGGAAGGCTCCTCAGACATTGC	qRT-PCR
TAR1 RV	At1g23320	CGCTGGTCAGAGTTATGAGACACC	qRT-PCR
TAR2 FW	At4g24670	GGTTGTGTCTCAGACAGTTGTGGG	qRT-PCR
TAR2 RV	At4g24670	GGTTGTGTCTCAAAGACCTGTC	qRT-PCR
TIP41 FW	Solyc10g049850	ATGGAGTTTTTGAGTCTTCTGC	qRT-PCR
TIP41 RV	Solyc10g049850	GCTGCGTTTCTGGCTTAGG	qRT-PCR
ToFZY1 FW	Solyc06g065630	GTACTCGACGTTGGAGCATTATC	qRT-PCR
ToFZY1 RV	Solyc06g065630	TGAAGAAATCATTTCCCTTAAACC	qRT-PCR
ToFZY2 FW	Solyc08g068160	AGGAATGGAGGTGTGTTTGG	qRT-PCR
ToFZY2 RV	Solyc08g068160	GGGACGTGTCACCGAGTAA	qRT-PCR

Table S4: CAPS / PCR-RFLP markers for genotyping.

PCR fragment	CAPS / RFLP	Wild-type product	Mutant product
<i>phyA-201</i>	HinfI	±190 bp	241 bp
<i>phyB-5</i>	BsaBI	666 bp	±250 bp
<i>phyA-1</i>	EcoNI	236 bp	±180 bp
<i>phyB1-1</i>	HinfI	±100 bp	193 bp
<i>phyB2-1</i>	FokI	±300 bp	536 bp

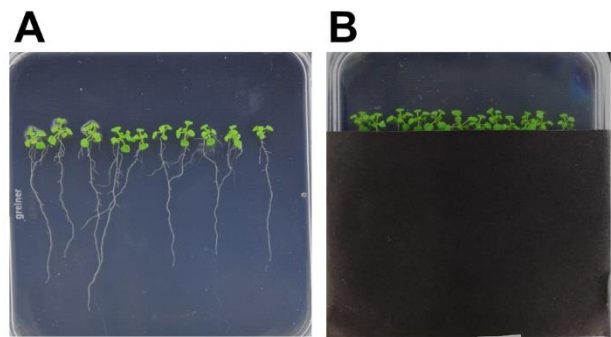


Figure S1: LGR and DGR growth conditions.

A. Arabidopsis seedlings grown in the light-grown root (LGR) condition, where the shoots and roots are exposed to light. **B.** Arabidopsis seedlings grown in the dark-grown (DGR) condition, where only the shoots are exposed to light.

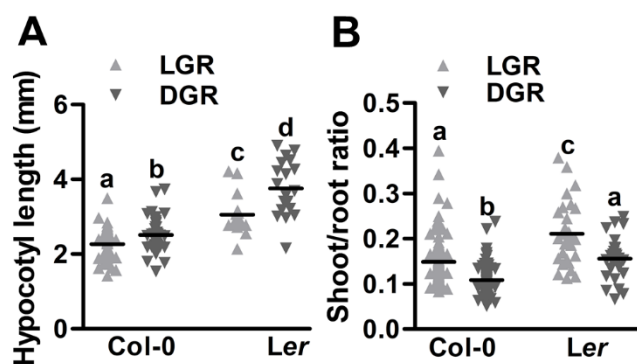


Figure S2: Arabidopsis DGR seedlings show a reduced shoot/root ratio despite their longer hypocotyls.

A. Quantification of the hypocotyl length of 7-day-old Arabidopsis seedlings of ecotypes Columbia (Col-0) and Landsberg *erecta* (Ler) that were grown in light-grown roots (LGR) or dark-grown roots (DGR) conditions. **B.** Quantification of the shoot/root ratio of 7-day-old Col-0 and Ler seedlings that were grown in LGR or DGR conditions. Hypocotyl lengths or shoot/root ratios were compared using a one-way ANOVA followed by a Tukey's test (letters **a**, **b**, **c**, and **d** indicate statistically different values, $p < 0.05$). In the graphs, the horizontal line indicates the mean, error bars indicating standard error of the mean are not visible due to limited variation, and triangles indicate values of biologically independent observations ($n=30$). Similar results were obtained from three independent experiments.

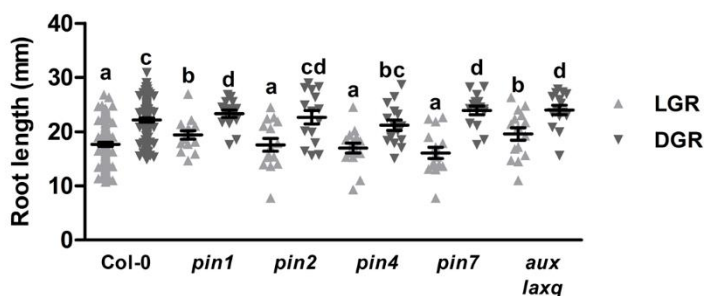
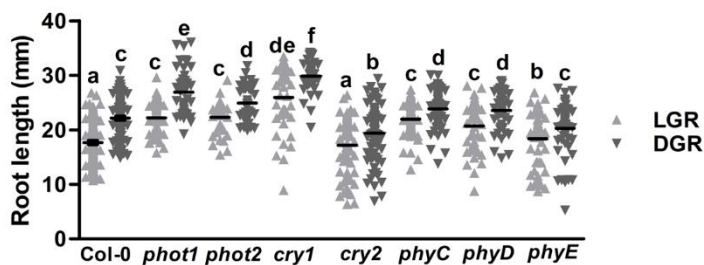
A**B**

Figure S3: Seedling roots of several Arabidopsis photoreceptor mutants are shorter in light-grown conditions.

A. Quantification of the primary root length of 7-day-old Arabidopsis pin-formed (*pin*) and auxin1/like-aux1 (*aux/lax*) mutants that were grown in LGR or DGR conditions. **B.** Quantification of the primary root length of 7-day-old Arabidopsis phototropin (*phot*), cryptochrome (*cry*) or phytochrome (*phy*) single mutants that were grown in LGR or DGR conditions. Primary root lengths were compared using a one-way ANOVA followed by a Tukey's test (letters **a**, **b**, **c**, **d**, **e**, and **f** indicate statistically different values, $p < 0.05$). In the graphs, the horizontal line indicates the mean, error bars represent standard error of the mean (for some not visible due to limited variation), and triangles indicate values of biologically independent observations ($n=30$). Similar results were obtained from three independent experiments.



Chapter 3

Regulation of early plant development by red
and blue light: A comparative analysis
between *Arabidopsis thaliana* and *Solanum
lycopersicum*.

**Kiki Spaninks¹, Jelmer van Lieshout¹, Wim van
Ieperen² and Remko Offringa¹**

Frontiers in Plant Science (2020) **11**:1-13

¹Plant Developmental Genetics, Institute of Biology Leiden,
Leiden University, Sylviusweg 72, 2333 BE, Leiden, Netherlands.

²Horticulture and Product Physiology Group, Wageningen
University and Research, Droevendaalsesteeg 1, 6708 PB,
Wageningen, Netherlands.



Abstract

In vertical farming, plants are grown in multi-layered growth chambers supplied with energy-efficient LEDs that produce less heat and can thus be placed in close proximity to the plants. The spectral quality control allowed by LED lighting potentially enables steering plant development towards desired phenotypes. However, this requires detailed knowledge on how light quality affects different developmental processes per plant species or even cultivar, and how well information from model plants translates to horticultural crops. Here we have grown the model dicot *Arabidopsis thaliana* (Arabidopsis) and the crop plant *Solanum lycopersicum* (tomato) under white or monochromatic red or blue LED conditions. In addition, seedlings were grown *in vitro* in either light-grown roots (LGR) or dark-grown roots (DGR) LED conditions. Our results present an overview of phenotypic traits that are sensitive to red or blue light, which may be used as a basis for application by tomato nurseries. Our comparative analysis showed that young tomato plants were remarkably indifferent to the LED conditions, with red and blue light effects on primary growth, but not on organ formation or flowering. In contrast, Arabidopsis appeared to be highly sensitive to light quality, as dramatic differences in shoot and root elongation, organ formation, and developmental phase transitions were observed between red, blue, and white LED conditions. Our results highlight once more that growth responses to environmental conditions can differ significantly between model and crop species. Understanding the molecular basis for this difference will be important for designing lighting systems tailored for specific crops.



Keywords: Tomato, Arabidopsis, LED lighting, growth, development, R/B light ratio, floral transition

Introduction

To ensure optimal plant performance in horticultural crops, it is required to understand how growth and development are affected by environmental factors. Light is a key environmental factor that not only affects the available sugars through photosynthesis, but also steers development through processes such as photomorphogenesis, phototropism and shade avoidance (Nemhauser and Chory, 2002; Goyal et al., 2013; Ballaré and Pierik, 2017). Studies have shown that light intensity can be used to modulate plant growth and ultimately yield in different species (Smeets and Garretsen, 1986; Zhou et al., 2009; Lu et al., 2017; Viršilė et al., 2019). Aside from its intensity, the spectral quality of light influences plant development by activating different families of photoreceptors that can detect light, ranging from UV-B to far-red. Blue light-activated receptor families include cryptochromes (CRYs) (Yu et al., 2010), phototropins (Christie, 2007) and Zeitlupes (ZTLs) (Suetsugu and Wada, 2013), whereas phytochromes (PHYs) respond to red and far-red light (Galvão and Fankhauser, 2015). Many artificial lights that are used in horticulture try to loosely mimic the spectrum of sunlight by including fractions of all the spectral colours. However, the development of LED technology has created new possibilities for spectral control that may lead to more energy efficient and economic lighting. For example, matching the LED spectral output to specific photoreceptor families can ensure optimal plant performance without



Chapter 3: Light quality regulates early plant development

wasting energy on non-productive wavelengths. Aside from spectral control, LEDs are more energy-efficient than traditional artificial lighting systems and are less detrimental to the environment when discarded, since they contain no toxic metals such as mercury (Morrow, 2008). Finally, LEDs produce less heat and are thus suitable for application in multi-layered vertical farming (SharathKumar et al., 2020).

To implement LED lighting in horticulture it is important to understand how the different colours in the spectrum influence all aspects of plant growth and development. Furthermore, developmental effects of specific LED spectra have been shown to vary between species (Dougher and Bugbee, 2001), suggesting that there are optimal light recipes for different species and even for different ecotypes or cultivars within these species. So far, most studies on spectral properties of light have focused on changes in the red/far-red (R/FR) ratio within the spectrum. At the top of the canopy, R/FR ratios are high, whereas low R/FR ratios are found lower in the canopy (Ballaré et al., 1990). In *Solanum lycopersicum* (tomato), LEDs have been used to add extra far-red light to the spectrum to study shade avoidance (Schrager-Lavelle et al., 2016), plant growth and yield (Ji et al., 2019; Kalaitzoglou et al., 2019) and vitamin production (Ntagkas et al., 2019) among others. Aside from studying R/FR ratios, LED lights can be used to study plant development in response to monochromatic light (red, far-red, yellow, green, or blue) or differential red/blue (R/B) light ratios. So far, most of these studies have been performed in crop species. For example, in tomato, light quality has been found to influence leaf development, assimilates, gas exchange, and biomass (Fan et al., 2013; Lanoue et al., 2017, 2018). However, most of these studies have focused



on one crop species, one wavelength, or only on one developmental trait. Moreover, photoreceptor function and downstream pathways have been studied extensively in *Arabidopsis thaliana* (Arabidopsis) (Wang et al., 2016; Lim et al., 2018; Schumacher et al., 2018), but only a small fraction of these pathways have been investigated in commercial crops. In contrast, many light-induced physiological traits have been studied in different crops (Kaiser et al., 2019; Pennisi et al., 2019; Song et al., 2019) but not in Arabidopsis.

Here we performed a comparative analysis between the commercial crop tomato and the genetic model dicot Arabidopsis, studying how monochromatic red or blue LED lighting, compared to white LED lighting, affects early plant development in these species by monitoring several morphological and developmental traits. Although monochromatic red or blue conditions are unlikely to be used in horticulture, this set-up allowed us to obtain more insights into the wavelength-specific effects on plant traits compared to when using different R/B light ratios. Our analyses showed that monochromatic red or blue LED treatments resulted in significant differences in primary growth of both Arabidopsis and tomato, when compared to white LED conditions. However, whereas red and blue light could be used to steer developmental phase transitions in Arabidopsis, in tomato these traits appeared to be surprisingly indifferent to the type of LED treatment. Our results offer an overview of phenotypic traits in young plants that are regulated by red or blue light, and also provide new insights in the conservation and divergence of these traits with respect to their light sensitivity between two plant species from different families.



Materials and Methods

Growth conditions and LED treatments.

In all experiments, plants were grown at a 16h photoperiod, under white, deep red, or blue Philips Greenpower LED research modules (Signify B.V., Eindhoven, the Netherlands) with a measured photon flux density of $120 \pm 10 \mu\text{mol m}^{-2}\text{s}^{-1}$ at the top of the canopy, a temperature of 21°C, and 70% relative humidity. The percentages of blue, green, red, and far-red wavelengths for the different LED modules are listed in **Table S1**. Experiments with the different LED treatments were performed simultaneously in the same growth chamber in separate compartments enclosed by white plastic screens with a proximal distance of 50 cm to the plants. For *in vitro* analysis of seedling development, two different light treatments were used in all three LED conditions: (1) seedlings were grown completely exposed to light (light-grown roots or LGR); or (2) seedlings were grown in a more “natural” light environment with shoots exposed to light and roots shielded from light using black paper covers (dark-grown roots or DGR) (based on Silva-Navas et al., 2015).

Plant lines and seed germination.

Arabidopsis wild-type ecotypes Columbia (Col-0) and Landsberg *erecta* (Ler) and tomato cultivar Moneymaker (MM) and the commercial hybrid Foundation (FO) were used in all experiments. This study includes both *in vitro* experiments where seedlings were grown on sterile growth medium as well as experiments where the plants were grown on soil. For *in vitro* experiments, *Arabidopsis* and tomato seeds were surface sterilised by incubating for 1



minute in 70% ethanol and 10 minutes in a 2-fold diluted commercial bleach solution (1% chlorine). Subsequently the seeds were washed five times with sterile water. Arabidopsis seeds were stratified for 5 days at 4°C in darkness and germinated on square plates (#688102, Greiner Bio-One™) containing MA medium (Masson and Paszkowski, 1992) supplemented with 1% (w/v) sucrose and 0.8% (w/v) Daishin agar. For efficient and simultaneous germination, plates with Arabidopsis seeds were placed vertically in white light for one day and then moved to the LED conditions (**Figure S1A**). Sterile tomato seeds were placed on sterilised, wet Whatman filter paper using forceps. Tomato seeds showed optimal germination in darkness (**Figure S1B**) and were therefore kept in darkness at 21 °C until 5 days after sowing. Germinated seeds were moved from the filter to square plates containing solid MA medium and placed vertically in the LED conditions. For *on soil* experiments, Arabidopsis seeds were sown on the soil surface and stratified for 5 days at 4°C in darkness. Subsequently the seeds were moved to white light to allow simultaneous germination. After one day in white light, the pots were placed in the LED conditions. Tomato seeds were placed approximately 2 cm under the soil surface and pots were directly placed in the LED conditions. The age of tomato plants was therefore expressed as days after sowing (DAS), instead of days after germination (DAG) used for Arabidopsis.

***In vitro* analysis of seedling development.**

At 7 days after germination (DAG), Arabidopsis seedlings were photographed, and primary root length and hypocotyl length were measured. Tomato seedlings were photographed at 5 DAG for primary root length and hypocotyl length measurements. All measurements were performed with ImageJ (Fiji)



Chapter 3: Light quality regulates early plant development

(Schindelin et al., 2012). The shoot-root ratio was calculated based on the measured primary root length and hypocotyl length. At 14 DAG, Arabidopsis seedlings were photographed, and the number of emerged lateral roots was counted using binoculars. Lateral roots could not be counted for tomato since tomato seedlings older than 6 DAG outgrew the square plates.

Analysis of leaf appearance and morphology.

The leaf appearance rate was measured throughout the experiment once or twice per week for tomato and Arabidopsis, respectively. Leaves were counted from the moment they were visible by eye. For Arabidopsis, the plants were grown until bolting. At this time, the rosettes were photographed, and rosette surface area (RSA) was measured. Individual rosette leaves were removed and photographed separately for length and width measurements of the leaf blade. Length/width ratio of rosette leaves was calculated based on these measurements. For tomato plants, compound leaves were removed at 45 DAS and photographed individually. Leaf surface area was measured for leaf #4 (fully developed, mature leaf) and leaf #6 (developing, young leaf). All of these measurements were performed with ImageJ (Fiji) (Schindelin et al., 2012).

Analysis of flowering time.

Arabidopsis flowering time was measured in number of days until bolting, or until the moment that the first flower buds were visible by eye. For tomato measurements, toothpicks were used to carefully push aside the young leaves from the apex. Flowering time was determined as the day on which small inflorescences became visible near the shoot apex. Individual plants were



photographed at one week after bolting for Arabidopsis and 30 DAS for tomato.

Analysis of stem development.

After Arabidopsis plants became reproductive, plant height measurements commenced. Plant height was measured twice a week until termination of the primary inflorescence meristem. At this time point, individual plants were photographed and the number of branches from the primary inflorescence were counted. Branches were categorised into primary shoots, secondary shoots and tertiary shoots, as previously described (Li et al., 2017). For tomato plants, hypocotyl length, epicotyl length and stem length were measured once a week until 45 DAS. At this time point, individual plants were photographed.

Statistical analysis and figures.

All experiments were performed with 20 or 30 biologically independent plants for tomato or Arabidopsis, respectively. For destructive measurements, 10 representative biological replicates were used. Data was obtained from either two or three independent experiments for *on soil* or *in vitro* experiments, respectively. Measurements under different LED conditions, or comparing different ecotypes or cultivars, were statistically analysed using a one-way ANOVA followed by a Tukey's honestly significant different (HSD) post hoc test. When comparing results from monochromatic (red or blue) with white (control) LED conditions, a two-sided Student's *t*-test was used. For *in vitro* experiments, LGR and DGR treatments using the same LED condition were also compared using a two-sided Student's *t*-test. All measurements were



plotted into graphs using GraphPad Prism 5 software. In the graphs, the colours of the dots, bars and lines indicate white, red, and blue LED conditions. All photographs were taken with a Nikon D5300 camera and edited in ImageJ (Fiji). Final figures were assembled using Microsoft PowerPoint.

Results

Red and blue light influence *in vitro* development of Arabidopsis and tomato seedlings.

Arabidopsis and tomato seedlings were grown in white, red, or blue LED conditions with either light-grown roots (LGR) or dark-grown roots (DGR). Treatment with monochromatic red or blue light strongly affected seedling growth of Arabidopsis ecotypes Col-0 (**Figure 1A**) and *Ler* (**Figure S4A**) and tomato cultivars MM (**Figure 1B**) and FO (**Figure S5A**). Hypocotyl growth was strongly enhanced in red light and reduced in blue light compared to white light, in both Arabidopsis and tomato seedlings grown either in DGR (**Figure 1C**) or LGR (**Figures S2A,C**) conditions, making it the most conserved trait regulated by light quality. Red- or blue light-induced alterations of primary root growth were only partially conserved between the two species. In both Arabidopsis (**Figure 1D**) and tomato (**Figure 1E**), seedlings grown in monochromatic blue LGR conditions had shorter roots than in white LGR conditions, whereas there was no difference between blue and white DGR conditions (with the exception of *Ler* DGR seedlings). This suggests that blue light inhibits root growth locally, and not through shoot-to-root signalling. In



monochromatic red light, *Arabidopsis*, but not tomato seedlings, showed reduced primary root growth compared to white light in DGR conditions, but not in LGR conditions (**Figures 1D,E**), suggesting that in *Arabidopsis* red LED conditions hamper root growth by shoot-to-root signalling. In conclusion, our results show that *in vitro* growth of both *Arabidopsis* and tomato seedlings can be altered by light quality. The local effect of light quality on primary root, and hypocotyl growth seems conserved between these two species, whereas the effect of light quality mediated by shoot-to-root signalling seems more species- or cultivar-dependent. In addition, our results suggest that light conditions with higher rather than lower R/B ratios, and dark-grown roots are optimal for *in vitro* seedling development.

Red light promotes shoot elongation in *Arabidopsis* and young tomato plants.

The height of a plant determines its ability to compete for light and therefore often correlates with leaf mass, seed production and longevity among others (Moles et al., 2009). For monopodial species such as *Arabidopsis*, stem growth is initiated once the plant becomes reproductive and continues until termination of the inflorescence meristems (IMs) (Schmitz and Theres, 1999). To investigate if shoot elongation can be modulated by light quality, *Arabidopsis* plants were grown in white, red, or blue LED conditions, until termination of the primary IM (Col-0: **Figure 2A** and *Ler*: **Figure S4E**). At this time, plant height of Col-0 and *Ler* ecotypes was significantly reduced in blue light and increased in red light, compared to white light (**Figure 2C**). In a series of weekly measurements, we observed that the primary IM of plants grown in monochromatic blue or red light produced flowers for approximately

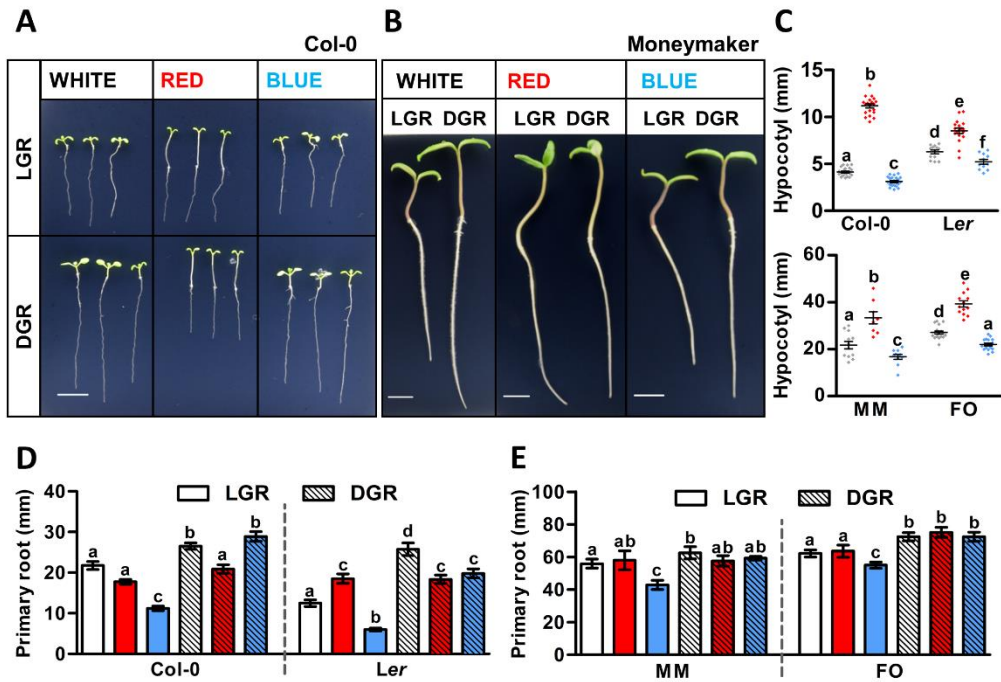


Figure 1: The effect of red and blue light on primary growth of Arabidopsis and tomato seedlings.

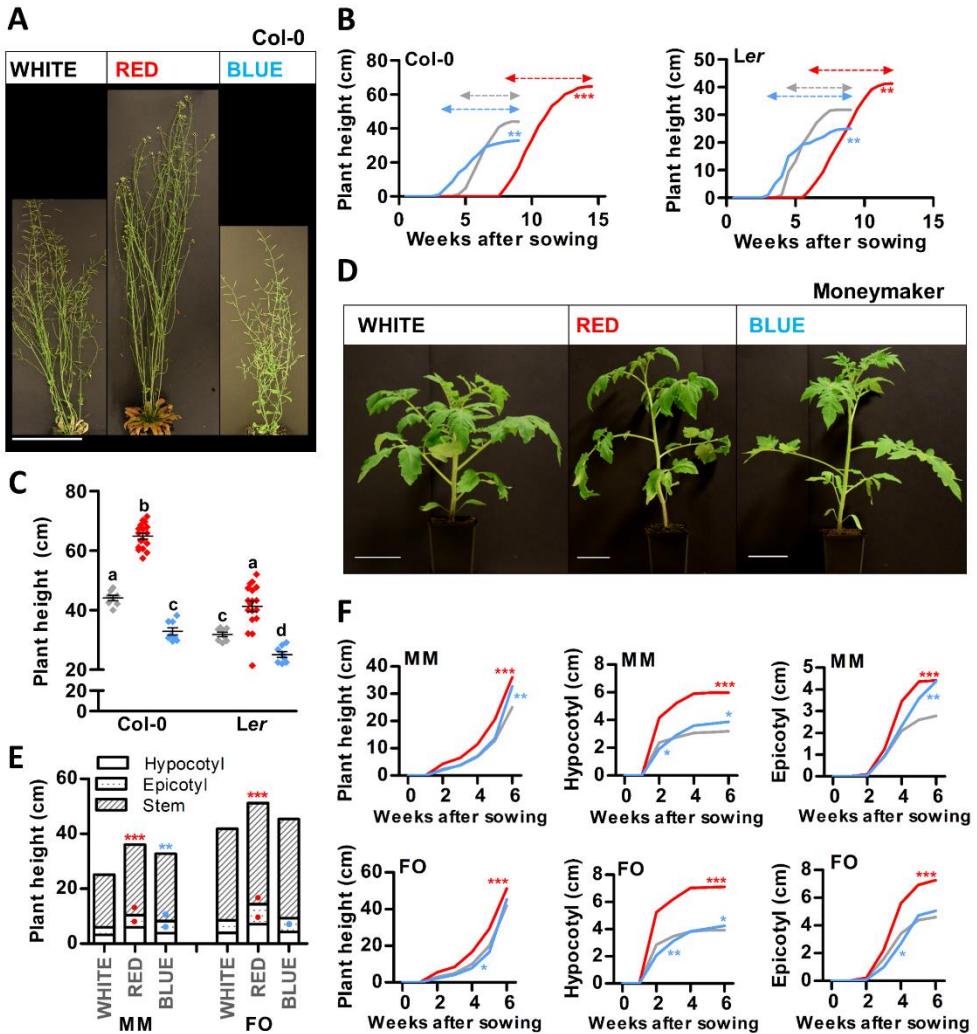
A-B. Representative 7-day-old Arabidopsis and 5-day-old tomato seedlings grown in white, red, or blue LED conditions. Seedlings of Arabidopsis ecotype Columbia (Col-0) (**A**) and tomato cultivar Moneymaker (MM) (**B**) were grown in light-grown roots (LGR) and dark-grown roots (DGR) LED conditions. For presentation purposes, seedlings were transferred to black agarose plates before photographing. Scale bars indicate 1 cm. **C-E.** Quantification of the hypocotyl length of DGR seedlings (**C**) and the primary root length of LGR and DGR seedlings (**D-E**) of Arabidopsis ecotypes Col-0 and *Landsberg erecta* (Ler) and tomato cultivars MM and Foundation (FO) as shown in **Figures 1A, S4A, 1B** and **S5A**, respectively. LED conditions and ecotypes or cultivars were compared using a one-way ANOVA followed by a Tukey's test (letters **a, b, c, d, e**, and **f** indicate statistically significant differences values, $p < 0.05$) in **C-E**. Error bars represent standard error of the mean in **C-E** ($n = 30$). Similar results were obtained in three independent experiments.



6 weeks, whereas in white light-grown plants the primary IM terminated after approximately 5 weeks (**Figure 2B**, dashed arrows). This slight extension of the reproductive phase in blue light compared to white light, indicated that the reduction of plant height in blue light is caused by reduced elongation of the shoot, and not by a shorter growth phase. In contrast, the elongated plants in red light might be caused by both enhanced elongation growth, and the extended reproductive phase, when compared to white light. As a sympodial plant, tomato initiates stem growth already during the vegetative growth phase (Schmitz and Theres, 1999). To investigate shoot elongation of tomato plants grown in white, red, or blue LED conditions, we measured hypocotyl length, epicotyl length and stem length (from epicotyl to SAM) every week for up to 45 days after sowing (DAS). At 45 DAS, red light-grown plants of both cultivars were taller than white light-grown plants (MM and FO: **Figure 2D-F** and **Figure S5D**). Also at earlier timepoints, tomato plants grown in red light had a significantly longer hypocotyl, epicotyl, and stem than white light grown plants (**Figures 2F**). At 45 DAS, MM plants grown in blue light were significantly taller than those grown in white light (**Figures 2D,E**), whereas FO plants only showed a significant increase in hypocotyl length in blue light (**Figure 2E** and **Figure S5D**). However, during our weekly measurements we observed that, at earlier time points (mainly before the appearance of inflorescence meristems), blue light-grown plants of both cultivars had shorter hypocotyls, epicotyls and stems compared to white light-grown plants (**Figures 2F**). This shows that, in tomato, the effects of monochromatic blue light treatment on shoot elongation are dependent on both cultivar and developmental stage. Taken together, our results show that the enhanced shoot elongation in monochromatic red LED conditions is conserved between



Chapter 3: Light quality regulates early plant development



Arabidopsis and tomato, whereas the effect of monochromatic blue light seems to vary between species and cultivars.



Figure 2: Red light promotes shoot growth in Arabidopsis and young tomato plants.

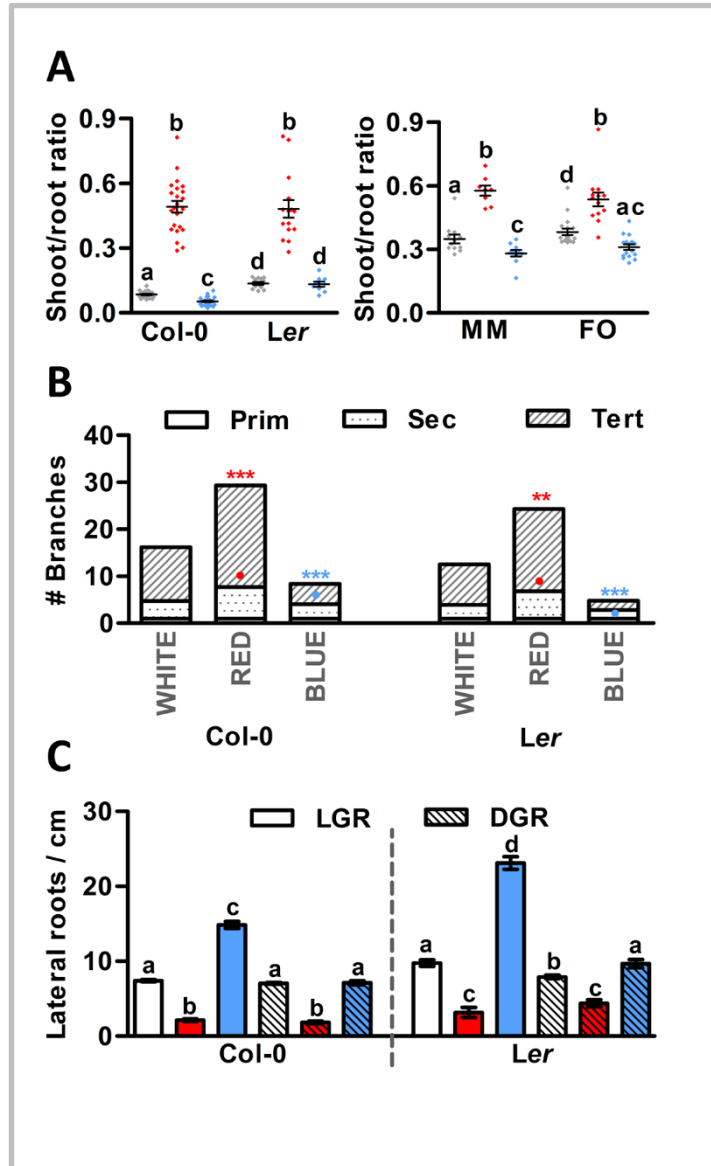
A. Representative Arabidopsis Columbia (Col-0) plants grown in white, red, or blue LED conditions until 4 weeks after bolting. **B-C.** Quantification of the plant height over time (**B**) or the plant height after termination of the primary inflorescence (**C**) of Arabidopsis Col-0 or Landsberg *erecta* (*Ler*) plants as shown in **Figures 2A** and **S4E**, respectively. **D.** Representative tomato Moneymaker (MM) plants grown in white, red, or blue LED conditions until 45 days after sowing (DAS). **E-F.** Quantification of the plant height at 45 DAS (**E**), or the plant height, hypocotyl length, or epicotyl length over time (**F**) of tomato MM or Foundation (FO) plants as shown in **Figures 2D** and **S5D**, respectively. LED conditions and ecotypes or cultivars were compared using a one-way ANOVA followed by a Tukey's test (letters **a**, **b**, **c**, and **d** indicate statistically significant differences, $p < 0.05$) in **C**. In **B**, and **E-F**, monochromatic LED conditions (red or blue) were compared to white (control) using a two-sided Student's *t*-test (asterisks indicate significant differences ($p < 0.05$) in time series in **B** and **F**, or in plant height in **E**, bullets indicate significant differences ($p < 0.05$) in hypocotyl or epicotyl length in **E**). Error bars represent standard error of the mean in **C**, standard errors for **B** and **E-F** are listed in **Table S2** ($n=20$). Dashed arrows in **B** represent the time from bolting until termination of the primary inflorescence. For presentation purposes, pots were placed in front of a black background in **A** and **D** before photographing. Scale bars indicate 10 cm in **A**, and 5 cm in **D**. Similar results were obtained in two independent experiments.



Chapter 3: Light quality regulates early plant development

Monochromatic red light promotes shoot growth and inhibits root branching in *Arabidopsis*.

In nature, the balance between shoot growth to increase photosynthetic capacity, and root growth to compete for soil nutrients is tightly controlled and dependent on the growth conditions and nutrient and water availability (Puig et al., 2012). In greenhouses, however, the growth conditions and availability of water and nutrients are generally good, making development of the root system less relevant. As a result, plant breeders of fruit-producing species have spent decades to optimise the growth and development of above-ground organs





(van der Ploeg et al., 2007), often at the cost of root development. In our *in vitro* experiments, monochromatic red conditions, either LGR or DGR, significantly enhanced the shoot-root ratio of both *Arabidopsis* and tomato seedlings (**Figure 3A** and **Figures S2B/D**). A mildly opposite effect was

Figure 3: Monochromatic red light promotes shoot growth and inhibits root branching in *Arabidopsis*.

A. Shoot-root ratio of 7-day-old *Arabidopsis* seedlings (left) and 5-day-old tomato seedlings (right), grown in white, red, or blue LED conditions. *Arabidopsis* ecotypes Columbia (Col-0) and Landsberg *erecta* (*Ler*), and tomato cultivars MoneyMaker (MM) and Foundation (FO) were grown in dark-grown roots (DGR) LED conditions. **B.** Number of primary (Prim), secondary (Sec) and tertiary (Tert) branches from the primary inflorescence of *Arabidopsis* Col-0 and *Ler* plants grown in LED conditions until termination of the primary inflorescence. **C.** Lateral root density of 14-day-old Col-0 and *Ler* seedlings grown in light-grown roots (LGR) and DGR LED conditions. Graph colours represent the LED conditions in **A** and **C**. LED conditions and ecotypes or cultivars were compared using a one-way ANOVA followed by a Tukey's test (letters **a**, **b**, **c**, and **d** indicate statistically significant differences, $p < 0.05$) in **A** and **C**. In **B**, monochromatic LED conditions (red or blue) were compared to white (control) using a two-sided Student's *t*-test (bullets indicate significant differences in secondary branches ($p < 0.05$), asterisks indicate significant differences in tertiary branches ($***p < 0.001$, $**p < 0.01$)). Error bars represent standard error from mean in **A** and **C** ($n = 30$), standard errors for **B** are listed in **Table S2** ($n = 20$). Similar results were obtained in three (**A** and **C**) or two (**B**) independent experiments.

observed in seedlings grown under monochromatic blue LED DGR conditions (**Figure 3A**). In LGR conditions, however, the shoot-root ratio was slightly increased (**Figures S2B,D**), which is most likely the result of the inhibition of primary root growth in monochromatic blue light (**Figures 1D,E**). This suggests that the balance between shoot and root elongation in *Arabidopsis* and



Chapter 3: Light quality regulates early plant development

tomato seedlings can be controlled by the R/B light ratio in the spectrum. Interestingly, analysis of the number of branches on the primary *Arabidopsis* inflorescence showed that bud formation from axillary meristems is greatly enhanced in red light compared to white light conditions (**Figure 3B**). In contrast, red light-grown *Arabidopsis* seedlings showed a significant decrease in lateral root density compared to those grown in white light, in both LGR and DGR conditions (**Figure 3C** and **Figure S3**). In monochromatic blue light, branching of the primary inflorescence was significantly reduced compared to white light (**Figure 3B**). The lateral root density of blue light DGR *Arabidopsis* seedlings was unaffected (**Figure 3C** and **Figure S3**), but was increased in LGR seedlings, most likely as a result of primary root growth inhibition in blue LGR conditions (**Figures 1D,E** and **Figure 3C**). To summarise, our results show that *Arabidopsis* plants grown in monochromatic red LED conditions show increased shoot elongation and branching, and decreased root branching compared to white light-grown plants. In contrast, the effect of monochromatic blue light is relatively mild, except for the strong inhibitory effect on root growth in LGR conditions. Tomato plants show the same increased shoot-root ratio in monochromatic red compared to white light, and a similar mild effect of monochromatic blue light, but the effects of red light on lateral organ formation in tomato shoots and roots remain to be determined.

Developmental phase transitions in *Arabidopsis* are promoted by blue light and delayed by red light.

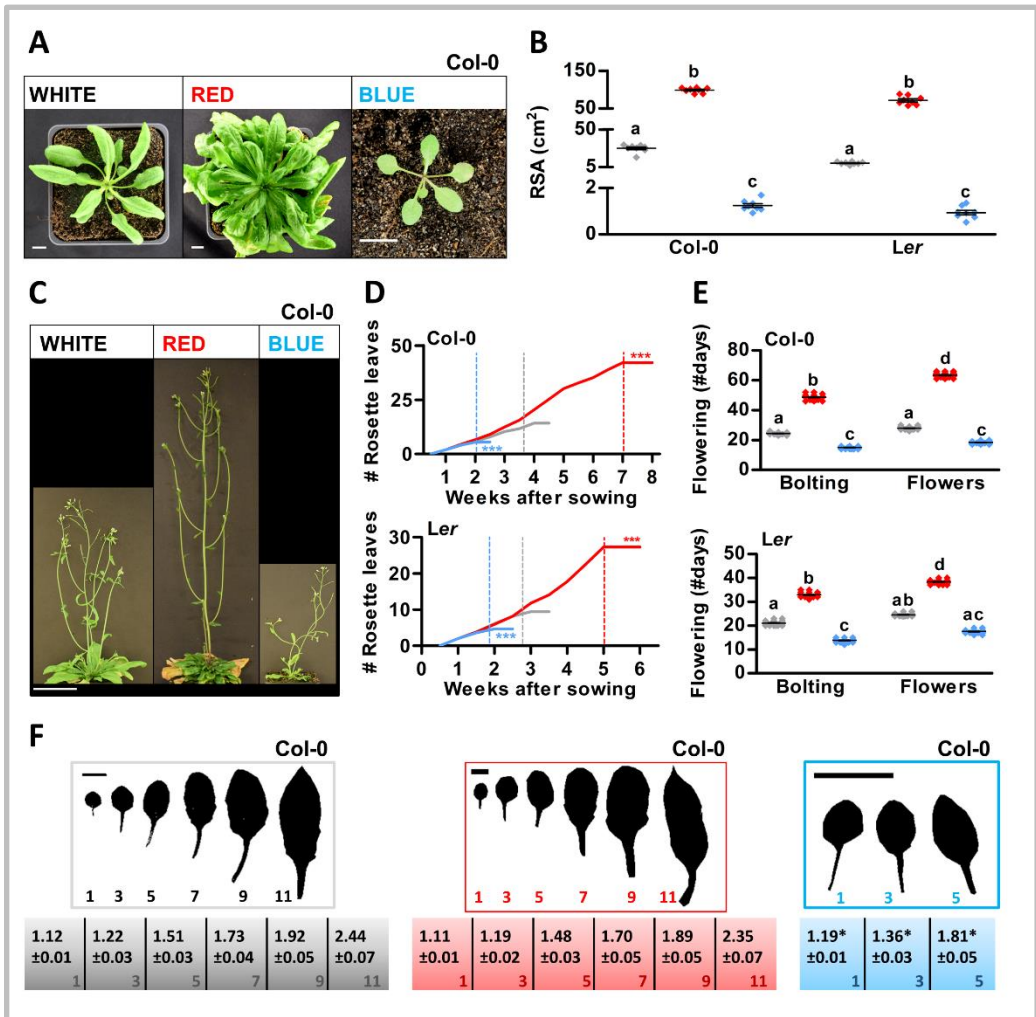
To ensure a high yield in crops, it is important that leaves are produced at an optimal rate and that the morphology of the leaf allows for optimal exposure to light (Mathan et al., 2016). Moreover, optimizing the timing of flowering is



crucial to ensure either a long vegetative phase (for leaf production in crop species such as lettuce or cabbage) or a short vegetative phase (for rapid breeding cycles or for fruit-producing species such as tomato). Previous studies that used light filters or continuous lighting indicated that developmental phase transitions in *Arabidopsis* can be modulated by light quality (Eskins, 1992; Guo et al., 1998). To investigate if similar phenotypes could be obtained using a LED setup with a 16h/8h day/night cycle, *Arabidopsis* plants were grown on soil in white, red, or blue LED conditions. In monochromatic blue light, the rosette size, expressed as rosette surface area (RSA), was greatly reduced, whereas white light-grown plants showed a regular rosette development, and monochromatic red light-grown plants developed large rosettes resembling those of *Arabidopsis* plants grown in short-day conditions (**Figures 4A,B** and **Figure S4B**) (Brandt et al., 2018). Both the increase of RSA in red LED conditions and the decrease of RSA in blue LED conditions correlated with significant changes in the timing of the plant's floral transition (Col-0: **Figures 4C-E** and *Ler*: **Figure S4D**). Col-0 and *Ler* plants that were grown in blue light produced a limited number of rosette leaves as they flowered extremely early, whereas plants that were grown in red light developed many rosette leaves during an extended vegetative phase due to late flowering (**Figures 4D,E**). In *Arabidopsis*, the floral transition is preceded by the juvenile-to-adult or vegetative phase transition, the occurrence of which can be determined by leaf heteroblasty. Juvenile leaves consist of a round leaf blade with a long petiole, with a length/width ratio of approximately 1, whereas adult leaves have a more serrated leaf blade with a short petiole, and with a length/width ratio of approximately 1.7 (Telfer et al., 1997). Based on their length/width ratio,



Chapter 3: Light quality regulates early plant development



leaves of blue light-grown plants seemed to mature significantly faster, although in *Ler*, no completely adult leaves were formed before the plants switched to the reproductive phase (Col-0: **Figure 4F** and *Ler*: **Figure S4C**). In red light-grown plants, the timing of the vegetative phase changes did not differ significantly from that of white light-grown plants, suggesting that, in contrast to the reproductive phase transition, the vegetative phase transition



Figure 4: Developmental phase transitions in Arabidopsis are promoted by blue light and delayed by red light.

A. Rosette phenotype of representative Arabidopsis plants of ecotype Columbia (Col-0) grown in white, red, or blue LED conditions. **B.** Quantification of rosette surface area (RSA) of Col-0 or Landsberg *erecta* (*Ler*) plants as shown in **Figures 4A** and **S4B**, respectively. **C.** Representative Arabidopsis Col-0 plants grown in LED conditions until one week after flowering. **D.** Rosette leaf appearance in Col-0 and *Ler* plants over time. **E.** Flowering time (until bolting, or until the appearance of flower buds) of Col-0 and *Ler* plants in number of days. **F.** Rosette leaves of representative Col-0 plants and length/width ratios of the leaf blade (\pm SE, $n=10$). Scale bars represent 1 cm in **A** and **F**, and 10 cm in **C**. Graph colours represent the LED conditions in **B**, **D**, and **E**. LED conditions and ecotypes were compared using a one-way ANOVA followed by a Tukey's test (letters **a**, **b**, **c**, and **d** indicate statistically significant differences, $p<0.05$) in **B** and **E**. In **D** and **F**, monochromatic LED conditions (red or blue) were compared to white (control) using a two-sided Student's *t*-test (asterisks indicate significant differences (* $p<0.05$, *** $p<0.001$)). Error bars represent standard error of the mean in **B** and **E** ($n=30$), standard errors for **D** are listed in **Table S2** ($n=30$). Dashed lines in **D** represent the time of bolting. Similar results were obtained in two independent experiments.

was not delayed by the monochromatic red light treatment. Altogether, our results show that especially the floral transition but also the vegetative phase transition in Arabidopsis are sensitive to light quality and can thus be modulated not only by day length but also by the R/B light ratio in the spectrum.



Developmental phase transitions in tomato are indifferent to the R/B light ratio.

To investigate if developmental phase transitions can be modulated by red and blue light in tomato as well, MM and FO plants were grown on soil in white, red, or blue LED conditions until the start of the reproductive phase, which was defined as the moment that the first inflorescences appeared near the shoot apex (**Figure 5A**). MM and FO plants became reproductive at approximately 30 and 32 DAS, respectively, in all three LED conditions (**Figure 5B**). In addition, the appearance rate of new compound leaves was the same in all three LED conditions and in both cultivars (**Figure 5C**). These results are in contrast to our observations in *Arabidopsis* and imply that developmental phase shifts in tomato are completely indifferent to the R/B light ratio. To investigate the sensitivity of tomato leaf morphology to red and blue light, MM and FO plants were grown in the three different LED conditions until 45 DAS. We used leaf #4 as a representative for fully developed leaves (MM: **Figure 5D** and FO: **Figure S5B**), and leaf #6 as a representative for young, not fully developed leaves (MM: **Figure 5E** and FO: **Figure S5C**) for leaf surface area (LSA) measurements. The LSA of leaf #4 was similar for plants grown in white and blue LED conditions (**Figure 5F**). However, leaf #6 of blue light-grown FO plants showed a decreased LSA, which is most likely a result of a slight delay in leaf development specific for this cultivar, and not a true effect of monochromatic blue light on leaf morphology. In contrast, monochromatic red LED conditions led to a significant decrease in LSA of leaf #4 in both cultivars (**Figure 5F**). Moreover, leaves of plants grown in red light showed epinasty (**Figures 5D,E** and **Figures S5B,C**), thus further reducing the effective LSA



for photosynthesis. In conclusion, light quality does have an effect on leaf morphology, and may alter photosynthetic capacity in tomato. However, these changes in leaf morphology do not influence the formation rate of new leaves or flowering time. Although developmental phase transitions in *Arabidopsis* are highly sensitive to light quality, to our surprise the same phase transitions in tomato appeared to be completely indifferent to the R/B light ratio.

Discussion

Recent developments in LED technology have created new possibilities for spectral control that allow us to use light quality to steer plant development (Morrow, 2008). Here we present an overview of the phenotypes that arise from growing *Arabidopsis* and young tomato plants in white or monochromatic red or blue LED lighting. During *in vitro* seedling development, hypocotyls were significantly more elongated in red light and shorter in blue light, compared to white light-grown *Arabidopsis* and tomato seedlings. This confirmed previously published results that were obtained with the use of light filters (Ballaré et al., 1995), or with lighting setups in which the light intensity differed greatly between LED conditions (Jensen et al., 1998). At later developmental stages, *Arabidopsis* and tomato plant height were significantly increased in monochromatic red light and decreased in monochromatic blue light. In tomato, however, the reduced plant elongation in monochromatic blue light was limited to early stages of plant development. These results are in line with previous studies in wheat (Monostori et al., 2018) and chili peppers (Gangadhar et al., 2012), and a recent greenhouse study in

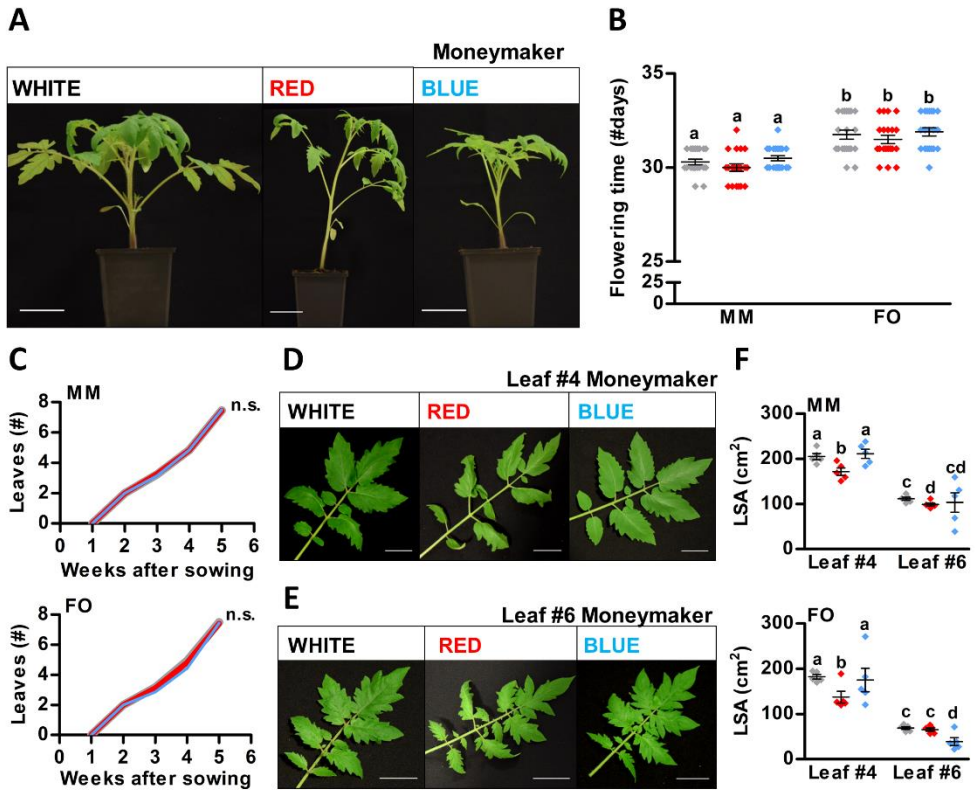


Figure 5: Developmental phase transitions in tomato are indifferent to R/B light ratios.

A. Representative tomato plants of cultivar Moneymaker (MM) grown in white, red, or blue LED conditions until 30 days after sowing (DAS). **B.** Flowering time of MM and Foundation (FO) plants in number of days. **C.** Leaf appearance over time in MM and FO plants. **D-E.** Representative compound leaves from MM plants grown in LED conditions until 45 DAS: leaf #4 (**D**) and leaf #6 (**E**). For presentation purposes, leaves were removed, flattened, and placed on black paper. **F.** Quantification of leaf surface area (LSA) of MM and FO leaves shown in **Figures D-E**, and **S5B-C**, respectively. Scale bars represent 5 cm in **A**, **D**, and **E**. Graph colours represent the LED conditions in **B**, **C**, and **F**. LED conditions and cultivars were compared using a one-way ANOVA followed by a Tukey's test (letters **a**, **b**, **c**, and **d** indicate statistically significant differences, $p < 0.05$) in **B** and **F**. In **C**, monochromatic LED conditions (red or blue) were compared to white (control) using a two-sided Student's *t*-test (n.s. indicates no significant differences between LED conditions ($p < 0.05$)). Error bars represent standard error of the mean in **B** and **F** ($n = 20$), standard errors for **C** are listed in **Table S2** ($n = 20$). Similar results were obtained in two independent experiments.



tomato where LEDs were used as supplemental lighting (Dieleman et al., 2019). However, monochromatic blue light has been reported to enhance hypocotyl growth in cucumber, indicating that there are species-specific differences (Hernández and Kubota, 2016). Primary shoot growth in white light-grown seedlings and plants was intermediate between that in monochromatic red or blue light-grown seedlings and plants, suggesting an antagonistic effect of both light conditions, with red light promoting and blue light inhibiting shoot growth. Since auxin, ethylene, gibberellic acid and brassinosteroids are the main phytohormones that regulate hypocotyl and stem elongation in response to light (Vandenbussche et al., 2005; Kurepin and Pharis, 2014), it is likely that red- and blue light-responsive photoreceptors interact with the corresponding hormone signalling pathways. We also observed a significant effect of red and blue light on primary root growth in *Arabidopsis* and tomato seedlings. By combining the different LED conditions with LGR (light-grown roots) and DGR (dark-grown roots) conditions, we were able to show that the reduced primary root growth in monochromatic blue light is caused by a local light-induced inhibition of root growth. As auxin and cytokinin are the main regulators of primary root growth (Su et al., 2011), we expect that activation of root-localised photoreceptors affects cytokinin levels and auxin gradients in the root apical meristem. In contrast, we observed reduced primary root growth in *Arabidopsis* seedlings grown in red DGR, but not LGR conditions, suggesting that red LED conditions inhibit root growth by altering the shoot to root signalling. In this case, we expect that activation of shoot-localised photoreceptors influences shoot to root transport of key signalling molecules such as HY5, HYH or auxin to modulate primary root growth (Chen et al., 2016; Van Gelderen et al., 2018). To summarise, our



Chapter 3: Light quality regulates early plant development

results show that primary growth of *Arabidopsis* and tomato can be modulated by changing the light quality at different developmental stages, and in different ecotypes or cultivars (**Table 1**). In this way, light quality may be used to steer primary growth towards compact and sturdy crop plants which can be grown in multi-layered growth chambers. In *Arabidopsis*, we observed a considerable increase in the shoot-root ratio in monochromatic red light, and a slight decrease in the shoot-root ratio in monochromatic blue light, which resulted from light-induced changes in hypocotyl growth and, to a lesser extent, primary root growth. Moreover, the lateral organ density in roots was greatly decreased in red LED conditions. Since the far-red light-activated phytochrome A has been shown to promote lateral root formation (Salisbury et al., 2007), it is likely that the low number of lateral roots in monochromatic red light results from red light-inactivation of this photoreceptor. Previous studies have shown that blue light photoreceptors suppress lateral root formation (Zeng et al., 2010; Moni et al., 2015). In contrast, we observed an increase in lateral root density in monochromatic blue light. We suspect that the strong decrease in primary root growth in blue LED conditions is responsible for an indirect increase in lateral root density similar to in white LED conditions. In contrast to the roots, shoot branching was significantly enhanced in monochromatic red light, and significantly decreased in monochromatic blue light, whereas white light-grown plants showed an intermediate phenotype. Shoot branching is promoted by cytokinin, and inhibited by strigolactones, either directly or through interactions with auxin (Domagalska and Leyser, 2011; Brewer et al., 2013). This suggests that red light might either enhance cytokinin signalling, or inhibit strigolactones, to promote shoot branching, and that an opposite effect on these phytohormones



might be expected for blue light. This hypothesis is in line with previous studies that show that the blue light photoreceptor cryptochrome 1 inhibits shoot branching, and that the red light-inducible phytochrome B promotes shoot branching through auxin signalling (Reddy and Finlayson, 2014; Zhai et al., 2020). Although we demonstrate that the balance between shoot and root development can be steered by the light quality in *Arabidopsis*, additional research is required for horticultural application.

Table 1: Primary growth of *Arabidopsis* and tomato is regulated by red and blue light.

Summary of the *Arabidopsis* and tomato primary growth phenotypes that were induced by monochromatic red or blue light in LGR conditions. Statistically significant differences between white light (control) and monochromatic LED conditions (red or blue) are indicated in this table ($p < 0.05$). When no statistical differences were found between LED conditions, it is indicated as “similar to white (W)”. Asterisks indicate results that are ecotype-, or cultivar-dependent. Double Asterisks indicate results that are time-dependent.

	<i>Arabidopsis</i>		<i>Tomato</i>	
	RED	BLUE	RED	BLUE
<i>Primary root growth</i>	* similar to W	shorter root	similar to W	shorter root
<i>Hypocotyl length</i>	longer hypocotyl	shorter hypocotyl	longer hypocotyl	shorter hypocotyl
<i>Shoot/root ratio</i>	higher S/R ratio	* similar to W	higher S/R ratio	similar to W
<i>Epicotyl length</i>	N/A	N/A	longer epicotyl	*shorter epicotyl
<i>Plant height</i>	taller plants	shorter plants	taller plants	**shorter/taller plants

Our comparative analysis identified a remarkable difference in the regulation of developmental phase transitions by light quality between *Arabidopsis* and tomato. We observed that *Arabidopsis* plants grown in monochromatic blue light developed very small rosettes and flowered early, whereas plants grown in monochromatic red light developed extremely big rosettes due to late



Chapter 3: Light quality regulates early plant development

flowering. Our results confirm previous studies in which light filters were used, or where plants were grown under continuous LED illumination, which excludes the effect of day-length. (Eskins, 1992; Guo et al., 1998). The light-induced changes in leaf length/width ratios, leaf formation and RSA in *Arabidopsis* are most likely the result of light quality-induced changes in both the juvenile to adult vegetative and the adult vegetative to reproductive phase transition (also referred to as the vegetative phase change and the floral transition, respectively). Strikingly, in contrast to *Arabidopsis*, these phase transitions in tomato were completely indifferent to red and blue light (**Table 2**). This might be a result of fundamental differences in plant architecture (monopodial versus sympodial growth), daylength sensitivity (long-day versus day-neutral) or life history (annual versus semi-perennial) between *Arabidopsis* and tomato, respectively. Similar to the phenotypes that we observed in *Arabidopsis*, strawberry and petunia have been shown to flower early in blue light and late in red light (Fukuda and Olsen, 2012; Fukuda et al., 2016; Yoshida et al., 2016). Petunia and tomato are both members of the *Solanaceae* family and are categorised as sympodial, semi-perennial plants. However, in contrast to tomato, petunia is not a day-neutral plant but a long-day plant, suggesting that photoperiodic sensitivity is a key characteristic of plants for which developmental phase transitions are sensitive to red or blue light. Because *Arabidopsis* plants grown in white light show an intermediate phenotype compared to those grown in either monochromatic red or blue LED conditions, a separate phase transition-promoting effect of blue light and a phase transition-delaying effect of red light should be considered. Previous studies have shown that blue light promotes flowering through photoreceptors of the cryptochrome and Zeitelupe families. In response to blue light, these



Table 2: Developmental phase transitions are modulated by red and blue light in Arabidopsis, but not in tomato.

Summary of the Arabidopsis and tomato developmental phenotypes that were induced by monochromatic red or blue light. Statistically significant differences between white light (control) and monochromatic LED conditions (red or blue) are indicated in this table ($p < 0.05$). When no statistical differences were found between monochromatic light and white light, it is indicated as “similar to white (W)”.

	<i>Arabidopsis</i>		<i>Tomato</i>	
	RED	BLUE	RED	BLUE
<i>Leaf formation</i>	more leaves	less leaves	similar to W	similar to W
<i>Leaf morphology</i>	bigger leaves / bigger rosette	smaller leaves / smaller rosette	smaller leaves	similar to W
<i>Flowering time</i>	late	Early	similar to W	similar to W

photoreceptors enhance expression of *CONSTANS* (*CO*). As a main integrator of circadian clock components and light signalling, *CO* promotes flowering through the florigen *FLOWERING LOCUS T*, in response to day length (Valverde, 2011). In day-neutral plant species, components of the photoperiodic pathway are likely non-existent, or unresponsive (Mizoguchi et al., 2007), which might explain the indifference of tomato plants to LED conditions that lack blue light. Although red light has been shown to inhibit flowering through targeted degradation of *CO* proteins (Lazaro et al., 2015), we do not expect that the flower-delaying effect of red light relies solely on photoperiodicity. Based on the length/width ratios of leaf blades, we suggest that meristems of plants grown in monochromatic blue light may mature faster, whereas meristems of plants grown in monochromatic red light mature at the same rate as those in white light. This suggests that red light might inhibit the ageing pathway, in addition to the photoperiodic pathway, to delay the floral



Chapter 3: Light quality regulates early plant development

transition. Therefore, LED conditions that lack red light would result in an early vegetative phase transition and early flowering. To summarise, our observations in *Arabidopsis* suggest a possibility to identify more (long-day) species in which developmental phase transitions can be steered by light quality, whereas our experiments in tomato demonstrate that tomato growers may change the R/B light ratio towards desired phenotypes, without affecting the timing of the developmental phase transitions. If we wish to apply the R/B light ratio to steer the timing of developmental phase transitions in horticulture, it will be necessary to further investigate the LED phenotypes in *Arabidopsis*, and to verify whether these are conserved in other species from the same or from different families. However, changes in the LED spectrum are likely to simultaneously modulate the activity of multiple photoreceptors, and the interplay between photoreceptors and their downstream targets adds another layer of complexity. For example, it has been shown that blue light-activated cryptochromes physically interact with the far-red/red light-inducible phytochromes, and with their downstream targets (Mas et al., 2000; Pedmale et al., 2016). Nonetheless, identification of the key photoreceptors, phytohormones, and downstream signalling targets that underly the phenotypes that we observed in this study will be the next step towards optimizing light quality-induced phenotypic traits for horticultural application, and to understand the divergence of these traits between plant species.

Conclusions

Our results demonstrate that light quality modulates different aspects of the growth and early development of *Arabidopsis* and tomato. In *Arabidopsis*,



treatment with monochromatic red light resulted in increased shoot growth and development (sometimes at the cost of root development), and delayed flowering, whereas plants grown in monochromatic blue light showed reduced shoot growth and development, and early flowering. In tomato plants grown in monochromatic red light we observed increased shoot growth and development, and a decrease in leaf surface area, whereas tomato plants grown in blue LED conditions showed reduced shoot growth in vegetative plants and increased shoot growth in flowering plants. Our comparative analysis showed that most of the primary growth responses to light quality were conserved between *Arabidopsis* and tomato (**Table 1**). In contrast, developmental phase transitions in *Arabidopsis* were highly sensitive to light quality, whereas these transitions in tomato were completely indifferent to red and blue light (**Table 2**).

Author contributions

KS, WvI and RO conceived and designed the experiments. KS and JvL performed the experiments, and KS performed the statistical analysis. KS, WvI and RO analysed the results, and KS and RO wrote the manuscript. All authors contributed to manuscript revision.



Chapter 3: Light quality regulates early plant development

Funding

This work was part of the research program “LED it be 50%” with project number 14212, which is partly financed by the Dutch Research Council (NWO).

Acknowledgements

We would like to thank Nunhems Netherlands BV for providing seeds of their commercial tomato hybrid line Foundation and Signify for providing the LED modules. We thank Fred Schenkel and Emiel Wiegers for help with design and construction of the LED lighting set-up, and Daliá Alves Carvalho for photon flux measurements and helpful suggestions. We acknowledge Jeroen Nels and Nakisa Echobardo for help with initial germination assays.



References

- Ballaré, C. L., Barnes, P. W., and Flint, S. D.** (1995). Inhibition of hypocotyl elongation by ultraviolet-B radiation in de-etiolating tomato seedlings. I. The photoreceptor. *Physiol. Plant.* 93, 584–592.
- Ballaré, C. L., and Pierik, R.** (2017). The shade-avoidance syndrome: Multiple signals and ecological consequences. *Plant Cell Environ.* 40, 2530–2543.
- Ballaré, C. L., Scopel, A. L., and Sánchez, R. A.** (1990). Far-red radiation reflected from adjacent leaves: An early signal of competition in plant canopies. *Science* 247, 329–332.
- Brandt, S., Fachinger, S., Tohge, T., Fernie, A. R., Braun, H. P., and Hildebrandt, T. M.** (2018). Extended darkness induces internal turnover of glucosinolates in *Arabidopsis thaliana* leaves. *PLoS One* 13, 1–15.
- Brewer, P. B., Koltai, H., and Beveridge, C. A.** (2013). Diverse roles of strigolactones in plant development. *Mol. Plant* 6, 18–28.
- Chen, X., Yao, Q., Gao, X., Jiang, C., Harberd, N. P., and Fu, X.** (2016). Shoot-to-root mobile transcription factor HY5 coordinates plant carbon and nitrogen acquisition. *Curr. Biol.* 26, 640–646.
- Christie, J. M.** (2007). Phototropin blue-light receptors. *Annu. Rev. Plant Biol.* 58, 21–45.
- Dieleman, J. A., De Visser, P. H. B., Meinen, E., Grit, J. G., and Dueck, T. A.** (2019). Integrating morphological and physiological responses of tomato plants to light quality to the crop level by 3D modeling. *Front. Plant Sci.* 10, 1–12.
- Domagalska, M. A., and Leyser, O.** (2011). Signal integration in the control of shoot branching. *Nat. Rev. Mol. Cell Biol.* 12, 211–221.
- Dougher, T. A. O., and Bugbee, B.** (2001). Differences in the response of wheat, soybean and lettuce to reduced blue radiation. *Photochem. Photobiol.* 73, 199–207.



Chapter 3: Light quality regulates early plant development

- Eskins, K.** (1992). Light-quality effects on *Arabidopsis* development. Red, blue and far-red regulation of flowering and morphology. *Physiol. Plant.* 86, 439–444.
- Fan, X. X., Xu, Z. G., Liu, X. Y., Tang, C. M., Wang, L. W., and Han, X.** (2013). Effects of light intensity on the growth and leaf development of young tomato plants grown under a combination of red and blue light. *Sci. Hortic.* 153, 50–55.
- Fukuda, N., Ajima, C., Yukawa, T., and Olsen, J. E.** (2016). Antagonistic action of blue and red light on shoot elongation in petunia depends on gibberellin, but the effects on flowering are not generally linked to gibberellin. *Environ. Exp. Bot.* 121, 102–111.
- Fukuda, N., and Olsen, J. E.** (2012). Short main shoot length and inhibition of floral bud development under red light condition can be recovered by application of gibberellin and cytokinin short main shoot length and inhibition of floral bud development under red light can be recovered by Ap. *Acta Hortic.* 956, 215–222.
- Galvão, V. C., and Fankhauser, C.** (2015). Sensing the light environment in plants: Photoreceptors and early signaling steps. *Curr. Opin. Neurobiol.* 34, 46–53.
- Gangadhar, B. H., Mishra, R. K., Pandian, G., and Park, S. W.** (2012). Comparative study of color, pungency, and biochemical composition in chili pepper (*Capsicum annuum*) under different light-emitting diode treatments. *HortScience* 47, 1729–1735.
- Goyal, A., Szarzynska, B., and Fankhauser, C.** (2013). Phototropism: At the crossroads of light-signaling pathways. *Trends Plant Sci.* 18, 393–401.
- Guo, H., Yang, H., Mockler, T. C., and Lin, C.** (1998). Regulation of flowering time by *Arabidopsis* photoreceptors. *Science* 279, 1360–1363.
- Hernández, R., and Kubota, C.** (2016). Physiological responses of cucumber seedlings under different blue and red photon flux ratios using LEDs. *Environ. Exp. Bot.* 121, 66–74.
- Jensen, P. J., Hangarter, R. P., and Estelle, M.** (1998). Auxin transport is required for hypocotyl elongation in light-grown but not dark-grown *Arabidopsis*. *Plant Physiol.* 116, 455–462.



- Ji, Y., Ouzounis, T., Courbier, S., Kaiser, E., Nguyen, P. T., Schouten, H. J., Visser, R. G. F., Pierik, R., Marcelis, L. F. M., and Heuvelink, E. (2019).** Far-red radiation increases dry mass partitioning to fruits but reduces *Botrytis cinerea* resistance in tomato. *Environ. Exp. Bot.* 168, 103889.
- Kaiser, E., Ouzounis, T., Giday, H., Schipper, R., Heuvelink, E., and Marcelis, L. F. M. (2019).** Adding blue to red supplemental light increases biomass and yield of greenhouse-grown tomatoes, but only to an optimum. *Front. Plant Sci.* 9, 1–11.
- Kalaitzoglou, P., van Ieperen, W., Harbinson, J., van der Meer, M., Martinakos, S., Weerheim, K., Nicole, C. C. S., and Marcelis, L. F. M. (2019).** Effects of continuous or end-of-day far-red light on tomato plant growth, morphology, light absorption, and fruit production. *Front. Plant Sci.* 10, 1–11.
- Kurepin, L. V., and Pharis, R. P. (2014).** Light signaling and the phytohormonal regulation of shoot growth. *Plant Sci.* 229, 280–289.
- Lanoue, J., Leonardos, E. D., and Grodzinski, B. (2018).** Effects of light quality and intensity on diurnal patterns and rates of photo-assimilate translocation and transpiration in tomato leaves. *Front. Plant Sci.* 9, 1–14.
- Lanoue, J., Leonardos, E. D., Ma, X., and Grodzinski, B. (2017).** The effect of spectral quality on daily patterns of gas exchange, biomass gain, and water-use-efficiency in tomatoes and lisianthus: An assessment of whole plant measurements. *Front. Plant Sci.* 8, 1–15.
- Lazaro, A., Mouriz, A., Piñeiro, M., and Jarillo, J. A. (2015).** Red light-mediated degradation of CONSTANS by the E3 ubiquitin ligase HOS1 regulates photoperiodic flowering in *Arabidopsis*. *Plant Cell* 27, 2437–2454.
- Li, F., De Storme, N., and Geelen, D. (2017).** Dynamics of male meiotic recombination frequency during plant development using fluorescent tagged lines in *Arabidopsis thaliana*. *Sci. Rep.* 7, 1–9.
- Lim, J., Park, J. H., Jung, S., Hwang, D., Nam, H. G., and Hong, S. (2018).** Antagonistic roles of phyA and phyB in far-red light-dependent leaf senescence in *Arabidopsis thaliana*. *Plant Cell Physiol.* 59, 1753–1764.



Chapter 3: Light quality regulates early plant development

- Lu, T., Meng, Z., Zhang, G., Qi, M., Sun, Z., Liu, Y., and Li, T.** (2017). Sub-high temperature and high light intensity induced irreversible inhibition on photosynthesis system of tomato plant (*Solanum lycopersicum* L.). *Front. Plant Sci.* 8, 1–16.
- Mas, P., Devlin, P. F., Panda, S., and Kay, S. A.** (2000). Functional interaction of phytochrome B and cryptochrome 2. *Nature* 408, 207–211.
- Masson, J., and Paszkowski, J.** (1992). The culture response of *Arabidopsis thaliana* protoplasts is determined by the growth conditions of donor plants. *Plant J.* 2, 829–833.
- Mathan, J., Bhattacharya, J., and Ranjan, A.** (2016). Enhancing crop yield by optimizing plant developmental features. *Dev.* 143, 3283–3294.
- Mizoguchi, T., Niinuma, K., and Yoshida, R.** (2007). Day-neutral response of photoperiodic flowering in tomatoes: Possible implications based on recent molecular genetics of Arabidopsis and rice. *Plant Biotechnol.* 24, 83–86.
- Moles, A. T., Warton, D. I., Warman, L., Swenson, N. G., Laffan, S. W., Zanne, A. E., Pitman, A., Hemmings, F. A., and Leishman, M. R.** (2009). Global patterns in plant height. *J. Ecol.* 97, 923–932.
- Moni, A., Lee, A. Y., Briggs, W. R., and Han, I. S.** (2015). The blue light receptor phototropin 1 suppresses lateral root growth by controlling cell elongation. *Plant Biol.* 17, 34–40.
- Monostori, I., Heilmann, M., Kocsy, G., Rakszegi, M., Ahres, M., Altenbach, S. B., Szalai, G., Pál, M., Toldi, D., Simon-Sarkadi, L., Harnos, N., Galiba, G., and Darko, E.** (2018). LED lighting – modification of growth, metabolism, yield and flour composition in wheat by spectral quality and intensity. *Front. Plant Sci.* 9, 1–16.
- Morrow, R. C.** (2008). LED lighting in horticulture. *HortScience* 43, 1947–1950.
- Nemhauser, J., and Chory, J.** (2002). Photomorphogenesis. *Arab. B.* 1, e0054.
- Ntagkas, N., Woltering, E., Bouras, S., De Vos, R. C., Dieleman, J. A., Nicole, C.**



- C. S., Labrie, C., and Marcelis, L. F. M.** (2019). Light-induced vitamin C accumulation in tomato fruits is independent of carbohydrate availability. *Plants* 8, 1–12.
- Pedmale, U. V., Huang, S. S. C., Zander, M., Cole, B. J., Hetzel, J., Ljung, K., Reis, P. A. B., Sridevi, P., Nito, K., Nery, J. R., Ecker, J. R., and Chory, J.** (2016). Cryptochromes interact directly with PIFs to control plant growth in limiting blue light. *Cell* 164, 233–245.
- Pennisi, G., Blasioli, S., Cellini, A., Maia, L., Crepaldi, A., Braschi, I., Spinelli, F., Nicola, S., Fernandez, J. A., Stanghellini, C., Marcelis, L. F. M., Orsini, F., and Gianquinto, G.** (2019). Unraveling the role of red:blue LED lights on resource use efficiency and nutritional properties of indoor grown sweet basil. *Front. Plant Sci.* 10, 1–14.
- Puig, J., Pauluzzi, G., Guiderdoni, E., and Gantet, P.** (2012). Regulation of shoot and root development through mutual signaling. *Mol. Plant* 5, 974–983.
- Reddy, S. K., and Finlayson, S. A.** (2014). Phytochrome B promotes branching in Arabidopsis by suppressing auxin signaling. *Plant Physiol.* 164, 1542–1550.
- Salisbury, F. J., Hall, A., Grierson, C. S., and Halliday, K. J.** (2007). Phytochrome coordinates Arabidopsis shoot and root development. *Plant J.* 50, 429–438.
- Schindelin, J., Arganda-Carreras, I., Frise, E., Kaynig, V., Longair, M., Pietzsch, T., Preibish, S., Rueden, C., Saalfeld, S., Schmid, B., Tinevez, J. Y., White, D. J., Hartenstein, V., Eliceiri, K., Tomancak, P., and Cardona, A.** (2012). Fiji: An open-source platform for biological-image analysis. *Nat. Methods* 9, 676–682.
- Schmitz, G., and Theres, K.** (1999). Genetic control of branching in Arabidopsis and tomato. *Curr. Opin. Plant Biol.* 2, 51–55.
- Schrager-Lavelle, A., Herrera, L. A., and Maloof, J. N.** (2016). Tomato phyE is required for shade avoidance in the absence of phyB1 and phyB2. *Front. Plant Sci.* 7, 1–9.
- Schumacher, P., Demarsy, E., Waridel, P., Petrolati, L. A., Trevisan, M., and**



Chapter 3: Light quality regulates early plant development

- Fankhauser, C.** (2018). A phosphorylation switch turns a positive regulator of phototropism into an inhibitor of the process. *Nat. Commun.* 9, 1–9.
- SharathKumar, M., Heuvelink, E., and Marcelis, L. F. M.** (2020). Vertical farming: moving from genetic to environmental modification. *Trends Plant Sci.* 25, 724–727.
- Silva-Navas, J., Moreno-Risueno, M. A., Manzano, C., Pallero-Baena, M., Navarro-Neila, S., Téllez-Robledo, B., Garcia-Mina, J. M., Baigorri, R., Gallego, F. J., and del Pozo, J. C.** (2015). D-Root: A system for cultivating plants with the roots in darkness or under different light conditions. *Plant J.* 84, 244–255.
- Smeets, L., and Garretsen, F.** (1986). Growth analyses of tomato genotypes grown under low night temperatures and low light intensity. *Euphytica* 35, 701–715.
- Song, J., Cao, K., Hao, Y., Song, S., Su, W., and Liu, H.** (2019). Hypocotyl elongation is regulated by supplemental blue and red light in cucumber seedling. *Gene* 707, 117–125.
- Su, Y. H., Liu, Y. B., and Zhang, X. S.** (2011). Auxin-cytokinin interaction regulates meristem development. *Mol. Plant* 4, 616–625.
- Suetsugu, N., and Wada, M.** (2013). Evolution of three LOV blue light receptor families in green plants and photosynthetic stramenopiles: Phototropin, ZTL/FKF1/LKP2 and aureochrome. *Plant Cell Physiol.* 54, 8–23.
- Telfer, A., Bollman, K. M., and Poethig, R. S.** (1997). Phase change and the regulation of trichome distribution in *Arabidopsis thaliana*. *Development* 124, 645–654.
- Valverde, F.** (2011). CONSTANS and the evolutionary origin of photoperiodic timing of flowering. *J. Exp. Bot.* 62, 2453–2463.
- Van der Ploeg, A., Van der Meer, M., and Heuvelink, E.** (2007). Breeding for a more energy efficient greenhouse tomato: Past and future perspectives. *Euphytica* 158, 129–138.



- Van Gelderen, K., Kang, C., and Pierik, R.** (2018). Light signaling, root development, and plasticity. *Plant Physiol.* 176, 1049–1060.
- Vandenbussche, F., Verbelen, J. P., and van der Straeten, D.** (2005). Of light and length: Regulation of hypocotyl growth in Arabidopsis. *BioEssays* 27, 275–284.
- Viršilė, A., Brazaitytė, A., Vaštakaitė-Kairienė, V., Miliauskienė, J., Jankauskienė, J., Novičkovas, A., and Samuolienė, G.** (2019). Lighting intensity and photoperiod serves tailoring nitrate assimilation indices in red and green baby leaf lettuce. *J. Sci. Food Agric.* 99, 6608–6619.
- Wang, Q., Zuo, Z., Wang, X., Gu, L., Yoshizumi, T., Yang, Z., Yang, L., Liu, Q., Liu, W., Han, Y. J., Kim, J. I., Liu, B., Wohlschlegel, J. A., Matsui, M., Oka, Y., and Lin, C.** (2016). Photoactivation and inactivation of *Arabidopsis* cryptochrome 2. *Science* 354, 343–347.
- Yoshida, H., Mizuta, D., Fukuda, N., Hikosaka, S., and Goto, E.** (2016). Effects of varying light quality from single-peak blue and red light-emitting diodes during nursery period on flowering, photosynthesis, growth, and fruit yield of everbearing strawberry. *Plant Biotechnol.* 33, 267–276.
- Yu, X., Liu, H., Klejnot, J., and Lin, C.** (2010). The cryptochrome blue light receptors. *Arab. B.* 8, e0135.
- Zeng, J., Wang, Q., Lin, J., Deng, K., Zhao, X., Tang, D., and Liu, X.** (2010). Arabidopsis cryptochrome-1 restrains lateral roots growth by inhibiting auxin transport. *J. Plant Physiol.* 167, 670–673.
- Zhai, H., Xiong, L., Li, H., Lyu, X., Yang, G., Zhao, T., Liu, J., and Liu, B.** (2020). Cryptochrome 1 inhibits shoot branching by repressing the self-activated transcription loop of PIF4 in Arabidopsis. *Plant Commun.* 1, 100042.
- Zhou, Y. H., Zhang, Y. Y., Zhao, X., Yu, H. J., Shi, K., and Yu, J. Q.** (2009). Impact of light variation on development of photoprotection, antioxidants, and nutritional value in *Lactuca sativa* L. *J. Agric. Food Chem.* 57, 5494–5500.



Supplementary Material (Tables S1-S2 and Figures S1-S5)

Table S1: LED modules.

This table indicates the percentages of blue, green, red, and far-red (FR) wavelengths for the white, red, and blue LED modules that were used in this study.

COLOUR	WAVELENGTHS	WHITE	RED	BLUE
BLUE	400-499	58%	0%	100%
GREEN	500-599	25%	0%	0%
RED	600-699	15%	100%	0%
FR	700-799	2%	0%	0%

Table S2: Standard error values.

In some figures, error bars were not included in the graphs for presentation purposes. These standard error values are listed in the table below. Abbreviations that are used: Arabidopsis (Ara), Tomato (Tom), Columbia (Col), Landsberg *erecta* (Ler), Moneymaker (MM), Foundation (FO), weeks after sowing (WAS), and days after sowing (DAS).

FIGURE	DATA POINT	MEAN VALUE	STANDARD ERROR
2B	Col-White-1WAS	0	0
2B	Col-White-2WAS	0	0
2B	Col-White-3WAS	0	0
2B	Col-White-4WAS	1.3	0.10
2B	Col-White-5WAS	12.8	1.78
2B	Col-White-6WAS	29.3	2.15
2B	Col-White-7WAS	40.7	3.62
2B	Col-White-8WAS	44.1	3.89



Chapter 3: Light quality regulates early plant development

2B	Col-White-9WAS	44.2	3.91
2B	Col-Blue-1WAS	0	0
2B	Col-Blue-2WAS	0	0
2B	Col-Blue-3WAS	4.7	0.32
2B	Col-Blue-4WAS	13.9	1.63
2B	Col-Blue-5WAS	21.6	2.09
2B	Col-Blue-6WAS	29.2	2.74
2B	Col-Blue-7WAS	31.3	3.68
2B	Col-Blue-8WAS	32.6	3.77
2B	Col-Blue-9WAS	32.9	3.81
2B	Col-Red-1WAS	0	0
2B	Col-Red-2WAS	0	0
2B	Col-Red-3WAS	0	0
2B	Col-Red-4WAS	0	0
2B	Col-Red-5WAS	0	0
2B	Col-Red-6WAS	0	0
2B	Col-Red-7WAS	0	0
2B	Col-Red-8WAS	10.6	0.51
2B	Col-Red-9WAS	26.4	1.77
2B	Col-Red-10WAS	41.5	3.49
2B	Col-Red-11WAS	53.2	4.21
2B	Col-Red-12WAS	60.1	4.87
2B	Col-Red-13WAS	63.8	5.02
2B	Col-Red-14WAS	64.8	5.11
2B	Ler-White-1WAS	0	0
2B	Ler-White-2WAS	0	0
2B	Ler-White-3WAS	0	0
2B	Ler-White-4WAS	9.5	0.61



Chapter 3: Light quality regulates early plant development

2B	Ler-White-5WAS	19.3	1.84
2B	Ler-White-6WAS	26.9	2.33
2B	Ler-White-7WAS	31.6	2.98
2B	Ler-White-8WAS	31.8	3.10
2B	Ler-White-9WAS	31.9	3.08
2B	Ler-Blue-1WAS	0	0
2B	Ler-Blue-2WAS	0	0
2B	Ler-Blue-3WAS	5.1	0.32
2B	Ler-Blue-4WAS	15.0	1.13
2B	Ler-Blue-5WAS	19.3	1.87
2B	Ler-Blue-6WAS	21.1	1.93
2B	Ler-Blue-7WAS	23.7	2.16
2B	Ler-Blue-8WAS	24.8	2.39
2B	Ler-Blue-9WAS	25.1	2.38
2B	Ler-Red-1WAS	0	0
2B	Ler-Red-2WAS	0	0
2B	Ler-Red-3WAS	0	0
2B	Ler-Red-4WAS	0	0
2B	Ler-Red-5WAS	0	0
2B	Ler-Red-6WAS	5.9	0.43
2B	Ler-Red-7WAS	14.5	1.17
2B	Ler-Red-8WAS	22.8	2.09
2B	Ler-Red-9WAS	32.3	2.96
2B	Ler-Red-10WAS	39.1	3.62
2B	Ler-Red-11WAS	41.2	3.90
2B	Ler-Red-12WAS	41.3	3.98
2E	MM-White-hypocotyl	3.2	0.11
2E	MM-White-epicotyl	2.8	0.28



Chapter 3: Light quality regulates early plant development

2E	MM-White-stem	19.1	0.93
2E	MM-Red-hypocotyl	5.9	0.13
2E	MM-Red-epicotyl	7.3	0.49
2E	MM-Red-stem	25.7	0.97
2E	MM-Blue-hypocotyl	3.9	0.24
2E	MM-Blue-epicotyl	3.8	0.44
2E	MM-Blue-stem	24.5	0.95
2E	FO-White-hypocotyl	3.9	0.14
2E	FO-White-epicotyl	4.6	0.17
2E	FO-White-stem	33.3	1.11
2E	FO-Red-hypocotyl	7.1	0.22
2E	FO-Red-epicotyl	7.3	0.49
2E	FO-Red-stem	36.8	1.02
2E	FO-Blue-hypocotyl	4.2	0.26
2E	FO-Blue-epicotyl	5.1	0.58
2E	FO-Blue-stem	36.1	1.39
2F	MM-White-height- 2WAS	2.5	0.07
2F	MM-White-height- 4WAS	6.8	0.21
2F	MM-White-height- 6WAS	25.1	0.92
2F	MM-Red-height-2WAS	4.2	0.08
2F	MM-Red-height-4WAS	11.5	0.31
2F	MM-Red-height-6WAS	36.1	0.75
2F	MM-Blue-height-2WAS	1.9	0.06
2F	MM-Blue-height-4WAS	7.2	0.23
2F	MM-Blue-height-6WAS	32.7	1.01



Chapter 3: Light quality regulates early plant development

2F	FO-White-height-2WAS	3.0	0.10
2F	FO-White-height-4WAS	9.9	0.27
2F	FO-White-height-6WAS	41.8	1.12
2F	FO-Red-height-2WAS	5.5	0.23
2F	FO-Red-height-4WAS	16.5	0.62
2F	FO-Red-height-6WAS	51.2	1.17
2F	FO-Blue-height-2WAS	2.2	0.14
2F	FO-Blue-height-4WAS	7.8	0.41
2F	FO-Blue-height-6WAS	45.4	1.65
2F	MM-White-hypocotyl- 2WAS	2.4	0.06
2F	MM-White-hypocotyl- 4WAS	3.1	0.08
2F	MM-White-hypocotyl- 6WAS	3.2	0.11
2F	MM-Red-hypocotyl- 2WAS	4.2	0.07
2F	MM-Red-hypocotyl- 4WAS	5.9	0.13
2F	MM-Red-hypocotyl- 6WAS	5.9	0.13
2F	MM-Blue-hypocotyl- 2WAS	1.9	0.05
2F	MM-Blue-hypocotyl- 4WAS	3.6	0.11
2F	MM-Blue-hypocotyl- 6WAS	3.9	0.24



Chapter 3: Light quality regulates early plant development

2F	FO-White-hypocotyl- 2WAS	2.9	0.09
2F	FO-White-hypocotyl- 4WAS	3.8	0.08
2F	FO-White-hypocotyl- 6WAS	3.9	0.14
2F	FO-Red-hypocotyl- 2WAS	5.2	0.21
2F	FO-Red-hypocotyl- 4WAS	7.0	0.19
2F	FO-Red-hypocotyl- 6WAS	7.1	0.22
2F	FO-Blue-hypocotyl- 2WAS	2.1	0.12
2F	FO-Blue-hypocotyl- 4WAS	3.8	0.14
2F	FO-Blue-hypocotyl- 6WAS	4.2	0.26
2F	MM-White-epicotyl- 2WAS	0.1	0.02
2F	MM-White-epicotyl- 4WAS	2.1	0.11
2F	MM-White-epicotyl- 6WAS	2.8	0.28
2F	MM-Red-epicotyl- 2WAS	0.1	0.02
2F	MM-Red-epicotyl- 4WAS	3.4	0.13



Chapter 3: Light quality regulates early plant development

2F	MM-Red-epicotyl- 6WAS	4.4	0.36
2F	MM-Blue-epicotyl- 2WAS	0.05	0.01
2F	MM-Blue-epicotyl- 4WAS	2.3	0.13
2F	MM-Blue-epicotyl- 6WAS	3.8	0.44
2F	FO-White-epicotyl- 2WAS	0.2	0.02
2F	FO-White-epicotyl- 4WAS	3.4	0.08
2F	FO-White-epicotyl- 6WAS	4.6	0.17
2F	FO-Red-epicotyl-2WAS	0.2	0.03
2F	FO-Red-epicotyl-4WAS	5.6	0.21
2F	FO-Red-epicotyl-6WAS	7.3	0.49
2F	FO-Blue-epicotyl-2WAS	0.1	0.03
2F	FO-Blue-epicotyl-4WAS	2.7	0.16
2F	FO-Blue-epicotyl-6WAS	5.1	0.58
3B	Col-White-secondary	3.7	0.19
3B	Col-White-tertiary	11.5	0.76
3B	Col-Red-secondary	6.7	0.46
3B	Col-Red-tertiary	21.6	3.59
3B	Col-Blue-secondary	3	0.14
3B	Col-Blue-tertiary	4.4	0.24
3B	Ler-White-secondary	2.9	0.19
3B	Ler-White-tertiary	8.6	0.86



Chapter 3: Light quality regulates early plant development

3B	Ler-Red-secondary	5.8	0.46
3B	Ler-Red-tertiary	17.5	3.12
3B	Ler-Blue-secondary	1.8	0.15
3B	Ler-Blue-tertiary	2	0.38
4D	Col-White-1WAS	2	0
4D	Col-White-2WAS	5.9	0.10
4D	Col-White-3WAS	10.3	0.18
4D	Col-White-4WAS	14.2	0.24
4D	Col-Red-1WAS	2	0
4D	Col-Red-2WAS	6.7	0.10
4D	Col-Red-3WAS	12.4	0.27
4D	Col-Red-4WAS	20.4	0.35
4D	Col-Red-5WAS	30.2	0.40
4D	Col-Red-6WAS	35.3	0.29
4D	Col-Red-7WAS	41.9	0.31
4D	Col-Red-8WAS	42.1	0.33
4D	Col-Blue-1WAS	2	0
4D	Col-Blue-2WAS	5.4	0.09
4D	Ler-White-1WAS	2	0
4D	Ler-White-2WAS	6.1	0.09
4D	Ler-White-3WAS	9.4	0.15
4D	Ler-Red-1WAS	2	0
4D	Ler-Red-2WAS	5.9	0.16
4D	Ler-Red-3WAS	11.8	0.22
4D	Ler-Red-4WAS	17.8	0.33
4D	Ler-Red-5WAS	27.1	0.47
4D	Ler-Red-6WAS	27.3	0.51
4D	Ler-Blue-1WAS	2	0



Chapter 3: Light quality regulates early plant development

4D	Ler-Blue-2WAS	4.6	0.10
5C	MM-White-1WAS	0	0
5C	MM-White-2WAS	2	0
5C	MM-White-3WAS	3.3	0.12
5C	MM-White-4WAS	4.9	0.16
5C	MM-White-5WAS	7.5	0.11
5C	MM-Red-1WAS	0	0
5C	MM-Red-2WAS	2	0
5C	MM-Red-3WAS	3.3	0.13
5C	MM-Red-4WAS	4.8	0.09
5C	MM-Red-5WAS	7.4	0.14
5C	MM-Blue-1WAS	0	0
5C	MM-Blue-2WAS	2	0
5C	MM-Blue-3WAS	3.2	0.16
5C	MM-Blue-4WAS	4.9	0.13
5C	MM-Blue-5WAS	7.5	0.11
5C	FO-White-1WAS	0	0
5C	FO-White-2WAS	2	0
5C	FO-White-3WAS	3.2	0.12
5C	FO-White-4WAS	4.9	0.10
5C	FO-White-5WAS	7.5	0.14
5C	FO-Red-1WAS	0	0
5C	FO-Red-2WAS	2	0
5C	FO-Red-3WAS	3.1	0.11
5C	FO-Red-4WAS	4.8	0.11
5C	FO-Red-5WAS	7.4	0.15
5C	FO-Blue-1WAS	0	0
5C	FO-Blue-2WAS	2	0



5C	FO-Blue-3WAS	2.9	0.17
5C	FO-Blue-4WAS	4.4	0.26
5C	FO-Blue-5WAS	7.4	0.17
S1A	Ara-White-1DAS	87.5	3.78
S1A	Ara-White-2DAS	94.3	1.26
S1A	Ara-White-3DAS	94.3	1.26
S1A	Ara-Red-1DAS	70.3	5.91
S1A	Ara-Red-2DAS	91.2	2.71
S1A	Ara-Red-3DAS	95.6	1.99
S1A	Ara-Blue-1DAS	64.2	5.32
S1A	Ara-Blue-2DAS	90.1	2.99
S1A	Ara-Blue-2DAS	93.8	2.04
S1B	Tom-White-4DAS	28.6	4.37
S1B	Tom-White-5DAS	64.3	2.51
S1B	Tom-White-6DAS	92.9	1.77
S1B	Tom-Red-4DAS	31.2	3.94
S1B	Tom-Red-5DAS	50.0	2.92
S1B	Tom-Red-6DAS	87.5	1.83
S1B	Tom-Blue-4DAS	6.7	3.01
S1B	Tom-Blue-5DAS	33.3	2.67
S1B	Tom-Blue-6DAS	33.3	2.67
S1B	Tom-Dark-4DAS	100	0.92
S1B	Tom-Dark-5DAS	100	0.92
S1B	Tom-Dark-6DAS	100	0.92



Chapter 3: Light quality regulates early plant development

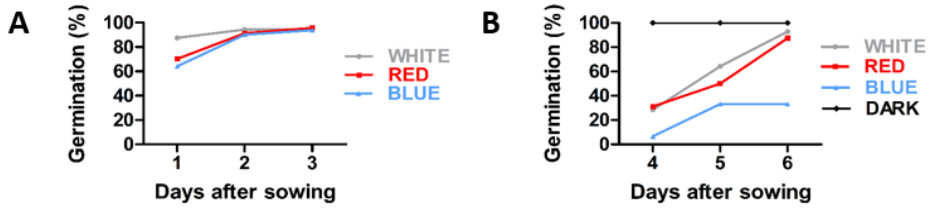


Figure S1: Arabidopsis and tomato germination assays.

A. Arabidopsis seeds showed optimal germination in white light. **B.** Tomato seeds showed optimal germination in darkness. Standard errors (from 3 technical replicates) are listed in **Table S2**.

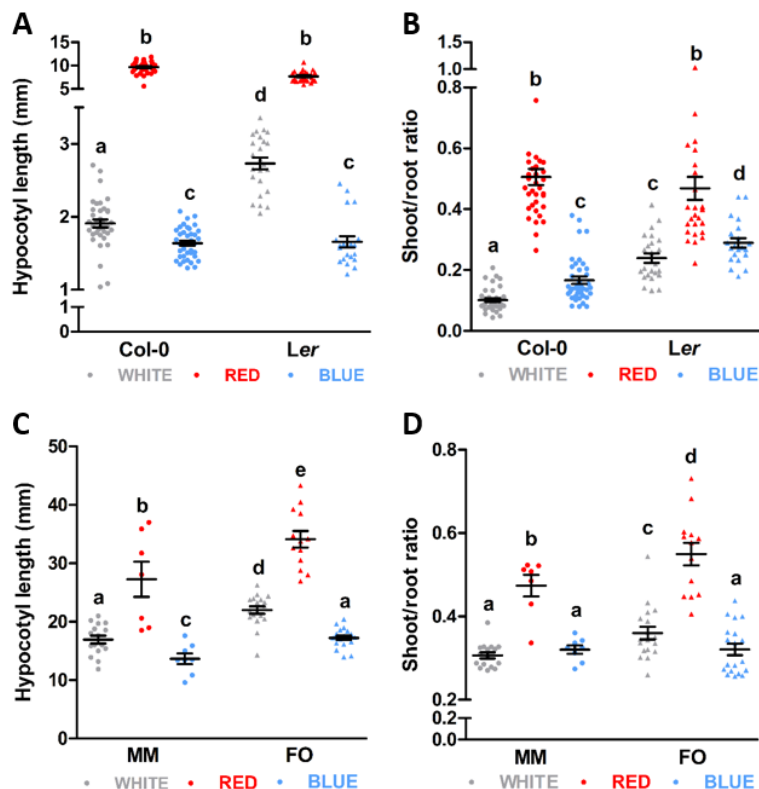


Figure S2: Quantification of Arabidopsis and tomato seedlings grown in light-grown roots (LGR) LED conditions.

A-B. Quantification of hypocotyl length (**A**) and shoot/root ratio (**B**) of 7-day-old Arabidopsis seedlings of ecotypes Columbia (Col-0) and Landsberg *erecta* (Ler) grown in white, red, or blue LED light-grown roots (LGR) conditions. **C-D.** Quantification of the hypocotyl length (**C**) and shoot/root ratio (**D**) of 5-day-old tomato seedlings of cultivars MoneyMaker (MM) and Foundation (FO). LED conditions and ecotypes / cultivars were compared using a one-way ANOVA followed by a Tukey's test (letters **a**, **b**, **c**, **d**, and **e** indicate statistically significant differences, $p < 0.05$). Error bars represent standard error of the mean in **A-B** ($n=30$) and **C-D** ($n=20$). Similar results were obtained in three independent experiments.

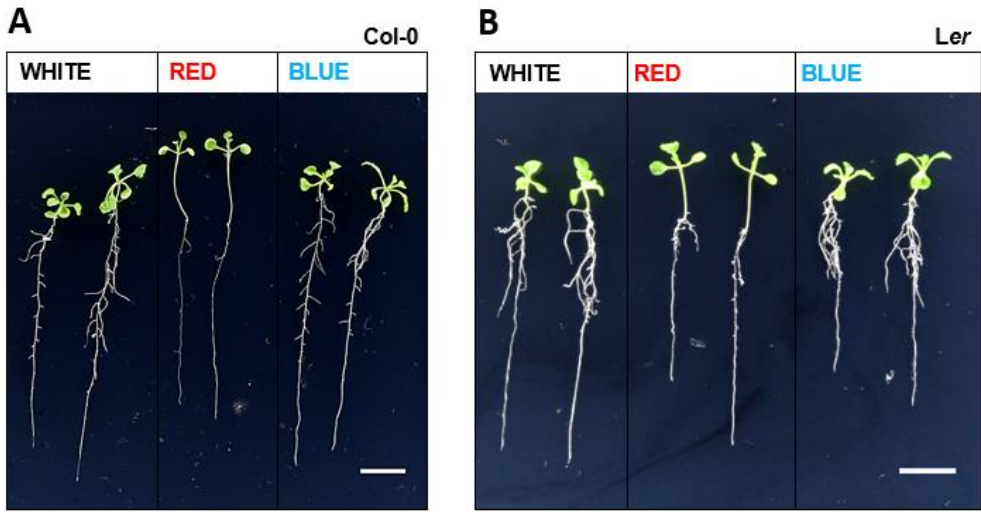


Figure S3: Phenotypes of 14-day-old Arabidopsis seedlings.

A. Representative 14-day-old Arabidopsis Columbia (Col-0) seedlings grown in dark-grown roots (DGR) white, red, or blue LED conditions. **B.** Representative 14-day-old Arabidopsis Landsberg *erecta* (Ler) seedlings grown in dark-grown roots (DGR) white, red, or blue LED conditions. For presentation purposes, seedlings were transferred to black agarose plates before photographing. Scale bars indicate 1 cm.

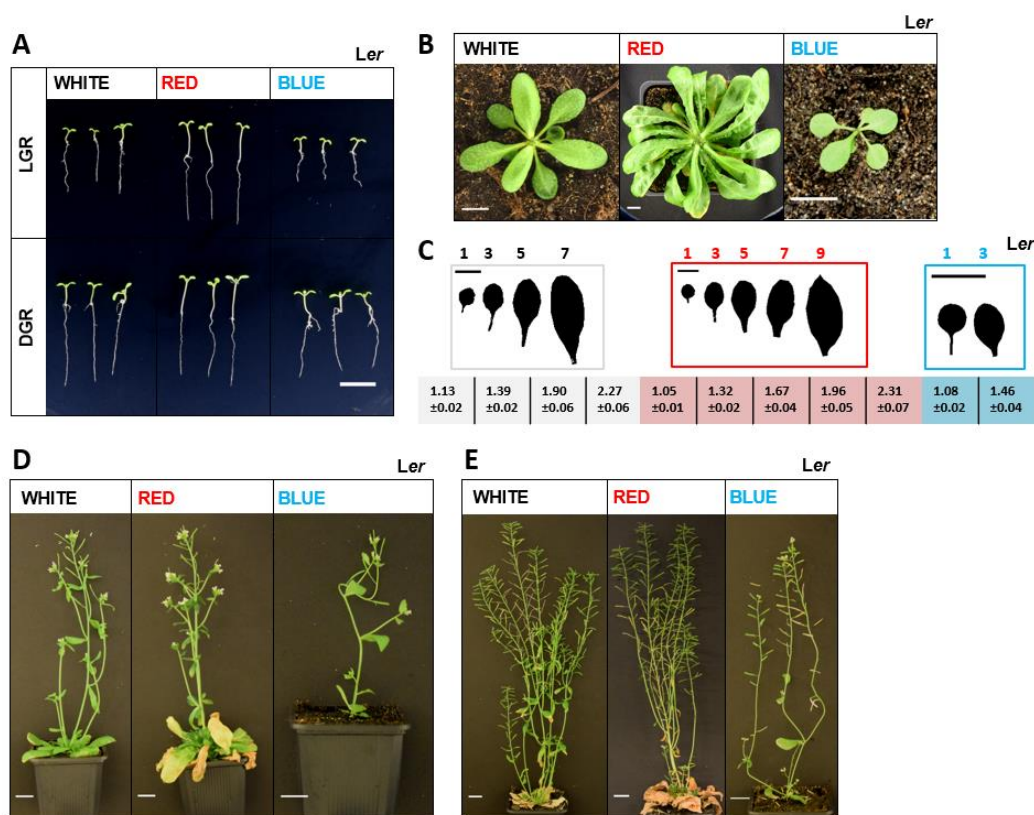
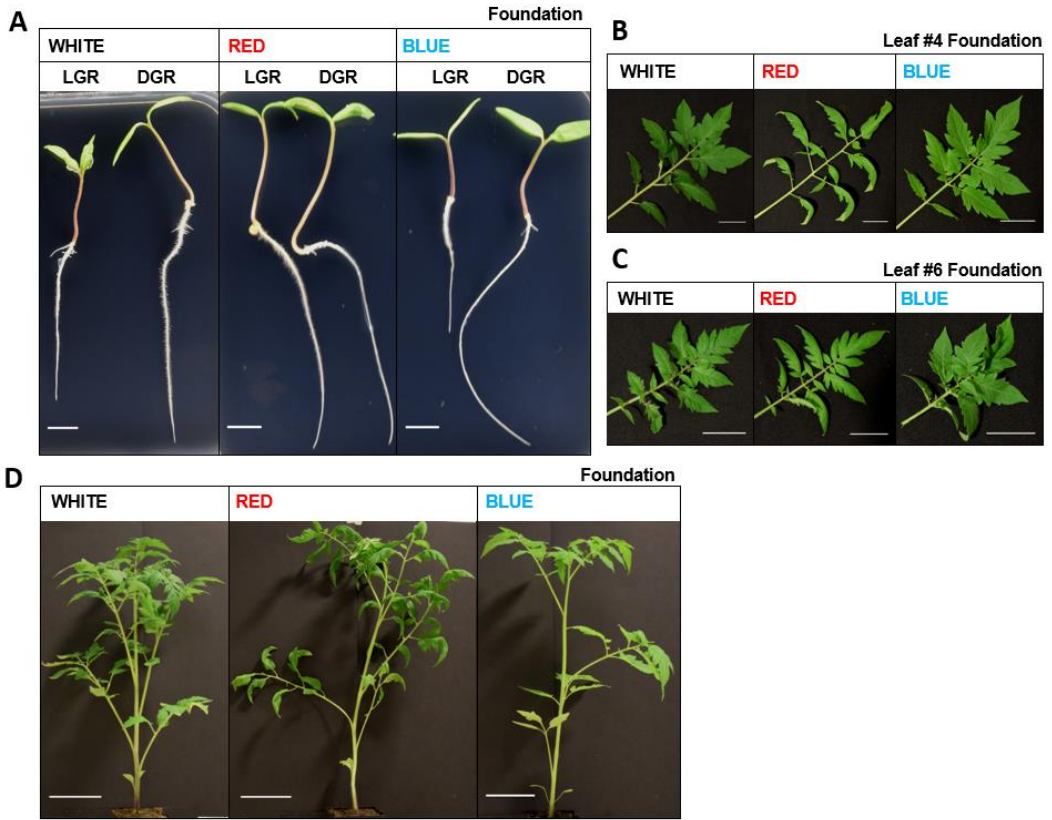


Figure S4: Phenotypes of *Arabidopsis Landsberg erecta* seedlings and plants grown under different LED lighting conditions.

A. Representative pictures of 7-day-old *Arabidopsis* seedlings of ecotype *Landsberg erecta* (*Ler*) grown in light-grown roots (LGR) or dark-grown roots (DGR) white, red, or blue LED conditions. For presentation purposes, seedlings were transferred to black agarose plates before photographing. **B.** Rosettes of representative *Ler* plants grown in white, red, or blue LED conditions. **C.** Rosette leaves of representative *Ler* plants and length/width ratios of the leaf blade (\pm SE). **D-E.** Representative *Ler* plants at one week (**D**) or 4 weeks after flowering (**E**). Monochromatic LED conditions (red or blue) were compared to white (control) using a two-sided Student's *t*-test (asterisks indicate statistically significant differences, $p < 0.05$) in **C** ($n = 10$). Scale bars indicate 1 cm. Similar results were obtained in two (**A**) or three (**B-E**) independent experiments.



Chapter 3: Light quality regulates early plant development





Chapter 4

Light quality regulates apical and primary radial growth of *Arabidopsis thaliana* and *Solanum lycopersicum*.

Kiki Spaninks¹, Gerda Lamers², Jelmer van Lieshout¹ and Remko Offringa¹

¹Plant Developmental Genetics, Institute of Biology Leiden, Leiden University, Sylviusweg 72, 2333 BE, Leiden, Netherlands.

²Core Facility Microscopy, Institute of Biology Leiden, Leiden University, Sylviusweg 72, 2333 BE, Leiden, Netherlands.



Abstract

For a horticultural crop such as tomato (*Solanum lycopersicum*), young plants are generally grown in the controlled environment of a growth chamber before their transfer to the greenhouse. For this initial growth phase, multi-layer systems can be applied to reduce space and energy costs. Here LEDs form the ideal lighting system, as they decouple light intensity from heating. Moreover, the spectral quality control of LEDs may be utilised to steer the plants towards a desired compact and sturdy phenotype. To achieve this, we must understand how light quality affects plant elongation and stem thickness during early plant development. Therefore we assessed apical and radial growth of tomato cultivars Moneymaker and Foundation, and *Arabidopsis thaliana* (*Arabidopsis*) ecotypes Columbia and Landsberg *erecta* grown in white, monochromatic red, or monochromatic blue light. Our histological and microscopic analysis revealed that the red LED condition increased cell elongation in hypocotyls and stems, whereas the blue LED condition decreased cell elongation, compared to white light-grown plants. This was observed in both species and correlated to hypocotyl length and plant height measurements from previous experiments. In seedlings, primary radial growth was affected by light quality in both species, resulting in thinner hypocotyls in the red LED condition, and thicker hypocotyls in the blue LED condition, compared to white light. However, in older plants, only *Arabidopsis* showed sensitivity of primary radial growth to light quality. Interestingly, the effect of red or blue light on *Arabidopsis* inflorescence stems was opposite to what was observed in hypocotyls. Possible effects of light quality on secondary radial growth remain to be investigated in both species. Finally, analysis of *Arabidopsis*



photoreceptor mutants suggested that cryptochromes and type II phytochromes are the main regulators of light-mediated apical and primary radial growth. To summarise, LEDs can be used to regulate both apical and primary radial plant growth, but the resulting phenotypes may be plant age- or species-specific.

Keywords: LEDs, apical growth, primary radial growth, histology, Arabidopsis, tomato

Introduction

Before the production cycle of a horticultural crop, such as tomato or cucumber, in greenhouses is started, young plants are generally grown in growth chambers (nurseries) until the appearance of the first truss. During this initial phase, plants may be grown in multi-layer systems to reduce space and energy costs. LED lights decouple light intensity from heating and can therefore be applied in these systems without the risk of overheating the plants. Moreover, spectral quality control of LEDs may be used to steer plant development into desired phenotypes. For tomato nurseries, uniform young plants that flower early and remain sturdy and compact until transport are the desired end product. To achieve this, both apical and radial stem growth should be tightly controlled. To avoid misinterpretation, we distinguish between “primary radial growth”, indicating an increase in stem thickness caused by cell growth in primary stem structures, and “secondary growth” where an increase in stem thickness results from cell divisions in the vascular or cork cambium. The stem is initiated in the rib zone (RZ) of the shoot apical



Chapter 4: Light quality affects apical and primary radial growth

meristem (SAM), where the central region gives rise to the pith, the boundary region to the vasculature, and the peripheral regions produce epidermal and cortex cells (Sachs, 1965). A key phytohormone for apical stem development, gibberellic acid (GA), promotes cell division in the RZ by relieving DELLA-inhibited class I TCP (TEOSINTE BRANCHED 1, CYCLOIDEA, PROLIFERATING CELL FACTOR) transcription factors (Davière et al., 2014). In addition, BRASSINAZOLE-RESISTANT 1 (BZR1) proteins physically interact with DELLAs, suggesting that GA indirectly regulates brassinosteroid (BR)-induced stem growth as well (Gallego-Bartolomé et al., 2012). Finally, interplay between auxin, abscisic acid and GA biosynthesis has been shown to regulate stem elongation (Ross et al., 2003; Seo et al., 2006; Oh et al., 2007). Modulation of apical stem growth by light quality and intensity has been linked to phytohormones, and has already been reported in several species (Zheng et al., 2019; Gawronska et al., 1995; Hisamatsu et al., 2005; Paradiso and Proietti, 2021), with the most well-known example being the shade avoidance syndrome where stem growth is increased under low light intensity or low red/far-red (R:FR) ratios. Different from apical growth, radial growth is initiated in lateral meristems that consist of a xylem- and phloem-producing vascular cambium, and a cork- and phelloderm-producing cork cambium (Barra-Jiménez and Ragni, 2017). Vascular stem cell proliferation and differentiation rely on the phytohormones auxin, cytokinin, BR, and their downstream signalling components. Proliferation of the vascular cambium is promoted directly through the ligand-receptor complex TRACHEARY ELEMENT DIFFERENTIATION (TDIF)-PHLOEM INTERCALATED WITH XYLEM (PXY), and indirectly through its activation of WUSCHEL-RELATED HOMEODOMAIN 4 (WOX4) and WOX14 transcription factors that



inhibit xylem differentiation (Suer et al., 2011; Etchells et al., 2013, 2016). Further towards the outside of the stem, HIGH CAMBIAL ACTIVITY 2 (HCA2) and LATERAL ORGAN BOUNDARIES DOMAIN 1 (LBD1) promote phloem formation, whereas VASCULAR-RELATED NAC-DOMAIN 6 (VND6) and VND7 are important for xylem production towards the inside of the stem (Kubo et al., 2005; Guo et al., 2008; Yordanov et al., 2010). Similar to apical stem growth, radial growth has been shown to respond to alterations in light quality, intensity, and day length. For example, low light intensity, short days, and low R:FR ratios all result in thicker stems in *Arabidopsis* and potato plants, respectively (MacMillan et al., 2013; Botterweg-Paredes et al., 2020; Li-Li et al., 2020). However, the underlying mechanisms remain to be elucidated. In order to steer plant growth towards the desired sturdy and compact phenotypes, a better understanding of light-regulated stem growth and development is required. In **chapter 3**, we observed that hypocotyl and stem elongation can be modulated by red or blue light in both *Arabidopsis thaliana* (*Arabidopsis*) and *Solanum lycopersicum* (tomato). To further investigate these observations, we performed histological and microscopic analyses on the hypocotyls and stems of *Arabidopsis* and tomato plants grown in white, red, or blue LED conditions. Here we show that apical growth of both hypocotyls and stems in response to light quality mostly relies on cell elongation. Furthermore, we confirmed that primary radial growth of hypocotyls and stems can be controlled by light quality in *Arabidopsis*, and that the stem phenotype is affected both by the formation of vascular bundles, and by primary xylem production. However, while tomato hypocotyls responded to light quality in a similar way, the primary radial growth in the stems of young tomato plants was indifferent to light quality, once again



Chapter 4: Light quality affects apical and primary radial growth

demonstrating that phenotypes from a genetic model organism may not always be translated to horticultural crops.

Results

Light quality regulates apical growth of *Arabidopsis* and tomato hypocotyls.

To assess the effect of light quality on hypocotyl elongation in *Arabidopsis*, seedlings of ecotype Columbia (Col-0) were grown for seven days in white, red, or blue LED conditions. As described in **chapter 3**, hypocotyls were longer in red light, and shorter in blue light, when compared to white light conditions (**Figure 1A, B**). Scanning electron microscopy analysis revealed that the hypocotyl epidermis cells were greatly affected by light quality (**Figure 1C**). Epidermal cells of seedlings grown in monochromatic red light were extremely elongated and appeared to be flaccid due to a possible loss of turgor, or rapid elongation. In contrast, seedlings grown in monochromatic blue light showed very small and turgid epidermal cells (**Figure 1C**). Next, we used stereomicroscopy to visualise the hypocotyls of 5-day-old wild-type tomato seedlings of both Moneymaker (MM) and the commercial hybrid Foundation (FO) grown in the different LED conditions. Hypocotyls of seedlings grown in monochromatic red light appeared to be greener, while hypocotyls of blue light-grown seedlings appeared slightly purple, compared

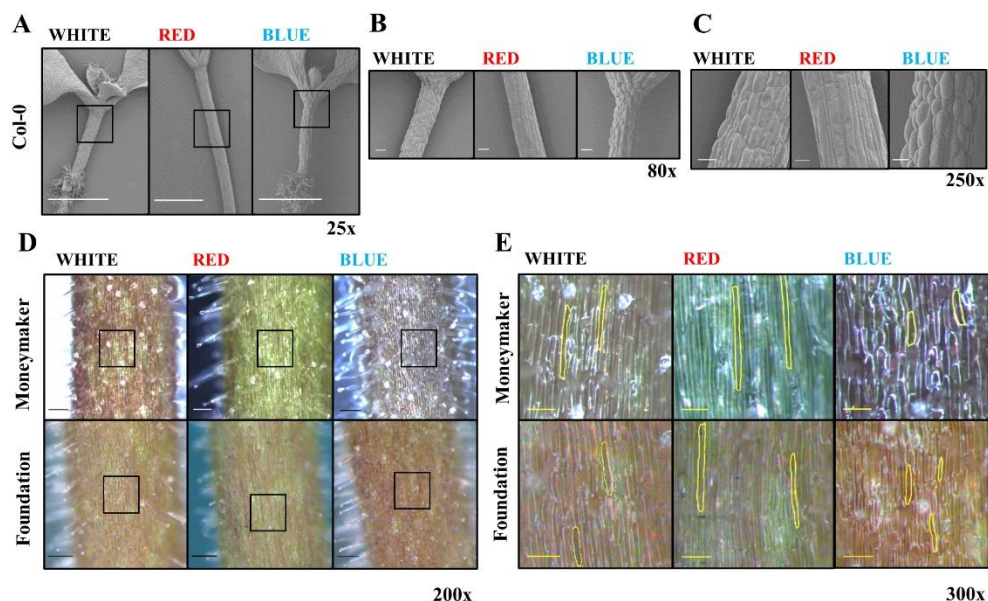


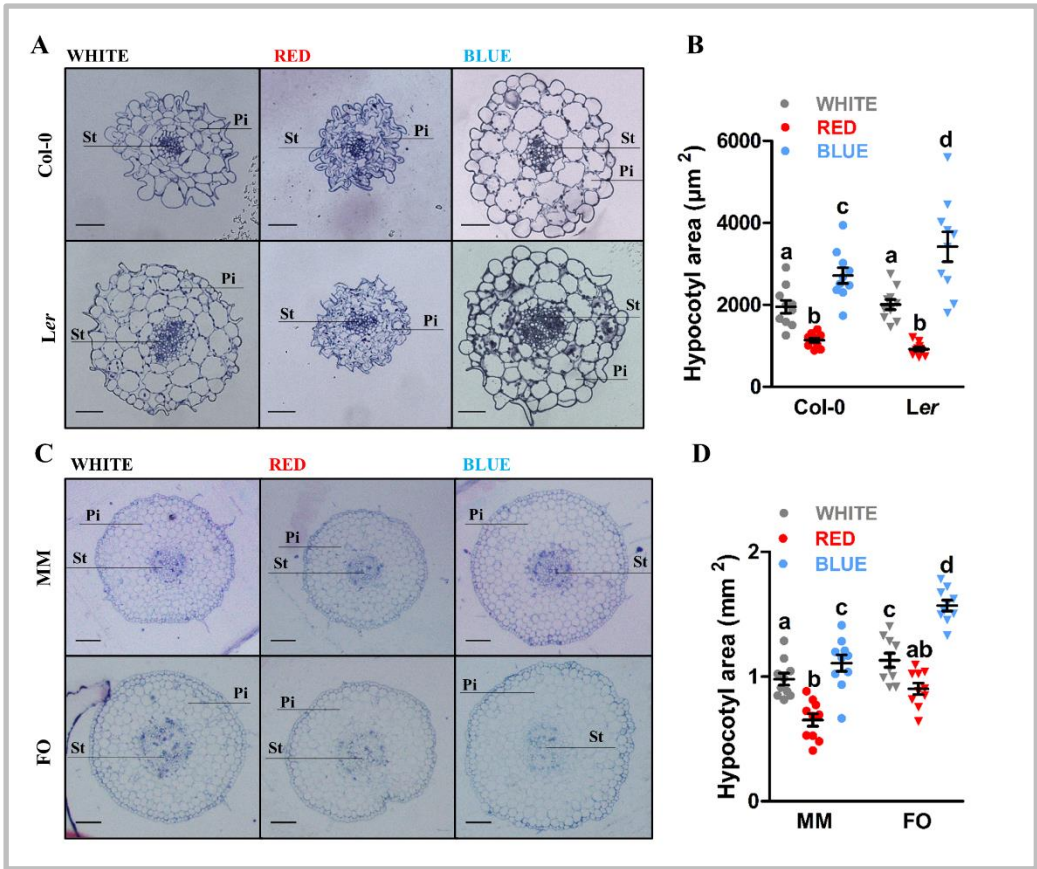
Figure 1: Light quality regulates epidermal cell elongation in *Arabidopsis* and tomato hypocotyls.

A-C: Scanning electron microscopy images of hypocotyls from 7-day-old *Arabidopsis* seedlings of ecotype Columbia (Col-0) that were grown in white, red, or blue LED conditions. **D-E:** Stereomicroscopy images of hypocotyls of 5-day-old tomato seedlings of cultivars MoneyMaker and Foundation that were grown in the different LED conditions. Hypocotyls were imaged at 25x (**A**), 80x (**B**), 250x (**C**), 200x (**D**), and 300x (**E**) magnification. Black boxes in **A** and **D** indicate the area that was further magnified in **B**, **C** and **E**, respectively. Single epidermal cells were highlighted in yellow in **E**. Scale bars indicate 1 mm (**A**), 100 μ m (**B**), 50 μ m (**C**), 200 μ m (**D**) and 150 μ m (**E**). Images shown are of representative seedlings (n=15), and similar results were obtained from two independent experiments.

to white light (**Figure 1D**). At a higher magnification, we observed that hypocotyl epidermis cells of red light-grown seedlings were elongated, whereas epidermis cells of seedlings grown in monochromatic blue light were



Chapter 4: Light quality affects apical and primary radial growth



shorter, compared to white light (**Figure 1E**). Together, these results show that hypocotyl elongation of both *Arabidopsis* and tomato seedlings can be modulated by light quality.

Light quality regulates primary radial growth of *Arabidopsis* and tomato hypocotyls.

Next, we investigated radial growth in hypocotyls of 7-day-old *Arabidopsis* seedlings of ecotypes Col-0 and *Landsberg erecta* (*Ler*) that were grown in the



Figure 2: Light quality regulates primary radial growth in *Arabidopsis* and tomato hypocotyls.

A. Light microscopy images of toluidine blue stained cross sections from hypocotyls of 7-day-old *Arabidopsis* seedlings of ecotypes Columbia (Col-0) and Landsberg *erecta* (*Ler*) grown in white, red, or blue LED conditions. **B.** Dot plot presenting the surface area of Col-0 and *Ler* hypocotyl cross sections in square micrometres (μm^2). **C.** Light microscopy images of toluidine blue stained cross sections from the hypocotyl of 5-day-old tomato seedlings of cultivars MoneyMaker (MM) and Foundation (FO) grown in white, red, or blue LED conditions. **D.** Dot plot presenting the surface area of MM and FO hypocotyl cross sections in square millimetres (mm^2). Scale bars indicate 10 μm in **A** and 150 μm in **C**. Pi=pith and St=stele in **A** and **C**. LED conditions and ecotypes were compared using a one-way ANOVA followed by a Tukey's test (letters **a**, **b**, **c**, and **d** indicate statistically significant differences, $p < 0.05$) in **B** and **D**. Error bars represent standard error from mean ($n=10$) in **B** and **D**. Similar results were obtained from two independent experiments.

different LED conditions. Toluidine blue stained cross sections showed that, both for *Arabidopsis* Col-0 and *Ler* ecotypes, in monochromatic red light, hypocotyls were thinner, whereas in blue light hypocotyls were thicker than in white light (**Figures 2A, B**). This difference in hypocotyl thickness appears to rely on cell size rather than cell number (**Figure 2A**). Analysis of the hypocotyls of 5-day-old tomato seedlings of MM and FO cultivars grown in white, red, or blue light showed that, similar to *Arabidopsis*, treatment with monochromatic red light resulted in thinner hypocotyls, and treatment with monochromatic blue light in thicker hypocotyls (**Figures 2C, D**). Furthermore,



Chapter 4: Light quality affects apical and primary radial growth

as in *Arabidopsis*, primary radial growth of tomato hypocotyls appeared to rely mostly on cell size (**Figure 2C**). Secondary growth was not observed in any of the *Arabidopsis* or tomato hypocotyls. To summarise, these results show that radial hypocotyl growth is affected by light quality in both *Arabidopsis* and tomato seedlings.

Light quality regulates apical growth of *Arabidopsis* and young tomato stems.

Next, we investigated the effect of light quality on apical stem growth in *Arabidopsis* and tomato plants. At 4 weeks after bolting, longitudinal sections of the basal internode of the main inflorescence of *Arabidopsis* plants of ecotypes Col-0 and *Ler* suggested that the size of cortex, vascular, and pith cells were affected by the LED conditions (**Figure 3A**). Measurements of the pith cells confirmed that the red LED condition increased pith cell length, whereas the blue LED condition decreased pith cell length, compared to white light. This difference was observed in both ecotypes, although for blue light it was less pronounced in *Ler* stems (**Figure 3B**). Longitudinal sections of the basal part (just above the epicotyl) of stems of 30-day-old tomato plants of MM and FO cultivars showed that treatment with monochromatic red or blue light affects the pith cells (**Figure 3C**). Quantification of pith cell length showed that, compared to white light, the red LED condition significantly increased pith cell length in the stems of both MM and FO, while the blue LED condition significantly increased pith cell length only in MM (**Figure 3D**). The longitudinal sections revealed that light quality can be used to modulate apical stem growth in both *Arabidopsis* and tomato, and that, similar to apical hypocotyl growth, these phenotypes rely (at least in part) on cell elongation.

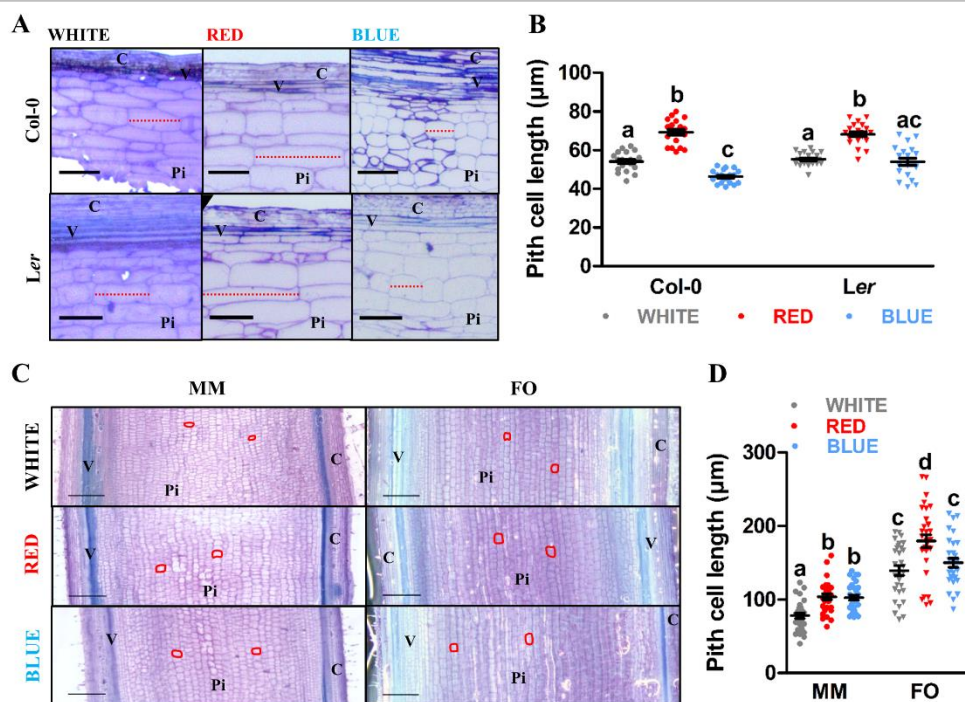


Figure 3: Light quality regulates pith cell elongation in Arabidopsis and tomato stems.

A. Light microscopy images of toluidine blue stained longitudinal sections from the most basal internode of the primary inflorescence of Arabidopsis plants (ecotypes Columbia (Col-0) and Landsberg *erecta* (Ler)) grown in white, red, or blue LED conditions. Stem segments were harvested at 4 weeks after bolting. The length of a representative pith cell is indicated by a red dotted line **B.** Dot plot presenting the pith cell length of Arabidopsis stems in micrometres (μm). **C.** Stereomicroscopy images of toluidine blue stained longitudinal sections from the basal part (above the epicotyl) of the stem of 30-day-old Moneymaker (MM) and Foundation (FO) tomato plants grown in the different LED conditions. Representative pith cells are highlighted in red. **D.** Dot plot presenting the pith cell length of tomato stems in μm . Scale bars indicate 50 μm in **A** and 1 mm in **C**. Pi=pith, V=vascular tissue and C=cortex in **A** and **C**. LED conditions and ecotypes were compared using a one-way ANOVA followed by a Tukey's test (letters **a**, **b**, **c**, and **d** indicate statistically significant differences, $p < 0.05$) in **B** and **D**. Error bars represent standard error from mean ($n=30$) in **B** and **D**. Similar results were obtained from two independent experiments.



Red and blue light regulate primary radial growth of Arabidopsis, but not of tomato stems.

For analysis of radial stem growth in Arabidopsis, we made cross-sections from the most basal internode of the primary inflorescence of Arabidopsis plants at 4 weeks after bolting. Stems of both Col-0 and Ler were thicker when grown in monochromatic red light, and thinner in monochromatic blue light, when compared to white light (**Figure 4A**). Quantification of the surface area of each cross-sectioned stem confirmed a statistically significant increase in red light, and decrease in blue light, when compared to white light (**Figure 4B**). At higher magnification, we observed structural differences in the different stem tissues. For example, the cortex and pith of stems from plants that were grown in blue light consisted of less layers than those from plants grown in white or red light (**Figure 4C**). But also the primary xylem width, and the number of vascular bundles were enhanced in red light and reduced in blue light compared to white light (**Figures 4D, E**). Interestingly, most of these differences in primary radial growth of Arabidopsis stems could already be observed at 1 week after bolting (**Figure S1**). Although no secondary xylem or phloem was observed in any of the samples, stems of Arabidopsis plants grown in red light contained interfascicular cambium, whereas no early signs of secondary growth were observed in plants grown in the white and blue LED condition. Next, we analysed cross sections of the stems of 30-day-old MM and FO tomato plants. Interestingly, the tomato stems showed a similar stem surface area in all three LED conditions (**Figure 5A, B**). In addition, we did not observe any differences in stem tissues (**Figure 5C**), xylem width or vascular bundle number (**Figure 5D, E**). These results indicate that primary

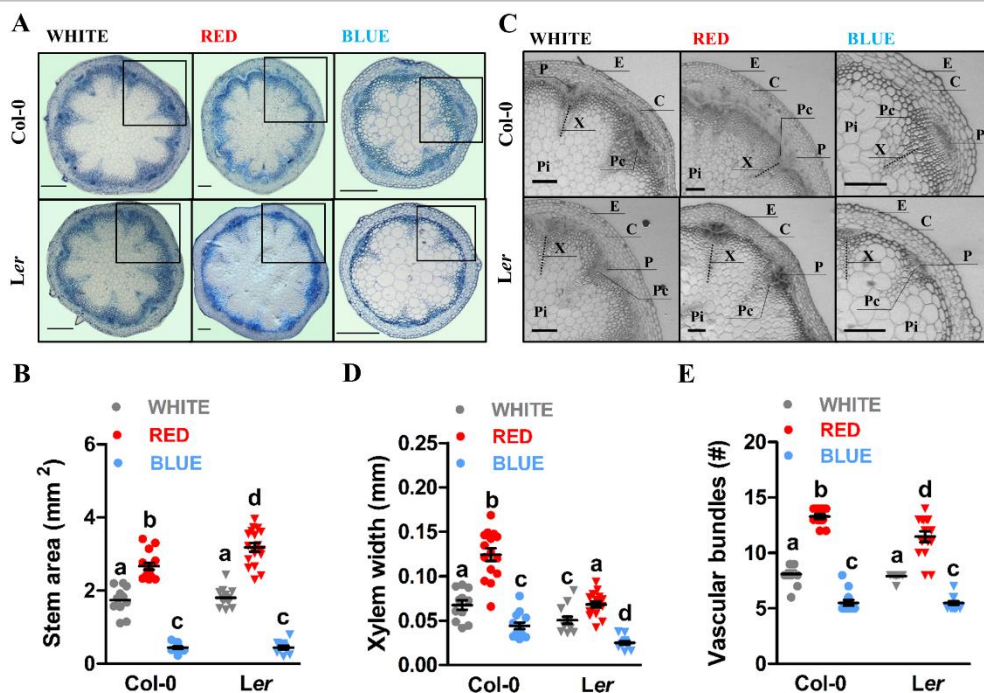


Figure 4: Light quality regulates primary radial growth of Arabidopsis stems.

A. Stereomicroscopy images of toluidine blue stained cross sections from the most basal internode of the primary inflorescence of Arabidopsis plants (ecotypes Columbia (Col-0) and Landsberg *erecta* (Ler)) grown in white, red, or blue LED conditions. Stem segments were harvested at 4 weeks after bolting. **B.** Dot plot presenting the surface area of Col-0 and *Ler* stem cross sections in square millimetres (mm²). **C.** 2x digital magnification of the boxed areas in **A** to show the vascular bundles in more detail (E=epidermis, C=cortex, P=phloem, Pc=procambium, X=xylem, and Pi=pith). **D.** The width (in mm) of the primary xylem tissue in Col-0 and *Ler* stems. Each dot represents the average of three measurements within one stem. **E.** The number of vascular bundles in Col-0 and *Ler* stems. Scale bars indicate 200 μ m in **A** and 100 μ m in **C**. LED conditions and ecotypes were compared using a one-way ANOVA followed by a Tukey's test (letters **a**, **b**, **c**, and **d** indicate statistically significant differences, $p < 0.05$) in **B**, **D** and **E**. Error bars represent standard error from mean ($n = 15$) in **B**, **D** and **E**. Similar results were obtained from two independent experiments.

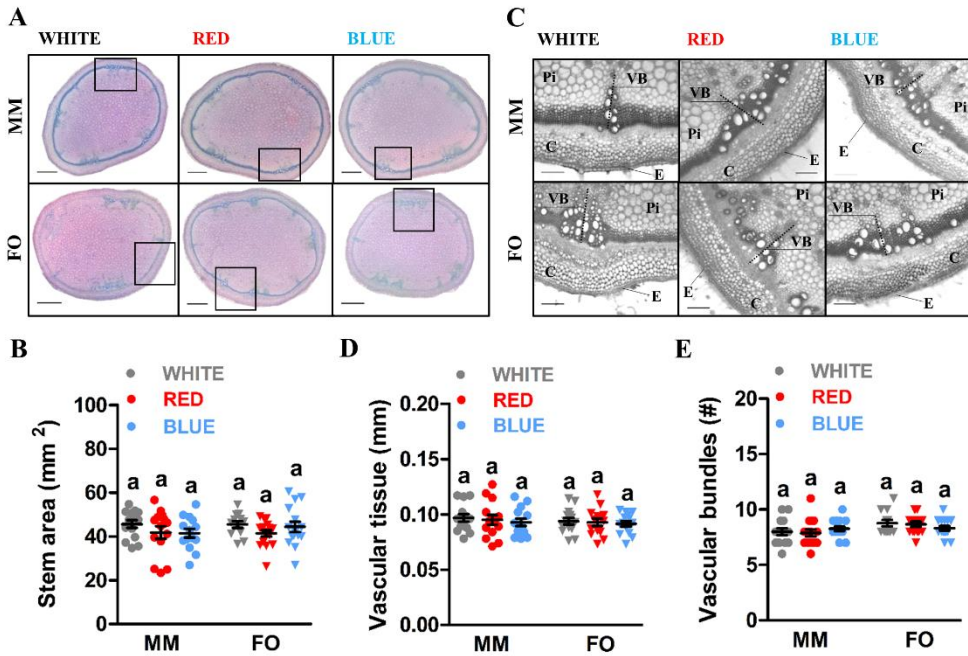


Figure 5: Primary radial growth of young tomato stems is indifferent to light quality.

A. Stereomicroscopy images of toluidine blue stained cross sections from the basal part (above the epicotyl) of the stem of 30-day-old tomato plants (cultivars MoneyMaker (MM) and Foundation (FO)) grown in white, red, or blue LED conditions. **B.** Dot plot presenting the surface area of MM and FO stem cross sections in square millimetres (mm²). **C.** 4x digital magnification of the boxed areas in **A** to show the vascular bundles in more detail (E=epidermis, C=cortex, VB=vascular bundle, and Pi=pith). Several magnifications were reoriented for easy comparison. **D.** The width (in mm) of the vascular tissue in MM and FO stems. Each dot represents the average of three measurements within one stem. **E.** The number of vascular bundles in MM and FO stems. Scale bars indicate 2 mm in **A** and 500 μ m in **C**. LED conditions and cultivars were compared using a one-way ANOVA followed by a Tukey's test (different letters indicate statistically significant differences, $p < 0.05$) in **B**, **D** and **E**. Error bars represent standard error from mean ($n=15$) in **B**, **D** and **E**. Similar results were obtained from two independent experiments.



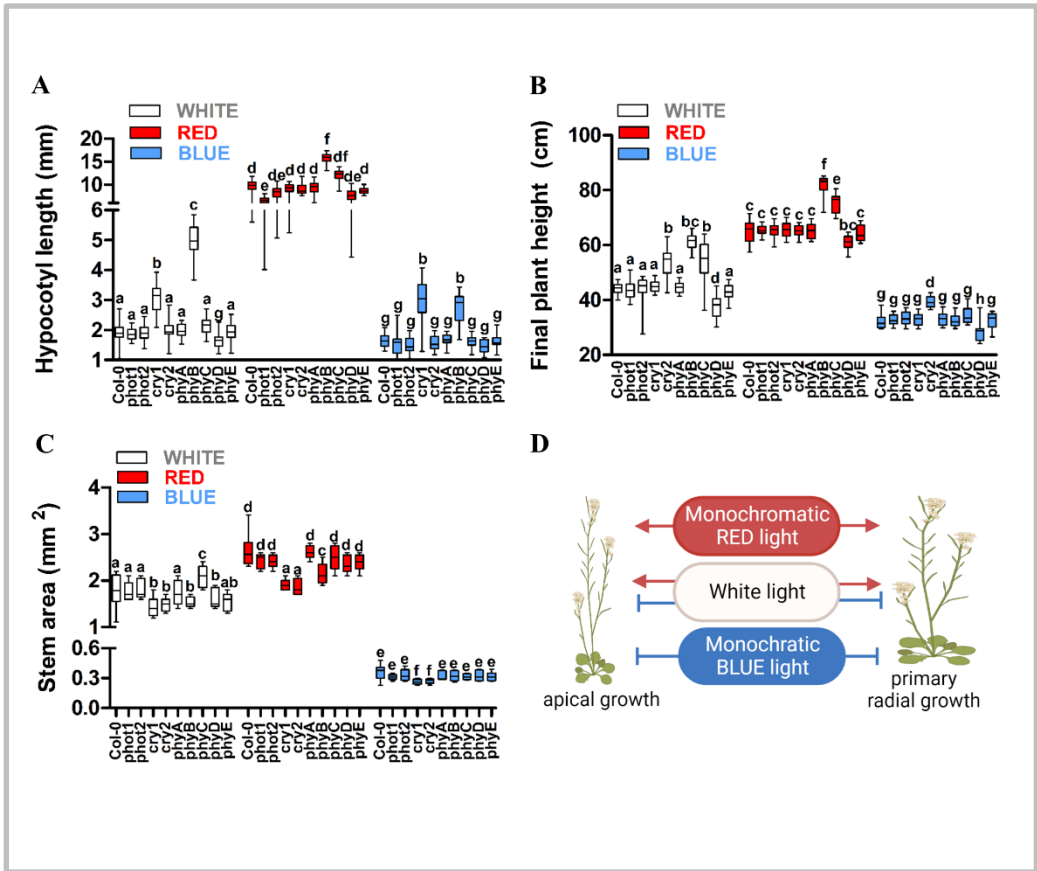
radial stem growth of *Arabidopsis* plants can be steered by red or blue light, while this appears to be impossible in young tomato plants. In addition, the effect of red and blue light on *Arabidopsis* primary radial growth are opposite in seedlings and reproductive plants.

Light-regulated apical and primary radial growth of *Arabidopsis* plants relies mostly on cryptochromes and type II phytochromes.

To investigate the role of photoreceptors in apical and primary radial growth, single mutants of the phytochrome (PHY), cryptochrome (CRY), or phototropin (PHOT) type of photoreceptors were grown in the different LED conditions. Like wild type, all mutants developed a longer hypocotyl in red light, and a shorter hypocotyl in white or blue light (**Figure 6A**). *cry1* seedlings had a longer hypocotyl than wild-type seedlings grown in white and monochromatic blue light, but not in monochromatic red light. The hypocotyl length of *phyB* seedlings was increased in all three LED conditions. In contrast, *phyD* and *phot1* seedlings had a slightly shorter hypocotyl in respectively white and monochromatic red light, compared to wild-type seedlings. All other photoreceptor mutants showed a hypocotyl phenotype similar to that of wild type in the different LED conditions (**Figure 6A**). The final plant height of all mutants, like wild type, was increased in red light and decreased in blue light. *cry2* plants showed an increase in plant height, compared to wild-type plants grown in white and monochromatic blue light. *phyB* and *phyC* plants were taller than wild-type plants grown in white and monochromatic red light. In contrast, *phyD* plants were shorter than wild-type plants grown in all three LED conditions. (**Figure 6B**). The stem thickness of most mutants, like wild type,



Chapter 4: Light quality affects apical and primary radial growth



was increased in red light and decreased in blue light. Only *cry1* and *cry2* plants had a thinner stem compared to wild-type plants in all three LED conditions, while *phyB* stems were only thinner in white and monochromatic red light. (**Figure 6C**). Altogether this data suggests that apical and primary radial growth of Arabidopsis is regulated by light quality, mostly via CRYs and type II PHYs (PHYB to PHYE) (**Figure 6D**). However, the positive effects of CRYs on primary radial growth are also observed in the red LED condition, suggesting putative interactions with PHYs, or light-independent functions of CRYs in this process.



Figure 6: Cryptochromes and Type II phytochromes regulate apical and primary radial growth in Arabidopsis.

A. Quantification of hypocotyl length of 7-day-old Arabidopsis photoreceptor mutants grown in white, red, or blue LED conditions. Single mutants of the following families were included: red / far-red light-sensing phytochromes (phys), and blue light-sensing cryptochromes (crys) and phototropins (phot). **B.** Plant height of Arabidopsis photoreceptor mutants grown in the different LED conditions. **C.** Box plot presenting the surface area of photoreceptor mutant stems in square millimetres (mm²). **D.** Simplified model of apical and primary radial growth of *Arabidopsis thaliana* in the different LED conditions. Monochromatic red light results in increased plant height and primary radial growth. In monochromatic blue light plant height is decreased (most likely resulting from CRY-mediated inhibition) and primary radial growth as well. In white light, the effects of red and blue light are balanced, resulting in an intermediate phenotype. To further confirm photoreceptor functions in white light, double and triple mutants should be studied to identify putative interactions between PHY and CRY signalling. LED conditions and plant lines were compared using a one-way ANOVA followed by a Tukey's test (letters **a**, **b**, **c**, **d**, **e**, and **f** indicate statistically significant differences, $p < 0.05$) in **A-C**. Error bars represent standard error from mean in **A-C** (n=20). Similar results were obtained from two independent experiments.

Discussion

If we wish to use LEDs to steer plants towards a short and compact architecture that is desired during the initial growth phase, we must understand how light quality regulates plant growth. In **chapter 3** we showed that treatment with monochromatic red light increased hypocotyl length and plant height in Arabidopsis and tomato, while the effect of monochromatic blue light was opposite. These results were consistent with other LED studies on Arabidopsis,



Chapter 4: Light quality affects apical and primary radial growth

and a greenhouse tomato study that used LEDs as supplemental lighting (Chen et al., 2020; Dieleman et al., 2019). Here we performed histological and microscopic analyses to further investigate apical and radial growth of stems and hypocotyls under different LED conditions.

Regulation of apical growth by light quality.

First, we further investigated apical growth of Arabidopsis and tomato hypocotyls and stems. Scanning electron microscopy revealed that the hypocotyl epidermal cells of Arabidopsis seedlings grown in monochromatic red light are extremely elongated (3-4 fold compared to white light) and appear flaccid. In contrast, blue light-grown seedlings had small and turgid epidermal cells. Although the effects of light quality on the epidermal cell elongation were clear, the microscopic analysis was insufficient to exclude an additional effect of light quality on cell division. Moreover, our analysis only allowed visualisation of the epidermis, thus other cell layers remain to be investigated. Since most hypocotyl cells are produced by cell divisions during embryogenesis, cell elongation is generally thought to be the driving force of hypocotyl growth (Gendreau et al., 1997). Stereomicroscopy images of tomato seedlings revealed a similar hypocotyl phenotype, suggesting that apical growth responses to light are conserved in these species. Furthermore, similar hypocotyl phenotypes have been reported in lettuce and chili peppers (Volmaro et al., 1998; Liu et al., 2019), while the blue light response of cucumber seedlings resulted in longer hypocotyls, thus indicating some species-specificity (Hernández and Kubota, 2016). Longitudinal sections of the primary inflorescence stems of Arabidopsis plants showed a similar increase in cell size in the red LED condition and decrease in the blue LED



condition. This suggests that apical growth of *Arabidopsis* is promoted by red wavelengths and inhibited by blue wavelengths throughout its life cycle. While similar effects of red and blue light on the plant height of wheat and chili peppers have been reported, these studies did not include any genetic or cell biological analyses (Gangadhar et al., 2012; Monostori et al., 2018). In line with these findings, our mutant analysis suggested that the blue light receptors CRY1 and CRY2 inhibit respectively hypocotyl and inflorescence stem elongation. Also, CRY1 has been reported to inhibit epidermal cell elongation in *Arabidopsis* hypocotyls grown during thermomorphogenesis (Ma et al., 2015). The role of the red light photoreceptors appeared to be more diverse with PHYB and PHYC inhibiting apical growth and PHYD promoting hypocotyl and stem elongation. PHYB has been reported to inhibit epidermal cell elongation in hypocotyls (Allen et al., 2019), however, its role in inhibiting apical stem growth has until now been limited to plant height studies without further histological or microscopic analysis (Weller et al., 2000; Cortés et al., 2016). Moreover, no roles for PHYC and PHYD in apical cell elongation have yet been reported. Our results suggest that the enhanced plant height in monochromatic red light, is partially mediated by PHYD, but most likely results mainly from CRY inactivation. Reduced apical growth in monochromatic blue light relies heavily on CRY inhibition of stem and hypocotyl elongation, and partially on PHYD inactivation (**Figure 6D**). In tomato, apical growth responses to light quality seem to change as the plant ages. While red or blue wavelengths respectively promote or inhibit apical growth in seedlings and young plants, the growth responses turn opposite in older, flowering plants (Yang et al., 2018). We expect this to be a gradual change over time, and that our 30-day-old plants that had only just started to



Chapter 4: Light quality affects apical and primary radial growth

flower were undergoing that transition at the time of measurements, thus explaining the increased pith cell length in the blue LED condition. To summarise, we clearly showed that red and blue light affect apical growth through cell elongation, although cell division remains to be investigated. During cell elongation, loosening of the normally rigid cell wall is required, while turgor pressure inside the vacuole drives expansion (Kaiser and Scheuring, 2020). Because our microscopic analysis revealed long and flaccid cells in the red LED condition, we hypothesise that these cell walls are loose, allowing the cells to grow rapidly while water uptake lags behind. In contrast, the blue LED condition might cause extremely rigid cell walls, causing vacuolar pressure to build, thus resulting in the observed small and turgid cells. Therefore we suggest that light quality affects both auxin-dependent cell wall acidification for cell wall loosening, and auxin-mediated vacuolar osmosis to regulate apical growth (Fendrych et al., 2016; Scheuring et al., 2016).

Regulation of primary radial growth by light quality.

We also investigated if, and how, light quality affects radial growth. Cross sections of *Arabidopsis* and tomato hypocotyls revealed that primary radial growth was decreased in monochromatic red light, and increased in monochromatic blue light, when compared to white light. Microscopic analysis showed that in both *Arabidopsis* and tomato seedlings this phenotype relied on cell size, rather than cell division. Similar hypocotyl phenotypes were observed in radish (Samuoliene et al., 2011). Moreover, since we did not observe any secondary growth in *Arabidopsis* or tomato hypocotyls, we cannot exclude additional light responses during later stages of radial hypocotyl growth. The hypocotyl cross sections of both species showed small flaccid pith



cells in the red LED condition, and big, turgid pith cells in the blue LED condition, in line with our scanning electron microscopy observations of epidermis cells. This suggests that the effects of light quality on apical and primary radial growth are interconnected during the seedling stage. Members of the *ERECTA* receptor kinase family have been shown to inhibit radial hypocotyl growth, while promoting apical hypocotyl growth (Ikematsu et al., 2017; Qu et al., 2017), and thus may be key factors in this interconnection. Interestingly, the radial growth phenotypes of both *Arabidopsis* and tomato changed throughout their development. In the stems of 30-day-old tomato plants, the primary radial growth was completely indifferent to red or blue light. A possible explanation for this may be that, as described above for apical growth, plants were in a transitional state at the time of measurements. Perhaps older tomato plants will show light-induced changes in primary radial growth, or even in secondary growth. On the other hand, in **chapter 3** we observed a similar indifference of tomato leaf production and flowering to red or blue light, suggesting this may result from fundamental differences in plant architecture and life cycle between species. Although radial stem growth has been correlated to light intensity in several species (Feng et al., 2019; Chung et al., 2020; Hamedalla et al., 2022), the effect of light quality has yet to be studied in most species. In *Arabidopsis*, we observed that the radial growth phenotypes turned opposite throughout their life cycle. In reproductive *Arabidopsis* plants, stem thickness increased in monochromatic red light, and decreased in monochromatic blue light, when compared to white light. Since secondary xylem and phloem were not yet visible in any of the *Arabidopsis* stems, the differential stem thickness was caused by changes in primary radial growth such as pith cell size and number, primary xylem width, and the number



Chapter 4: Light quality affects apical and primary radial growth

of vascular bundles. This is consistent with a radial growth-promoting role of the red light photoreceptors PHYB and PHYD that was revealed by our mutant analysis (**Figure 6D**). Surprisingly, *cry* mutants also showed a reduced stem thickness, compared to wild-type seedlings, thus suggesting radial-growth promoting functions for these blue light photoreceptors as well. However, since *cry* stems were also significantly shorter in the red LED condition, we expect that these phenotypes are either not light-dependent at all, or that they require CRY interaction with phytochromes. In line with our observations, PHYB has been reported to promote radial stem growth in maize (Wies et al., 2019). Our histological analysis of Arabidopsis stems revealed changes in primary xylem width and in the number and size of pith cells in the different LED conditions, that correlated to the stem thickness. In addition, the changes in vascular bundle numbers correlated to more branching in monochromatic red light, and reduced branching in the blue LED condition (**chapter 3**). Therefore we hypothesise that light quality regulates primary radial growth both through auxin-mediated vascular patterning, lateral organ formation, and primary xylem differentiation (Baima et al., 2001; Fàbregas et al., 2015). To summarise, the use of LEDs opens up new possibilities to steer primary radial growth in young plants, but additional experiments in different species, and at different developmental stages are required. Moreover, the appearance of an interfascicular cambium in stems of Arabidopsis plants grown in red light, but not in stems of plants grown in white or blue light, suggests the possibility for light quality to steer secondary growth, in addition to primary radial growth, in older plants. For tomato, optimisation of the red : blue ratio might be required to obtain sturdy plants by enhancing primary radial growth and reducing apical growth. From **chapter 3** we know that this will not affect



plastochron nor flowering time, two other important traits during the initial growth phase of tomato plants.

Materials and Methods

Growth conditions and LED treatments.

In all experiments, plants were grown at a 16 h photoperiod, under white, deep red, or blue Philips Greenpower LED research modules (Signify B.V., Eindhoven, Netherlands) with a measured photon flux density of $120 \pm 10 \mu\text{mol m}^{-2} \text{s}^{-1}$ at the top of the canopy, a temperature of 21°C, and 70% relative humidity. The percentages of blue, green, red, and far-red wavelengths for the different LED modules are listed in **Table S1** of **chapter 3**. Experiments with the different LED treatments were performed simultaneously in the same growth chamber in separate compartments enclosed by white plastic screens with a proximal distance of 50 cm to the plants.

Plant lines and seed germination.

Arabidopsis thaliana (Arabidopsis) ecotypes Columbia (Col-0) and Landsberg *erecta* (Ler), and *Solanum lycopersicum* (tomato) cultivars Moneymaker (MM) and Foundation (FO) were used as wild-type accessions. All wild-type and mutant lines that were used have been described before and are listed in **Table S1**. All Arabidopsis mutants (T-DNA insertion lines in Col-0 background) were genotyped with the primers listed in **Table S2**. Arabidopsis seeds were sown on the soil surface and stratified for 5 days at 4°C in darkness before they were placed in white light to allow simultaneous germination



Chapter 4: Light quality affects apical and primary radial growth

(**Chapter 3, Figure S1A**). After one day in white light, the seeds were moved to the LED conditions. Tomato seeds were planted approximately 2 cm under the soil surface and placed directly in the LED conditions (**Chapter 3, Figure S1B**). The age of tomato plants was expressed in days after sowing (DAS), whereas the age of Arabidopsis plants was expressed in days after germination (DAG).

Imaging of hypocotyl epidermis.

Hypocotyls of 7-day-old Arabidopsis seedlings were cut directly below the transition zone and fixed in 2% paraformaldehyde (PFA) and 1% glutaraldehyde in 1x phosphate-buffered saline (PBS) solution for 2 hours at 21°C, and overnight at 4°C. Fixed hypocotyls were washed twice with 1x PBS and dehydrated in a graded acetone series (70%, 80%, 90%, 96% and 100%) under vacuum. Acetone suspensions were transferred to a Bal-Tec CDP030 critical point dryer where acetone was replaced by liquid carbon dioxide. Samples were fixed to stubs and sputter coated with gold using the SEM Coating unit 5100 (Polaron Equipment Ltd.). Gold was discharged by admitting pressurised argon in a low vacuum environment, and coated samples were kept under dry vacuum conditions. Samples were imaged with a JEOL SEM 6400 scanning electron microscope at magnifications of 25x, 80x, and 250x. Hypocotyls of 5-day-old tomato seedlings were cut directly below the transition zone and mounted onto a glass slide using 1% low melting point (LMP) agarose (#16520050, Thermo ScientificTM) and imaged with a Leica MZ16FA equipped with a Leica DFC420C camera.



Fixation and epon embedding of hypocotyls and stems.

Hypocotyls of 7-day-old *Arabidopsis* seedlings and 5-day-old tomato seedlings were cut directly below the transition zone using a razorblade (Wilkinson Sword) and fixed overnight in a 4% PFA in 1x PBS solution. Stems of *Arabidopsis* plants at 1 and 4 weeks after bolting were cut at the base of the main inflorescence using a razorblade and kept on ice. Stem segments of at least 1 cm in size were fixed in 4% PFA in 1x PBS for 2 hours at 21°C, and overnight at 4°C. Fixed hypocotyls and stems were washed twice with 1x PBS and dehydrated in a graded ethanol series (70%, 80%, 90%, 96% and 100%) under vacuum. After dehydration, the tissues were placed in propylene oxide and subsequently in a 1:1 propylene oxide: Epon mixture overnight. The Epon-drenched tissues were embedded in epoxy resin moulds that dried overnight at 60°C, and were stored at 21°C. At 45 DAS, tomato stems were cut directly below the third leaf using a razor blade. The stems were kept on ice until fixation in 4% PFA in 1x PBS for 2 hours at 21°C, and overnight at 4°C. The fixed stems were washed twice with 1x PBS and stored in 70% ethanol at 4°C.

Sectioning and imaging of hypocotyls and stems.

Epon-embedded hypocotyls and stems were trimmed and 3-4 µm sections were cut with a Leica RM2265 rotary microtome equipped with a glass knife. The sections were mounted on a glass slide and stained with filtered 0.01% aqueous toluidine blue. A droplet of Epon was placed on the stained sections and covered with a glass coverslip. For tomato stems, sectioning was performed using a razor blade (very thin free-hand sectioning). The sections were stained with 6% aqueous toluidine blue, washed with MilliQ water, and



Chapter 4: Light quality affects apical and primary radial growth

mounted on a glass slide without cover slip. All stem sections were imaged with a Leica MZ16FA equipped with a Leica DFC420C camera, and all hypocotyl sections were imaged with Zeiss Axioscope A1 equipped with a Zeiss AxioCam MRc5 camera.

Plant phenotyping.

To measure hypocotyl length, *Arabidopsis* and tomato seedlings were grown in the LED conditions and photographed at 7 DAG and 5 DAS, respectively. Plant height was measured with a tape-measure in *Arabidopsis* plants after termination of the primary inflorescence meristem. Microscopic images of longitudinal sections were used to measure pith cell length, whereas cross section images were used to measure the stem area and xylem width, and to count the number of vascular bundles. All image measurements were performed using ImageJ (Fiji) software (Schindelin et al., 2012).

Statistical analysis and figures.

All experiments were performed with two technical replicates of 15 or 20 biologically independent plants for tomato and *Arabidopsis*, respectively. Measurements under different LED conditions, or comparing different plant lines, were statistically analysed using a one-way ANOVA followed by a Tukey's honestly significant different (HSD) post hoc test and plotted into graphs using GraphPad Prism 5 software. In the graphs, the colours of the dots and lines indicate white, red, and blue LED conditions. Microscopic images were edited in ImageJ (Fiji). Schematic models were generated with BioRender software. Final figures were assembled using Microsoft PowerPoint.



Author contributions

KS and RO conceived and designed the experiments. KS and JvL performed the experiments. KS and GL performed the microscopic analysis, and KS performed the statistical analysis. KS and RO analysed the results and wrote the manuscript. All authors contributed to manuscript revision.

Funding

This work was part of the research program “LED it be 50%” with project number 14212, which is partly financed by the Dutch Research Council (NWO).

Acknowledgements

We would like to thank Nunhems Netherlands B.V. for providing us with seeds of their commercial hybrid line Foundation and Signify B.V. for providing the LED modules. We thank Merijn de Bakker for microtome instructions and Arezoo Rahimi for help with fresh sectioning.



References

- Allen, J. I., Guo, K., Zhang, D., Ince, M., and Jammes, F. (2019). ABA-glucose ester hydrolyzing enzyme ATBG1 and PHYB antagonistically regulate stomatal development. *PLoS One* 14, e0218605.
- Baima, S., Possenti, M., Matteucci, A., Wisman, E., Altamura, M. M., Ruberti, I., and Morelli, G. (2001). The Arabidopsis ATHB-8 HD-Zip protein acts as a differentiation-promoting transcription factor of the vascular meristems. *Plant Physiol.* 126, 643-655.
- Barra-Jiménez, A., and Ragni, L. (2017). Secondary development in the stem: when Arabidopsis and trees are closer than it seems. *Curr. Opin. Plant Biol.* 35, 145–151.
- Botterweg-Paredes, E., Blaakmeer, A., Hong, S. Y., Sun, B., Mineri, L., Kruusvee, V., Xie, Y., Straub, D., Ménard, D., Pesquet, E., and Wenkel S. (2020). Light affects tissue patterning of the hypocotyl in the shade-avoidance response. *PLoS Genet.* 16, e1008678.
- Chen, L., Huang, X.-X., Zhao, S.-M., Xiao, D.-W., Xiao, L.-T., Tong, J.-H., Wang, W. S., Li, Y., J., Ding, Z., and Hou, B. K. (2020). IPyA glucosylation mediates light and temperature signaling to regulate auxin-dependent hypocotyl elongation in Arabidopsis. *Proc. Natl. Acad. Sci. U. S. A.* 117, 6910-6917.
- Christians, M. J., Gingerich, D. J., Hua, Z., Lauer, T. D., and Vierstra, R. D. (2012). The light-response BTB1 and BTB2 proteins assemble nuclear ubiquitin ligases that modify phytochrome B and D signaling in Arabidopsis. *Plant Physiol.* 160, 118–134.
- Chung, G. J., Lee, J. H., and Oh, M. M. (2020). Growth and acclimation of in vitro-propagated ‘M9’ apple rootstock plantlets according to light intensity. *Hortic. Environ. Biotechnol.* 61, 501–510.
- Cortés, L. E., Weldegergis, B. T., Boccalandro, H. E., Dicke, M., and Ballaré, C. L. (2016). Trading direct for indirect defense? Phytochrome B inactivation in tomato attenuates direct anti-herbivore defenses whilst enhancing volatile-mediated attraction of predators. *New Phytol.* 212, 1057–1071.



- Davière, J. M., Wild, M., Regnault, T., Baumberger, N., Eisler, H., Genschik, P., and Achard, P.** (2014). Class I TCP-DELLA interactions in inflorescence shoot apex determine plant height. *Curr. Biol.* 24, 1923–1928.
- Dieleman, J. A., De Visser, P. H. B., Meinen, E., Grit, J. G., and Dueck, T. A.** (2019). Integrating morphological and physiological responses of tomato plants to light quality to the crop level by 3D modeling. *Front. Plant Sci.* 10, 1–12.
- Etchells, J. P., Provost, C. M., Mishr, L., and Turner, S. R.** (2013). WOX4 and WOX14 act downstream of the PXY receptor kinase to regulate plant vascular proliferation independently of any role in vascular organisation. *Development* 140, 2224–2234.
- Etchells, J. P., Smit, M. E., Gaudinier, A., Williams, C. J., and Brady, S. M.** (2016). A brief history of the TDIF-PXY signalling module: balancing meristem identity and differentiation during vascular development. *New Phytol.* 209, 474–484.
- Fàbregas, N., Formosa-Jordan, P., Confraria, A., Siligato, R., Alonso, J. M., Swarup, R., Bennet, M. J., Mähönen, A. P., Caño-Delgado, A. I., and Ibañes, M.** (2015). Auxin influx carriers control vascular patterning and xylem differentiation in *Arabidopsis thaliana*. *PLoS Genet.* 11, e1005183.
- Fendrych, M., Leung, J., and Friml, J.** (2016). TIR1/AFB-Aux/IAA auxin perception mediates rapid cell wall acidification and growth of *Arabidopsis* hypocotyls. *Elife* 5.
- Feng, L., Raza, M. A., Li, Z., Chen, Y., Khalid, M. H. Bin, Du, J., Liu, W., Wu, X., Song, C., Yu, L., Zhang, Z., Yuan, S., Yang, W., and Yang, F.** (2019). The influence of light intensity and leaf movement on photosynthesis characteristics and carbon balance of Soybean. *Front. Plant Sci.* 9, 1952.
- Gallego-Bartolomé, J., Minguet, E. G., Marín, J. A., Prat, S., Blázquez, M. A., and Alabadí, D.** (2010). Transcriptional diversification and functional conservation between DELLA proteins in *Arabidopsis*. *Mol. Biol. Evol.* 27, 1247–1256.
- Gangadhar, B. H., Mishra, R. K., Pandian, G., and Park, S. W.** (2012). Comparative study of color, pungency, and biochemical composition in chili



Chapter 4: Light quality affects apical and primary radial growth

pepper (*Capsicum annuum*) under different light-emitting diode treatments. *HortScience* 47, 1729–1735.

Gawronska, H., Yang, Y. Y., Furukawa, K., Kendrick, R. E., Takahashi, N., and Kamiya, Y. (1995). Effects of low irradiance stress on gibberellin levels in pea seedlings. *Plant Cell Physiol.* 36, 1361–1367.

Gendreau, E., Traas, J., Demos', T., Crandjeau, O., Caboche, M., and Hofte, H. (1997). Cellular basis of hypocotyl growth in *Arabidopsis thaliana*. *Plant Physiol.* 11, 295–305.

Guo, H., Yang, H., Mockler, T. C., and Lin, C. (1998). Regulation of flowering time by *Arabidopsis* photoreceptors. *Science* 279, 1360–1363.

Guo, M., Thomas, J., Collins, G., and Timmermans, M. C. P. (2008). Direct repression of KNOX loci by the ASYMMETRIC LEAVES1 complex of *Arabidopsis*. *Plant Cell* 20, 48–58.

Hamedalla, A. M., Ali, M. M., Ali, W. M., Ahmed, M. A. A., Kaseb, M. O., Kalaji, H. M., Gajc-Wolska, J., and Yousef, A. F. (2022). Increasing the performance of cucumber (*Cucumis sativus* L.) seedlings by LED illumination. *Sci. Reports* 12, 1–12.

Hernández, R., and Kubota, C. (2016). Physiological responses of cucumber seedlings under different blue and red photon flux ratios using LEDs. *Environ. Exp. Bot.* 121, 66–74.

Hisamatsu, T., King, R. W., Helliwell, C. A., and Koshioka, M. (2005). The involvement of gibberellin 20-oxidase genes in phytochrome-regulated petiole elongation of *Arabidopsis*. *Plant Physiol.* 138, 1106–1116.

Ikematsu, S., Tasaka, M., Torii, K. U., and Uchida, N. (2017). ERECTA-family receptor kinase genes redundantly prevent premature progression of secondary growth in the *Arabidopsis* hypocotyl. *New Phytol.* 213, 1697–1709.

Kaiser, S., and Scheuring, D. (2020). To lead or to follow: Contribution of the plant vacuole to cell growth. *Front. Plant Sci.* 11, 553.

Koncz, C., Chua*, N.-H., Schell, J., and Rédei, G. P. (1992). A heuristic glance at the past of *Arabidopsis* genetics. *Methods Arab. Res.* 1–15.



- Kubo, M., Udagawa, M., Nishikubo, N., Horiguchi, G., Yamaguchi, M., Ito, J., Mimura, T., Fukuda, H., and Demura, T.** (2005). Transcription switches for protoxylem and metaxylem vessel formation. *Genes Dev.* 19, 1855–1860.
- Li-Li, C., Zhang, K., Gong, X.-C., Wang, H.-Y., You-Hui, G., Wang, X.-Q., Zeng, Z. H., and Hu, Y. G.** (2020). Effects of different LEDs light spectrum on the growth, leaf anatomy, and chloroplast ultrastructure of potato plantlets in vitro and minituber production after transplanting in the greenhouse. *J. Integr. Agric.* 2020, 108–119.
- Liu, N., Ji, F., Xu, L., and He, D.** (2019). Effects of LED light quality on the growth of pepper seedling in plant factory. *Int. J. Agric. Biol. Eng.* 12, 44–50.
- Ma, D., Li, X., Guo, Y., Chu, J., Fang, S., Yan, C., Noel, J. P., and Liu, H.** (2016). Cryptochrome 1 interacts with PIF4 to regulate high temperature-mediated hypocotyl elongation in response to blue light. *Proc. Natl. Acad. Sci. U. S. A.* 113, 224–229.
- MacMillan, C. P., O'Donnell, P. J., Smit, A. M., Evans, R., Stachurski, Z. H., Torr, K., West, M., Baltunis, J., and Strabala, T. J.** (2013). A survey of the natural variation in biomechanical and cell wall properties in inflorescence stems reveals new insights into the utility of *Arabidopsis* as a wood model. *Funct. Plant Biol.* 40, 662–676.
- Mayfield, J. D., Folta, K. M., Paul, A. L., and Ferl, R. J.** (2007). The 14-3-3 proteins μ and ν influence transition to flowering and early phytochrome response. *Plant Physiol.* 145, 1692–1702.
- McElver, J., Tzafrir, I., Aux, G., Rogers, R., Ashby, C., Smith, K., Thomas, C., Schetter, A., Zhou, Q., Cushman, M. A., Tossberg, J., Nickle, T., Levin, J. Z., Law, M., Meinke, D., and Patton, D.** (2001). Insertional mutagenesis of genes required for seed development in *Arabidopsis thaliana*. *Genetics* 159, 1751–1763.
- Monostori, I., Heilmann, M., Kocsy, G., Rakszegi, M., Ahres, M., Altenbach, S. B., Szalai, G., Pál, M., Toldi, D., Simon-Sarkadi, L., Harnos, N., Galiba, G., and Darko, E.** (2018). LED lighting – modification of growth, metabolism, yield and flour composition in wheat by spectral quality and intensity. *Front. Plant Sci.* 9, 1–16.



Chapter 4: Light quality affects apical and primary radial growth

- Monte, E., Alonso, J. M., Ecker, J. R., Zhang, Y., Li, X., Young, J., Austin-Phillips, S., and Quail, P. H.** (2003). Isolation and characterization of phyC mutants in *Arabidopsis* reveals complex crosstalk between phytochrome signaling pathways. *Plant Cell* 15, 1962–1980.
- Oh, E., Yamaguchi, S., Hu, J., Yusuke, J., Jung, B., Paik, I., Lee, H. S., Sun, T. P., Kamiya, Y., and Choi, G.** (2007). PIL5, a phytochrome-interacting bHLH protein, regulates gibberellin responsiveness by binding directly to the GAI and RGA promoters in *Arabidopsis* seeds. *Plant Cell* 19, 1192–1208.
- Paradiso, R., and Proietti, S.** (2021). Light-quality manipulation to control plant growth and photomorphogenesis in greenhouse horticulture: the state of the art and the opportunities of modern LED systems. *J. Plant Growth Regul.* 41, 742–780.
- Qu, X., Zhao, Z., and Tian, Z.** (2017). ERECTA regulates cell elongation by activating auxin biosynthesis in *Arabidopsis thaliana*. *Front. Plant Sci.* 8, 1688.
- Ross, J. J., O'Neill, D. P., and Rathbone, D. A.** (2003). Auxin-gibberellin interactions in pea: integrating the old with the new. *J. Plant Growth Regul.* 22, 99–108.
- Ruckle, M. E., DeMarco, S. M., and Larkin, R. M.** (2007). Plastid signals remodel light signaling networks and are essential for efficient chloroplast biogenesis in *Arabidopsis*. *Plant Cell* 19, 3944–3960.
- Sachs, R. M.** (1965). Stem Elongation. *Annu. Rev. Plant Physiol.* 16, 73–96.
- Samuoliene, G., Sirtautas, R., Brazaityte, A., Sakalauskaite, J., Sakalauskiene, S., and Duchovskis, P.** (2011). The impact of red and blue light-emitting diode illumination on radish physiological indices. *Cent. Eur. J. Biol.* 6, 821–828.
- Scheuring, D., Löffke, C., Krüger, F., Kittelmann, M., Eisa, A., Hughes, L., Smith, R. S., Hawes, C., Schumacher, K., Kleine-Vehn, J.** (2016). Actin-dependent vacuolar occupancy of the cell determines auxin-induced growth repression. *Proc. Natl. Acad. Sci. U. S. A.* 113, 452–457.
- Schindelin, J., Arganda-Carreras, I., Frise, E., Kaynig, V., Longair, M., Pietzsch, T., Preibish, S., Rueden, C., Saalfeld, S., Schmid, B., Tinevez, J. Y., White,**



- D. J., Hartenstein, V., Eliceiri, K., Tomancak, P., and Cardona, A.** (2012). Fiji: An open-source platform for biological-image analysis. *Nat. Methods* 9, 676–682.
- Seo, M., Hanada, A., Kuwahara, A., Endo, A., Okamoto, M., Yamauchi, Y., North, H., Marion-Poll, A., Sun, T. P., Koshiba, T., Kamiya, Y., Yamguchi, S., and Nambara, E.** (2006). Regulation of hormone metabolism in Arabidopsis seeds: phytochrome regulation of abscisic acid metabolism and abscisic acid regulation of gibberellin metabolism. *Plant J.* 48, 354–366.
- Suer, S., Agusti, J., Sanchez, P., Schwarz, M., and Greb, T.** (2011). WOX4 imparts auxin responsiveness to cambium cells in Arabidopsis. *Plant Cell* 23, 3247–3259.
- Volmaro, C., Pontin, M., Luna, V., Baraldi, R., and Bottini, R.** (1998). Blue light control of hypocotyl elongation in etiolated seedlings of *Lactuca sativa* (L.) cv. Grand Rapids related to exogenous growth regulators and endogenous IAA, GA3 and abscisic acid. *Plant Growth Regul.* 26, 165–173.
- Warnasooriya, S. N., Porter, K. J., and Montgomery, B. L.** (2011). Tissue- and isoform-specific phytochrome regulation of light-dependent anthocyanin accumulation in *Arabidopsis thaliana*. *Plant Signal. Behav.* 6, 624–631.
- Weller, J. L., Schreuder, M. E. L., Smith, H., Koornneef, M., and Kendrick, R. E.** (2000). Physiological interactions of phytochromes A, B1 and B2 in the control of development in tomato. *Plant J.* 24, 345–356.
- Wies, G., Mantese, A. I., Casal, J. J., and Maddonni, G. Á.** (2019). Phytochrome B enhances plant growth, biomass and grain yield in field-grown maize. *Ann. Bot.* 123, 1079–1088.
- Yang, X., Xu, H., Shao, L., Li, T., Wang, Y., and Wang, R.** (2018). Response of photosynthetic capacity of tomato leaves to different LED light wavelength. *Environ. Exp. Bot.* 150, 161–171.
- Yordanov, Y. S., Regan, S., and Busov, V.** (2010). Members of the LATERAL ORGAN BOUNDARIES DOMAIN transcription factor family are involved in the regulation of secondary growth in *Populus*. *Plant Cell* 22, 3662–3677.



Chapter 4: Light quality affects apical and primary radial growth

Zheng, L., He, H., and Song, W. (2019). Application of light-emitting diodes and the effect of light quality on horticultural crops: A review. *HortSci.* 54, 1656-1661.



Supplementary Material (Tables S1-S2 and Figure S1)

Table S1: Plant lines used in this study.

Arabidopsis and tomato seeds were obtained from Nottingham Arabidopsis Stock Centre (NASC), or a kind gift from Nunhems Netherlands BV.

PLANT LINE	DESCRIPTION	SOURCE	REFERENCE
Columbia (Col-0)	Natural Arabidopsis accession	NASC	-
Landsberg <i>erecta</i> (Ler)	Natural Arabidopsis accession	NASC	-
Moneymaker (MM)	Non-hybrid tomato cultivar	Nunhems BV	-
Foundation (FO)	Hybrid tomato cultivar	Nunhems BV	-
<i>phyA</i> (SALK_014575)	T-DNA insertion in At1g09570	NASC	Ruckle et al., 2007
<i>phyB</i> (SALK_022035)	T-DNA insertion in At2g18790	NASC	Mayfield et al., 2007
<i>phyC</i> (<i>phyC</i> -3)	3 kbp deletion in At5g35840	NASC	Monte et al., 2003
<i>phyD</i> (SALK_027956)	T-DNA insertion in At4g16250	NASC	Christians et al., 2012
<i>phyE</i> (SALK_092529)	T-DNA insertion in At4g18130	NASC	Warnasooriya et al., 2011
<i>cry1</i> (SALK_069292)	T-DNA insertion in At4g08920	NASC	Ruckle et al., 2007
<i>cry2</i> (<i>cry2</i> -1)	2 kbp deletion in At1g04400	NASC	Guo et al., 1998
<i>phot1</i> (SAIL_1232_C01)	T-DNA insertion in At3g45780	NASC	McElver et al., 2001
<i>phot2</i> (SALK_142275)	T-DNA insertion in At5g58140	NASC	Ruckle et al., 2007



Chapter 4: Light quality affects apical and primary radial growth

Table S2: Primers used in this study.

For genotyping of SAIL and SALK T-DNA insertion lines, gene-specific primers were combined with the LB1 or the LBb1.3 forward primer, respectively.

PRIMER NAME	TARGET GENE	SEQUENCE 5' → 3'	EXPERIMENT
LB1	N/A	GCCTTTTCAGAAATGGATAAATA	Genotyping
LBb1.3	N/A	ATTTTGCCGATTTTCGGAAC	Genotyping
<i>phyA</i> FW	At1g09570	CCAGTCAGCTCAGCAATTTTC	Genotyping
<i>phyA</i> RV	At1g09570	AATGCAAAACATGCTAGGGTG	Genotyping
<i>phyB</i> FW	At2g18790	CATCATCAGCATCATGTCACC	Genotyping
<i>phyB</i> RV	At2g18790	TTCACGAAGGCAAAAGAGTTG	Genotyping
<i>phyC</i> FW	At5g35840	ATGTCATCGAACACTTCACG	Genotyping
<i>phyC</i> RV	At5g35840	TCAAATCAAGGGAAATTCTG	Genotyping
<i>phyD</i> FW	At4g16250	AACCCGGTAGAATCAGAATGG	Genotyping
<i>phyD</i> RV	At4g16250	ATCGGTTACAGTGAAAATGCG	Genotyping
<i>phyE</i> FW	At4g18130	AAAGAGGCGGTCTAGTTCAGC	Genotyping
<i>phyE</i> RV	At4g18130	TATCAGTGGTAAACCCGTCG	Genotyping
<i>cry1</i> FW	At4g08920	TTCATGCCACTTGGTTAGACC	Genotyping
<i>cry1</i> RV	At4g08920	TCCCGACAGACTGGATACATC	Genotyping
<i>cry2</i> FW	At1g04400	ATGAAGATGGACAAAAAGAC	Genotyping
<i>cry2</i> RV	At1g04400	TCATTTGCAACCATTTTTTC	Genotyping
<i>phot1</i> FW	At3g45780	ACATAGGATGCAGCAGAAACG	Genotyping
<i>phot1</i> RV	At3g45780	CAGTAGACTGGTGGGCTCTTG	Genotyping
<i>phot2</i> FW	At5g58140	TCCATCTCCTTTGAATGATGC	Genotyping
<i>phot2</i> RV	At5g58140	AGTGTCATTGCTCACGGATTC	Genotyping

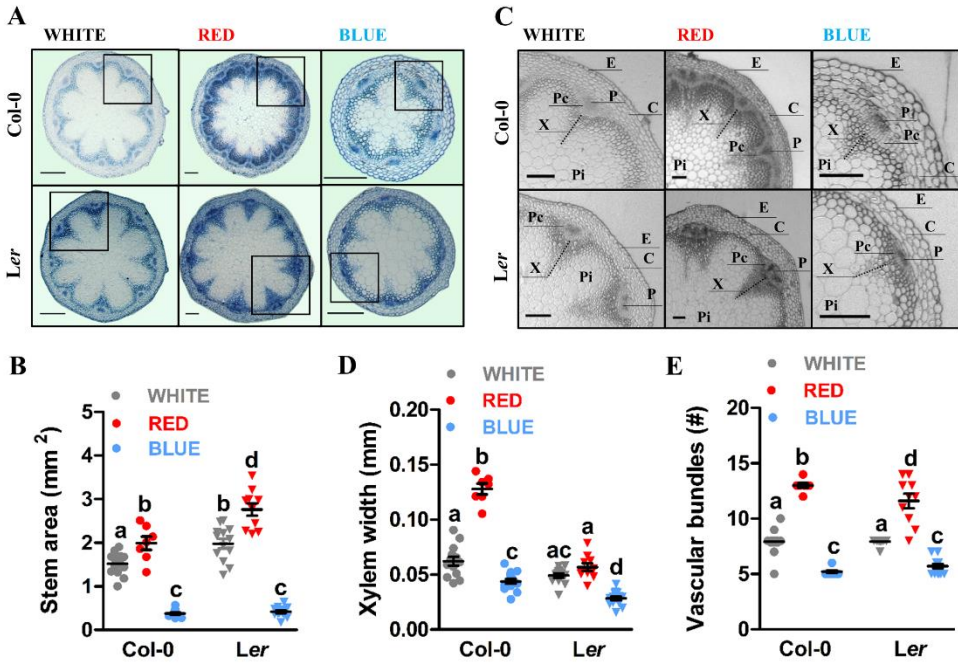


Figure S1: Light quality affects primary radial growth of Arabidopsis stems already at 1 week after bolting.

A. Stereomicroscopy images of toluidine blue stained cross sections from the most basal internode of the primary inflorescence of Arabidopsis plants (ecotypes Columbia (Col-0) and Landsberg *erecta* (Ler)) grown in white, red, or blue LED conditions. Stem segments were harvested at 1 week after bolting. **B.** Dot plot presenting the surface area of Col-0 and Ler stem cross sections in square millimetres (mm²). **C.** 2x digital magnification of the boxed areas in **A** to show the vascular bundles in more detail (E=epidermis, C=cortex, P=phloem, Pc=procambium, X=xylem, and Pi=pith). Several magnifications were reoriented for easy comparison. **D.** The width (in mm) of the primary xylem tissue in Col-0 and Ler stems. Each dot represents the average of three measurements within one stem. **E.** The number of vascular bundles in Col-0 and Ler stems. Scale bars indicate 200 μ m in **A** and 100 μ m in **C**. LED conditions and ecotypes were compared using a one-way ANOVA followed by a Tukey's test (letters **a**, **b**, **c**, and **d** indicate statistically significant differences, $p < 0.05$) in **B**, **D** and **E**. Error bars represent standard error from mean ($n=15$) in **B**, **D** and **E**. Similar results were obtained from two independent experiments.



Chapter 5

Light quality regulates flowering through the photoperiodic and age pathways.

Kiki Spaninks¹ and Remko Offringa¹

¹Plant Developmental Genetics, Institute of Biology Leiden,
Leiden University, Sylviusweg 72, 2333 BE, Leiden, Netherlands.



Abstract

For leafy horticultural crops, such as lettuce and cabbage, delayed flowering is essential for quality crop production, whereas breeders require early flowering to speed up seed production cycles and breeding programs. Environmental cues such as temperature, photoperiod, or light quality have been used to control flowering time and especially the currently available LED technology allows accurate spectral quality control. Although previous LED studies have shown that many phenotypic traits of different plant species can be modulated by light quality, most of their underlying molecular mechanisms remain unknown, which makes their application on other crop species unpredictable. Here, we combined genetic studies of flowering pathways in the long-day model dicot *Arabidopsis thaliana* (Arabidopsis), with physiological experiments in long-day and day-neutral *Lactuca sativa* (lettuce) and *Solanum lycopersicum* (tomato) plants. Using LEDs, we confirmed that blue light must be present in the spectrum to activate the photoperiodic pathway to promote flowering in the long-day plant species. In addition, we identified a new flowering-inhibiting role for red light in the spectrum that represses the age pathway in long-day and (some) day-neutral plant species. We identified PHYB as an inhibitor of plant ageing through its activation of *microRNA156*, which represses the flower-promoting SQUAMOSA-PROMOTER BINDING PROTEIN-LIKE (SPL) transcription factors. Our findings identify a molecular pathway that integrates plant ageing and light quality in Arabidopsis, and that may be conserved in important crop species.



Keywords: Flowering, Photoperiod, Ageing, PHYB, miR156, SPLs, GIGANTEA

Introduction

Various environmental factors, such as light, temperature and stress determine the timing of the floral transition, and thus offer potential control over the plant life cycle (Thomas, 2006; Cho et al., 2017). In horticulture, environmental control of flowering would be useful to speed up production cycles for important crops such as tomato (*Solanum lycopersicum*). Moreover, plant breeding programs would greatly benefit from floral induction in response to changing environmental cues, especially in plants species that have been bred towards late flowering, such as lettuce (*Lactuca sativa*). Because of their possibility for spectral quality control, LEDs may be used to steer plant development towards early or late flowering (Morrow, 2008; SharathKumar et al., 2020). To achieve this, we must elucidate the molecular mechanisms that underly the flowering response to light quality and explore how these mechanisms are conserved in different plant species. The effect of light quality on flowering has been extensively studied with the use of photoreceptor mutants in the genetic model dicot *Arabidopsis thaliana* (Arabidopsis). In Arabidopsis, diurnal accumulation of the blue light photoreceptor *FLAVIN-BINDING, KELCH REPEAT, F-BOX 1* (FKF1) and the nuclear protein *GIGANTEA* (GI) coincides during long day photoperiods. FKF1, through interaction with its two other blue light-activated family members *ZEITLUPE* (ZTL) and *LOV KELCH PROTEIN 2* (LKP2), associates with GI to inhibit



Chapter 5: Light quality regulates flowering

expression of *CYCLING DOF FACTORs* (CDFs) that repress expression of *CONSTANS* (*CO*) (Sawa et al., 2007; Fornara et al., 2009). In addition, *CO* transcription is promoted by the blue light receptor cryptochrome 2 (*CRY2*) and the FR-activated phytochrome A (*PHYA*) (Valverde et al., 2004; Liu et al., 2008). As a result, *CO* levels rise and peak during the late afternoon, which subsequently results in elevated expression of *FLOWERING LOCUS T* (*FT*) at the end of the day (Samach et al., 2000). Finally, this *FT* peak promotes flowering through activation of floral meristem identity genes such as *APETALA 1* (*API*) and *FRUITFULL* (*FUL*) (Abe et al., 2005; Wigge et al., 2005). In contrast to blue and FR light-inducible photoreceptors, the red light-activated phytochrome B (*PHYB*) inhibits flowering through targeted degradation of *CO* (Valverde et al., 2004; Lazaro et al., 2015), and possibly through inhibition of *GI*, an interaction opposite to *PHYB* function during hypocotyl elongation (Huq et al., 2000). Although photoreceptor studies in *Arabidopsis* have contributed greatly to the understanding of photoperiodic flowering, light quality studies using LEDs, where the activity of all photoreceptors are influenced simultaneously, remain limited. Moreover, light quality responses should be investigated in different long-day (LD), short-day (SD) and day-neutral (DN) species. As a main integrator of circadian clock components and light signalling, homologs of *CO* have been identified in both LD and SD species (Robert et al., 1998; Yano et al., 2000; Campoli et al., 2012; Yang et al., 2014), suggesting that the photoperiodic pathway is the main light-regulated flowering pathway. However, this would also suggest that flowering of DN species is either indifferent to light quality, which is in line with our previous study in tomato (**chapter 3**), or that light quality regulates flowering through other pathways as well. In addition to the photoperiodic pathway, the



floral transition depends on four other pathways: vernalization, gibberellic acid (GA), autonomous regulation, and plant ageing (Teotia and Tang, 2015). Although studies concerning the effect of light quality on these other pathways remain limited, there is some evidence for light-regulated flowering that is photoperiod-independent. For example, *Arabidopsis phyB* mutant plants show early flowering compared to wild type, both under LD and SD photoperiods (Reed et al., 1993), thus indicating an additional photoperiod-independent role for PHYB in flowering. Moreover, diurnal expression levels of *CO* and *FT* are similar in *phyB* and wild-type plants, suggesting once more that PHYB may act independent of photoperiod. Although PHYB modulates responsiveness to GA during hypocotyl elongation, PHYB-dependent flowering has been shown to be GA-independent (Blázquez and Weigel, 1999). However, two recent shade avoidance studies show that downstream signalling targets of PHYA, and possibly of PHYB, modulate plant ageing. Under low R:FR ratios, *microRNA156* (*miR156*) is repressed, which alleviates its inhibitory effect on the expression of SQUAMOSA-PROMOTER BINDING PROTEIN-LIKE (SPL) transcription factors (Xie et al., 2017, 2020). Subsequently, SPLs directly enhance expression of the floral integrators *SUPPRESSOR OF OVEREXPRESSION OF CONSTANS 1* (*SOC1*) and *FT*, or indirectly through elevation of *microRNA172* (*miR172*) levels that inhibit *APETALA 2* (*AP2*)-like repressors of flowering (Zheng et al., 2019). Although the shade avoidance studies suggest a putative role for (F)R light in the regulation of flowering through the age pathway, the photoreceptors that are involved, and the underlying molecular mechanisms remain to be clarified. Moreover, LED studies are required to confirm if plant ageing can be regulated by light quality, and if this pathway can be exploited towards preferred flowering phenotypes.



Chapter 5: Light quality regulates flowering

As a follow-up of our experiments in **chapter 3**, we used LEDs to study the timing of the floral transition by changes in light quality in Arabidopsis, tomato, and lettuce plants. Treatment with monochromatic red light resulted in late flowering in LD Arabidopsis and lettuce plants, but not in DN tomato and lettuce plants. Moreover, Arabidopsis plants grown in the red LED condition failed to establish *CO* and *FT* peaks at the end of the day, which confirmed that blue light must be present in the spectrum to activate the photoperiodic pathway in this species. In contrast, treatment with monochromatic blue light caused early flowering in LD plant species, as well as in a DN lettuce accession. Expression analysis of *GI*, *miR156*, *miR172*, *SPLs*, *FT* and *SOC1* revealed that early flowering in the blue LED condition resulted in part from a lack of PHYB-dependent inhibition of the age pathway. In conclusion, we showed that the age pathway is repressed by the presence of red light in the spectrum, thereby revealing a long sought-after photoperiod-independent function for PHYB in the inhibition of flowering.

Results

Shoot development is greatly influenced by red and blue light in Arabidopsis, but not in tomato.

In **chapter 3** we observed that Arabidopsis development is greatly influenced by light quality. Although many traits were influenced by red or blue light, the most intriguing phenotype was observed in the shoot of Arabidopsis plants. To follow up, we performed weekly imaging of Arabidopsis plants grown in

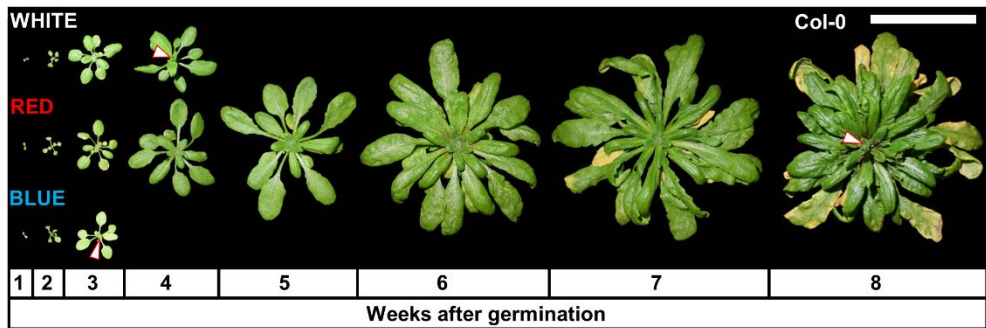


Figure 1: Arabidopsis shoot development is greatly influenced by red and blue light.

Representative Arabidopsis plants of ecotype Columbia (Col-0) that were grown in white, red, or blue LED conditions. Plants were photographed every week from 7 days after germination until bolting. For presentation purposes, rosettes were object selected and copy/pasted on a black background using ImageJ (Fiji) software. White arrowheads indicate the first visible flower buds. The scale bar indicates 5 cm. Similar results were obtained in three independent experiments.












white, red, or blue LED conditions (**Figure 1**). In white LED light, rosette leaf numbers (14 ± 0.3) and flowering time (24 ± 0.5 days) resembled development of Arabidopsis plants grown under regular fluorescent tube lighting systems (**Figure 1 (top panel), Figure 2A**). Plants that were grown in monochromatic red light developed large rosettes (42 ± 0.4 leaves) and flowered extremely late (48 ± 0.7 days), resembling Arabidopsis development under SD conditions in white light (**Figure 1 (middle panel), Figure 2A**). In contrast, treatment with monochromatic blue light resulted in small rosettes ($5-6 \pm 0.1$ leaves) and very early flowering (15 ± 0.4 days) (**Figure 1 (bottom panel), Figure 2A**). Treatment with monochromatic red light resulted in a remarkable decrease in plastochron (flowering time divided by the total number of rosette leaves: 1.1



Chapter 5: Light quality regulates flowering

Table 1: Arabidopsis leaf heteroblasty is altered in monochromatic blue light.

Leaf morphology, length/width (L/W) ratio (\pm SE, $n=10$) of the leaf blades, and appearance of abaxial trichomes of *Arabidopsis Columbia* (Col-0) plants that were grown in white, red, or blue LED conditions. For presentation purposes, leaf images were changed into black and white images using ImageJ (Fiji) software. Monochromatic LED conditions (red or blue) were compared to white (control) using a two-sided Student's *t*-test (asterisks indicate significant differences * $p<0.05$). Similar results were obtained in two independent experiments.

LED CONDITION	TRAIT	LEAF #1	LEAF #3	LEAF #5	LEAF #7
WHITE	Morphology				
	L/W ratio	1.14 \pm 0.01	1.25 \pm 0.03	1.54 \pm 0.04	1.76 \pm 0.05
	Abaxial trichomes	No	No	No	Yes
RED	Morphology				
	L/W ratio	1.10 \pm 0.01	1.23 \pm 0.04	1.51 \pm 0.05	1.75 \pm 0.05
	Abaxial trichomes	No	No	No	Yes
BLUE	Morphology				N/A
	L/W ratio	*1.21 \pm 0.01	*1.38 \pm 0.04	*1.89 \pm 0.05	N/A
	Abaxial trichomes	No	No	No	N/A

days) compared to white light (1.8 days), whereas plastochron was significantly increased in monochromatic blue light (2.8 days) (**Figure 2B**). Confocal imaging of shoot apices of *Arabidopsis pDR5::GFP* plants showed that, compared to white light, the shoot apex was significantly enlarged in the red LED condition, and significantly reduced in the blue LED condition (**Figure 2C, D**). Moreover, in the blue LED condition, the relative *pDR5::GFP* signal in the shoot meristem was significantly reduced compared to white and red LED conditions (**Figure 2E**). Leaf blade measurements revealed that



rosette leaves of plants grown in monochromatic blue light had a significantly higher length/width ratio, when compared to white or red LED conditions (**Table 1**), suggesting early vegetative phase change (VPC). However, no abaxial trichomes were present on rosette leaves of plants grown in monochromatic blue light (**Table 1**), whereas in the white and red LED conditions they were indicative of VPC around leaf number 6 or 7. Interestingly, we did not observe any differences in tomato compound leaf numbers, plastochron, shoot meristem size, or *pDR5::YFP* signals between the LED conditions (**Figure S1**). In summary, this data implied that red and blue light have an antagonistic effect on leaf initiation and growth of *Arabidopsis*, but not of tomato plants.

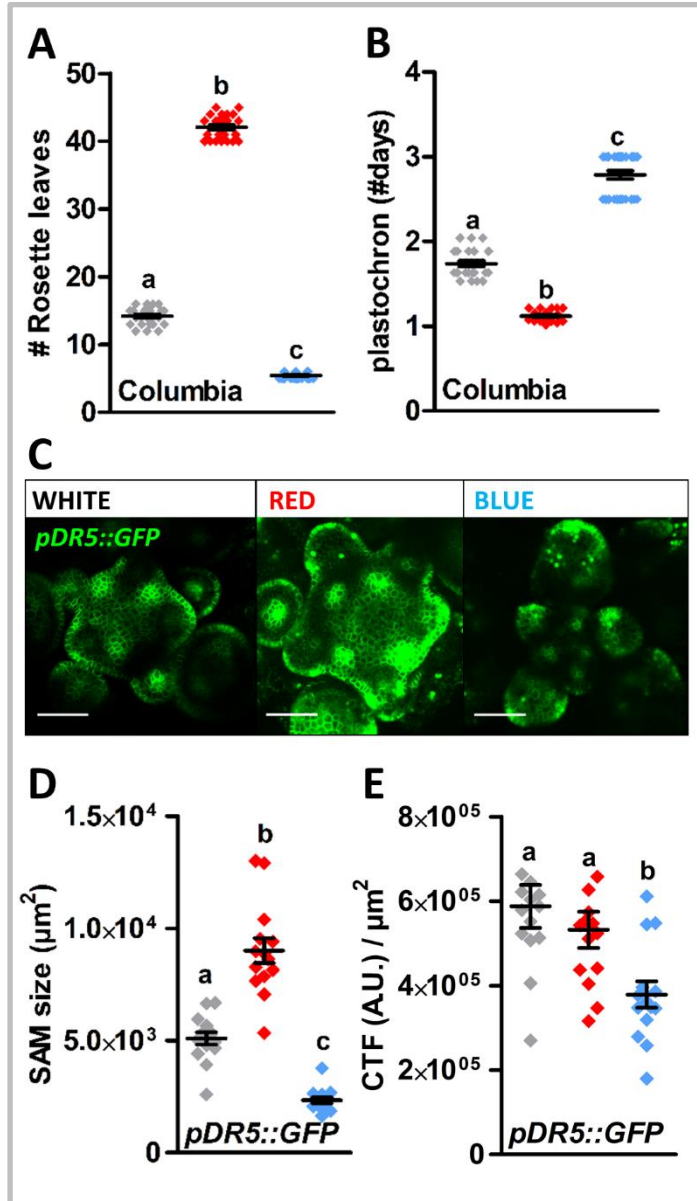
Late flowering in monochromatic red light is caused by inactivation of the photoperiodic pathway.

Because we previously observed that light quality affects flowering of LD *Arabidopsis* plants, but not of DN tomato plants (**chapter 3**), we next investigated the key photoreceptors involved in the photoperiodic pathway: the Zeitlupe family. Analysis of *Arabidopsis ztl*, *fkf1*, and *lkp* mutants showed a significant delay in flowering of the mutants compared to wild-type plants in both white and blue LED conditions. In monochromatic red light, flowering time of the mutants was similar to that of wild-type plants, confirming that the presence of blue light in the spectrum, perceived by the ZTL family of photoreceptors, is required to promote flowering (**Figure 3A**). Next, we investigated the diurnal expression patterns of *GI*, *CO*, and *FT* in 14-day-old wild-type *Arabidopsis* plants grown in the different LED conditions. In white light, expression of *GI* peaked around Zeitgeber time (ZT) 9, which induced



Chapter 5: Light quality regulates flowering

CO peaks around ZT12 and ZT18. Subsequently, the presence of a *CO* peak at the end of the day promoted *FT* expression around ZT15 (**Figures 3B-D**). In monochromatic red light, the *GI* peak was significantly reduced compared to white light (**Figure 3B**). As a likely result of this, plants grown in the red LED condition failed to establish the *CO* peaks that would induce *FT* expression (**Figures 3C, D**). This explains why LD Arabidopsis plants, that were grown in monochromatic red light, develop similar to SD grown plants. In monochromatic blue light, peaks in *GI* and *CO* expression occurred simultaneously with, but were significantly higher than, those of white light-grown plants (**Figures 3B, C**). *FT*





expression levels were significantly higher at all time points in blue LED conditions. In addition, the *FT* expression levels peaked throughout a longer period of time (**Figure 3D**), hence the extremely early flowering. To investigate if photoperiod-sensitivity is required for regulation of the floral

Figure 2: Red and blue light act antagonistically on organ formation at the shoot apical meristem in Arabidopsis.

A. Rosette leaf number until flowering of Arabidopsis Columbia (Col-0) plants grown in white, red, or blue LED conditions. **B.** Plastochron length (number of rosette leaves divided by the days until flowering) of Col-0 plants grown in the different LED conditions. **C.** Confocal images of representative shoot apices of Arabidopsis *pDR5::GFP* plants grown in the different LED conditions. **D.** Shoot apical meristem (SAM) surface area (in μm^2) of Arabidopsis *pDR5::GFP* plants grown in the different LED conditions. **E.** Corrected Total Fluorescence (CTF) of the *pDR5::GFP* signal in Arbitrary Units (A.U.) in shoot apices of Arabidopsis plants grown in the different LED conditions. Graph colours represent white, red, or blue LED conditions in **A**, **B**, **D** and **E**. Scale bars indicate 50 μm in **C**. LED conditions were compared using a one-way ANOVA followed by a Tukey's test (letters **a**, **b**, and **c** indicate statistically significant differences, $p < 0.05$) in **A**, **B**, **D** and **E**. Error bars represent standard error from mean in **A**, **B**, **D** and **E**. Similar results were obtained in two independent experiments.

transition by red or blue light, we compared the development of LD Arabidopsis and DN tomato plants to two lettuce accessions with different photoperiod-sensitivities: Meikoningin (LD) and Gaardenier (DN) (**Figure S2**). In LD lettuce plants, we observed early flowering in monochromatic blue light, and late flowering in monochromatic red light (**Figures 4A, B**).

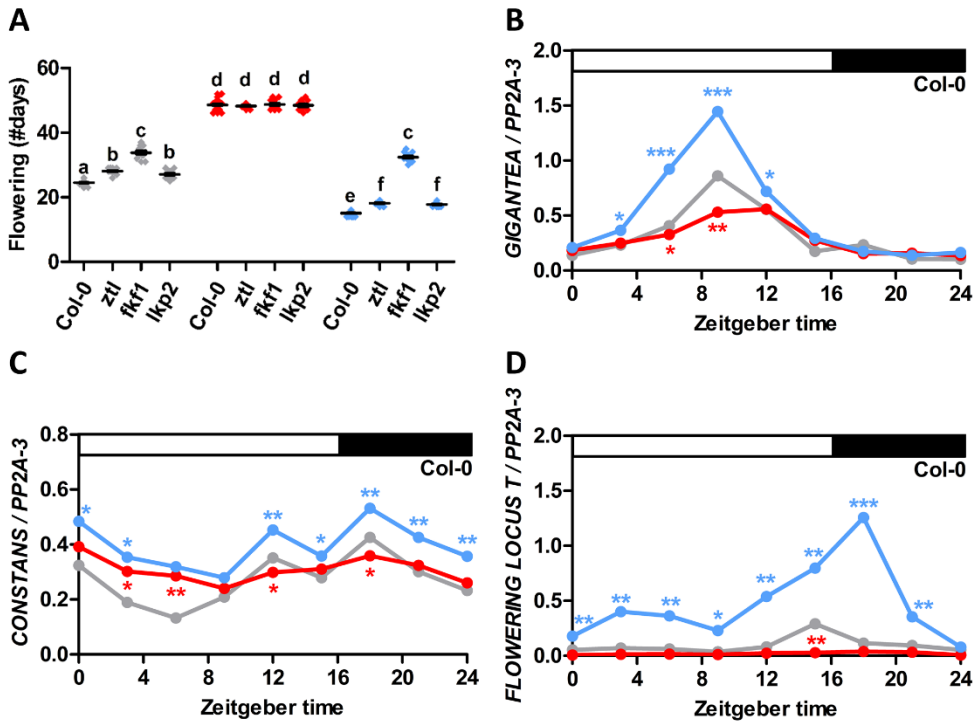


Figure 3: The Arabidopsis photoperiodic pathway is inactive in spectra that lack blue light.

A. Flowering time of Arabidopsis Columbia (Col-0) and photoreceptor mutants *ztl*, *fkl1* and *lkp2* grown in white, red, or blue LED conditions. **B-D.** Diurnal gene expression patterns of *GIGANTEA* (**B**), *CONSTANS* (**C**) and *FLOWERING LOCUS T* (**D**) in 14-day-old wild-type Arabidopsis plants that were grown in white, red, or blue LED conditions. Graph colours represent the different LED conditions. LED conditions and wild types or mutants were compared using a one-way ANOVA followed by a Tukey's test (letters **a**, **b**, **c**, **d**, **e**, and **f** indicate statistically significant differences, $p < 0.05$) in **A**. In **B-D**, monochromatic LED conditions (red or blue) were compared to white (control) using a two-sided Student's *t*-test (asterisks indicate significant differences at a specific time point (** $p < 0.01$, *** $p < 0.001$, * $p < 0.05$)). For presentation purposes, not all time points that were significantly different between white and red LED conditions (**Table S3**) were labelled with asterisks in **D**. Error bars represent standard error from mean in **A** ($n = 30$), standard errors and *p*-values for **B-D** are listed in **Table S3**. Similar results were obtained in three independent experiments.

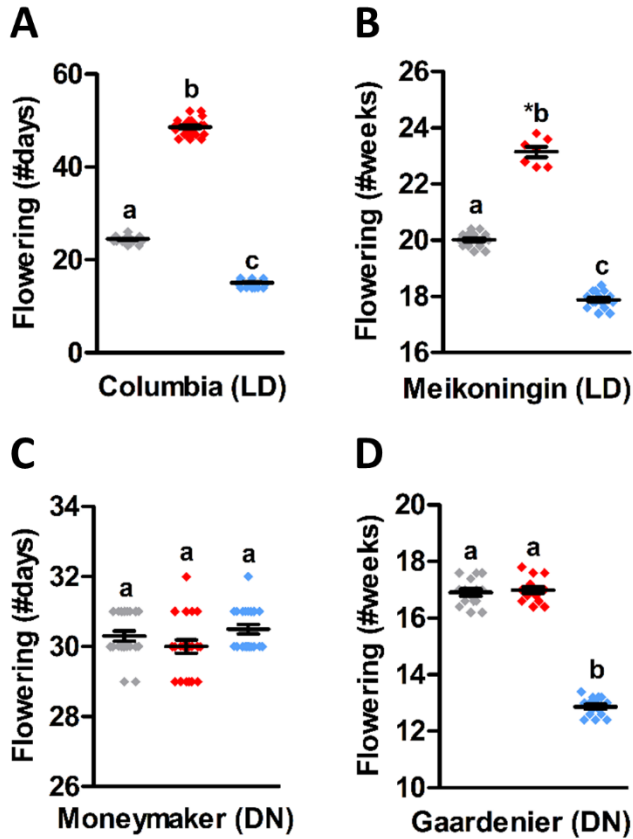


Figure 4: Late flowering in monochromatic red light relies on day length sensitivity.

A-B. Flowering time of long-day (LD) plants: *Arabidopsis* ecotype Columbia (**A**), and lettuce variety Meikoningin (**B**) grown in white, red, or blue LED conditions. **C-D.** Flowering time of day-neutral (DN) plants: tomato cv. Moneymaker (**C**), and lettuce variety Gaardenier (**D**) grown in the different LED conditions. Graph colours represent the different LED conditions. LED conditions were compared using a one-way ANOVA followed by a Tukey's test (letters **a**, **b**, and **c** indicate statistically significant differences, $p < 0.05$). Error bars represent standard error from mean. Similar results were obtained in two (**B/D**) or three (**A/C**) independent experiments.



As expected, late flowering in the red LED condition was lost in DN lettuce plants. Interestingly, early flowering in monochromatic blue light was observed in DN lettuce plants, but not in DN tomato plants (**Figures 4C,D**). The combined data of Arabidopsis, tomato, and lettuce suggested that late flowering in monochromatic red light relies mainly on inactivation of the blue light Zeitlupe photoreceptor-driven photoperiodic pathway, and can thus be observed in LD, but not in DN plant species.

Early flowering in monochromatic blue light is caused by upregulation of the age pathway.

We observed early flowering in the DN lettuce cultivar Gaardenier plants that were grown in monochromatic blue light (**Figure 4D**), which suggested that in these plants, flower induction relies on a flowering pathway other than the photoperiodic pathway. The increased plastochron, length/width ratios of the leaf blade and enhanced *GI* expression that we observed in Arabidopsis plants grown in the blue LED condition together pointed towards the age pathway (Jung et al., 2007; Wang et al., 2008; Wu et al., 2009). To investigate this, we focused on expression of known regulators of VPC in the rosettes of 5- to 15-day-old Arabidopsis plants grown in the different LED conditions. The expression of *miR156* was significantly reduced in monochromatic blue light, compared to white and monochromatic red light (**Figure 5A**). As a likely result, gene expression levels of *miR172*, *SPL2*, *SPL9*, *SPL10*, *SPL11*, and *SPL15* were significantly higher in the blue LED condition than in the other LED conditions (**Figures 5B, D, E, F, G, I**). The expression of the newly identified plant longevity gene *AHL15* (Karami et al., 2020; Rahimi et al., 2022) was not altered in monochromatic blue light, but was significantly

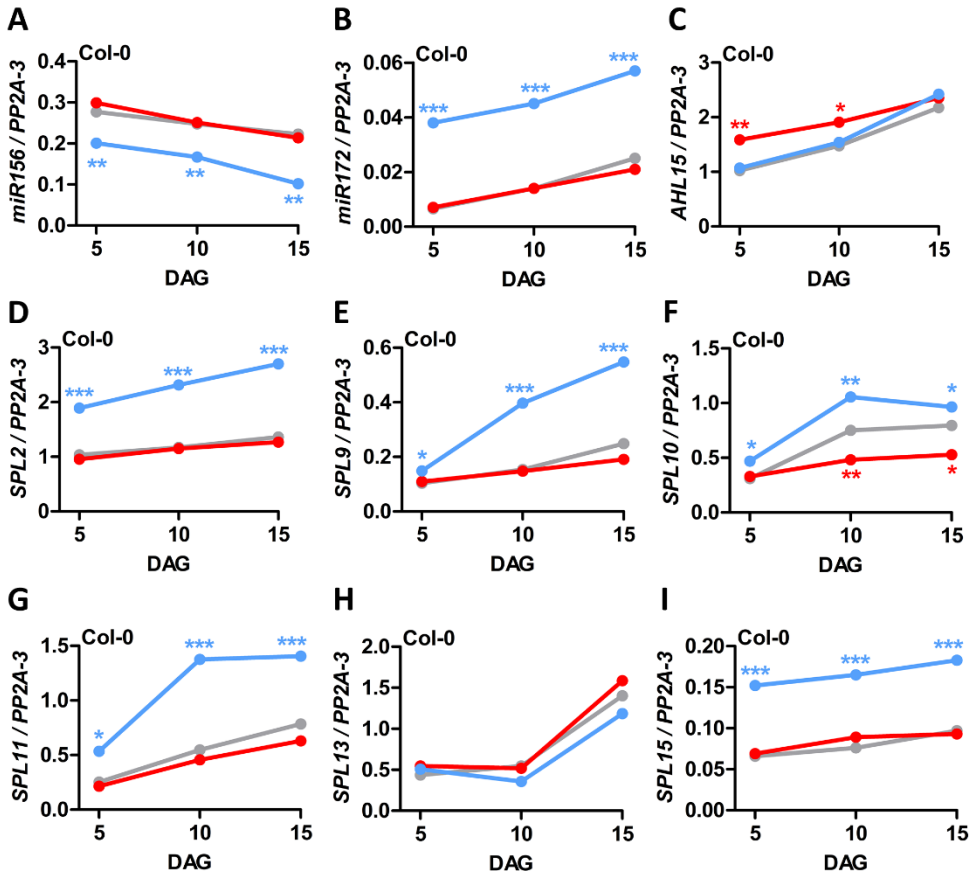


Figure 5: The Arabidopsis age pathway is promoted in spectra that lack red light.

A-I. Quantitative RT-PCR analysis of genes involved in the age pathway in Arabidopsis plants of ecotype Columbia (Col-0) grown in white, red, or blue LED conditions. Relative expression levels of *miR156* (**A**), *miR172* (**B**), *AHL15* (**C**), *SPL2* (**D**), *SPL9* (**E**), *SPL10* (**F**), *SPL11* (**G**), *SPL13* (**H**), and *SPL15* (**I**) at 5, 10 and 15 days after germination (DAG). Graph colours represent the different LED conditions. Monochromatic LED conditions (red or blue) were compared to white (control) using a two-sided Student's *t*-test (asterisks indicate significant differences at a specific time point (***p*<0.001, ***p*<0.01, **p*<0.05)). Standard errors and *p*-values are listed in **Table S3**. Similar results were obtained in three independent experiments.



higher in 5- and 10-day-old plants grown in monochromatic red light (**Figure 5C**). Expression of *SPL10* was significantly decreased in 5- to 15-day-old Arabidopsis plants grown in monochromatic red light (**Figures 5F and 6D**), whereas the expression of all other *SPLs* was similar in the white and red LED conditions. *SPL4*, *SPL6*, and *SPL13* expression levels were indifferent to the LED conditions (**Figures 5H and S3A-D**). For *SPL5*, gene expression was significantly higher in monochromatic blue light, compared to white and monochromatic red light, but its overall expression levels were extremely low (**Figure S3B**). Analysis of the expression of *SPL2*, *SPL3*, *SPL9*, *SPL10*, *SPL11*, and *SPL15* at 10-25 days after germination, which comprises the floral transition in monochromatic blue and white light-grown plants, showed again a significant increase of these age pathway genes in monochromatic blue light (**Figure 6A-F**). Because the same *SPL* genes already showed elevated expression in 5- to 15-day-old plants grown in monochromatic blue light, whereas expression of the floral integrators *FT* and *SOC1* was only elevated in 15- and 20-day-old plants (**Figure 6G, H**), it is likely that early flowering in monochromatic blue light results from increased *SPL* expression. To confirm this, we tested mutant plant lines with reduced (*spl9spl15* or *p35S::miR156*) or enhanced (*p35S::MIM156*) *SPL* expression levels. Flowering of *p35S::miR156* or *spl9 spl15* double mutant plants was delayed in the white and blue LED conditions, compared to wild-type plants, whereas *p35S::MIM156* plants flowered earlier than wild-type in white light, and later than wild-type in monochromatic blue light (**Figure S3E**). In monochromatic red light, flowering time of all three lines was similar to wild-type plants, corroborating our previous conclusion that late flowering in monochromatic red light relies largely on the absence of blue light-stimulation of the photoperiod pathway

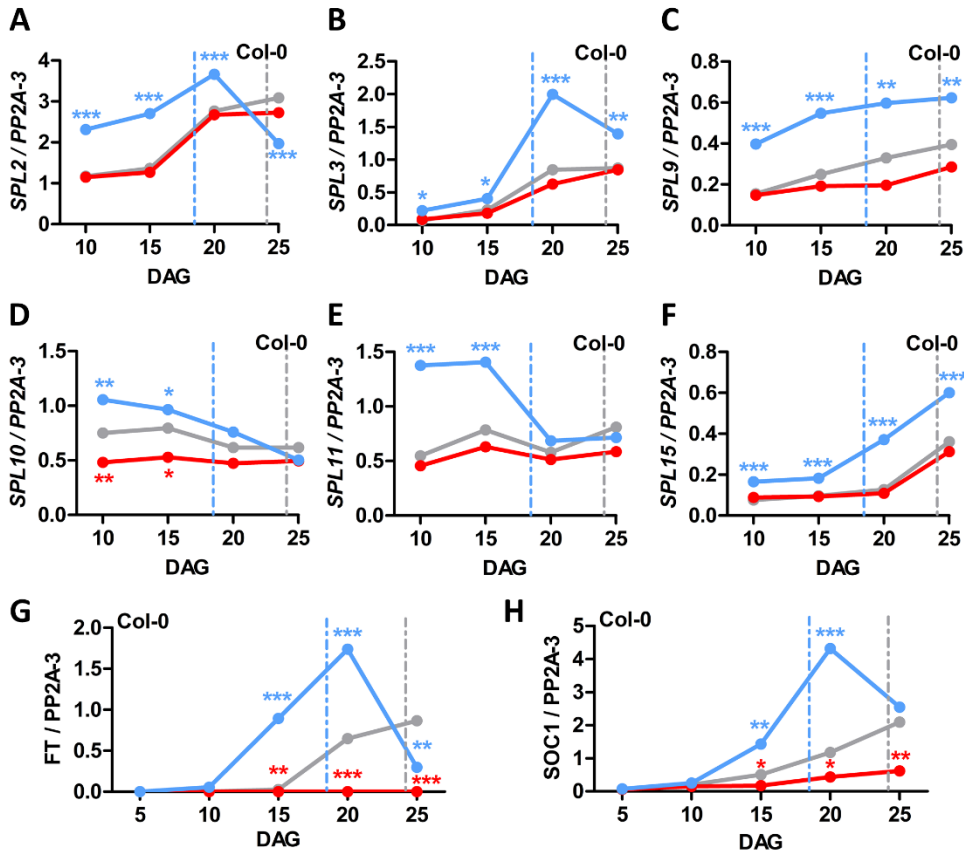


Figure 6: Early flowering in spectra that lack red light results from accelerated ageing.

A-F. Quantitative RT-PCR analysis of *SPL* genes that induce flowering in *Arabidopsis Columbia* (Col-0) plants that were grown in white, red, or blue LED conditions at 10, 15, 20, and 25 days after germination (DAG). Relative expression levels of *SPL2* (A), *SPL3* (B), *SPL9* (C), *SPL10* (D), *SPL11* (E) and *SPL15* (F). **G-H.** Quantitative RT-PCR analysis of the floral integrators *FT* (G) and *SOC1* (H) in Col-0 plants that were grown in different LED conditions at 5, 10, 15, 20, and 25 DAG. Graph colours represent the different LED conditions, dashed lines represent the moment of bolting. Monochromatic LED conditions (red or blue) were compared to white (control) using a two-sided Student's *t*-test (asterisks indicate significant differences at a specific time point (*** $p < 0.001$, ** $p < 0.01$, * $p < 0.05$)). Standard errors and *p*-values are listed in **Table S3**. Similar results were obtained in three independent experiments.



(**Figure S3E**). Interestingly, the flowering time of *p35S::miR156*, *p35S::MIM156* and *spl9 spl15* double mutant in monochromatic blue light did not significantly differ from that of wild-type plants flowering in white light (**Figure S3E**), suggesting that disruption of the *miR156-SPL* module of the age pathway results in a (partial) rescue of the early flowering phenotype in the blue LED condition. Our quantitative RT-PCR data, together with flowering time analysis, suggests that shoot meristems age faster in monochromatic blue light, ultimately resulting in early flowering.

In spectra that contain red light, Arabidopsis PHYB inhibits flowering by repressing the age pathway.

The results described above suggest that shoots of plants grown in monochromatic blue light (thus lacking red light in the spectrum) mature early compared to those grown in white or red LED conditions, implying that red light actively inhibits the age pathway. To investigate this, we analysed photoreceptors of the red/FR light-sensitive phytochrome (PHY) family. Analysis of *phyA*, *phyB*, *phyC*, *phyD*, and *phyE* single mutants showed a significant early flowering of *phyB* mutants compared to wild type or other *phy* mutant plants in both white and red LED conditions, and to a lesser extent, in the blue LED condition (**Figure 7A**), suggesting a putative role for PHYB in inhibition of plant ageing. Since PHYB has been proposed to repress *GI* expression, which promotes *miR172* (Huq et al., 2000; Jung et al., 2007), we analysed its expression in *phyB* plants grown in the different LED conditions. Expression of *GI* was similar in *phyB* plants grown in white and monochromatic blue light, thus further supporting the PHYB-GI interaction, and possibly explaining the elevated diurnal *GI* expression in Col-0 plants



grown in monochromatic blue light (**Figure 3B**). However, its expression was significantly lower in 15-day-old *phyB* plants grown in red light (**Figure 7B**), which is most likely a side-effect of inactivation of the photoperiodic pathway in this LED condition. Next, we investigated the plant ageing regulators that were differentially expressed in wild-type plants grown in monochromatic blue light, compared to red or white light (**Figure 5**). Except for *SPL10* expression in the red LED condition, the differential expression of *miR156*, *miR172*, *SPL2*, *SPL9*, *SPL11*, and *SPL15* in the different LED conditions was lost in *phyB* plants (**Figures 7C-I**). This suggests that, in wild-type plants, the differential expression of these ageing regulators between the blue LED condition and the white or red LED conditions relies on PHYB activation. To summarise, our data suggests that, in the LD plant *Arabidopsis*, PHYB signalling suppresses the age pathway through *miRNAs*, *SPLs*, and *GI* in response to the presence of red light in the spectrum.

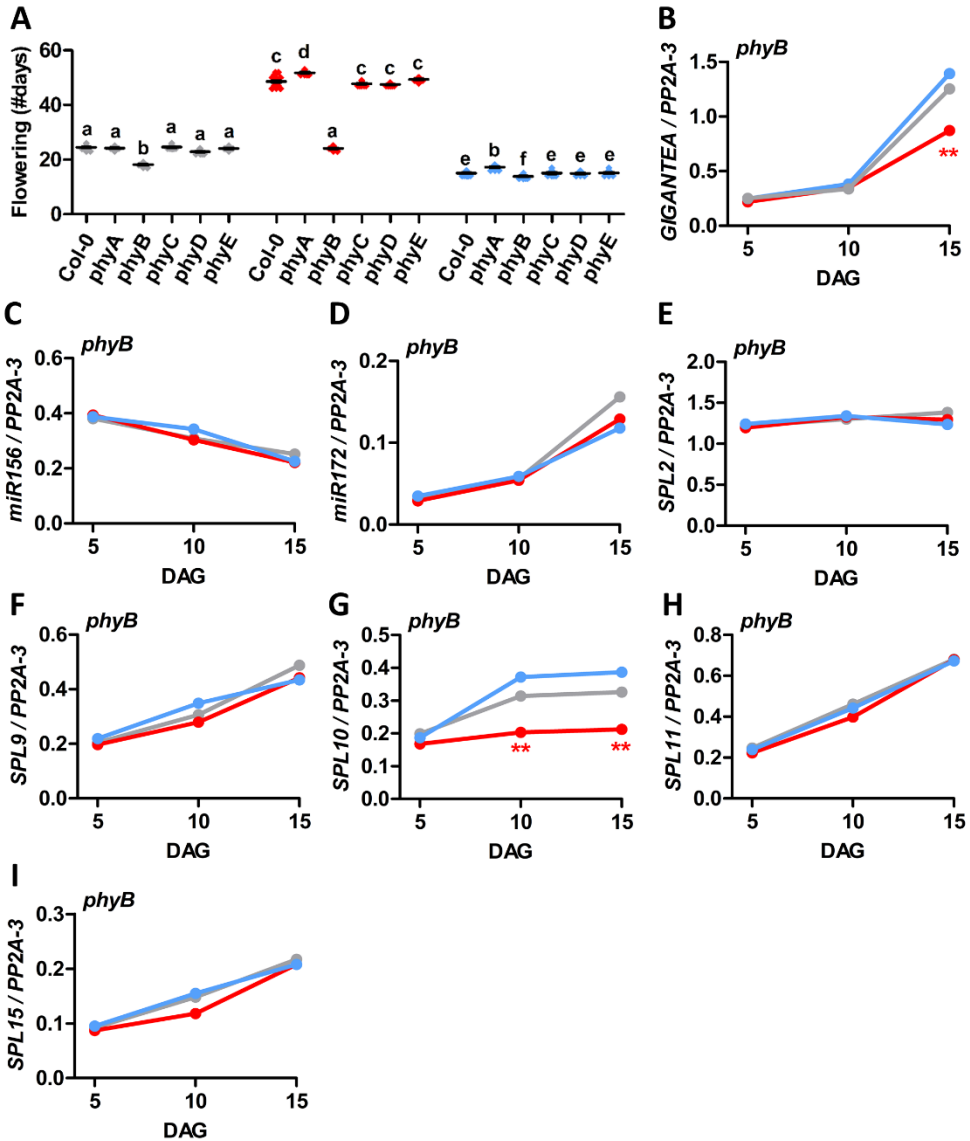
Discussion

In **chapter 3**, we observed that *Arabidopsis* shoot development is greatly influenced by light quality, whereas tomato shoots remained indifferent to red or blue light. Here, we further investigated the formation of *Arabidopsis* and tomato shoot organs, and their correlation to flowering time. *Arabidopsis* plants grown in monochromatic red light developed more rosette leaves, and at a higher pace, which correlated to a large shoot apex, and an extended vegetative phase caused by late flowering. In contrast, *Arabidopsis* plants grown in monochromatic blue light developed only a few leaves and at a



Chapter 5: Light quality regulates flowering

significantly slower rate than white- or red light-grown plants. In addition to a small shoot apex and a shortened vegetative phase due to extremely early flowering, the auxin response in the shoot apex was decreased in the blue LED condition. Interestingly, in tomato plants, leaf number, plastochron, flowering





time, and size of, and auxin response in, the shoot meristem were all indifferent to monochromatic red and blue light treatments. Since *Arabidopsis* is a LD plant, and tomato a DN species, we aimed to explain this difference by investigating the photoperiodic pathway. In monochromatic red light (thus

Figure 7: *Arabidopsis* PHYB inhibits flowering by repressing the age pathway.

A. Flowering time of *Arabidopsis* Columbia (Col-0) and photoreceptor mutants *phyA*, *phyB*, *phyC*, *phyD*, and *phyE* grown in white, red, or blue LED conditions.

B-I. Quantitative RT-PCR analysis of genes involved in the age pathway in Col-0 and *phyB* plants grown in the different LED conditions. Relative expression levels of *GIGANTEA* (**B**), *miR156* (**C**), *miR172* (**D**), *SPL2* (**E**), *SPL9* (**F**), *SPL10* (**G**), *SPL11* (**H**), and *SPL15* (**I**) at 5, 10, and 15 days after germination (DAG). Graph colours represent the different LED conditions. LED conditions and wildtypes or mutants were compared using a one-way ANOVA followed by a Tukey's test (letters **a**, **b**, **c**, **d**, **e**, and **f** indicate statistically significant differences, $p < 0.05$) in **A**. In **B-I**, monochromatic LED conditions (red or blue) were compared to white (control) using a two-sided Student's *t*-test (asterisks indicate significant differences at a specific time point (** $p < 0.01$)). Error bars represent standard error from mean in **A** ($n=30$), standard errors and *p*-values for **B-I** are listed in **Table S3**. Similar results were obtained in three independent experiments.



Chapter 5: Light quality regulates flowering

lacking blue light in the spectrum), the inactivity of photoreceptors of the Zeitzlupe family resulted in a significant decrease in *GI* and *CO* expression, and thus Arabidopsis plants failed to establish a peak in *FT* expression at the end of the day to induce flowering. Although *GI*, *CO*, and *FT* levels were significantly elevated in Arabidopsis plants grown in the blue LED condition, early flowering of a DN lettuce accession in monochromatic blue light suggested that this phenotype could be photoperiod-independent. Gene expression analysis of components of the age pathway showed that *miR156*, *miR172*, *SPL2*, *SPL3*, *SPL9*, *SPL10*, *SPL11*, and *SPL15* were differentially expressed in monochromatic blue light (thus lacking red light in the spectrum), when compared to white and red LED conditions. Subsequently, *SOC1* and *FT* levels were elevated in 15- to 25-day-old Arabidopsis plants grown in the blue LED condition, suggesting that the presence of red light in the spectrum is required to repress the age pathway and thereby delay VPC and flowering. In addition to early flowering, *phyB* mutants lost the differential expression of *miR156*, *miR172*, *SPL2*, *SPL9*, *SPL10*, *SPL11*, and *SPL15* between the white and blue LED conditions, confirming that PHYB represses the age pathway in light spectra that contain red light.

Light quality regulates shoot organ formation and morphology.

The rosette phenotype of Arabidopsis plants grown in the different LED conditions resulted from changes in flowering time and plastochron, that correlated to significant differences in shoot apex size. The accumulation of stem cells in the meristem determines its size, and is regulated by *CLAVATA* (*CLV*) genes that have been shown to respond to changes in photoperiod (Jeong and Clark, 2005). Therefore, the altered meristem size of Arabidopsis plants



grown in monochromatic red or blue light likely correlates to changes in photoperiodic regulation. This hypothesis was further supported by the complete indifference of DN tomato apices to these light treatments. Interestingly, we also observed a decreased auxin response in *Arabidopsis* shoot apices of plants grown in monochromatic blue light, that was not observed in tomato shoot apices. Since auxin regulates the initiation of new leaf primordia (Lee et al., 2019), this decrease in auxin response suggested that, similar to a dark treatment, the blue LED condition somehow interferes with PIN1-dependent auxin flux in the shoot apex (Yoshida et al., 2011). This implies that there are either functional differences in auxin-dependent primordia initiation between *Arabidopsis* and tomato, or that auxin responses in the shoot apex may be (partially) photoperiod-sensitive in LD plants, and thus indifferent to red or blue light in DN species. Aside from initiation and outgrowth of new leaves, monochromatic blue light treatment of *Arabidopsis* plants also affected the morphology of rosette leaves. Leaf blades of plants grown in this LED condition had a significantly higher length/width (L/W) ratio than those of plants grown in white or red LED conditions, and even reached beyond 1.7, which is indicative of adult leaves (Telfer et al., 1997). However, these leaves did not show other characteristics of adult leaves such as abaxial trichomes, or serrated margins. Based on leaf heteroblasty, these plants would thus not be identified as adult vegetative, suggesting that VPC was incomplete in these plants. By definition, VPC is described as the acquisition of flowering competence (Huijser and Schmid, 2011), which implies that all reproductive plants have completed this developmental phase transition. However, *Arabidopsis* plants grown in the blue LED condition already flowered after the production of only 5-6 leaves that lacked most adult



Chapter 5: Light quality regulates flowering

characteristics. Therefore, we speculate that either the widely used leaf heteroblasty characteristics are not completely reliable for the identification of adult vegetative plants, or that plants become reproductive after a (partially) incomplete VPC when grown in monochromatic blue light. Although VPC and the floral transition are uncoupled in woody species (Huijser and Schmid, 2011), this is not common for *Arabidopsis*. However, leaf heteroblasty of white- and monochromatic red light-grown plants suggested that VPC occurs simultaneously in these LED conditions, while their floral transition occurs at different time points, indicating that spectra that lack blue light specifically delay the floral transition, independent of VPC.

Light quality regulates photoperiodic flowering.

In the past decades, many flowering studies have been conducted in photoperiod-sensitive LD and SD species to show that blue light photoreceptors of the *Zeitlupe* and cryptochrome families, and red/FR light-responsive phytochromes regulate photoperiodic flowering (Wu and Hanzawa, 2014). However, their responses had not been tested in LED lighting setups that simultaneously modulate multiple photoreceptors, and their putative interactions. Therefore, we analysed *Arabidopsis* photoreceptor mutants of the *Zeitlupe* family in the three LED conditions to confirm that the flowering response of these photoreceptors is only activated in spectra that contain blue light. Upon photoactivation, these photoreceptors interact with *GI* to inhibit CDFs and thereby alleviate their repression of *CO*, subsequently resulting in upregulation of the floral integrator *FT* (Samach et al., 2000; Sawa et al., 2007; Fornara et al., 2009). Our analysis of diurnal expression patterns confirmed that the presence of blue light is required in the spectrum to promote *GI*, *CO*,



and *FT* to induce flowering. Moreover, since flowering of DN tomato and lettuce accessions was indifferent to treatment with monochromatic red light, we showed that spectra that contain blue light can only promote flowering in photoperiod-sensitive species. In contrast to the red LED condition, *Arabidopsis* plants grown in white or monochromatic blue light did establish sufficient *GI* and *CO* expression to induce an end-of-day *FT* peak. Although FR light-activated PHYA has been shown to promote flowering as well (Valverde et al., 2004), we showed that FR light is not necessarily required to induce the photoperiodic pathway in LD plants. While elevated *FT* expression in monochromatic blue light, compared to white light, could have resulted from a previously described role for PHYB in targeted CO protein degradation (Valverde et al., 2004; Lazaro et al., 2015), a PHYB-GI interaction has been suggested as well (Huq et al., 2000). In conclusion, we verified that the presence of blue light in the spectrum, through activation of the Zeitzlupe photoreceptor family, promotes photoperiodic flowering. Our results suggest that, although flower-promoting roles for PHYA and CRY2 and a flower-inhibiting role for PHYB have been described, their role in photoperiodic flowering appears to be subordinate (**Figure 8**).

Light quality regulates plant ageing.

In addition to altered leaf heteroblasty of *Arabidopsis* plants grown in monochromatic blue light, we observed early flowering, not only in both LD species, but also in the DN lettuce accession, suggesting that the absence of red light in this spectrum promotes flowering in a photoperiod-independent manner. These results led us to further investigate the age pathway. Upregulation of five out of six VPC-associated *SPL* genes in plants grown in



Chapter 5: Light quality regulates flowering

monochromatic

blue light, which combined with the increased L/W ratio of their rosette leaves, strongly suggested early VPC. The subsequent increase in *FT* and *SOC1* expression and flowering analysis of the *spl9 spl15* double mutant and *p35S::miR156* and *p35S::MIM156* lines confirmed the correlation between the miR156-SPL module and early flowering in monochromatic blue light. Altogether, this

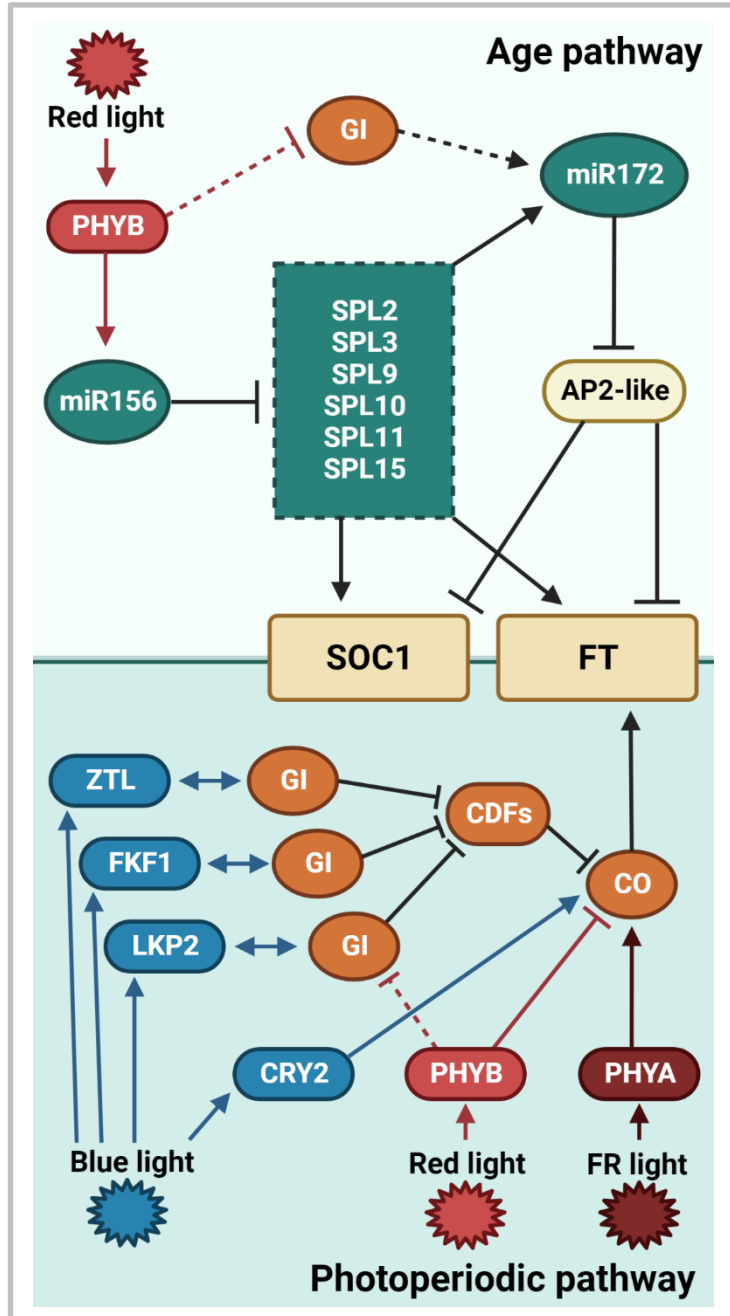




Figure 8: Model for regulation of the Arabidopsis floral transition by light quality.

The floral transition in Arabidopsis is regulated by light quality through both the age pathway (top) and the photoperiodic pathway (bottom). In spectra that contain red light, PHYB inhibits flowering through the age pathway in two ways: (1) PHYB promotes *miR156*, thereby enhancing its repression of *SPLs*, which reduces both their direct and indirect (through *miR172*) promotion of *SOC1* and *FT*. (this work) (2) We hypothesise an additional red light response where PHYB inhibits *GI* expression, thereby reducing its activation of *miR172*, which may lead to accumulation of AP2-like transcription factors that inhibit floral integrators *SOC1* and *FT* (this work; Huq et al., 2000; Jung et al., 2007). Furthermore, light quality regulates flowering through the photoperiodic pathway. In spectra that contain blue light, photoreceptors of the Zeirlupe family (ZTL, FKF1, and LKP2, this work) and CRY2 (Liu et al., 2008) promote flowering by modulation of *CO*, either directly (CRY2), or indirectly through complex formation with *GI* (Zeirlupes) that inhibits CDFs which repress *CO* expression. In addition, far-red (FR) light promotes *CO* expression through PHYA (Valverde et al., 2004). In spectra that contain red light, photoperiodic flowering is inhibited through PHYB-dependent degradation of CO proteins, and possibly also by decreasing *GI* expression (Valverde et al., 2004, this work, Huq et al, 2000). If modulation of CO levels by light quality leads to a CO peak at the end of the day, its subsequent promotion of *FT* is sufficient to induce flowering.

suggested that, in white and red LED conditions (where red light is present in the spectra), the age pathway is inhibited to delay both VPC and the floral transition, whereas this inhibition does not occur in the blue LED condition (that lacks red light in the spectrum). Based on early flowering of *phyB* in white and monochromatic red light, and on the fact that *phyB* mutants flower early both under inductive LD photoperiods, and non-inductive SD



Chapter 5: Light quality regulates flowering

photoperiods (Reed et al., 1993), we selected PHYB as a putative inhibitor of plant ageing. In *phyB* mutants, components of the miR156-SPL module were no longer differentially expressed in monochromatic blue light, thus confirming inhibition of the age pathway by PHYB. Although PHYB-promoted expression of *miR156* through degradation of PHYTOCHROME INTERACTING FACTORS (PIFs) has been described in a shade avoidance study (Xie et al., 2017), its effect on delaying VPC and flowering has not been reported yet. By revealing this long sought-after photoperiod-independent role for PHYB, we showed that light quality may be used to regulate VPC and flowering of some DN plant species, as well as LD plant species. In addition to regulation of the age pathway in a photoperiod-independent manner, a possible photoperiod-dependent function of PHYB in the age pathway should be considered as well. Diurnal *GI* expression levels in wild-type *Arabidopsis* plants grown in monochromatic blue light were significantly higher than in white light, however, in *phyB* mutants this difference was lost, thus further supporting the previously proposed PHYB-GI interaction (Huq et al., 2000). Interestingly, GI has been shown to promote *miR172* expression (Jung et al., 2007), supporting the possibility of a putative photoperiod-dependent role for PHYB in plant ageing (**Figure 8**). Surprisingly, DN tomato plants, in contrast to the DN lettuce accession, did not flower early in the blue LED condition. Since components of the age pathway have been identified in tomato (Zhang et al., 2011; Salinas et al., 2012; Li et al., 2013), a possible explanation for the indifference of tomato plants may be the lack of a true *PHYB* orthologue. Tomato *PHYB1* and *PHYB2* arose from an independent duplication in *Solanaceae* (Pratt et al., 1995), suggesting that PHYB function in plant ageing may not be conserved in *Solanaceae* species. To summarise, we showed that



the presence of red light in the spectrum is required for the activation of PHYB, which promotes *miR156*, resulting in decreased *SPL*, *FT* and *SOC1* expression that inhibits VPC and flowering (**Figure 8**).

Materials and Methods

Growth conditions and LED treatments

In all experiments, plants were grown at a 16h photoperiod, under white, deep red, or blue Philips Greenpower LED research modules (Signify B.V., Eindhoven, the Netherlands) with a measured photon flux density of $120 \pm 10 \mu\text{mol m}^{-2}\text{s}^{-1}$ at the top of the canopy, a temperature of 21°C, and 70% relative humidity. The percentages of blue, green, red, and far-red wavelengths for the different LED modules are listed in **Table S1** of **chapter 3**. Experiments with the different LED treatments were performed simultaneously in the same growth chamber in separate compartments enclosed by white plastic screens with a proximal distance of 50 cm to the plants.

Plant lines and seed germination

Experiments were performed with *Arabidopsis thaliana* (*Arabidopsis*) ecotype Columbia (Col-0), *Solanum lycopersicum* (tomato) cultivar Moneymaker (MM) and *Lactuca sativa* (lettuce) cultivars Meikoningin (long-day) or Gaardenier (day-neutral). *Arabidopsis* and tomato mutant or reporter lines that were used have been described before and are listed in **Table S1**. *Arabidopsis* mutant lines were genotyped using the primers listed in **Table S2**. *Arabidopsis* seeds were sown on the soil surface and stratified for 5 days at 4°C in darkness.



Chapter 5: Light quality regulates flowering

Subsequently the seeds were moved to white light to allow simultaneous germination. After one day in white light, the pots were placed in the LED conditions. Tomato and lettuce seeds were placed approximately 2 cm under the soil surface and the pots were directly placed in the LED conditions.

Analysis of leaf formation, morphology, and flowering time

Arabidopsis rosette leaves or tomato compound leaves were counted every week from the moment they were visible by eye, until the floral transition. Plastochron was calculated based on the number of leaves and the number of days until the floral transition. *Arabidopsis* rosettes were photographed every week, until bolting. At this time, individual rosette leaves were removed, flattened, and photographed for measurements to calculate the length/width ratio of the leaf blade. All measurements were performed with ImageJ (Fiji) (Schindelin et al., 2012). The individual rosette leaves were also analysed under a Leica MZ12 light microscope to score for the presence of abaxial trichomes. *Arabidopsis* flowering time was measured in number of days until bolting. For tomato, toothpicks were used to carefully push aside the young leaves from the apex. Flowering time was determined as the day on which small inflorescences became visible near the shoot apex. In lettuce plants, flowering was determined by the number of days until an inflorescence became visible above the head. At this time, representative tomato and lettuce plants were photographed.

Microscopic analysis of the shoot apex

Primary inflorescences of *Arabidopsis pDR5::GFP* plants at 1 week after bolting were dissected using 0.3 mm x 13 mm needles (#304000, BD



MicroalanceTM). All flowers, flower buds, and stage IV and V primordia were removed to expose the shoot apex. Dissected Arabidopsis shoot apices were mounted on a glass slide using 1% Low Melting Point (LMP) agarose (#16520050, Thermo ScientificTM). To visualise *pDR5::GFP*, a Zeiss LSM5 Exciter/Axiolmager equipped with a 40x water objective and a 488 nm argon laser with a 505-530 nm band pass filter was used. The shoots of 25-day-old tomato *pDR5::YFP* plants were dissected using tweezers. All leaves and primordia that were visible by eye were removed to expose the shoot apex. Dissected tomato shoot apices were mounted on a glass slide using 1% LMP agarose and imaged with a Leica MZ16FA equipped with a Leica DFC420C camera. YFP fluorescence was detected using a 510/20 nm excitation filter and a 560/40 nm emission filter. Based on the microscopic images, the meristem size of Arabidopsis and tomato was measured using ImageJ (Fiji) software. To quantify the fluorescent signals, the corrected total cell fluorescence (CTCF) method (McCloy et al., 2014) was slightly adjusted to quantify the corrected total fluorescence (CTF) of the shoot apex. $CTF = \text{integrated density} - (\text{area of shoot apex} * \text{mean fluorescence of background readings})$. For images of Arabidopsis shoot apices, the CTF was also corrected for the differences in SAM size between LED conditions.

RNA extraction and qRT-PCR

All tissues that were used for RNA extraction were frozen in liquid nitrogen directly after harvesting within their respective LED condition. For each experiment, five different plants from the same LED condition were pooled and used for RNA extraction. Three biological replicates were used for each plant line per LED condition, with three technical replicates. For analysis of



Chapter 5: Light quality regulates flowering

diurnal expression patterns, RNA was extracted from the rosettes of 14-day-old *Arabidopsis* plants, at the following time points: Zeitgeber time (ZT)0 (07.00), ZT3 (10.00), ZT6 (13.00), ZT9 (16.00), ZT12 (19.00), ZT15 (22.00), ZT18 (01.00), ZT21 (04.00) and ZT24 (07.00). For analysis of gene expression throughout development, RNA was extracted from the rosettes of 5-, 10-, 15-, 20-, or 25-day-old *Arabidopsis* plants (always at ZT9). Frozen tissue samples were ground with a TissueLyser II (#85300, Qiagen). Total RNA was extracted from the ground tissue using an RNeasy® Plant Mini kit (#74904, Qiagen), and used for first strand cDNA synthesis with the RevertAid First Strand cDNA Synthesis kit (#K1621, Thermo Scientific™). For miRNAs, total RNA was reverse transcribed with the SnoR101 reverse primer, and a miRNA-specific RT primer. For qRT-PCR, the cDNA was diluted 10x and used with TB Green Premix Ex Taq II (Tli RNase H Plus) (#RR820B, Takara) and the CFX96 Touch™ Real-Time PCR Detection System (#1855196, Bio-Rad). CT values were obtained using Bio-Rad CFX manager 3.1. The relative expression level of genes of interest was calculated according to the Livak method (Livak and Schmittgen, 2001), using *PP2A-3* (At2g42500) as a reference gene. All primers that were used for qRT-PCR experiments are listed in **Table S2**.

Statistical analysis and figures

For phenotypic analysis (leaf formation, flowering time), 20 tomato or lettuce plants, and 30 *Arabidopsis* plants were grown in each LED condition. For analysis of *Arabidopsis* leaf morphology, 10 representative biological replicates were used for each leaf number (1, 3, 5, and 7). For microscopic analysis of *Arabidopsis* and tomato shoot apices, images of 20 individual shoot apices were used to calculate meristem size and corrected total fluorescence



(CTF). In qRT-PCR experiments, rosettes of 10 individual plants were pooled for RNA extraction. For each data point, the mean of 3 cDNA samples, derived from 3 different RNA samples, was plotted in the graph. All data was obtained from either two (lettuce flowering, leaf morphology, microscopic analysis) or three independent experiments (phenotypic analysis of *Arabidopsis* and tomato, RT-qPCR). For phenotypic and microscopic analysis, the different LED conditions, or wild types and mutants, were compared using a one-way ANOVA followed by a Tukey's honestly significant different (HSD) post hoc test. In qRT-PCR experiments, monochromatic LED conditions (red or blue) were compared to white light using a two-sided Student's *t*-test. All measurements were plotted into graphs using GraphPad Prism 5 software. In the graphs, the colours of the dots and lines indicate white, red, and blue LED conditions. All photographs were taken with a Nikon D5300 camera and edited in ImageJ (Fiji). Schematic models were generated with BioRender software. Final figures were assembled using Microsoft PowerPoint.

Author contributions

KS and RO conceived and designed the experiments. KS performed the experiments and the statistical analysis. KS and RO analysed the results and wrote the manuscript.



Funding

This work was part of the research program “LED it be 50%” with project number 14212, which is partly financed by the Dutch Research Council (NWO).

Acknowledgements

We would like to thank Signify for providing the LED modules, and Cris Kuhlemeier for providing seeds of the tomato *pDR5::YFP* reporter. We acknowledge Fred Schenkel and Emiel Wiegers for help with design and construction of the LED frame, and Peter Schellekens and Carlos Galvan-Ampudia for help with shoot apex dissection protocols.



References

- Abe, M., Kobayashi, Y., Yamamoto, S., Daimon, Y., Yamaguchi, A., Ikeda, Y., Ichinoki, H., Notaguchi, M., Goto, K., and Araki, T. (2005). FD, a bZIP protein mediating signals from the floral pathway integrator FT at the shoot apex. *Science* 309, 1052–1056.
- Ben-Gera, H., Shwartz, I., Shao, M. R., Shani, E., Estelle, M., and Ori, N. (2012). ENTIRE and GOBLET promote leaflet development in tomato by modulating auxin response. *Plant J.* 70, 903–915.
- Blázquez, M. A., and Weigel, D. (1999). Independent regulation of flowering by phytochrome B and gibberellins in Arabidopsis. *Plant Physiol.* 120, 1025–1032.
- Campoli, C., Drosse, B., Searle, I., Coupland, G., and Von Korff, M. (2012). Functional characterisation of HvCO1, the barley (*Hordeum vulgare*) flowering time ortholog of CONSTANS. *Plant J.* 69, 868–880.
- Cheng, X. F., and Wang, Z. Y. (2005). Overexpression of COL9, a CONSTANS-LIKE gene, delays flowering by reducing expression of CO and FT in *Arabidopsis thaliana*. *Plant J.* 43, 758–768.
- Cho, L. H., Yoon, J., and An, G. (2017). The control of flowering time by environmental factors. *Plant J.* 90, 708–719.
- Christians, M. J., Gingerich, D. J., Hua, Z., Lauer, T. D., and Vierstra, R. D. (2012). The light-response BTB1 and BTB2 proteins assemble nuclear ubiquitin ligases that modify phytochrome B and D signaling in Arabidopsis. *Plant Physiol.* 160, 118–134.
- Fornara, F., Panigrahi, K. C. S., Gissot, L., Sauerbrunn, N., Rühl, M., Jarillo, J. A., and Coupland, G. (2009). Arabidopsis DOF transcription factors act redundantly to reduce CONSTANS expression and are essential for a photoperiodic flowering response. *Dev. Cell* 17, 75–86.
- Franco-Zorrilla, J. M., Valli, A., Todesco, M., Mateos, I., Puga, M. I., Rubio-Somoza, I., Leyva, A., Weigel, D., García, A., and Paz-Ares, J. (2007). Target mimicry provides a new mechanism for regulation of microRNA activity. *Nat. Genet.* 39, 1033–1037.
- Huijser, P., and Schmid, M. (2011). The control of developmental phase transitions



Chapter 5: Light quality regulates flowering

in plants. *Development* 138, 4117–4129.

- Huq, E., Tepperman, J. M., and Quail, P. H.** (2000). GIGANTEA is a nuclear protein involved in phytochrome signaling in Arabidopsis. *Proc. Natl. Acad. Sci. U. S. A.* 97, 9789–9794.
- Jeong, S., and Clark, S. E.** (2005). Photoperiod regulates flower meristem development in *Arabidopsis thaliana*. *Genetics* 169, 907–915.
- Jung, J. H., Seo, Y. H., Pil, J. S., Reyes, J. L., Yun, J., Chua, N. H., and Park, C. M.** (2007). The GIGANTEA-regulated microRNA172 mediates photoperiodic flowering independent of CONSTANS in Arabidopsis. *Plant Cell* 19, 2736–2748.
- Karami, O., Rahimi, A., Khan, M., Bemer, M., Hazarika, R. R., Mak, P., Compier, M., van Noort, V., and Offringa, R.** (2020). A suppressor of axillary meristem maturation promotes longevity in flowering plants. *Nat. Plants* 6, 368–376.
- Koncz, C., Chua*, N.-H., Schell, J., and Rédei, G. P.** (1992). A heuristic glance at the past of Arabidopsis genetics. *Methods Arab. Res.* , 1–15.
- Lazaro, A., Mouriz, A., Piñeiro, M., and Jarillo, J. A.** (2015). Red light-mediated degradation of constans by the e3 ubiquitin ligase hos1 regulates photoperiodic flowering in Arabidopsis. *Plant Cell* 27, 2437–2454. .
- Lee, Z. H., Hirakawa, T., Yamaguchi, N., and Ito, T.** (2019). The roles of plant hormones and their interactions with regulatory genes in determining meristem activity. *Int. J. Mol. Sci.* 20, 4065.
- Li, J., Luan, Y., Zhai, J., Liu, P., and Xia, X.** (2013). Bioinformatic analysis of functional characteristics of miR172 family in tomato. *J. Northeast Agric. Univ.* 20, 19–27.
- Liu, L. J., Zhang, Y. C., Li, Q. H., Sang, Y., Mao, J., Lian, H. L., Wang, L., and Yang, H. Q.** (2008). COP1-mediated ubiquitination of CONSTANS is implicated in cryptochrome regulation of flowering in Arabidopsis. *Plant Cell* 20, 292–306.
- Livak, K. J., and Schmittgen, T. D.** (2001). Analysis of relative gene expression data using real-time quantitative PCR and the 2- $\Delta\Delta$ CT method. *Methods* 25,



402–408.

- Martin-Tryon, E. L., Kreps, J. A., and Harmer, S. L.** (2007). GIGANTEA acts in blue light signaling and has biochemically separable roles in circadian clock and flowering time regulation. *Plant Physiol.* 143, 473–486.
- Mayfield, J. D., Folta, K. M., Paul, A. L., and Ferl, R. J.** (2007). The 14-3-3 proteins μ and ν influence transition to flowering and early phytochrome response. *Plant Physiol.* 145, 1692–1702.
- McCloy, R. A., Rogers, S., Caldon, C. E., Lorca, T., Castro, A., and Burgess, A.** (2014). Partial inhibition of Cdk1 in G2 phase overrides the SAC and decouples mitotic events. *Cell Cycle* 13, 1400–1412.
- Monte, E., Alonso, J. M., Ecker, J. R., Zhang, Y., Li, X., Young, J., Austin-Phillips, S., and Quail, P. H.** (2003). Isolation and characterization of phyC mutants in Arabidopsis reveals complex crosstalk between phytochrome signaling pathways. *Plant Cell* 15, 1962–1980.
- Morrow, R. C.** (2008). LED lighting in horticulture. *HortScience* 43, 1947–1950.
- Ottenschläger, I., Wolff, P., Wolverton, C., Bhalerao, R. P., Sandberg, G., Ishikawa, H., Evans, M., and Palme, K.** (2003). Gravity-regulated differential auxin transport from columella to lateral root cap cells. *Proc. Natl. Acad. Sci. U. S. A.* 100, 2987–2991.
- Pratt, L. H., Cordonnier-Pratt, M. M., Hauser, B., and Caboche, M.** (1995). Tomato contains two differentially expressed genes encoding B-type phytochromes, neither of which can be considered an ortholog of Arabidopsis phytochrome B. *Planta* 197, 203–206.
- Rahimi, A., Karami, O., Balazadeh, S., and Offringa, R.** (2022). miR156-independent repression of the ageing pathway by longevity-promoting AHL proteins in Arabidopsis. *New Phytol.* 235, 2424–2438.
- Reed, J. W., Nagpal, P., Poole, D. S., Furuya, M., and Chory, J.** (1993). Mutations in the gene for the red/far-red light receptor phytochrome B alter cell elongation and physiological responses throughout Arabidopsis development. *Plant Cell* 5, 147–157.
- Robert, L. S., Robson, F., Sharpe, A., Lydiate, D., and Coupland, G.** (1998).



Chapter 5: Light quality regulates flowering

Conserved structure and function of the Arabidopsis flowering time gene CONSTANS in *Brassica napus*. *Plant Mol. Biol.* 37, 763–772.

Ruckle, M. E., DeMarco, S. M., and Larkin, R. M. (2007). Plastid signals remodel light signaling networks and are essential for efficient chloroplast biogenesis in Arabidopsis. *Plant Cell* 19, 3944–3960.

Salinas, M., Xing, S., Höhmann, S., Berndtgen, R., and Huijser, P. (2012). Genomic organization, phylogenetic comparison and differential expression of the SBP-box family of transcription factors in tomato. *Planta* 235, 1171–1184.

Samach, A., Onouchi, H., Gold, S. E., Ditta, G. S., Schwarz-Sommer, Z., Yanofsky, M. F., and Coupland, G. (2000). Distinct roles of constans target genes in reproductive development of Arabidopsis. *Science* 288, 1613–1616.

Sawa, M., Nusinow, D. A., Kay, S. A., and Imaizumi, T. (2007). FKF1 and GIGANTEA complex formation is required for day-length measurement in Arabidopsis. *Science* 318, 261–265.

Schindelin, J., Arganda-Carreras, I., Frise, E., Kaynig, V., Longair, M., Pietzsch, T., Preibish, S., Rueden, C., Saalfeld, S., Schmid, B., Tinevez, J. Y., White, D. J., Hartenstein, V., Eliceiri, K., Tomancak, P., and Cardona, A. (2012). Fiji: An open-source platform for biological-image analysis. *Nat. Methods* 9, 676–682.

Schwab, R., Palatnik, J. F., Riester, M., Schommer, C., Schmid, M., and Weigel, D. (2005). Specific effects of microRNAs on the plant transcriptome. *Dev. Cell* 8, 517–527.

Schwarz, S., Grande, A. V., Bujdoso, N., Saedler, H., and Huijser, P. (2008). The microRNA regulated SBP-box genes SPL9 and SPL15 control shoot maturation in Arabidopsis. *Plant Mol. Biol.* 67, 183–195.

SharathKumar, M., Heuvelink, E., and Marcelis, L. F. M. (2020). Vertical farming: moving from genetic to environmental modification. *Trends Plant Sci.* 25, 724–727.

Takase, T., Nishiyama, Y., Tanihigashi, H., Ogura, Y., Miyazaki, Y., Yamada, Y., and Kiyosue, T. (2011). LOV KELCH PROTEIN2 and ZEITLUPE repress Arabidopsis photoperiodic flowering under non-inductive conditions, dependent



- on FLAVIN-BINDING KELCH REPEAT F - BOX1. *Plant J.* 67, 608–621.
- Telfer, A., Bollman, K. M., and Poethig, R. S.** (1997). Phase change and the regulation of trichome distribution in *Arabidopsis thaliana*. *Development* 124, 645–654.
- Teotia, S., and Tang, G.** (2015). To bloom or not to bloom: Role of microRNAs in plant flowering. *Mol. Plant* 8, 359–377.
- Thomas, B.** (2006). Light signals and flowering. *J. Exp. Bot.* 57, 3387–3393.
- Valverde, F., Mouradov, A., Soppe, W., Ravenscroft, D., Samach, A., and Coupland, G.** (2004). Photoreceptor regulation of CONSTANS protein in photoperiodic flowering. *Science* 303, 1003–1006.
- Wang, J. W., Schwab, R., Czech, B., Mica, E., and Weigel, D.** (2008). Dual effects of miR156-targeted SPL genes and CYP78A5/KLUH on plastochron length and organ size in *Arabidopsis thaliana*. *Plant Cell* 20, 1231–1243.
- Warnasooriya, S. N., Porter, K. J., and Montgomery, B. L.** (2011). Tissue- and isoform-specific phytochrome regulation of light-dependent anthocyanin accumulation in *Arabidopsis thaliana*. *Plant Signal. Behav.* 6, 624–631.
- Wigge, P. A., Kim, M. C., Jaeger, K. E., Busch, W., Schmid, M., Lohmann, J. U., and Weigel, D.** (2005). Integration of spatial and temporal information during floral induction in *Arabidopsis*. *Science* 309, 1056–1059.
- Wu, F., and Hanzawa, Y.** (2014). Photoperiodic control of flowering in plants. *Handbook of plant and crop physiology* 121–138.
- Wu, G., Park, M. Y., Conway, S. R., Wang, J. W., Weigel, D., and Poethig, R. S.** (2009). The sequential action of miR156 and miR172 regulates developmental timing in *Arabidopsis*. *Cell* 138, 750–759.
- Xie, Y., Liu, Y., Wang, H., Ma, X., Wang, B., Wu, G., and Wang, H.** (2017). Phytochrome-interacting factors directly suppress MIR156 expression to enhance shade-avoidance syndrome in *Arabidopsis*. *Nat. Commun.* 8, 348.
- Xie, Y., Zhou, Q., Zhao, Y., Li, Q., Liu, Y., Ma, M., Wang, B., Shen, R., Zheng, Z., and Wang, H.** (2020). FHY3 and FAR1 integrate light signals with the miR156-SPL module-mediated aging pathway to regulate *Arabidopsis*



Chapter 5: Light quality regulates flowering

flowering. *Mol. Plant* 13, 483–498.

- Yang, S., Weers, B. D., Morishige, D. T., and Mullet, J. E.** (2014). CONSTANS is a photoperiod regulated activator of flowering in sorghum. *BMC Plant Biol.* 14, 1–15.
- Yano, M., Katayose, Y., Ashikari, M., Yamanouchi, U., Monna, L., Fuse, T., Baba, T., Yamamoto, K., Umehara, Y., Nagamura, Y. and Sasaki, T.** (2000). Hd1, a major photoperiod sensitivity quantitative trait locus in rice, is closely related to the Arabidopsis flowering time gene CONSTANS. *Plant Cell* 12, 2473–2483.
- Yoshida, S., Mandel, T., and Kuhlemeier, C.** (2011). Stem cell activation by light guides plant organogenesis. *Genes Dev.* 25, 1439–1450.
- Zhang, X., Zou, Z., Zhang, J., Zhang, Y., Han, Q., Hu, T., Xu, X., Liu, H., Li, H., and Ye, Z.** (2011). Over-expression of sly-miR156a in tomato results in multiple vegetative and reproductive trait alterations and partial phenocopy of the sft mutant. *FEBS Lett.* 585, 435–439.
- Zheng, C., Ye, M., Sang, M., and Wu, R.** (2019). A regulatory network for mir156-spl module in *Arabidopsis thaliana*. *Int. J. Mol. Sci.* 20, 6166.



Supplementary Material (Tables S1-S3 and Figure S1-S3)

Table S1: Plant lines used in this study.

Arabidopsis, tomato, and lettuce seeds were obtained from Nottingham Arabidopsis Stock Centre (NASC), Tomato Genetics Resource Centre (TGRC), and HortiTops, respectively.

PLANT LINE	DESCRIPTION	SOURCE	REFERENCE
Columbia (Col-0)	Natural Arabidopsis ecotype	-	Koncz et al., 1992
Moneymaker (MM)	Standard non-hybrid tomato cultivar	TGRC	-
Meikoningin (MK)	Long-day lettuce cultivar	HortiTops	-
Gaardenier (GD)	Day-neutral lettuce cultivar	HortiTops	-
<i>phyA</i> (SALK_014575)	T-DNA insertion in At1g09570	NASC	Ruckle et al., 2007
<i>phyB</i> (SALK_022035)	T-DNA insertion in At2g18790	NASC	Mayfield et al., 2007
<i>phyC</i> (<i>phyC-3</i>)	3 kbp deletion in At5g35840	NASC	Monte et al., 2003
<i>phyD</i> (SALK_027956)	T-DNA insertion in At4g16250	NASC	Christians et al., 2012
<i>phyE</i> (SALK_092529)	T-DNA insertion in At4g18130	NASC	Warnasooriya et al., 2011
<i>ztl</i> (SALK_069091)	T-DNA insertion in At5g57360	NASC	Martin-Tryon et al., 2007
<i>fkf1</i> (SALK_059480)	T-DNA insertion in At1g68050	NASC	Cheng and Wang, 2005
<i>lkp2</i> (SALK_036083)	T-DNA insertion in At2g18915	NASC	Takase et al., 2011
<i>spl9 spl15</i>	Double mutant in At2g42200 and At3g57920	NASC	Schwarz et al., 2008
<i>p35S::miR156b</i>	Overexpression of <i>miR156</i> in Col-0	NASC	Schwab et al., 2005
<i>p35S::MIM156</i>	Overexpression of <i>miR156</i> target mimic in Col-0	NASC	Franco-Zorrilla et al., 2007
<i>pDR5::GFP</i>	Synthetic auxin-responsive reporter in Col-0	-	Ottenschläger et al., 2003



Chapter 5: Light quality regulates flowering

<i>pDR5::YFP</i>	Synthetic auxin-responsive reporter in tomato M82	Kuhlemeier	Ben-Gera et al., 2012
------------------	---------------------------------------------------	------------	-----------------------

Table S2: Primers used in this study.

PRIMER NAME	TARGET GENE	SEQUENCE 5' → 3'	EXPERIMENT
LB1 (SAIL T-DNA)	N/A	GCCTTTTCAGAA ATGGATAAATA	Genotyping
LBb1.3 (SALK T-DNA)	N/A	ATTTTGCCGATT TCGGAAC	Genotyping
<i>phyA</i> FW	At1g09570	CCAGTCAGCTCA GCAATTTTC	Genotyping
<i>phyA</i> RV	At1g09570	AATGCAAAACAT GCTAGGGTG	Genotyping
<i>phyB</i> FW	At2g18790	CATCATCAGCAT CATGTCACC	Genotyping
<i>phyB</i> RV	At2g18790	TTCACGAAGGCA AAAGAGTTG	Genotyping
<i>phyC</i> FW	At5g35840	ATGTCATCGAAC ACTTCACG	Genotyping
<i>phyC</i> RV	At5g35840	TCAAATCAAGGG AAATTCTG	Genotyping
<i>phyD</i> FW	At4g16250	AACCCGGTAGAA TCAGAATGG	Genotyping
<i>phyD</i> RV	At4g16250	ATCGGTTACAGT GAAAATGCG	Genotyping
<i>phyE</i> FW	At4g18130	AAAGAGGCGGT CTAGTTCAGC	Genotyping
<i>phyE</i> RV	At4g18130	TATCAGTGGTTA AACCCGTCG	Genotyping
<i>ztl</i> FW	At5g57360	GGACCGTTTGCT AAAAGAAGG	Genotyping
<i>ztl</i> RV	At5g57360	GTGTCACTTAGA AGAACGCCG	Genotyping
<i>fkf1</i> FW	At1g68050	GCATGGTCGAGT AACAAGGAG	Genotyping
<i>fkf1</i> RV	At1g68050	TGATGCAGAGTG	Genotyping



<i>lkp2</i> FW	At2g18915	TCCTGAGTG GGAGATCCATCT TTCCGAAAG	Genotyping
<i>lkp2</i> RV	At2g18915	CTCTTTTCTTCGC TCGATTCC	Genotyping
<i>spl9</i> FW	At2g42200	TGGTTCCTCCACT GAGTCATC	Genotyping
<i>spl9</i> RV	At2g42200	GCTCATTATGAC CAGCGAGTC	Genotyping
<i>spl15</i> FW	At3g57920	TGTTGGTGTCTG AAGTTGCTG	Genotyping
<i>spl15</i> RV	At3g57920	TCCACCGAGTCT TCTTCACTC	Genotyping
SnoR101 RV		AGCATCAGCAGA CCAGTAGTT	RT miRNA
miR156 FW-RT	At2g25095	GTCGTATCCAGTG CAGGGTCCGAGGT ATTCGCACTGGAT ACGACGTGCTCA	RT miRNA
miR172 FW-RT	At5g04275	GTCGTATCCAGTG CAGGGTCCGAGGT ATTCGCACTGGAT ACGACATGCAG	RT miRNA
PP2A-3 FW	At2g42500	ACGTGGCCAAAA TGATGCAA	qRT-PCR
PP2A-3 RV	At2g42500	TCATGTTCTCCAC AACCGCT	qRT-PCR
GIGANTEA FW	At1g22770	GGGTAAATATGC TGCTGGAGA	qRT-PCR
GIGANTEA RV	At1g22770	CAGTATGACACC AGCTCCATT	qRT-PCR
CONSTANS FW	At5g15840	CTACAACGACAA TGGTTCCATTAAC	qRT-PCR
CONSTANS RV	At5g15840	CAGGGTCAGGTT GTTGC	qRT-PCR
FT FW	At1g65480	CTGGAACAACCT TTGGCAAT	qRT-PCR
FT RV	At1g65480	TACACTGTTTGCC TGCCAAG	qRT-PCR
miR156-A FW	At2g25095	CTTCGTTCTCTAT GTCTCAATCTCTC	qRT-PCR
miR156-A RV	At2g25095	TGATTAAAGGCT	qRT-PCR



Chapter 5: Light quality regulates flowering

		AAAGGTCTCCTC	
miR172-B FW	At5g04275	TTTCTCAAGCTTTA GGTATTTGTAG	qRT-PCR
miR172-B RV	At5g04275	TCGGCGGATCCATG GAAGAAAGCTC	qRT-PCR
AHL15 FW	At3g55560	AAGAGCAGCCGCTT CAACTA	qRT-PCR
AHL15 RV	At3g55560	TGTTGAGCCATTTGA TGACC	qRT-PCR
SPL2 FW	At5g43270	TTTCCGATACCGAGC ACAATAG	qRT-PCR
SPL2 RV	At5g43270	TACGGGTTGGAGGTT GCTTGAGG	qRT-PCR
SPL3 FW	At2g33810	ATGAGTATGAGAAGA AGCAAAGCG	qRT-PCR
SPL3 RV	At2g33810	TCCACTACTACTTGTA GCTTTACCT	qRT-PCR
SPL4 FW	At1g53160	TCAAGGGTAGAGATG ACACTTCCTAT	qRT-PCR
SPL4 RV	At1g53160	TCTCCTTCGTGGCTCT GAAACTTC	qRT-PCR
SPL5 FW	At3g15270	CGATAGGTGCACTGTT AATTTGACT	qRT-PCR
SPL5 RV	At3g15270	TCTGGTAGCTCATGAA ACCTGCTGCA	qRT-PCR
SPL6 FW	At1g69170	ACAGTGCAGCAGGTTT CATTTCTC	qRT-PCR
SPL6 RV	At1g69170	CTCCAGAACTTGTTG CCTACTAC	qRT-PCR
SPL9 FW	At2g42200	AATTGGCGACTCAAAC TGTG	qRT-PCR
SPL9 RV	At2g42200	CTGAAGAAGCTCGCC ATGTA	qRT-PCR
SPL10 FW	At1g27370	CAGACAAAGGTGTGG GAGAATGCTC	qRT-PCR
SPL10 RV	At1g27370	TAGGGAAAGTGCCAA ATATTGGCG	qRT-PCR
SPL11 FW	At1g27360	AGTCCAAGTTTCAACT TCATGGCG	qRT-PCR
SPL11 RV	At1g27360	GAACAGAGTAGAGAA AATGGCTGC	qRT-PCR
SPL13 FW	At5g50570	GCTCGAGAACCGCAT	qRT-PCR



		CGTT	
SPL13 RV	At5g50570	CCCGTAAAAAAC TGTCTCAACTGCT	qRT-PCR
SPL15 FW	At3g57920	TGAATGTTTTATC ACATGGAAGCTC	qRT-PCR
SPL15 RV	At3g57920	TCATCGAGTCGAA ACCAGAAGATG	qRT-PCR
SOC1 FW	At3g57920	ATAGGAACATGCT CAATCGAGGAGCTG	qRT-PCR
SOC1 RV	At3g57920	TTTCTTGAAGAAC AAGGTAACCCAATG	qRT-PCR

Table S3: Standard errors and p-values.

In some figures, error bars and statistics were not included in the graphs for presentation purposes. These values are listed in the table below. Significance indicates whether or not red or blue LED conditions are significantly different from white LED conditions, based on a two-sided Student's *t*-test ($p < 0.05$). Abbreviations that are used: Standard error (SE), Zeitgeber time (ZT); not available (N/A); days after germination (DAG); and phytochrome B mutant (*phyB*).

FIGURE	DATA POINT	MEAN \pm SE	SIGNIFICANCE	P-VALUE
3B	ZT0-WHITE	0.138 \pm 0.025	N/A	N/A
3B	ZT3-WHITE	0.233 \pm 0.046	N/A	N/A
3B	ZT6-WHITE	0.408 \pm 0.030	N/A	N/A
3B	ZT9-WHITE	0.861 \pm 0.073	N/A	N/A
3B	ZT12-WHITE	0.557 \pm 0.031	N/A	N/A
3B	ZT15-WHITE	0.175 \pm 0.049	N/A	N/A
3B	ZT18-WHITE	0.235 \pm 0.026	N/A	N/A
3B	ZT21-WHITE	0.105 \pm 0.003	N/A	N/A
3B	ZT24-WHITE	0.102 \pm 0.009	N/A	N/A
3B	ZT0-RED	0.184 \pm 0.040	No	0.479
3B	ZT3-RED	0.249 \pm 0.046	No	0.849
3B	ZT6-RED	0.328 \pm 0.047	Yes	0.041
3B	ZT9-RED	0.531 \pm 0.072	Yes	0.006
3B	ZT12-RED	0.559 \pm 0.051	No	0.976
3B	ZT15-RED	0.274 \pm 0.015	No	0.191
3B	ZT18-RED	0.154 \pm 0.008	No	0.073



Chapter 5: Light quality regulates flowering

3B	ZT21-RED	0.157±0.018	No	0.086
3B	ZT24-RED	0.137±0.008	No	0.088
3B	ZT0-BLUE	0.208±0.030	No	0.222
3B	ZT3-BLUE	0.366±0.021	Yes	0.039
3B	ZT6-BLUE	0.923±0.073	Yes	0.00081
3B	ZT9-BLUE	1.446±0.181	Yes	0.00094
3B	ZT12-BLUE	0.719±0.028	Yes	0.034
3B	ZT15-BLUE	0.293±0.036	No	0.186
3B	ZT18-BLUE	0.175±0.022	No	0.228
3B	ZT21-BLUE	0.139±0.016	No	0.159
3B	ZT24-BLUE	0.165±0.009	No	0.172
3C	ZT0-WHITE	0.324±0.048	N/A	N/A
3C	ZT3-WHITE	0.189±0.036	N/A	N/A
3C	ZT6-WHITE	0.133±0.005	N/A	N/A
3C	ZT9-WHITE	0.209±0.031	N/A	N/A
3C	ZT12-WHITE	0.351±0.005	N/A	N/A
3C	ZT15-WHITE	0.279±0.050	N/A	N/A
3C	ZT18-WHITE	0.426±0.019	N/A	N/A
3C	ZT21-WHITE	0.301±0.005	N/A	N/A
3C	ZT24-WHITE	0.233±0.027	N/A	N/A
3C	ZT0-RED	0.392±0.055	No	0.491
3C	ZT3-RED	0.302±0.039	Yes	0.047
3C	ZT6-RED	0.286±0.050	Yes	0.008
3C	ZT9-RED	0.240±0.032	No	0.604
3C	ZT12-RED	0.299±0.012	Yes	0.039
3C	ZT15-RED	0.311±0.039	No	0.103
3C	ZT18-RED	0.359±0.040	Yes	0.013
3C	ZT21-RED	0.324±0.026	No	0.319
3C	ZT24-RED	0.261±0.007	No	0.154
3C	ZT0-BLUE	0.484±0.043	Yes	0.041
3C	ZT3-BLUE	0.354±0.047	Yes	0.022
3C	ZT6-BLUE	0.319±0.025	No	0.114
3C	ZT9-BLUE	0.279±0.011	No	0.159
3C	ZT12-BLUE	0.453±0.048	Yes	0.004
3C	ZT15-BLUE	0.358±0.033	Yes	0.034
3C	ZT18-BLUE	0.532±0.041	Yes	0.007
3C	ZT21-BLUE	0.426±0.016	Yes	0.009
3C	ZT24-BLUE	0.357±0.017	Yes	0.009
3D	ZT0-WHITE	0.053±0.011	N/A	N/A
3D	ZT3-WHITE	0.071±0.003	N/A	N/A
3D	ZT6-WHITE	0.063±0.007	N/A	N/A
3D	ZT9-WHITE	0.038±0.004	N/A	N/A



3D	ZT12-WHITE	0.081±0.008	N/A	N/A
3D	ZT15-WHITE	0.291±0.017	N/A	N/A
3D	ZT18-WHITE	0.115±0.014	N/A	N/A
3D	ZT21-WHITE	0.094±0.026	N/A	N/A
3D	ZT24-WHITE	0.054±0.007	N/A	N/A
3D	ZT0-RED	0.007±0.0002	Yes	0.025
3D	ZT3-RED	0.013±0.002	Yes	0.0002
3D	ZT6-RED	0.016±0.001	Yes	0.007
3D	ZT9-RED	0.012±0.002	Yes	0.007
3D	ZT12-RED	0.025±0.003	Yes	0.007
3D	ZT15-RED	0.028±0.002	Yes	0.002
3D	ZT18-RED	0.039±0.006	Yes	0.016
3D	ZT21-RED	0.032±0.0004	Yes	0.024
3D	ZT24-RED	0.008±0.002	Yes	0.007
3D	ZT0-BLUE	0.179±0.011	Yes	0.003
3D	ZT3-BLUE	0.401±0.048	Yes	0.005
3D	ZT6-BLUE	0.364±0.033	Yes	0.002
3D	ZT9-BLUE	0.229±0.014	Yes	0.039
3D	ZT12-BLUE	0.539±0.016	Yes	0.003
3D	ZT15-BLUE	0.798±0.026	Yes	0.001
3D	ZT18-BLUE	1.258±0.076	Yes	0.0003
3D	ZT21-BLUE	0.355±0.083	Yes	0.006
3D	ZT24-BLUE	0.079±0.011	No	0.193
5A	5 DAG-WHITE	0.277±0.012	N/A	N/A
5A	10 DAG-WHITE	0.248±0.029	N/A	N/A
5A	15 DAG-WHITE	0.223±0.0007	N/A	N/A
5A	5 DAG-RED	0.299±0.067	No	0.807
5A	10 DAG-RED	0.251±0.006	No	0.550
5A	15 DAG-RED	0.214±0.038	No	0.861
5A	5 DAG-BLUE	0.201±0.016	Yes	0.003
5A	10 DAG-BLUE	0.167±0.004	Yes	0.002
5A	15 DAG-BLUE	0.102±0.009	Yes	0.001
5B	5 DAG-WHITE	0.007±0.0004	N/A	N/A
5B	10 DAG-WHITE	0.014±0.0007	N/A	N/A
5B	15 DAG-WHITE	0.025±0.0007	N/A	N/A
5B	5 DAG-RED	0.007±0.0004	No	0.791
5B	10 DAG-RED	0.014±0.0008	No	0.326
5B	15 DAG-RED	0.021±0.001	No	0.530
5B	5 DAG-BLUE	0.038±0.008	Yes	0.0009
5B	10 DAG-BLUE	0.045±0.003	Yes	0.0008
5B	15 DAG-BLUE	0.057±0.004	Yes	0.0008
5C	5 DAG-WHITE	1.023±0.036	N/A	N/A



Chapter 5: Light quality regulates flowering

5C	10 DAG-WHITE	1.478±0.062	N/A	N/A
5C	15 DAG-WHITE	2.174±0.026	N/A	N/A
5C	5 DAG-RED	1.588±0.169	Yes	0.009
5C	10 DAG-RED	1.910±0.091	Yes	0.027
5C	15 DAG-RED	2.355±0.258	No	0.601
5C	5 DAG-BLUE	1.071±0.037	No	0.485
5C	10 DAG-BLUE	1.539±0.066	No	0.217
5C	15 DAG-BLUE	2.422±0.506	No	0.709
5D	5 DAG-WHITE	1.038±0.002	N/A	N/A
5D	10 DAG-WHITE	1.173±0.028	N/A	N/A
5D	15 DAG-WHITE	1.363±0.135	N/A	N/A
5D	5 DAG-RED	0.956±0.217	No	0.697
5D	10 DAG-RED	1.149±0.132	No	0.821
5D	15 DAG-RED	1.268±0.104	No	0.669
5D	5 DAG-BLUE	1.892±0.176	Yes	0.0009
5D	10 DAG-BLUE	2.314±0.095	Yes	0.0008
5D	15 DAG-BLUE	2.701±0.509	Yes	0.0009
5E	5 DAG-WHITE	0.104±0.008	N/A	N/A
5E	10 DAG-WHITE	0.154±0.007	N/A	N/A
5E	15 DAG-WHITE	0.249±0.016	N/A	N/A
5E	5 DAG-RED	0.110±0.031	No	0.884
5E	10 DAG-RED	0.148±0.018	No	0.912
5E	15 DAG-RED	0.191±0.016	No	0.101
5E	5 DAG-BLUE	0.149±0.007	Yes	0.024
5E	10 DAG-BLUE	0.397±0.022	Yes	0.0009
5E	15 DAG-BLUE	0.548±0.030	Yes	0.0007
5F	5 DAG-WHITE	0.311±0.041	N/A	N/A
5F	10 DAG-WHITE	0.751±0.033	N/A	N/A
5F	15 DAG-WHITE	0.795±0.043	N/A	N/A
5F	5 DAG-RED	0.329±0.087	No	0.889
5F	10 DAG-RED	0.481±0.033	Yes	0.007
5F	15 DAG-RED	0.528±0.027	Yes	0.013
5F	5 DAG-BLUE	0.469±0.048	Yes	0.041
5F	10 DAG-BLUE	1.057±0.018	Yes	0.003
5F	15 DAG-BLUE	0.966±0.084	Yes	0.031
5G	5 DAG-WHITE	0.254±0.021	N/A	N/A
5G	10 DAG-WHITE	0.548±0.017	N/A	N/A
5G	15 DAG-WHITE	0.785±0.004	N/A	N/A
5G	5 DAG-RED	0.214±0.038	No	0.499
5G	10 DAG-RED	0.457±0.052	No	0.628
5G	15 DAG-RED	0.631±0.051	No	0.561



5G	5 DAG-BLUE	0.534±0.064	Yes	0.024
5G	10 DAG-BLUE	1.375±0.074	Yes	0.0007
5G	15 DAG-BLUE	1.405±0.148	Yes	0.0008
5H	5 DAG-WHITE	0.436±0.006	N/A	N/A
5H	10 DAG-WHITE	0.548±0.046	N/A	N/A
5H	15 DAG-WHITE	1.402±0.060	N/A	N/A
5H	5 DAG-RED	0.546±0.078	No	0.317
5H	10 DAG-RED	0.518±0.006	No	0.628
5H	15 DAG-RED	1.585±0.159	No	0.431
5H	5 DAG-BLUE	0.506±0.055	No	0.357
5H	10 DAG-BLUE	0.357±0.031	No	0.217
5H	15 DAG-BLUE	1.184±0.046	No	0.079
5I	5 DAG-WHITE	0.066±0.007	N/A	N/A
5I	10 DAG-WHITE	0.076±0.002	N/A	N/A
5I	15 DAG-WHITE	0.097±0.004	N/A	N/A
5I	5 DAG-RED	0.069±0.015	No	0.873
5I	10 DAG-RED	0.089±0.011	No	0.572
5I	15 DAG-RED	0.093±0.006	No	0.512
5I	5 DAG-BLUE	0.152±0.009	Yes	0.0005
5I	10 DAG-BLUE	0.165±0.007	Yes	0.0008
5I	15 DAG-BLUE	0.183±0.013	Yes	0.0006
6A	10 DAG-WHITE	1.173±0.028	N/A	N/A
6A	15 DAG-WHITE	1.363±0.135	N/A	N/A
6A	20 DAG-WHITE	2.766±0.125	N/A	N/A
6A	25 DAG-WHITE	3.089±0.049	N/A	N/A
6A	10 DAG-RED	1.149±0.132	No	0.821
6A	15 DAG-RED	1.268±0.104	No	0.669
6A	20 DAG-RED	2.676±0.007	No	0.588
6A	25 DAG-RED	2.727±0.051	No	0.371
6A	10 DAG-BLUE	2.314±0.095	Yes	0.0008
6A	15 DAG-BLUE	2.701±0.509	Yes	0.0009
6A	20 DAG-BLUE	3.663±0.133	Yes	0.0009
6A	25 DAG-BLUE	1.968±0.021	Yes	0.0006
6B	10 DAG-WHITE	0.071±0.0004	N/A	N/A
6B	15 DAG-WHITE	0.231±0.002	N/A	N/A
6B	20 DAG-WHITE	0.847±0.047	N/A	N/A
6B	25 DAG-WHITE	0.869±0.028	N/A	N/A
6B	10 DAG-RED	0.085±0.005	No	0.672
6B	15 DAG-RED	0.182±0.038	No	0.353
6B	20 DAG-RED	0.626±0.068	No	0.095
6B	25 DAG-RED	0.847±0.048	No	0.749



Chapter 5: Light quality regulates flowering

6B	10 DAG-BLUE	0.219±0.004	Yes	0.021
6B	15 DAG-BLUE	0.404±0.026	Yes	0.017
6B	20 DAG-BLUE	1.996±0.036	Yes	0.0007
6B	25 DAG-BLUE	1.392±0.028	Yes	0.003
6C	10 DAG-WHITE	0.154±0.007	N/A	N/A
6C	15 DAG-WHITE	0.249±0.016	N/A	N/A
6C	20 DAG-WHITE	0.329±0.012	N/A	N/A
6C	25 DAG-WHITE	0.395±0.020	N/A	N/A
6C	10 DAG-RED	0.148±0.018	No	0.912
6C	15 DAG-RED	0.191±0.016	No	0.101
6C	20 DAG-RED	0.196±0.019	No	0.124
6C	25 DAG-RED	0.285±0.018	No	0.219
6C	10 DAG-BLUE	0.397±0.022	Yes	0.0009
6C	15 DAG-BLUE	0.548±0.030	Yes	0.0007
6C	20 DAG-BLUE	0.597±0.005	Yes	0.008
6C	25 DAG-BLUE	0.623±0.017	Yes	0.005
6D	10 DAG-WHITE	0.751±0.033	N/A	N/A
6D	15 DAG-WHITE	0.795±0.043	N/A	N/A
6D	20 DAG-WHITE	0.617±0.041	N/A	N/A
6D	25 DAG-WHITE	0.617±0.008	N/A	N/A
6D	10 DAG-RED	0.481±0.033	Yes	0.007
6D	15 DAG-RED	0.528±0.027	Yes	0.013
6D	20 DAG-RED	0.474±0.020	No	0.065
6D	25 DAG-RED	0.494±0.015	No	0.078
6D	10 DAG-BLUE	1.057±0.018	Yes	0.003
6D	15 DAG-BLUE	0.966±0.084	Yes	0.031
6D	20 DAG-BLUE	0.759±0.024	No	0.072
6D	25 DAG-BLUE	0.503±0.037	No	0.077
6E	10 DAG-WHITE	0.548±0.017	N/A	N/A
6E	15 DAG-WHITE	0.785±0.004	N/A	N/A
6E	20 DAG-WHITE	0.579±0.041	N/A	N/A
6E	25 DAG-WHITE	0.811±0.039	N/A	N/A
6E	10 DAG-RED	0.457±0.052	No	0.628
6E	15 DAG-RED	0.631±0.051	No	0.561
6E	20 DAG-RED	0.514±0.037	No	0.338
6E	25 DAG-RED	0.586±0.020	No	0.092
6E	10 DAG-BLUE	1.375±0.074	Yes	0.0007
6E	15 DAG-BLUE	1.405±0.148	Yes	0.0008
6E	20 DAG-BLUE	0.685±0.016	No	0.081
6E	25 DAG-BLUE	0.716±0.032	No	0.192
6F	10 DAG-WHITE	0.076±0.002	N/A	N/A



6F	15 DAG-WHITE	0.097±0.004	N/A	N/A
6F	20 DAG-WHITE	0.127±0.003	N/A	N/A
6F	25 DAG-WHITE	0.361±0.007	N/A	N/A
6F	10 DAG-RED	0.089±0.011	No	0.572
6F	15 DAG-RED	0.093±0.006	No	0.512
6F	20 DAG-RED	0.109±0.012	No	0.299
6F	25 DAG-RED	0.312±0.022	No	0.163
6F	10 DAG-BLUE	0.165±0.007	Yes	0.0008
6F	15 DAG-BLUE	0.183±0.013	Yes	0.0006
6F	20 DAG-BLUE	0.371±0.004	Yes	0.0004
6F	25 DAG-BLUE	0.601±0.003	Yes	0.0003
6G	5 DAG-WHITE	0.0005±0.0001	N/A	N/A
6G	10 DAG-WHITE	0.0024±0.0009	N/A	N/A
6G	15 DAG-WHITE	0.0260±0.008	N/A	N/A
6G	20 DAG-WHITE	0.6470±0.087	N/A	N/A
6G	25 DAG-WHITE	0.8650±0.167	N/A	N/A
6G	5 DAG-RED	0.0003±0.0001	No	0.388
6G	10 DAG-RED	0.0005±0.0002	No	0.071
6G	15 DAG-RED	0.0007±0.0002	Yes	0.008
6G	20 DAG-RED	0.0011±0.0003	Yes	0.0009
6G	25 DAG-RED	0.0021±0.0002	Yes	0.0006
6G	5 DAG-BLUE	0.0009±0.0001	No	0.094
6G	10 DAG-BLUE	0.0050±0.001	No	0.127
6G	15 DAG-BLUE	0.8950±0.086	Yes	0.0005
6G	20 DAG-BLUE	1.7390±0.288	Yes	0.0004
6G	25 DAG-BLUE	0.2290±0.059	Yes	0.007
6H	5 DAG-WHITE	0.076±0.008	N/A	N/A
6H	10 DAG-WHITE	0.199±0.011	N/A	N/A
6H	15 DAG-WHITE	0.503±0.093	N/A	N/A
6H	20 DAG-WHITE	1.176±0.275	N/A	N/A
6H	25 DAG-WHITE	2.095±0.522	N/A	N/A
6H	5 DAG-RED	0.059±0.009	No	0.783
6H	10 DAG-RED	0.151±0.029	No	0.668
6H	15 DAG-RED	0.176±0.044	Yes	0.03
6H	20 DAG-RED	0.433±0.092	Yes	0.02
6H	25 DAG-RED	0.617±0.113	Yes	0.007
6H	5 DAG-BLUE	0.072±0.007	No	0.924
6H	10 DAG-BLUE	0.253±0.029	No	0.645
6H	15 DAG-BLUE	1.430±0.466	Yes	0.006
6H	20 DAG-BLUE	4.320±0.942	Yes	0.0004
6H	25 DAG-BLUE	2.545±0.618	No	0.781
7B	10 DAG-BLUE	0.251±0.029	N/A	N/A



Chapter 5: Light quality regulates flowering

7B	15 DAG-BLUE	0.337±0.027	N/A	N/A
7B	20 DAG-BLUE	1.253±0.166	N/A	N/A
7B	25 DAG-BLUE	0.219±0.031	No	0.481
7B	<i>phyB</i> 10 DAG-RED	0.349±0.041	No	0.844
7B	<i>phyB</i> 15 DAG-RED	1.081±0.129	Yes	0.006
7B	<i>phyB</i> 5 DAG-BLUE	0.249±0.021	No	0.911
7B	<i>phyB</i> 10 DAG-BLUE	0.382±0.066	No	0.625
7B	<i>phyB</i> 15 DAG-BLUE	1.492±0.063	No	0.073
7C	<i>phyB</i> 5 DAG-WHITE	0.381±0.041	N/A	N/A
7C	<i>phyB</i> 10 DAG-WHITE	0.309±0.005	N/A	N/A
7C	<i>phyB</i> 15 DAG-WHITE	0.252±0.026	N/A	N/A
7C	<i>phyB</i> 5 DAG-RED	0.394±0.052	No	0.812
7C	<i>phyB</i> 10 DAG-RED	0.304±0.012	No	0.772
7C	<i>phyB</i> 15 DAG-RED	0.222±0.044	No	0.544
7C	<i>phyB</i> 5 DAG-BLUE	0.388±0.052	No	0.851
7C	<i>phyB</i> 10 DAG-BLUE	0.343±0.020	No	0.592
7C	<i>phyB</i> 15 DAG-BLUE	0.226±0.052	No	0.492
7D	<i>phyB</i> 5 DAG-WHITE	0.031±0.003	N/A	N/A
7D	<i>phyB</i> 10 DAG-WHITE	0.056±0.009	N/A	N/A
7D	<i>phyB</i> 15 DAG-WHITE	0.156±0.044	N/A	N/A
7D	<i>phyB</i> 5 DAG-RED	0.029±0.008	No	0.932
7D	<i>phyB</i> 10 DAG-RED	0.054±0.019	No	0.873



7D	<i>phyB</i> 15 DAG-RED	0.129±0.013	No	0.684
7D	<i>phyB</i> 5 DAG-BLUE	0.035±0.006	No	0.889
7D	<i>phyB</i> 10 DAG-BLUE	0.059±0.003	No	0.932
7D	<i>phyB</i> 15 DAG-BLUE	0.118±0.009	No	0.425
7E	<i>phyB</i> 5 DAG-WHITE	1.216±0.024	N/A	N/A
7E	<i>phyB</i> 10 DAG-WHITE	1.301±0.055	N/A	N/A
7E	<i>phyB</i> 15 DAG-WHITE	1.382±0.020	N/A	N/A
7E	<i>phyB</i> 5 DAG-RED	1.195±0.056	No	0.728
7E	<i>phyB</i> 10 DAG-RED	1.326±0.058	No	0.814
7E	<i>phyB</i> 15 DAG-RED	1.296±0.121	No	0.595
7E	<i>phyB</i> 5 DAG-BLUE	1.241±0.071	No	0.526
7E	<i>phyB</i> 10 DAG-BLUE	1.339±0.059	No	0.732
7E	<i>phyB</i> 15 DAG-BLUE	1.237±0.137	No	0.439
7F	<i>phyB</i> 5 DAG-WHITE	0.205±0.037	N/A	N/A
7F	<i>phyB</i> 10 DAG-WHITE	0.306±0.053	N/A	N/A
7F	<i>phyB</i> 15 DAG-WHITE	0.488±0.051	N/A	N/A
7F	<i>phyB</i> 5 DAG-RED	0.197±0.035	No	0.466
7F	<i>phyB</i> 10 DAG-RED	0.219±0.046	No	0.329
7F	<i>phyB</i> 15 DAG-RED	0.442±0.021	No	0.523
7F	<i>phyB</i> 5 DAG-BLUE	0.219±0.031	No	0.782
7F	<i>phyB</i> 10 DAG-BLUE	0.349±0.029	No	0.583



Chapter 5: Light quality regulates flowering

7F	<i>phyB</i> 15 DAG-BLUE	0.434±0.045	No	0.551
7G	<i>phyB</i> 5 DAG-WHITE	0.199±0.062	N/A	N/A
7G	<i>phyB</i> 10 DAG-WHITE	0.314±0.031	N/A	N/A
7G	<i>phyB</i> 15 DAG-WHITE	0.326±0.051	N/A	N/A
7G	<i>phyB</i> 5 DAG-RED	0.128±0.037	No	0.417
7G	<i>phyB</i> 10 DAG-RED	0.203±0.024	Yes	0.007
7G	<i>phyB</i> 15 DAG-RED	0.212±0.062	Yes	0.006
7G	<i>phyB</i> 5 DAG-BLUE	0.187±0.018	No	0.622
7G	<i>phyB</i> 10 DAG-BLUE	0.372±0.029	No	0.185
7G	<i>phyB</i> 15 DAG-BLUE	0.387±0.023	No	0.172
7H	<i>phyB</i> 5 DAG-WHITE	0.247±0.044	N/A	N/A
7H	<i>phyB</i> 10 DAG-WHITE	0.462±0.014	N/A	N/A
7H	<i>phyB</i> 15 DAG-WHITE	0.681±0.145	N/A	N/A
7H	<i>phyB</i> 5 DAG-RED	0.223±0.066	No	0.483
7H	<i>phyB</i> 10 DAG-RED	0.398±0.039	No	0.273
7H	<i>phyB</i> 15 DAG-RED	0.679±0.072	No	0.993
7H	<i>phyB</i> 5 DAG-BLUE	0.239±0.051	No	0.728
7H	<i>phyB</i> 10 DAG-BLUE	0.442±0.033	No	0.681
7H	<i>phyB</i> 15 DAG-BLUE	0.673±0.168	No	0.978
7I	<i>phyB</i> 5 DAG-WHITE	0.092±0.005	N/A	N/A
7I	<i>phyB</i> 10 DAG-WHITE	0.148±0.007	N/A	N/A



7I	<i>phyB</i> 15 DAG-WHITE	0.217±0.069	N/A	N/A
7I	<i>phyB</i> 5 DAG-RED	0.087±0.004	No	0.726
7I	<i>phyB</i> 10 DAG-RED	0.118±0.007	No	0.087
7I	<i>phyB</i> 15 DAG-RED	0.208±0.029	No	0.928
7I	<i>phyB</i> 5 DAG-BLUE	0.095±0.005	No	0.891
7I	<i>phyB</i> 10 DAG-BLUE	0.155±0.020	No	0.805
7I	<i>phyB</i> 15 DAG-BLUE	0.208±0.015	No	0.923
S3A	10 DAG-WHITE	0.181±0.011	N/A	N/A
S3A	15 DAG-WHITE	0.236±0.016	N/A	N/A
S3A	20 DAG-WHITE	0.530±0.026	N/A	N/A
S3A	25 DAG-WHITE	1.052±0.041	N/A	N/A
S3A	10 DAG-RED	0.162±0.022	No	0.472
S3A	15 DAG-RED	0.183±0.020	No	0.178
S3A	20 DAG-RED	0.538±0.083	No	0.646
S3A	25 DAG-RED	0.726±0.037	No	0.102
S3A	10 DAG-BLUE	0.176±0.019	No	0.872
S3A	15 DAG-BLUE	0.244±0.031	No	0.858
S3A	20 DAG-BLUE	0.563±0.021	No	0.246
S3A	25 DAG-BLUE	1.431±0.019	No	0.192
S3B	10 DAG-WHITE	3.9E-05±9.3E-06	N/A	N/A
S3B	15 DAG-WHITE	0.0005±4.5E-05	N/A	N/A
S3B	20 DAG-WHITE	0.0001±9.4E-06	N/A	N/A
S3B	25 DAG-WHITE	0.0001±3.8E-06	N/A	N/A
S3B	10 DAG-RED	2.7E-05±1.1E-04	No	0.189
S3B	15 DAG-RED	0.0004±3.9E-05	No	0.377
S3B	20 DAG-RED	8.8E-05±1.5E-05	No	0.093
S3B	25 DAG-RED	0.0003±3.6E-05	No	0.096
S3B	10 DAG-BLUE	7.1E-05±7.3E-06	Yes	0.043
S3B	15 DAG-BLUE	0.001±0.0002	Yes	0.031
S3B	20 DAG-BLUE	0.0005±4.2E-05	Yes	0.041



Chapter 5: Light quality regulates flowering

S3B	25 DAG-BLUE	6.2E-05±2.6E-06	Yes	0.023
S3C	10 DAG-WHITE	0.314±0.013	N/A	N/A
S3C	15 DAG-WHITE	0.256±0.019	N/A	N/A
S3C	20 DAG-WHITE	0.242±0.017	N/A	N/A
S3C	25 DAG-WHITE	0.361±0.008	N/A	N/A
S3C	10 DAG-RED	0.384±0.009	No	0.584
S3C	15 DAG-RED	0.191±0.008	No	0.178
S3C	20 DAG-RED	0.211±0.010	No	0.279
S3C	25 DAG-RED	0.341±0.012	No	0.335
S3C	10 DAG-BLUE	0.314±0.067	No	0.913
S3C	15 DAG-BLUE	0.183±0.010	No	0.052
S3C	20 DAG-BLUE	0.225±0.014	No	0.569
S3C	25 DAG-BLUE	0.253±0.012	No	0.089
S3D	10 DAG-WHITE	0.548±0.046	N/A	N/A
S3D	15 DAG-WHITE	1.402±0.060	N/A	N/A
S3D	20 DAG-WHITE	1.207±0.051	N/A	N/A
S3D	25 DAG-WHITE	1.141±0.038	N/A	N/A
S3D	10 DAG-RED	0.518±0.006	No	0.628
S3D	15 DAG-RED	1.585±0.159	No	0.431
S3D	20 DAG-RED	1.263±0.097	No	0.695
S3D	25 DAG-RED	0.938±0.053	No	0.165
S3D	10 DAG-BLUE	0.357±0.011	No	0.172
S3D	15 DAG-BLUE	1.184±0.046	No	0.102
S3D	20 DAG-BLUE	0.876±0.044	No	0.118
S3D	25 DAG-BLUE	0.972±0.029	No	0.129

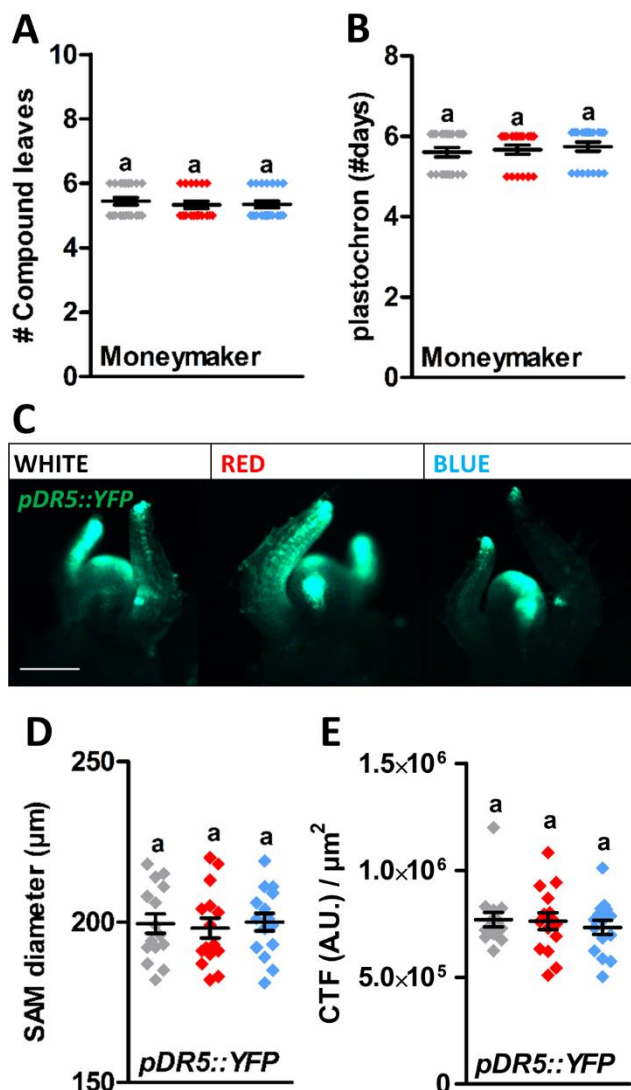


Figure S1: Tomato shoot development is indifferent to red and blue light.

A. Number of compound leaves of tomato cultivar MoneyMaker (MM) plants grown in white, red, or blue LED conditions until the floral transition. **B.** Plastochron length (in number of days) of MM plants grown in the different LED conditions. **C.** Stereo-fluorescence microscopy images of representative shoot apices of tomato *pDR5::YFP* plants grown in the different LED conditions. **D.** SAM diameter (in μm) of tomato *pDR5::YFP* plants grown in the different LED conditions. **E.** Corrected Total Fluorescence (CTF) of the *pDR5::YFP* signal in Arbitrary Units (A.U.) in shoot apices of tomato plants grown in the different LED conditions.

Graph colours represent white, red, or blue LED conditions in **A**, **B**, **D** and **E**. Scale bars indicate 100 μm in **C**. LED conditions were compared using a one-way ANOVA followed by a Tukey's test (different letters indicate statistically significant differences, $p < 0.05$) in **A**, **B**, **D** and **E**. Error bars represent standard error from mean in **A**, **B**, **D** and **E**. Similar results were obtained in two independent experiments.

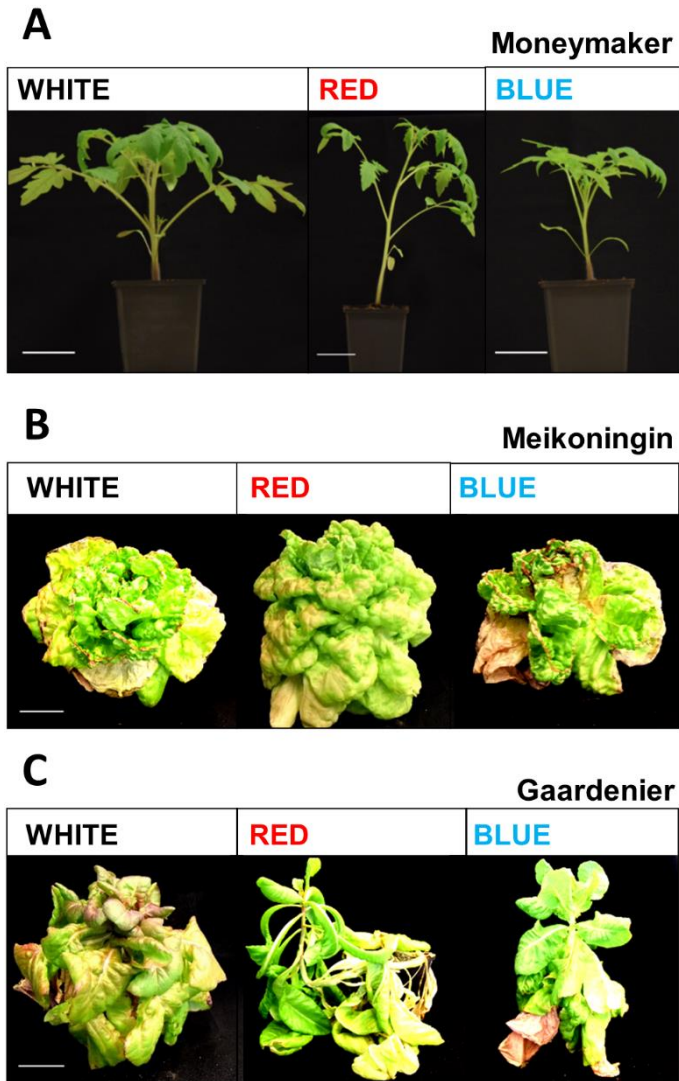


Figure S2: Phenotypes of tomato and lettuce plants grown in the LED conditions.

Representative tomato and lettuce plants that were grown in white, red, or blue LED conditions until the floral transition. **A.** 30-day-old tomato plants of the day-neutral cultivar Moneymaker. **B.** 12-weeks-old lettuce plants of the long-day variety Meikoningin. **C.** 12-weeks-old lettuce plants of the day-neutral variety Gaardenier. Scale bars indicate 5 cm in **A** and 10 cm in **B-C**. Similar results were obtained in either two (lettuce) or three (tomato) independent experiments.

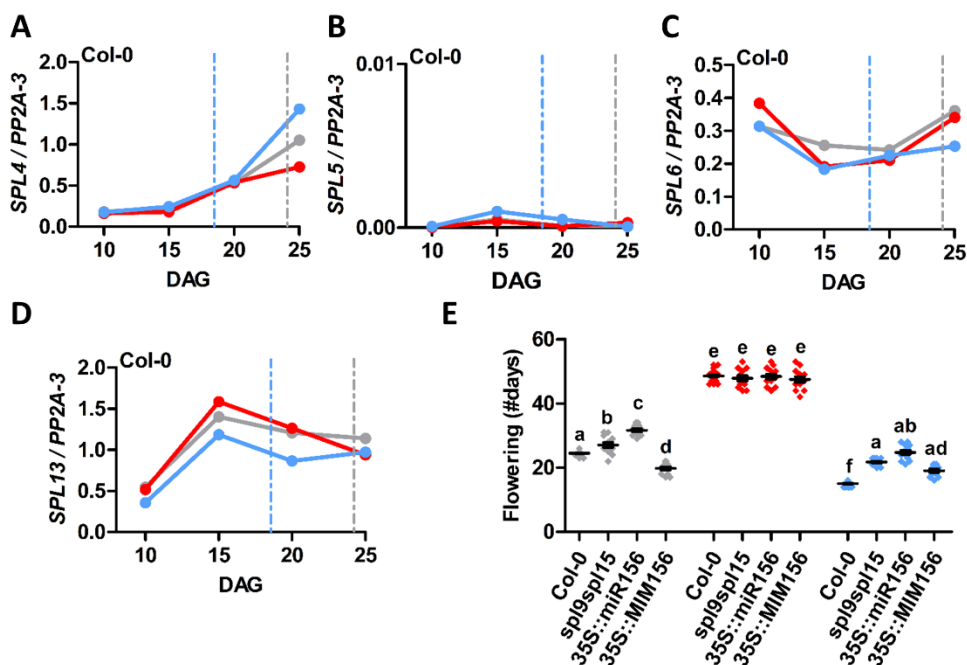


Figure S3: Early flowering in the absence of red light results from accelerated ageing.

A-D. Quantitative RT-PCR analysis of genes involved in the age pathway. Analysis was performed on Arabidopsis Columbia (Col-0) plants that were grown in white, red, or blue LED conditions at 10, 15, 20, and 25 days after germination (DAG). Relative expression levels of *SPL4* (**A**), *SPL5* (**B**), *SPL6* (**C**), and *SPL13* (**D**). **E.** Flowering time of Arabidopsis Columbia (Col-0), *p35S::miR156b*, *p35S::MIM156*, and *spl9 spl15* double mutant plants grown in the different LED conditions. Graph colours represent the different LED conditions. Monochromatic LED conditions (red or blue) were compared to white (control) using a two-sided Student's *t*-test (asterisks indicate significant differences at a specific time point (**p*<0.05)) in **A-D**. In **E**, LED conditions and wild types or mutants were compared using a one-way ANOVA followed by a Tukey's test (letters **a**, **b**, **c**, **d**, **e**, and **f** indicate statistically significant differences, *p*<0.05). Error bars represent standard error from mean in **E** (*n*=30), standard errors and *p*-values for **A-D** are listed in **Table S3**. Similar results were obtained in three (**A-D**) or two (**E**) independent experiments.



Summary



Young horticultural plants such as *Solanum lycopersicum* (tomato) are relatively small and require less light, thus opening up possibilities to be grown in multi-layers that require less space and energy. Since light-emitting diodes (LEDs) decouple light intensity from heating, they can be applied in such “vertical farming” growth systems. Moreover, LEDs offer spectral quality control that may be used to steer plant development. To achieve this, the effect of light quality on growth and developmental processes via the different light-sensing “photoreceptors” must be revealed. The photoreceptor families respond to different wavelengths (colours) within the spectrum: phytochromes (PHYs) are sensitive to red and far-red light, phototropins (PHOTs), cryptochromes (CRYs), and Zeitlupes (ZTLs) respond to blue light, and the UV-RESISTANCE LOCUS 8 (UVR8) receptor is activated by UV-B light.

Chapter 1 reviews the discovery and protein structures of, and signalling pathways triggered by, the different photoreceptors in land plants. Next, we discuss the role of each photoreceptor during different phases of plant development, and their interplay with major hormonal signalling pathways. After seed germination, the embryo matures from heterotrophic to fully photoautotrophic, and at this stage, light becomes a requirement for further development. Following seed germination, darkness promotes apical hypocotyl growth in seedlings to ensure rapid emergence from the soil. After emergence, light activates PHYs and CRYs to inhibit hypocotyl elongation and promote apical hook opening, thereby exposing the shoot apical meristem (SAM). Subsequently, the SAM responds to light by producing leaves and by initiating signalling cascades that modulate the architecture of the root. A widely-studied example of light-regulated plant growth is shade avoidance, where PHY signalling results in apical dominance, hyponastic leaves, and

early flowering, in response to low light intensity or low red: far-red ratios. Aside from the light responses that are described above, plants also monitor changes in light intensity and quality to become reproductive. For long-day (LD) plants, such as the genetic model dicot *Arabidopsis thaliana* (*Arabidopsis*), flowering is promoted in late spring through connections between ZTL photoreceptors and the circadian clock. In contrast, day-neutral (DN) plants, such as tomato, flower in response to other autonomous and hormonal pathways, regardless of day length. Therefore, at the end of **chapter 1**, we also discuss the major differences in light-associated genes and phenotypes between the genetic model dicot *Arabidopsis* and the horticultural crop tomato. In **chapter 2** we investigated how direct exposure of roots to light alters primary root growth of seedlings. We introduced a system to grow *Arabidopsis* and tomato seedlings in a “more natural” *in vitro* environment: the dark-grown roots (DGR) condition. Compared to traditional *in vitro* conditions with light-grown roots (LGR), DGR seedlings showed a better developed root system. Further analysis showed that red light activates root-localised PHYB proteins, that subsequently inhibit PHYTOCHROME INTERACTING FACTOR (PIF) 4, an activator of the auxin biosynthesis gene *YUCCA 6*. In a similar way, PHYA was found to inhibit PIF1, an activator of *YUCCA 4* and *YUCCA 6*, in response to far-red light. Subsequently this results in a suboptimal auxin concentration in the root apical meristem of LGR seedlings, ultimately leading to shorter roots. In DGR seedlings, PHYA- and PHYB-mediated inhibition of auxin biosynthesis does not occur, thereby creating optimal auxin levels for root growth. Proof-of-principle experiments in tomato suggested that the mechanism is at least partially conserved in plants. In **chapter 3**, *Arabidopsis* and tomato plants were grown in three different light



Summary

conditions: white light (control), monochromatic red light, and monochromatic blue light. Monochromatic red light promoted apical growth, resulting in longer hypocotyls and stems, and a higher shoot/root ratio in *Arabidopsis* and tomato plants. In contrast, monochromatic blue light resulted in shorter hypocotyls and stems, and a lower shoot/root ratio. Adult *Arabidopsis* plants developed a large rosette, flowered extremely late, and showed enhanced branching in the red LED condition, whereas blue light-grown plants flowered extremely early and developed only very few rosette leaves and branches. Interestingly, lateral organ formation and flowering of tomato plants appeared to be remarkably indifferent to the LED conditions, highlighting once more that responses in horticultural crops can greatly differ from what is observed in the genetic model plant *Arabidopsis*. In **chapter 4** we further investigated the hypocotyl and stem phenotypes that were observed in the different LED treatments. We showed that monochromatic red light promotes apical hypocotyl growth in seedlings, while decreasing its primary radial growth in both *Arabidopsis* and tomato seedlings. In contrast, treatment with monochromatic blue light resulted in shorter and thicker hypocotyls, when compared to white light. Histological and microscopic analysis revealed that these phenotypes were caused by changes in epidermal and pith cell sizes, suggesting that light quality affects cell wall loosening and vacuolar expansion to regulate hypocotyl growth. Interestingly, we observed that primary radial growth of adult tomato plants was completely indifferent to red and blue light, similar to leaf production and flowering. In contrast, primary radial growth of adult *Arabidopsis* plants was affected by light quality, resulting in thick stems in monochromatic red light, and thin stems in monochromatic blue light. These phenotypes were correlated to changes in primary xylem width and the number

of vascular bundles. Finally, analysis of Arabidopsis photoreceptor mutants suggested that CRYs and PHYs play an important role in light-regulated apical and primary radial growth. **Chapter 5** explores the leaf and flowering phenotypes that were observed in the different LED treatments in more detail. In monochromatic red light, an increase in Arabidopsis SAM size and an extended vegetative phase resulted in the production of an extremely big rosette, while the blue LED condition had an opposite effect. Interestingly, tomato SAMs were indifferent to light quality, resulting in the same number of leaves and flowering time in the different LED conditions. This suggested that light-regulated flowering of LD Arabidopsis plants was correlated to daylength sensitivity. Mutant and gene expression analysis confirmed that the photoperiodic pathway is only activated by light spectra that contain blue light,









	Red Light		Blue Light	
	Arabidopsis	Tomato	Arabidopsis	Tomato
	 <p>Long, thin hypocotyl</p> <p>Short root, few lateral roots</p>	 <p>Long, thin hypocotyl</p> <p>Normal root length</p>	 <p>Short, thick hypocotyl</p> <p>Short root, many lateral roots</p>	 <p>Short, thick hypocotyl</p> <p>Short root</p>
	 <p>Big rosette, late flowering</p> <p>Long, thick stems with many branches</p>	 <p>Normal flowering time</p> <p>Long stems with normal thickness</p>	 <p>Small rosette, early flowering</p> <p>Short, thin stems with few branches</p>	 <p>Normal flowering time</p> <p>Long stems with normal thickness</p>

Figure 1: Growth and development of Arabidopsis and tomato plants grown in red or blue light.

Summary of the Arabidopsis and tomato phenotypes that were observed in monochromatic red light (left) or monochromatic blue light (right), when compared to white light. “normal” indicates that the phenotype does not deviate from what was observed in white light.



while only spectra that contain red light activate the age pathway. Additional gene expression and *phy* mutant analysis showed that PHYB-mediated inhibition of the age pathway delays flowering in response to red light. This explains why Arabidopsis and lettuce plants flowered early in the blue LED condition that lacks red light, thus leaving PHYB in its inactive Pr conformation. Based on the work presented in this thesis we can conclude that red and blue light often act antagonistically during many aspects of plant growth and development. In addition, by including both Arabidopsis and tomato plants in our studies, we showed that light quality responses are not necessarily conserved between species, thus highlighting the importance of crop research in addition to the use of genetic model plants (**Figure 1**).



Samenvatting



Jonge planten van gewassen zoals *Solanum lycopersicum* (tomaat) zijn relatief klein, waardoor ze minder behoefte hebben aan een hoge lichtintensiteit. Om ruimte en energie te besparen, zouden deze jonge planten in meerdere lagen boven elkaar gegroeid kunnen worden. Omdat “light-emitting diode” (LED) lampen geen extra hitte produceren bij het bereiken van een hoge lichtintensiteit, kunnen ze worden gebruikt in dergelijke “vertical farming” groeisystemen. Bovendien geeft het gebruik van LEDs de optie om de intensiteiten van verschillende golflengtes (kleuren) in het lichtspectrum aan te passen om daarmee de plantenontwikkeling gericht te sturen. Daartoe moet wel duidelijk zijn hoe de lichtkwaliteit (spectrum) via verschillende lichtgevoelige “fotoreceptoren” ontwikkelings- en groei- processen in de plant beïnvloedt. Fotoreceptorfamilies worden geactiveerd door verschillende golflengtes in het spectrum: fytochromen (PHYs) zijn gevoelig voor rood en ver-rood licht, fototropines (PHOTs), cryptochromen (CRYs) en zeitlupes (ZTLs) worden geactiveerd door blauw licht, en de UV-RESISTANCE LOCUS 8 (UVR8) receptor reageert op UV-B licht. In **hoofdstuk 1** worden de ontdekking, de eiwitstructuren en de signaaltransductieroutes van de verschillende fotoreceptoren geïntroduceerd. Vervolgens wordt de rol van elke fotoreceptor tijdens verschillende stadia van plantenontwikkeling besproken, en hoe dit interacteert met de signaaltransductie van plantenhormonen. Na de kieming van een zaadje ondergaat het plantenembryo in het licht een transitie van heterotrofisch naar foto-autotrofisch. Kieming in de donkere aarde resulteert in etiolatie van de zaailing, waarbij snelle apicale groei van de hypocotyl ervoor zorgt dat de scheut snel het licht kan bereiken. Eenmaal in het licht worden PHYs en CRYs geactiveerd, die zorgen voor remming van de hypocotylgroei en voor opening van de zaadlobben zodat het scheut apicale

meristeem (SAM) blootgesteld wordt aan het licht. Dit stimuleert de productie van bladeren, en een signaaltransductie vanuit het SAM die de wortelgroei reguleert. Een van de meest bestudeerde licht-gereguleerde processen in planten is de schaduwreactie, waarbij de lichtintensiteit of de rood:ver-rood ratio laag is. Deze reactie wordt gemedieerd door een PHY signaaltransductie die resulteert in sterke lengte groei van de stengel, hyponastische bladeren en vroege bloei. Behalve de-etiolatie en de schaduwreactie wordt ook de transitie van vegetatieve groei naar reproductieve groei gereguleerd door licht. In lange-dag (LD) planten, zoals de genetische modelplant *Arabidopsis thaliana* (Arabidopsis), wordt bloei geïnduceerd door de langere daglengte aan het einde van de lente, via interacties tussen ZTL fotoreceptoren en het circadiaanse ritme (biologische klok). Dag-neutrale (DN) planten zoals tomaat worden reproductief op basis van autonome en hormonale regulatie, en zijn ongevoelig voor daglengte. Aan het einde van **hoofdstuk 1** worden de overige verschillen tussen Arabidopsis en tomaat behandeld, waarbij gefocust wordt op de genen en processen die geassocieerd worden met licht. In **hoofdstuk 2** is onderzocht hoe primaire wortelgroei van zaailingen wordt beïnvloed door directe belichting van de wortels. Arabidopsis en tomatenzaailingen werden gegroeid in een “meer natuurlijke” *in vitro* omgeving met de scheut in het licht en de wortels in het donker: de zogenaamde dark-grown roots (DGR) conditie. In vergelijking met traditionele *in vitro* systemen waarbij de gehele zaailing belicht wordt (LGR condities), zorgt de DGR conditie voor een betere ontwikkeling van het wortelsysteem. Met behulp van mutanten, reporterlijnen, auxine behandelingen, enten, en genexpressie analyse hebben we laten zien dat PHYB fotoreceptoren in de wortel geactiveerd worden door rood licht. Dit resulteert in inhibitie van PHYTOCHROME INTERACTING FACTOR (PIF)





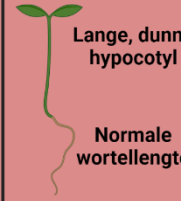
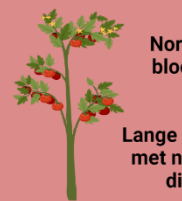

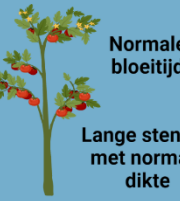


4, een activator van het auxine biosynthese gen *YUCCA 6*. Op een vergelijkbare manier wordt PIF1 (een activator van *YUCCA 4* en *YUCCA 6*) geremd door PHYA als reactie op ver-rood licht. In de LGR conditie veroorzaakt dit een suboptimale auxine concentratie in het wortelmeristeem, wat resulteert in kortere wortels. In de DGR conditie vindt de PHYA- en PHYB-gereguleerde remming van auxine biosynthese niet plaats, waardoor de auxine concentratie in het meristeem optimaal is voor wortelgroei. Wortels van DGR tomatenzaailingen waren ook langer dan die van LGR zaailingen, wat suggereert dat de respons van wortels op directe belichting in ieder geval gedeeltelijk geconserveerd is in planten. In **hoofdstuk 3** zijn Arabidopsis en tomatenplanten gegroeid in een LED systeem met drie verschillende licht condities: wit licht (controle), monochromatisch rood licht, en monochromatisch blauw licht. Monochromatisch rood licht bevorderde de apicale groei van zowel Arabidopsis als tomatenplanten, waardoor deze een langere hypocotyl en stengel, en een hogere scheut/wortel ratio hadden. Monochromatisch blauw licht had een tegenovergesteld effect resulterend in een kortere hypocotyl en stengel, en een lage scheut/wortel ratio. In oudere Arabidopsis planten resulteerde de rode LED conditie in een grote rozet, extreem late bloei, en veel vertakkingen op de primaire boeiwijze, terwijl de blauwe LED conditie zorgde voor weinig bladeren en vertakkingen, en erg vroege bloei. Verassend genoeg bleken deze processen in tomaat volledig ongevoelig voor rode en blauwe golflengten te zijn. Dit benadrukt nogmaals dat lichtreacties die onderzocht zijn in de modelplant Arabidopsis daarnaast ook in relevante gewassen onderzocht moeten worden. In **hoofdstuk 4** zijn de hypocotyl- en stengelfenotypes vanuit de LED condities in meer detail onderzocht. Deze analyses lieten zien dat in monochromatisch rood licht de

primaire radiale groei geremd werd, terwijl deze LED conditie de apicale hypocotylgroei in Arabidopsis en tomatenzaailingen juist bevorderde. In beide soorten had monochromatisch blauw licht een antagonistisch effect. Histologie en microscopische analyse lieten zien dat deze fenotypes ontstaan door verschillen in de grootte van epidermis- en pithcellen, wat suggereert dat lichtkwaliteit hypocotylgroei reguleert door het gericht verslappen van de celwand en door opzwellen van de vacuole. Bij oudere tomatenplanten bleek de primaire radiale stengelgroei, net als de bladproductie en bloei, ongevoelig voor lichtkwaliteit, terwijl er wel een effect van lichtkwaliteit op de primaire radiale groei van Arabidopsis stengels werd geobserveerd. De rode LED conditie veroorzaakte dikke stengels, terwijl de Arabidopsis planten in de blauwe LED conditie dunne stengels hadden. Deze fenotypes resulteerden uit verschillen in primaire xyleem differentiatie en het aantal vasculaire bundels. Tenslotte bleek uit een mutant analyse dat CRYs en PHYs een belangrijke rol spelen in de lichtregulatie van apicale en primaire radiale groei. In **hoofdstuk 5** zijn de blad en bloei fenotypes van Arabidopsis en tomatenplanten in de verschillende LED condities in meer detail onderzocht. In monochromatisch rood licht was het SAM van Arabidopsis planten vergroot. Dit resulteerde, samen met een langere vegetatieve groeifase, in een extreem grote rozet. De blauwe LED conditie had nogmaals een tegenovergesteld effect op het fenotype. In DN tomatenplanten was het SAM ongevoelig voor lichtkwaliteit waardoor hetzelfde aantal bladeren en dezelfde bloeitijd werden geobserveerd in alle LED condities. Dit suggereerde dat de lichtspectrum-gevoeligheid van bloei in Arabidopsis correleert met daglengte-gevoeligheid. Genexpressie en mutant analyses bevestigden dat de fotoperiode signaaltransductie, en dus versnelde bloei, geactiveerd wordt door blauw licht, terwijl de veroudering, en



dus ook bloei, geremd wordt door rood licht. Tenslotte heeft verdere analyse geleid tot de conclusie dat rood licht-geactiveerde PHYB fotoreceptoren de bloei uitstellen via de verouderings signaaltransductie. Dit verklaart waarom Arabidopsis en sla planten vroeg bloeiden in de blauwe LED conditie (zonder rode golflengten), waar PHYB alleen aanwezig is in de inactieve vorm. Uit dit proefschrift kunnen we concluderen dat rood en blauw licht vaak een antagonistisch effect hebben op plantengroei en -ontwikkeling. Omdat we Arabidopsis en tomaat hebben gebruikt in dit onderzoek, hebben we zowel gelijkenissen als verschillen ontdekt in hoe deze twee soorten op het lichtspectrum reageren (**Figuur 1**). Dit benadrukt nogmaals hoe belangrijk het is om naast genetische modelorganismen ook relevante gewassen in het onderzoek te betrekken.

Arabidopsis	 <p>Lange, dunne hypocotyl Korte wortel met weinig zijwortels</p>	 <p>Grote rozet, late bloei Lange, dikke stengels met veel vertakkingen</p>	 <p>Korte, dikke hypocotyl Korte wortel met veel zijwortels</p>	 <p>Kleine rozet, vroege bloei Korte, dunne stengels met weinig vertakkingen</p>
	 <p>Lange, dunne hypocotyl Normale wortellengte</p>	 <p>Normale bloeitijd Lange stengels met normale dikte</p>	 <p>Korte, dikke hypocotyl Korte wortel</p>	 <p>Normale bloeitijd Lange stengels met normale dikte</p>

Figuur 1: Ontwikkeling en groei van Arabidopsis en tomatenplanten in rood of blauw licht.

Overzicht van de fenotypen die geobserveerd zijn in Arabidopsis en tomatenplanten na groei in monochromatisch rood licht (links) of monochromatisch blauw licht (rechts), ten opzichte van wit licht. “normaal” geeft aan dat het fenotype in de LED conditie hetzelfde was als in wit licht.



List of abbreviations



List of abbreviations

Abbreviation	Description
<i>a</i>	y-intercept
ABA	Absciscic acid
ABCB19	ATP-BINDING CASSETTE B19
ABCG14	ATP-BINDING CASSETTE G14
AFB	AUXIN-BINDING F-BOX PROTEINS
AGL24	AGAMOUS-LIKE 24
AHL15	AT-HOOK MOTIF CONTAINING NUCLEAR LOCALIZED 15
AHP6	ARABIDOPSIS HISTIDINE PHOSPHOTRANSFER PROTEIN 6
AIL6	AINTEGUMENTA-LIKE 6
AM	axillary meristem
ANT	AINTEGUMENTA
AP	APETALA
Arabidopsis	<i>Arabidopsis thaliana</i>
ARF(s)	AUXIN REPSONSE FACTOR(s)
arg	arginine
ARR(s)	ARABIDOPSIS RESPONSE REGULATOR(s)
A.U.	arbitrary units
AUX1	AUXIN-RESISTANT 1
AUX/IAA(s)	AUXIN / INDOLE-3-ACETIC ACID PROTEIN(s)
<i>b</i>	regression coefficient (slope)
B	blue
BES1	BRI1-EMS-SUPPRESSOR 1
BGR	blue-grown roots
bHLH	basic helix-loop-helix
BIL1	BRASSINOSTEROID-INSENSITIVE 2-LIKE 1

BR	brassinosteroids
BZR1	BRASSINAZOLE-RESISTANT 1
CAL	CAULIFLOWER
CAPS	cleaved amplified polymorphic sequence
CCE	CRY C-terminal extension
CDF(s)	CYCLING DOF FACTOR(s)
CIB(s)	CRY2-INTERACTING bHLH(s)
CK	cytokinin
CKX2	CYTOKININ DEHYDROGENASE 2
CLV	CLAVATA
CO	CONSTANS
Col-0	Columbia
COP	CONSTITUTIVE PHOTOMORPHOGENIC
CPD	cyclobutane pyrimidine dimer
CRY(s)	cryptochrome(s)
CSN	COP9 signalosome
CTCF	corrected total cell fluorescence
CTF	corrected total fluorescence
CZ	central zone
DAG	days after germination
DAS	days after sowing
DET	DE-ETIOLATED
DGR	dark-grown roots
DN	day-neutral
DNA	deoxyribonucleic acid
Ehd1	Early heading date 1
EIN3	ETHYLENE-INSENSITIVE 3
ERF(s)	ETHYLENE RESPONSE FACTOR(s)



List of abbreviations

ET	ethylene
FAD	flavin adenine dinucleotide
FAR1	FAR-RED IMPAIRED RESPONSE 1
FHL	FHY1-like
FHY	FAR-RED ELONGATED HYPOCOTYL
FIL	FILAMENTOUS FLOWER
FKF1	FLAVIN-BINDING KELCH REPEAT 1
FLC	FLOWERING LOCUS C
FMN	flavin mononucleotide
FO	Foundation
FR	far-red
FT	FLOWERING LOCUS T
FUL	FRUITFULL
FUS	FUSCA
FW	forward
GA	gibberellic acid
GFP	green fluorescent protein
GI	GIGANTEA
HAM	HAIRY MERISTEM
HCA2	HIGH CAMBIAL ACTIVITY 2
Hd1	Heading date 1
Hd3a	Heading date 3a
HEC	HECATE
HFR1	LONG HYPOCOTYL IN FAR-RED 1
HIR	high irradiance response
HKRD	Histidine kinase-related domain
HSD	honestly significant different
HY4	ELONGATED HYPOCOTYL 4 (CRY1)

HY5	ELONGATED HYPOCOTYL 5
HYH	HY5 HOMOLOGUE
IAA	indole-3-acetic acid (auxin)
IM	inflorescence meristem
JA	jasmonic acid
KRP2	KIP-RELATED PROTEIN 2
LAF1	LONG AFTER FAR-RED LIGHT
LAX	LIKE-AUX1
LBD	LATERAL ORGAN BOUNDARIES DOMAIN
LD	long-day
LED(s)	light-emitting diode(s)
<i>Ler</i>	Landsberg <i>erecta</i>
Lettuce	<i>Lactuca sativa</i>
LFR	low fluence response
LFY	LEAFY
LGR	light-grown roots
LKP2	LOV KELCH PROTEIN 2
LMP	low melting point
LOG	LONELY GUY
LOV	light, oxygen, or voltage
LSA	leaf surface area
L/W ratio	length / width ratio
miR	microRNA
MM	Moneymaker
MP	MONOPTEROS (ARF5)
NAA	1-naphthaleneacetic acid
NASC	Nottingham Arabidopsis Stock Centre
NBs	nuclear bodies



List of abbreviations

NFY(s)	NUCLEAR FACTOR Y(s)
NLS	nuclear localisation signal
nm	nanometre
NPA	1-naphthylphthalamic acid
NPH1	NON-PHOTOTROPIC HYPOCOTYL 1 (PHOT1)
NPH3	NON-PHOTOTROPIC HYPOCOTYL 3
NPL1	NPH1-like 1 (PHOT2)
n.s.	not significant
NOW	Dutch Research Council (Nederlandse organisatie voor Wetenschappelijk Onderzoek)
OC	organizing centre
PAR	photosynthetically active radiation
PAT	polar auxin transport
PBS	phosphate-buffered saline
PCR-RFLP	PCR- restriction fragment length polymorphism
PFA	paraformaldehyde
Pfr	FR-absorbing form of phytochromes
PHOT(s)	phototropin(s)
PHR	photolyase homologous region
PHY(s)	phytochrome(s)
PI	propidium iodide
PIF(s)	PHYTOCHROME INTERACTING FACTOR(s)
PIN	PIN-FORMED
PKS	PHYTOCHROME KINASE SUBSTRATE
PLT3	PLETHORA 3
PP2A	PROTEIN PHOSPHATASE 2A
PPF	photosynthetic photon flux
Pr	R-absorbing form of phytochromes

Prim	primary
PRR(s)	PSEUDO-RESPONSE REGULATOR(s)
PXY	PHLOEM INTERCALATED WITH XYLEM
PZ	peripheral zone
PΦB	phytochromobilin tetrapyrrole chromophore
QC	quiescent centre
<i>r</i>	correlation coefficient
R	red
RAM	root apical meristem
R/B	red/blue ratio
R:FR	red/far-red ratio
RGR	red-grown roots
ROS	reactive oxygen species
RSA	rosette surface area
RTP2	ROOT PHOTOTROPISM 2
RUP	REPRESSOR OF UV-B PHOTOMORPHOGENESIS
RV	reversed
RZ	rib zone
SAM	shoot apical meristem
SCF	Skp, Cullin, and F-box
SD	short-day
SE	standard error
Sec	secondary
SEP3	SEPALLATA 3
ser	serine
SOC1	SUPPRESSOR OF CONSTANS 1
SPA1	SUPPRESSOR OF PHYA 1



List of abbreviations

SPL(s)	SQUAMOSA PROMOTER BINDING PROTEIN-LIKE(s)
STM	SHOOT MERISTEMLESS
TAA1	TRYPTOPHAN AMINOTRANSFERASE OF ARABIDOPSIS 1
TAR	TRYPTOPHAN AMINOTRANSFERASE RELATED
TCP	TEOSINTE BRANCHED 1, CYCLOIDEA, PROLIFERATING CELL FACTOR
TDIF	TRACHEARY ELEMENT DIFFERENTIATION
Tert	tertiary
TFL1	TERMINAL FLOWER 1
TGRC	Tomato Genetics Resource Centre
thr	threonine
THz	terahertz
TIP41	TAP42-interacting protein
TIR1	TRANSPORT INHIBITOR RESPONSE 1
TMO6	TARGET OF MONOPTEROS 6
TOC1	TIMING OF CAB EXPRESSION 1
TOE	TARGET OF EARLY ACTIVATION TAGGED
ToFZHY	tomato YUCCA orthologue
tomato	<i>Solanum lycopersicum</i>
TOR	TARGET OF RAPAMYCIN
trp	tryptophan
UV	ultra-violet
UV-B	ultra-violet B
UVR8	UV RESISTANCE LOCUS 8
VIN3	VERNALIZATION INSENSITIVE 3
VLFR	very low fluence response

VND	VASCULAR-RELATED NAC-DOMAIN
VPC	vegetative phase change
VRN	VERNALIZATION
W	white
WAS	weeks after sowing
WOX	WUSCHEL-RELATED HOMEBOX
WUS	WUSCHEL
YFP	yellow fluorescent protein
YUC	YUCCA
ZT	Zeitgeber time
ZTL(s)	ZEITLUPE(s)



Curriculum vitae



Kiki Spaninks was born on November 25th, 1990, in Voorburg, the Netherlands. After graduating from 't Stedelijk College in Zoetermeer, she started her Biology study at Leiden University in 2008. She obtained her BSc degree with a minor in modern drug discovery (chemistry) in 2011. Her BSc programme included an internship at the Molecular Cell Biology department of the Institute of Biology Leiden (IBL) under the supervision of Prof. dr. A.H. Meijer and PhD student M. van der Vaart, where she studied the role of nitric oxide during the innate immune response of MyD88-deficient zebrafish against *Mycobacterium marinum*. In 2011, she continued with the Master study Biology at Leiden University, with a specialisation in Molecular and Cellular Biosciences that included two internships. During the first internship at the Molecular Genetics department of the IBL, she applied multi-colour BiFC to visualise the translocation of *Agrobacterium tumefaciens* virulence proteins to *Saccharomyces cerevisiae* (yeast) under the supervision of dr. G.P.H. van Heusden and PhD student P.A. Sakalis. In the second internship with dr. H.J.M. Linthorst and PhD student Y. Zhou at the Plant Cell Physiology department of the IBL, she investigated the putative function of EDS5 as a salicylic acid transporter using yeast as a model organism. After receiving her MSc degree in 2013, she spent six months studying proteolysis in human tissue macrophages at the Erasmus Medical Centre in Rotterdam under the supervision of Prof. dr. J.J.M. van Dongen. In 2015, Kiki started as a PhD student in the Plant Developmental Genetics group of Prof. dr. R. Offringa at the IBL, as part of the NWO/STW funded LED it be 50% consortium. Here she studied the effects of light quality on the early plant development of *Arabidopsis thaliana* and *Solanum lycopersicum*, of which the results are described in this thesis. In 2020, she continued to work in the Offringa group

as post-doctoral researcher to study tipburn as part of the NWO/TTW funded LettuceKnow consortium. From October 2022 on she works as Assistant Professor at the IBL focusing on teaching and researching shoot-root signalling *in planta*.

